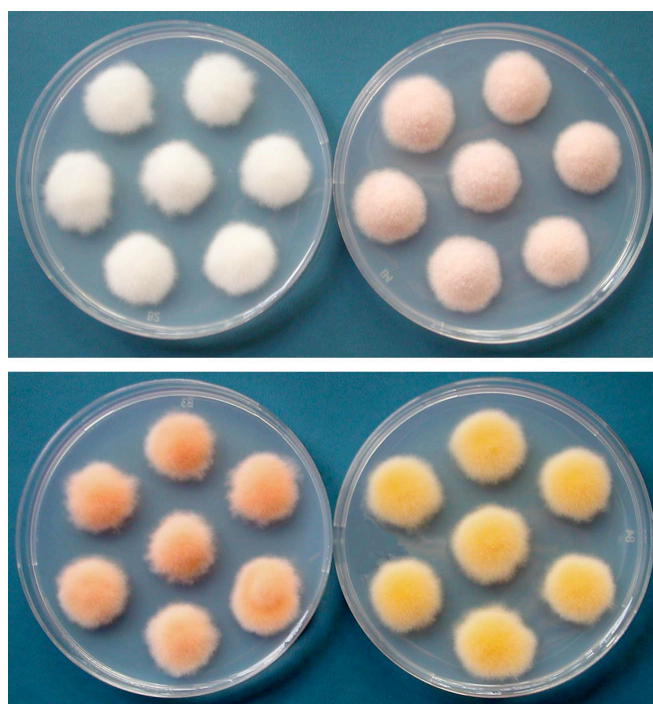


UNIVERSIDAD DE SEVILLA  
DEPARTAMENTO DE GÉNETICA



**Análisis funcional de enzimas de la  
carotenogénesis y fotoproteínas en hongos**



TESIS DOCTORAL

Alejandro Fernández Estrada

Sevilla, Febrero de 2009





UNIVERSIDAD DE SEVILLA  
FACULTAD DE BIOLOGÍA  
DEPARTAMENTO DE GENÉTICA



# **Análisis funcional de enzimas de la carotenogénesis y fotoproteínas en hongos**

Trabajo presentado por el licenciado  
**Alejandro Fernández Estrada**

Para optar al grado de Doctor Europeo en  
Ciencias Biológicas por la Universidad de Sevilla

Sevilla, Febrero de 2009

Director de trabajo:  
Dr Javier Ávalos Cordero  
Profesor titular de Genética  
Departamento de Genética, Facultad de Biología, Universidad de Sevilla

El director de la Tesis

El doctorando

Dr Javier Ávalos Cordero

Alejandro Fernández Estrada



Dedicado a mis padres,  
mi hermano y a Alejandra



# ÍNDICE DE CONTENIDOS

## INTRODUCCIÓN

1. Organismos utilizados en este trabajo	1
1.1 Manipulación y características generales de los organismos objeto de estudio.	1
1.2 Descripción y ciclo de vida de <i>Fusarium fujikuroi</i>	
1.2.1 El género <i>Fusarium</i> .	2
1.2.2 Ciclo de vida de <i>Fusarium</i> .	
4      1.2.3 Ciclo infectivo de <i>Fusarium fujikuroi</i> .	6
1.3 Descripción y ciclo de vida de <i>Neurospora</i> .	7
1.3.1 Características generales.	7
1.3.2 Ciclo de vida de <i>Neurospora</i> .	7
1.3.3 <i>Neurospora</i> como organismo modelo.	9
1.3.4 <i>Neurospora</i> como modelo de silenciamiento génico.	12
1.4 Descripción y ciclo de vida de <i>Ustilago maydis</i> .	13
1.4.1 Características generales de <i>Ustilago maydis</i> .	13
1.4.2 Ciclo infectivo de <i>U. maydis</i> .	14
2. Fotorreceptores.	16
2.1 Fotorrespuestas en hongos.	16
2.2 <i>Neurospora</i> como modelo de fotorreceptores en hongos.	17
2.2.1 Estructura del sistema fotorreceptor WC.	17
2.2.2 Funcionamiento del complejo WC.	20
2.2.3 Papel de VIVID en la fotoadaptación del complejo WC.	21
2.2.4 Genes fotoinducibles en <i>Neurospora</i> .	22
2.3 Opsinas.	23
2.3.1 Estructura de las opsinas.	24
2.3.2 Opsinas en hongos.	25
2.3.3 Opsinas en <i>Fusarium</i> .	36
3. Metabolismo secundario de hongos.	27
3.1 Metabolismo secundario de <i>Fusarium</i> .	27
3.1.1 Síntesis de policétidos en <i>Fusarium fujikuroi</i> :	
bicaverinas y fusarinas.	28
3.1.2 Los terpenoides.	29
3.1.3 Síntesis de giberelinas.	31

3.2 Los carotenoides.	32
3.2.1 Carotenogénesis de hongos.	33
3.2.2 Carotenogénesis en <i>Fusarium fujikuroi</i> .	35
3.2.3 Carotenogénesis en <i>N. crassa</i> .	38
3.2.4 Síntesis de carotenoides en <i>Ustilago</i> .	41
OBJETIVOS	43
RESULTADOS	47
Capítulo 1. The <i>ylo-1</i> gene encodes an aldehyde dehydrogenase responsible for the last reaction in the <i>Neurospora</i> carotenoid pathway	49
Abstract	51
1. Introduction	52
2. Results	55
2.1 Carotenoid pattern of the <i>ylo-1</i> mutant	55
2.2 Identification of the putative <i>ylo-1</i> gene in the <i>Neurospora</i> genome	57
2.3 Genetic identification of NCU04013 as the <i>ylo-1</i> gene	58
2.4 Characterization of YLO-1 enzymatic activity	60
2.5 Expression of <i>ylo-1</i>	62
3. Discussion	64
4. Experimental Procedures	68
4.1 <i>Neurospora</i> strains and culture conditions	68
4.2 Transformation and southern blot analysis	68
4.3 Real-time RT-PCR analyses	69
4.4 In vitro protein expression and enzyme assays	69
4.5 Analytical methods	70
Acknowledgements	71
Capítulo 2. Novel apocarotenoid intermediates in <i>Neurospora crassa</i> mutants imply a new biosynthetic reaction sequence leading to neurosporaxanthin formation	73
Abstract	75
1. Introduction	76
2. Material and Methods	79
2.1 Strains and growth conditions	79
2.2 Construction of plasmids	79
2.3 In vivo and in vitro analyses	80
2.4 Analytical methods	80

3. Results	81
3.1. Generation of a 3,4-didehydrolycopene accumulating <i>E. coli</i> strain	81
3.2. CAO-2 converted 3,4-didehydrolycopene into apo-4'-lycopenal	82
3.3. Analyses of the <i>ylo-1</i> mutant	84
3.4. Analyses of the reddish <i>al-2</i> mutant JA26	86
3. Discussion	86
Acknowledgements	91

Capítulo 3. The White Collar protein WcoA of <i>Fusarium fujikuroi</i> is not required for photocarotenogenesis, but plays a role in the regulation of secondary metabolism and conidiation	93
Abstract	95
1. Introduction	96
2. Material and Methods	98
2.1 Strains and culture conditions	98
2.2. Cloning of <i>wcoA</i>	98
2.3. Transformation	99
2.4 Molecular techniques	100
2.5. Chemical analyses and conidia production	101
2.6. Sequence analyses	101
3. Results	102
3.1. Cloning and sequence of the <i>wc-1</i> orthologue of <i>F. fujikuroi</i> , <i>wcoA</i>	102
3.2. <i>wcoA</i> expression	104
3.3. Gene disruption of <i>wcoA</i>	106
3.4. Carotenoid biosynthesis in <i>wcoA</i> disruptant strains	107
3.5. Production of other metabolites by the <i>wcoA</i> disruptant strains	109
3.6. Effect of the <i>wcoA</i> mutation on conidiation	111
3. Discussion	112
Acknowledgements	116

Capítulo 4. Regulation and targeted mutation of <i>opsA</i> , coding for the NOP-1 opsin orthologue in <i>Fusarium fujikuroi</i>	117
Abstract	119
1. Introduction	120
2. Results	123
2.1 Proteins from the opsin family in <i>Fusarium</i>	123
2.2 Gene <i>opsA</i> from <i>F. fujikuroi</i>	126
2.3 Generation and phenotypic characterization of <i>opsA</i> mutants	129
2.4 Effect of <i>opsA</i> and <i>car</i> mutations on the expression of <i>car</i> genes	130
3. Discussion	134

4. Material and Methods	138
4.1 Strains and culture conditions	138
4.2 Cloning and sequencing of <i>opsA</i>	138
4.3 Fusarium transformation	139
4.4 Generation of <i>opsA</i> , <i>carB</i> and <i>carRA</i> mutants	140
4.5 Molecular techniques	141
4.6 Analytical methods, conidia production and pathogenicity assay	143
4.7 Sequence analyses	143
Acknowledgements	143
Capítulo 5. $\beta$ -carotene and retinal biosynthesis in <i>Ustilago maydis</i>	145
Abstract	147
1. Introduction	148
2. Results	151
2.1 <i>U. maydis</i> accumulates $\beta$ -carotene as the sole carotenoid	151
2.2 <i>U. maydis</i> $\beta$ -carotene content is reduced by low pH value and not affected by light or H <sub>2</sub> O <sub>2</sub>	152
2.3 $\beta$ -carotene biosynthesis genes occur in <i>U. maydis</i>	152
2.4 The <i>U. maydis</i> enzyme Cco1 catalyzes retinal synthesis in vitro	155
2.5 <i>U. maydis</i> $\beta$ -carotene content is determined by Cco1	155
2.6 Retinal is not found in <i>U. maydis</i> $\Delta$ <i>cco1</i> mutants	158
2.7 <i>car</i> and <i>ops</i> genes are differentially regulated	155
3. Discussion	161
4. Material and Methods	164
4.1 Strains and Growth conditions	164
4.2 Plasmid and strain constructions	165
4.3 DNA and RNA procedures	166
4.4 Expression analyses	166
4.5 Carotenoid analyses	167
4.6 Enzymatic assays	167
4.7 Pathogenicity assay	168
4.8 Sequence analyses	168
Acknowledgements	168
DISCUSIÓN GENERAL	169
D.1 Rutas biosintéticas de carotenoides en <i>Neurospora</i>	171
D.2 La proteína WcoA de <i>Fusarium</i>	177
D.3 Las opsinas de <i>Fusarium</i> y <i>Ustilago</i>	181



CONCLUSIONES.	187
REFERENCIAS.	191

## 1. Organismos utilizados en este trabajo.

### 1.1 Manipulación y características generales de los organismos objeto de estudio.

Por sus sencillos ciclos de vida y fácil manejo en el laboratorio, los hongos son excelentes objetos de estudio en investigación. Algunos de ellos, han destacado como modelos genéticos y de abordaje de problemas biológicos básicos, como es el caso de *Neurospora crassa* (Perkins y Davis, 2000b). Este hongo, que contribuyó a mediados del siglo XX al desarrollo de conceptos pioneros en la Genética, como la relación entre genes y enzimas (citado en cualquier libro de texto de Genética), es actualmente uno de los microorganismos mejor conocidos a nivel molecular (Perkins y Davis, 2000b). La nutrida comunidad científica lo utiliza como organismo modelo dispone de una de las más completas colecciones de estirpes mutantes y herramientas genéticas. En la actualidad persiste como sistema de estudio especialmente fructífero en ciertas áreas, como son los mecanismos naturales de inactivación génica o la fotobiología. La gran cantidad de información acumulada sobre su biología y su manipulación han potenciado el interés por su posible uso biotecnológico (<http://www.neugenes.com>, Perkins y Davis, 2000a).

Otros hongos no están tan desarrollados metodológicamente, pero justifican su elección por sus usos aplicados o por la influencia que ejercen sobre la actividad humana. Ese es el caso, por ej. de las especies del género *Fusarium*, empleadas como modelos de patogénesis vegetal o de producción de metabolitos secundarios. En el primer caso merece especial mención *Fusarium oxysporum*, ampliamente estudiado por su actividad fitopatogénica (Ortoneda et al., 2004). En el segundo caso, ocupa un puesto relevante *Fusarium fujikuroi* por su capacidad de producir giberelinas, hormonas casi exclusivas del reino vegetal (Tudzynski, 2005). Estos compuestos no son más que un ejemplo de los numerosos metabolitos producidos por diferentes especies de este género (Medentsev y Akimenko, 1998). Muchas de ellas, incluyendo *F. fujikuroi* (Avalos et al., 2007) producen metabolitos tóxicos conocidos globalmente como micotoxinas, cuya presencia en plantas infectadas por el hongo puede representar un problema de salud pública (Nelson et al., 1994).

El tercer hongo utilizado en esta Tesis, *U. maydis*, se ha puesto de moda en los últimos años como modelo de patogénesis, en este caso sobre el maíz, al que es capaz de alterar de forma muy profunda su fisiología (Banuett, 1995). Un aspecto inédito de esta patogénesis es su interés culinario, ya que las mazorcas de maíz infectadas constituyen un manjar en algunos países, como México (Ruiz-Herrera y Martínez-Espinoza 1998). Las peculiaridades de su ciclo de vida dimórfico y su ciclo sexual, dependiente de la interacción con la planta, lo han convertido en un modelo de referencia en las bases moleculares de ambos procesos, con contribuciones especialmente relevantes en lo que

respecta a sus rutas de transducción de señales. La versatilidad metodológica de este organismo ha motivado la extensión de su uso para abordar otros problemas biológicos básicos (Steinberg y Pérez-Martín 2008).

A continuación se detallan los aspectos más relevantes de la biología de estos hongos.

## **1.2 Descripción y ciclo de vida de *Fusarium fujikuroi***

### **1.2.1 El género *Fusarium***

El género *Fusarium*, definido por Link en 1809 (ver tabla A1, Booth, 1971), está formado por un grupo de hongos imperfectos que poseen esporas fusiformes, a lo que debe su nombre, y que se denominan conidios. Los hongos imperfectos son aquellos a los que no se les ha observado ciclo sexual, de manera que se carece de la base para clasificarlos dentro de algunos de los grandes grupos de hongos, definidos originalmente por las estructuras sexuales características en su ciclo de vida (ascas, basidios, oosporas o zigosporas). La nomenclatura de este grupo de hongos es confusa, ya que muchas de sus stirpes se han rebautizado como otros géneros por la simple razón de haber observado sus capacidad de desarrollar el ciclo sexual en el laboratorio. Así, distintas especies de *Fusarium* “imperfectas” (anamorfos) cambiaron de nombre al subir a la categoría de “forma perfecta” (teleomorfo). Así ocurrió por ejemplo, con *Fusarium solani* y *Fusarium moniliforme*, que pasaron a llamarse *Nectria haematococca* y *Gibberella fujikuroi*, respectivamente. La costumbre de asignar al hongo “imperfecto” un género transitorio en espera de que el investigador pueda observar las estructuras desarrolladas en el ciclo sexual solo han causado confusión a la comunidad científica, y no ha supuesto ninguna ventaja desde el punto de vista taxonómico.

Un caso particularmente confuso, aunque en sentido contrario, lo constituye la especie “perfecta” *Gibberella fujikuroi*, usada para determinar diferentes especies fértiles de *Fusarium* aunque no fueran capaces de cruzar entre sí. *Gibberella fujikuroi* es un grupo de hongos haplontes y normalmente heterotálicos, nombre que se aplica a las especies o variedades en las que los sexos están separados en individuos diferentes. Por el contrario, se habla de hongos homotálicos cuando los dos sexos se encuentran en el mismo individuo (hermafroditismo). En *Gibberella fujikuroi* los dos tipos sexuales se denominan (+) y (-), lo que depende a su vez, de la presencia de dos alelos diferentes de los *loci* MAT-1 y MAT-2 (Steenkamp et al., 2000). En función de la capacidad de cruzar, se han incluido en esta especie hasta nueve grupos de cruzamiento, nombrados por una letra desde la A a la I (Tabla A2). El concepto de esta especie ha ido evolucionando en la dirección de considerar cada grupo de cruzamiento como una especie diferente, por lo que en la literatura se

<b>División</b>	<i>Ascomycota</i>
<b>Clase</b>	<i>Euascomycetes</i>
<b>Orden</b>	<i>Hypocreales</i>
<b>Familia</b>	<i>Hypocreaceae</i>
<b>Género</b>	<i>Fusarium</i>
<b>Especies</b>	<i>F. oxysporum</i> , <i>F. solani</i> , <i>F. verticilloides</i> , <i>F. fujikuroi</i> , <i>F. chlamydosporum</i> , etc.

**Tabla II.** Clasificación filogenética del género *Fusarium*.

refieren a ella habitualmente como “species complex” o complejo de especies. Paradójicamente, el error de su denominación compartida se ha corregido usando para cada grupo de cruzamiento el nombre de la especie de *Fusarium* anteriormente “imperfecta” (Tabla A2). La separación actual en nueve especies ha sido confirmada posteriormente por datos moleculares (Nirenberg y O'Donnell 1998, Steenkamp et al., 2000). La especie utilizada en esta Tesis corresponde al grupo de cruzamiento C del complejo, denominada *Fusarium fujikuroi*.

Cada una de las especies del género *Fusarium* parasita preferentemente una planta (Kuhlman, 1983; Voigt et al., 1995; Leslie y Klein, 1996). Algunas especies nunca se han conseguido cruzar en el laboratorio y por tanto se libraron de la confusión taxonómica. Tal es el caso del anamorfo *Fusarium oxysporum*, que incluye variedades (“*forma specialis*”) especializadas en patogenizar diferentes plantas. Así, por ejemplo, las “*forma specialis*” *lycopersici* o *phaseoli* infectan específicamente las plantas del tomate o la judía, respectivamente. Sin embargo, otros teleomorfos son homotáticos a pesar de que presentan los dos alelos de los genes MAT, como es el caso de *Gibberella zeae* (Kerényi et al., 2004).

Ocasionalmente las especies del género *Fusarium* causan infecciones en la especie humana (queratitis, onicomiosis, etc.). Éstas son infrecuentes y poco peligrosas en individuos sanos, pero son más comunes y pueden tener consecuencias más graves en pacientes inmunodeprimidos (Austwick, 1984). La plaga del sida, que azota la humanidad en las últimas décadas, ha elevado la importancia del problema y el interés de su estudio. Las infecciones provocadas por el género *Fusarium* se incluyen dentro de las hialohifomicosis, o infecciones por hongos oportunistas que presentan hifas hialinas septadas, e incluyen queratomycosis, úlceras y onicomycosis (Guarro y Gené, 1995). Su amplia distribución se atribuye a su versatilidad metabólica, que le permite crecer en muy diferentes sustratos, y a su eficaz mecanismo de dispersión. El viento y la lluvia juegan un importante papel en su diseminación; se ha demostrado que el aire puede llevar las esporas hasta 400 km de distancia.

Grupo de cruzamiento	Especie	Referencia	Referencia anterior
A	<i>verticillioides</i>	O'Donnell et al 1998	Wineland, 1924
B	<i>sacchari</i>	“	Nelson et al., 1983
C	<i>fujikuroi</i>	“	Nirenberg, 1976
D	<i>proliferatum</i>	“	Kuhlman, 1982
E	<i>subglutinans</i>	“	Nelson et al., 1983
F	<i>thapsicum</i>	“	Klittich et al., 1997
G	<i>nygamai</i>	“	Klaasen y Nelson, 1996
H	<i>circinatum</i>	Britz et al., 1999	
I	<i>konzum</i>	Zeller et al., 2003	

**Tabla 12** Especies de *Fusarium* pertenecientes al “complejo *Gibberella fujikuroi*”, dentro del cual constituyen el grupo de cruzamiento indicado. En la tercera columna, se indican las referencias donde se definió su nombre como especie y en la cuarta columna referencias anteriores a su nombramiento como especie independiente.

### 1.2.2 Ciclo de vida de *Fusarium*

*Fusarium* se reproduce asexualmente mediante la formación de esporas denominadas conidios (Fig. 11). Se distinguen dos tipos de conidios: los microconidios, pequeños, fusiformes y uninucleados (Avalos et al., 1985), y los macroconidios, más grandes, arqueados, tabicados y presumiblemente multinucleados (Kuhlman, 1983). Muchas especies producen en condiciones desfavorables, como el calor o la sequía, formas especiales de resistencia esféricas y de pared muy gruesa, llamadas clamidosporas.

En su ciclo patogénico, *Fusarium* comienza generalmente la infección por la raíz, posiblemente a partir de clamidosporas presentes en el suelo, o bien por las anteras de las flores, a partir de conidios dispersados por el viento. Se produce entonces una invasión del micelio por el interior de la planta, generalmente en Primavera. La invasión del micelio es potenciada por el estrés hídrico asociado a la llegada del verano y culmina con la infección del grano o su dispersión en forma de conidios a través del viento. Aunque no es frecuente observarlo en la naturaleza, en ocasiones se desarrollan peritecios, estructuras sexuales que alojan los productos meióticos encerrados en ascas. En *Fusarium* las ascas contienen tétradas con cuatro ascosporas desordenadas. En el laboratorio se puede reproducir el ciclo sexual entre estirpes compatibles cultivándolas en un medio adecuado (Sidhu, 1983a; Klittich y Leslie, 1988).

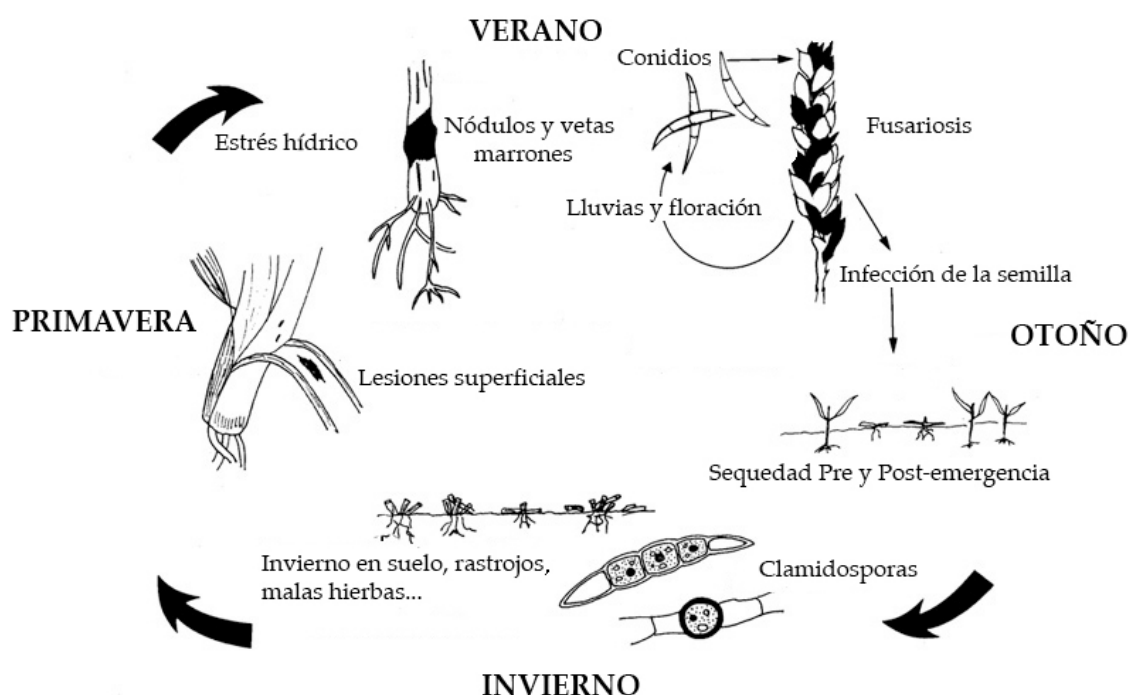


**Fig. 11.** Ciclo de vida de *Fusarium*

También se obtienen con facilidad en algunas especies heterocariontes por anastomosis espontánea de hifas de estirpes genéticamente diferentes (Ming et al., 1966; Correll et al., 1987; Adams et al., 1987) o, de forma más elaborada, mediante fusión de protoplastos (Adams et al., 1987). Sin embargo, los heterocariontes a menudo no se pueden formar a causa de fenómenos de incompatibilidad vegetativa entre estirpes diferentes (Puhalla y Spieth, 1983; 1985), o de autoincompatibilidad en el caso de mutantes derivados de una misma estirpe parental (Correll et al., 1989).

Los conidios dispersados y las clamidosporas se acumulan en el suelo, malas hierbas o rastrojos y son el inóculo para la siguiente estación. Cuando las condiciones de humedad y temperatura son propicias, durante la primavera, se produce de nuevo la infección de la planta y se cierra el ciclo. Eventualmente los conidios se encuentran en el interior del grano proveniente de una planta infectada, y si se usa para la cosecha siguiente puede provocar la infección de la plántula. En ese caso, los síntomas son tempranos y la enfermedad, denominada entonces "tizón de la plántula", produce debilitamiento o muerte prematura de la misma (Fig. 11).

Al contrario que la mayoría de las especies de *Fusarium*, *F. fujikuroi* produce prácticamente solo microconidios. Esta característica representa una ventaja metodológica, ya que los microconidios poseen un solo núcleo y facilitan el aislamiento de estirpes con mutaciones recesivas (Avalos et al., 1985). Como consecuencia, su exposición a diversos agentes mutagénicos, físicos o químicos, produce elevadas tasas de mutación (Puhalla y Spieth, 1983; Avalos et al., 1985). En esta Tesis se ha utilizado solo una estirpe de

*Fusarium fujikuroi* denominada *FKMC1995*, de sexo (-) y vegetativamente autocompatible.

### 1.2.3 Ciclo infectivo de *Fusarium fujikuroi*

Como ya se ha mencionado, cada especie del género *Fusarium* infecta de forma preferente una especie vegetal. En el caso de *F. fujikuroi* esa planta es el arroz (Desjardins et al., 2000). La enfermedad que provoca en sus cultivos se conoce desde antiguo en Japón como *bakanae* o “planta loca”. Debido a la forma de siembra del arroz, la infección se produce principalmente a través de la semilla, transcurriendo al menos un mes hasta que empiezan a manifestarse externamente los síntomas. Estos son fácilmente reconocibles por la mayor altura y delgadez de las plantas infectadas, que muestran además síntomas de clorosis. La mayor altura es consecuencia de una elongación anómala del tallo debida a que el hongo produce giberelinas, hormonas vegetales inductoras del crecimiento. La elongación del tallo es tal y su grosor tan fino que generalmente acaba quebrándose. La infección continúa habitualmente hasta la muerte de la planta. En ocasiones consigue sobrevivir y formar panículas, pero vacías de semillas. La fácil propagación de la enfermedad llega a causar pérdidas considerables en las cosechas, motivo del inicio del estudio de este organismo en Japón en la primera mitad del siglo XX (Hori, 1989). Cuando las plantas enfermas entran en senescencia, el micelio del hongo emerge entre sus nódulos por encima del nivel del agua y produce conidios, ocurriendo también en niveles más bajos del tallo cuando se drena el arrozal. Las esporas producidas contaminan la superficie de las semillas sanas durante la cosecha, lo que las inutiliza para el consumo humano. Las esporas pueden aguantar hasta la siguiente cosecha tanto en el suelo como en la semilla facilitando así el siguiente ciclo de infección incluso en campos previamente no infectados.

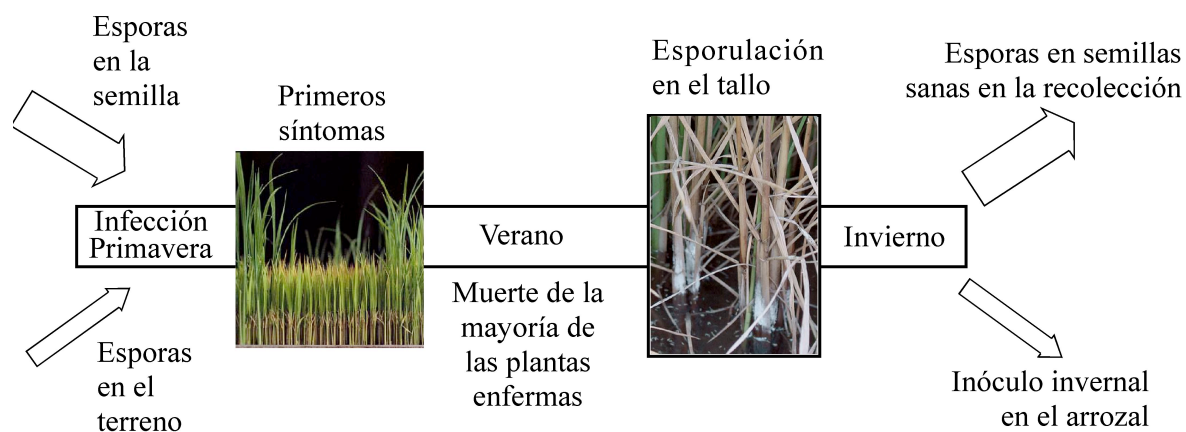


**Fig. 12.** Ciclo de infección de *Fusarium fujikuroi* en el arroz.

Como ya se ha mencionado, en ocasiones pueden encontrarse dos estirpes de sexo compatible y formar peritecios, cuyas ascosporas sirven también como inóculo para una nueva infección (Fig. I2).

### 1.3 Descripción y ciclo de vida de *N. crassa*

#### 1.3.1 Características generales

*N. crassa* es un hongo filamentoso heterotálico perteneciente a la clase Ascomycetes. Como *Fusarium*, produce peritecios con productos meióticos encerrados en sacos membranosos llamados ascas, pero en este caso las ascosporas están ordenadas. Este hecho, y la fácil reproducción de su ciclo sexual en el laboratorio, hacen de este hongo un excelente modelo genético. *N. crassa* no es un hongo patógeno, y se encuentra en la naturaleza en áreas húmedas tropicales y subtropicales (Turner et al., 2001), aunque



**Fig. I3.** *Neurospora* creciendo sobre la corteza de un árbol quemado.

esporádicamente también se ha observado en regiones templadas del noroeste de América y en el sur de Europa (Jacobson et al., 2006). Tras un incendio, este hongo es uno de los primeros colonizadores de la vegetación arrasada (Fig. I3). Este hecho indica un versátil metabolismo degradativo que incluye enzimas líticas como las celulasas, que facilitan su crecimiento sobre la madera quemada (Fig. I3).

#### 1.3.2 Ciclo de vida de *N. crassa*.

Como *Fusarium*, *N. crassa* es un hongo filamentoso que crece en forma de células cilíndricas de crecimiento apical, denominadas hifas, que se ramifican, y forman un denso entramado o red denominado micelio. Las hifas son tabicadas y multinucleadas y sus núcleos son haploides. Los tabiques presentan poros que permiten el paso de macromoléculas entre los compartimentos vecinos, y probablemente también de orgánulos, incluyendo los núcleos (Lew, 2005).

El ciclo de vida de *N. crassa* posee una fase asexual y otra sexual. La exposición al aire, aún más en condiciones de escasez de nutrientes, inducen la formación de esporas asexuales o macroconidios (Fig. I4). Este proceso se inicia con la formación de estrangulamientos en las hifas aéreas que posteriormente se cierran formando cadenas de células independientes o macroconidios, cada uno de ellos con varios núcleos. Estas esporas, que se producen en enorme número, son estructuras de resistencia que pueden



durar varios años (Springer, 1993). La acumulación de carotenoides (ver sección 3.2.3) en las esporas le confiere al micelio aéreo de *N. crassa* un característico color anaranjado. Las esporas están adaptadas para su inmediata dispersión aérea, ya que se liberan con facilidad. Como consecuencia los investigadores deben adoptar precauciones especiales en su manipulación en el laboratorio. Así, este hongo suele incubarse en tubos de agar inclinado cerrados con algodón, ya que la falta de hermeticidad de las cajas de Petri no impide la salida de las esporas. Las grandes masas de macroconidios producidas en la superficie de los cultivos de *N. crassa*, formando largos rosarios, confiere un típico aspecto polvoriento a la superficie de este hongo.

*N. crassa* produce también microconidios, más pequeños y uninucleados, formados asexualmente dentro de la hifa vegetativa y liberados al medio tras la rotura de su pared celular (Lowry et al., 1967). Estas esporas son de color marrón grisáceo y muestran una baja tasa de germinación. Se ha propuesto que funcionan como elementos fertilizadores masculinos en los cruzamientos (Dodge et al., 1948), aunque este papel también ya es llevado a cabo por los macroconidios.

El ciclo sexual de *N. crassa* (Fig. I4) requiere la presencia de dos estirpes de distinto sexo. El tipo sexual está determinado por formas alternativas de una región genéticamente compleja, denominadas *mat A* y *mat a* para cada sexo (Glass et al., 1988). En condiciones de hambre de nitrógeno o carbono, algunas de las hifas vegetativas pueden iniciar el ciclo sexual (Westergaard y Hirsch, 1954). El proceso empieza con la acumulación de hifas entrelazadas en distintos lugares para formar los protoperitecios, que rodean a unas células especializadas que forman la ascogonia. Los protoperitecios producen otro tipos de hifas especializadas denominadas tricóginas, las cuales reconocen el conidio de distinto tipo sexual mediante señales hormonales (Bistis, 1996). El reconocimiento entre dos estirpes de sexo opuesto (*A* y *a*) de lugar a la fusión de la hifa tricógina con el conidio y a la migración de uno de los núcleos de éste a través de la hifa hasta la ascogonia. La pared del protoperitecio se desarrolla y pasa a llamarse peritecio, donde se desarrollan los primordios de las futuras ascas o “crozier”. Los núcleos de ambos sexos se dividen varias veces y posteriormente dos núcleos de sexo opuesto se unen para generar un núcleo diploide. Tras multiplicarse por mitosis, cada núcleo diploide sufre meiosis y genera una tétrada ordenada. Los cuatro productos meióticos se dividen una vez más por mitosis generando un asca con ocho ascosporas (Raju, 1980). Cada peritecio puede formar hasta 400 ascas.

El aumento de la presión osmótica dentro del asca provoca una explosión, liberándose las ascosporas maduras, que son disparadas al exterior por una apertura en el protoperitecio. Las ascosporas son muy resistentes al calor, y su germinación es activada por choque térmico, cualidad posiblemente desarrollada evolutivamente como adaptación para la colonización de la materia vegetal tras los incendios. La germinación de la ascospora regenera el micelio vegetativo y cierra su ciclo (Springer, 1993). Este ciclo

sexual muestra variaciones entre distintas especies de *N. crassa*. Algunas especies son homotáticas y carecen de conidios (Dutta et al., 1976; Dutta, 1976) y una especie, *N. crassa tetrasperma*, es pseudohomotática, conteniendo sus micelios núcleos de los dos tipos sexuales (Raju y Leslie, 1992).

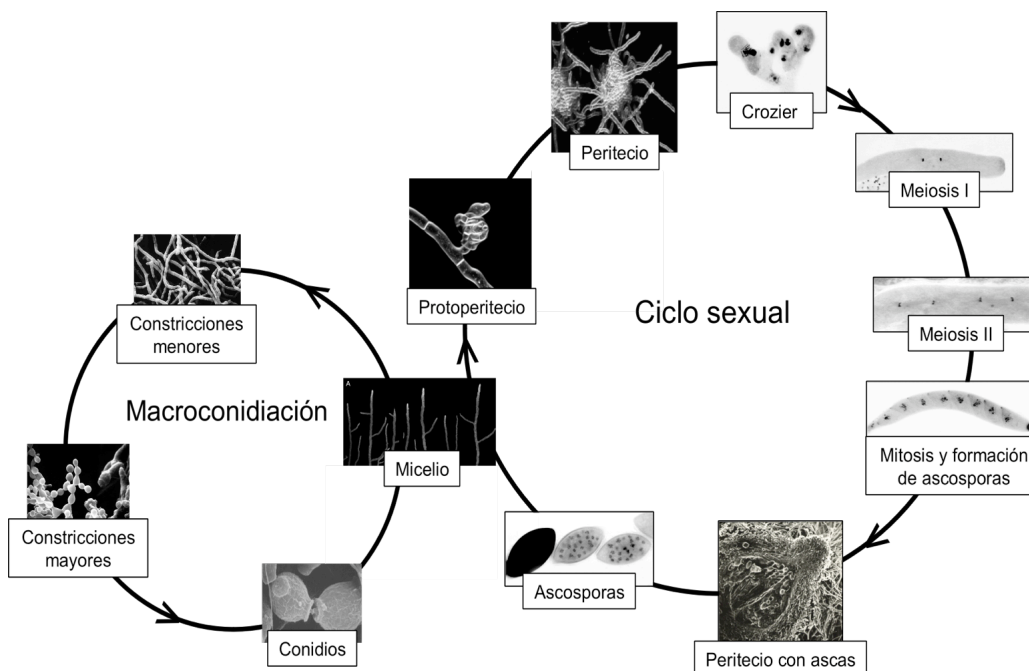


**Fig. 14.** Ciclo de vida de *N. crassa*. (Imágenes de N.B. Raju, M. Springer y N. Read).

### 1.3.3 *N. crassa* como organismo modelo.

*N. crassa* se conoce desde 1843, cuando se encontró como contaminante en la industria panadera y posteriormente también en la naturaleza en las masas vegetales devastadas por los incendios. Originalmente denominado *Monilia sitophila*, no fue hasta principios del siglo XX cuando se observaron por primera vez sus estructuras sexuales y se renombró como *N. crassa* (Shear y Dodge, 1927). Una vez identificados los dos tipos sexuales, se iniciaron los estudios de las segregaciones mendelianas de sus productos meióticos. Su sencillo cultivo en el laboratorio y la facilidad para obtener mutantes a partir de sus conidios, producidas en abundancia por su micelio aéreo, potenció el uso experimental de este hongo como modelo genético. En 1941 Beadle y Tatum, estudiando por primera vez rutas metabólicas utilizando mutantes nutricionales de *N. crassa*, y demostraron que los genes controlan los procesos fundamentales de la vida, que les llevó a proponer su hipótesis de “un gen una enzima” (Beadle y Tatum, 1941). La gran cantidad de información generada por el uso de este hongo como material de estudio ha dado lugar a diferentes revisiones y libros, entre los que destaca un completo compendio genético

(Perkins et al., 2001). Resultado de la interacción entre los distintos grupos de investigación de *N. crassa*, mayoritariamente estadounidenses, surgió el *Fungal Genetics Stock Center* (<http://www.fgsc.net/>), institución que centraliza, organiza y distribuye los datos y materiales generados, incluyendo una vasta colección de mutantes, vectores y genotecas. Una consecuencia de la actividad de esta institución es el *Fungal Genetics Newsletter* (<http://www.fgsc.net/newslet.html>), concebido como un boletín interno de publicación rápida de resultados, complementario a las publicaciones tradicionales. De esta forma, gran cantidad de resultados experimentales laterales que habitualmente se acaban perdiendo almacenados en un archivador han estado a disposición de esta dinámica comunidad de investigadores. El FGSC ha extendido más recientemente su actividad a otros hongos y a la información proporcionada por la secuenciación de sus genomas, y centraliza también las convocatorias de los congresos especializados.

El potencial experimental de *N. crassa* compite con éxito en algunos aspectos con el microorganismo líder en la genética molecular de los eucariotas, la levadura *Saccharomyces cerevisiae*. Su mayor sencillez en comparación con los hongos filamentosos hace de ella un objeto de trabajo inútil en algunas áreas de investigación, como por ejemplo la fotobiología, aspecto en el que como se verá más adelante, *N. crassa* muestra una notable complejidad. Es precisamente su utilización para investigar problemas inabordables con *S. cerevisiae* lo que ha justificado los esfuerzos dedicados a este hongo en las últimas décadas.

*N. crassa* fue el primer hongo en ser transformado con ADN exógeno (Mishra y Tatum, 1973), incluso antes que *S. cerevisiae*, y el primer hongo filamentosos en ser transformado con ADN plasmídico (Case et al., 1979), en ambos casos mediante la obtención de protoplastos competentes. Los elevados números de transformantes producidos permiten la clonación de genes mediante transformación con genotecas (Vollmer y Yanofsky, 1986). Se obtienen transformantes también por otros métodos, como la electroporación (Chakraborty et al., 1991), la transferencia desde *Agrobacterium tumefaciens* (de Groot et al., 1998) o la biobalística (Armaleo et al., 1990). La facilidad de su transformación se debe a la eficacia de sus mecanismos de recombinación no homóloga, cuyos genes responsables fueron recientemente identificados (Ishibashi et al., 2006; Watanabe et al., 1997).

Estas facilidades experimentales han sido explotadas para investigar diferentes procesos, algunos de ellos descubiertos en este organismo. Destacan los mecanismos de inactivación génica de secuencias duplicadas por metilación del ADN ("RIP", Galagan y Selker, 2004) o por silenciamiento génico post-transcripcional (Romano y Macino, 1992), así como los mecanismos de reparación del ADN (Davis, 2000; Sato et al., 2008). Actualmente *N. crassa* es un organismo extensamente utilizado para estudios de fotobiología y ritmo circadiano (Dunlap et al., 2007b), así como modelo de desarrollo y

diferenciación celular (Banno et al., 2005, Cano-Domínguez et al., 2008). Aunque no patógeno, también se ha usado como modelo de patogénesis para otros hongos donde las herramientas de biología molecular no estaban desarrolladas (Sweigard y Ebbole, 2001). Se dispone además de una extensa colección de estirpes naturales provenientes de todo el mundo (proyecto liderado por el Dr. David Perkins y en la actualidad por el Dr. David Jacobson).

La mayor complejidad de un hongo filamentoso como *N. crassa* frente a *S. cerevisiae* queda reflejada en el mayor tamaño de su genoma (39 Mb frente a los 11 Mb de la levadura) y su mayor número de genes (unos 10.000 frente a aproximadamente 5.800). Muchos de ellos han sido localizado por recombinación en sus siete cromosomas, para los que se ha elaborado un completo mapa genético. La disponibilidad de esta información, resultado de la integración de resultados de numerosos laboratorios durante décadas de trabajo, ha facilitado posteriormente la identificación y clonación de muchos genes, especialmente tras la secuenciación del genoma, el primero disponible en un hongo filamentoso (Galagan et al., 2003). El análisis del genoma y la correspondiente anotación de sus genes ha proporcionado información muy valiosa a los investigadores, accesible a través de un servidor del Broad Institute ( <http://www.broad.mit.edu/annotation/genome/N.crassa/home.html>).

Actualmente se lleva a cabo un programa de mutación dirigida de todos sus genes, próximo a su culminación, sacando provecho de las herramientas disponibles para generación de mutantes nulos. Los experimentos de reemplazamiento génico por transformación, tradicionalmente dificultados en este hongo por la alta frecuencia de recombinación no homóloga (80%), han sido facilitados enormemente por la utilización de mutantes de los genes *mus-51* o *mus-52*, homólogos de genes de mamífero responsables de la unión inespecífica de extremos de ADN generados por roturas de doble cadena (Ninomiya et al., 2004). En estos mutantes, la frecuencia de recombinación homóloga alcanza el 100%. Además de la disponibilidad de mutantes de cualquiera de sus genes, limitado únicamente por que sean viables, están disponibles numerosos datos sobre su expresión génica provenientes de análisis de “microarrays” de muestras de ARN procedentes de diferentes condiciones de crecimiento, estadios de desarrollo y fondos genéticos (Dunlap et al., 2007). La información generada se centraliza también en una página del FGSC dedicada exclusivamente a este hongo (<http://www.fgsc.net/N.crassa/N.crassa.html>) y ha dado lugar a diversas revisiones (Borkovich et al., 2004; Davis, 2000; Davis y Perkins, 2002; Perkins y Davis, 2000).

### 1.3.4 *N. crassa* como modelo de silenciamiento génico

Una de las vanguardias de la Genética molecular actual la constituye el estudio de los mecanismos de inactivación génica mediante ARN, utilizados tanto para regulación de la expresión génica (miRNA) como para protección frente a duplicaciones génicas o invasión de ADN exógeno (siRNA). *N. crassa* es un hongo pionero en la investigación de uno de estos mecanismos, conocido como “quelling” (Romano y Macino, 1992). El proceso tiene lugar en micelio vegetativo, y consiste en la identificación del ARN expresado a partir de genes duplicados mediante la formación de estructuras secundarias reconocidas por una helicasa de ADN denominada QDE-3 (Cogoni y Macino, 1999a). Esto dispara un proceso complejo en el que interviene una polimerasa dependiente de ARN (QDE-1, Cogoni y Macino, 1999b) y dos ribonucleasas de tipo DICER (DCL-1 y DCL-2). Estas enzimas que generan moléculas de ARN de pequeño tamaño (siRNAs, de “small interference RNAs” Catalanotto et al., 2004) usadas como molde para reconocer el ARN duplicado y formar segmentos bicatenarios, los cuales son degradados por un complejo multiprotéico llamado RISC (“**R**NA-**I**nduced **S**ilencing **C**omplex”). Al contrario que el proceso RIP, este mecanismo no produce a menudo el silenciamiento total del gen diana, lo que hace de ésta una útil herramienta para analizar el fenotipo de la inactivación parcial de genes cuyo pérdida completa sería inviable para el hongo.

Además, *N. crassa* posee otros dos mecanismos de silenciamiento, esta vez a nivel de ADN. Así, el mecanismo RIP (“**R**epet-**I**nduced **P**oint mutation”, Selker, 1990) consiste en la detección e inactivación de secuencias duplicadas durante la fase haploide dicariótica de la reproducción sexual. Para que el proceso se ponga en marcha es suficiente con que el segmento duplicado alcance los 400 pb (Watters et al., 1999) y que al menos coincidan el 80% de las bases (Cambareri et al., 1991). El mecanismo produce hipermetilación de las dos secuencias repetidas y numerosas mutaciones GC→TA (Cambareri et al., 1989). Este proceso ha sido profusamente utilizado como método de mutagénesis dirigida, consistente en introducir una copia extra del gen diana por transformación, cruzar el transformante con una estirpe silvestre de sexo contrario e identificar sus mutantes RIP en la descendencia. Las ventajas evolutivas de este mecanismo no son claras, ya que teóricamente limita la capacidad del genoma para tolerar duplicaciones génicas que faciliten la aparición de nuevas funciones génicas (Galagan y Selker, 2004). El sesgo mutacional del proceso permite identificar en el genoma numerosas reliquias de duplicaciones ancestrales inactivadas.

Por último, *N. crassa* posee otro mecanismo de silenciamiento meiótico generado por ADN no apareado (MSUD, “**M**eiotic **S**ilencing by **U**npaired **D**NA”), un proceso que tiene lugar después de la cariogamia. Cuando no se detecta una secuencia de ADN en el cromosoma opuesto, la región que no aparea desencadena una señal que es capaz de

inactivar todas las secuencias homólogas en el genoma (Shiu et al., 2001).

## 1.4 Descripción y ciclo de vida de *Ustilago maydis*

### 1.4.1 Características generales de *U. maydis*.

Entre la gran diversidad de enfermedades vegetales causadas por hongos figuran los denominados carbones, originadas por basidiomicetos del orden Ustilaginales y que están distribuidos por todo el mundo afectando a muchas especies de plantas de interés económico, principalmente cereales. Generalmente no son especies de gran espectro infectivo, y cada especie se limita a un estrecho rango de plantas. Sin embargo, existen más de 1.100 especies diferentes de este orden, cuya actividad patogénica en conjunto representa un problema económico importante (Agrios, 2005).

*U. maydis* es el agente responsable del carbón del maíz (Banuett, 1995; Kahmann et al., 1999). A diferencia de *Fusarium* o *N. crassa*, hongos ascomicetos miceliales, *U. maydis* es un hongo basidiomiceto, dimórfico (levadura / micelio) y con un ciclo sexual dependiente de la planta que infecta. Su ciclo de vida consta de una fase haploide, saprofítica, en la que crece como levadura dividiéndose por gemación (Fig. I6), y otra fase dicarionte, que solo se da en el interior de la planta, en la que crece como micelio (Banuett 1992). La fase dicarionte se inicia con el encuentro ocasional de dos células de sexo contrario, que se reconocen mediante un sistema de señalización feromona-receptor. Cada célula responde formando un filamento o tubo de conjugación que crece a favor de gradiente de feromona hasta establecer contacto físico (Fig. I6) (Snetselaar et al., 1996). Las dos hifas sexualmente compatibles se fusionan formando un único citoplasma dicarionte que mantiene un crecimiento polar filamentoso. La hifa así formada, llamado filamento infectivo (Fig. I6) (Fischer y Holton, 1957), mantienen el ciclo mitótico de sus núcleos detenidos en fase G2 (García-Muse et al, 2004), independientemente de la longitud que alcance. Este estado se mantiene hasta que el filamento entra en contacto con la planta. El resto de su ciclo de vida tiene lugar en íntima interacción con la planta del maíz, en donde lleva a cabo el proceso infectivo. El peculiar *modus operandi* de *Ustilago* para iniciar la infección, incluyendo su parada del ciclo celular, ha sido objeto de estudio detallado (Martínez-Espinoza et al. 2002; Flor-Parra et al., 2006; Nadal et al., 2008) y han hecho de este hongo un sistema biológico cada vez más empleado en investigación. Su manejo en el laboratorio tiene ventajas, ya que crece rápido en comparación con otros hongos y se han desarrollado todas las técnicas básicas para su manipulación genética. El estudio de la patogénesis en *U. maydis* ha hecho posible entender los mecanismos en otros hongos patógenos y ha permitido el diseño de estrategias de biocontrol contra infecciones (Martínez-Espinoza et al. 2002).

### 1.4.2 Ciclo infectivo de *U. maydis*

En el proceso previo a la infección es determinante la capacidad de la hifa dicarionte formada para crecer de forma polarizada sobre la superficie de la planta hasta encontrar un lugar de penetración. Los mecanismos de entrada a la planta son diversos y diferentes especies de *Ustilago* utilizan estrategias distintas de invasión. Algunas entran por heridas producidas en la planta, bien por accidentes naturales, bien por la acción de insectos u otros animales, incluyendo el hombre (por ejemplo, talas y podas). Otras entran por aberturas naturales, como son los estomas. En ocasiones, la vía de acceso de estos patógenos es la raíz, ya que esta menos expuesta a la desecación y posee un menor número de capas de tejidos a través de las cuales permear el agua y otro nutrientes. Al margen de las posibilidades que pueden brindar las heridas o las aberturas naturales de las plantas, muchos hongos han diseñado estrategias activas de penetración. Este es el caso de los hongos que forman apresorios, estructuras diferenciadas generadas sobre la superficie de la planta con el objetivo de superar sus barreras de entrada (Deising et al., 2000). Estas estructuras han sido especialmente estudiadas en *Magnaporthe grisea*, y en las especies de *Colletotrichum* (Fig. I5). Son estructuras ensanchadas, separadas del tubo germinal por un septo, que se adhieren a la superficie y destruyen la cutícula por presión, permitiendo el acceso al interior de la planta (Mendgen et al., 1996; Talbot, 2003). *U. maydis* genera apresorios menos desarrollados, consistentes en un engrosamiento del extremo de la hifa infectiva (Snetselaar y Mims, 1992, 1993). Aunque se desconoce exactamente el mecanismo de penetración, se cree que en lugar de ejercer fuerza física, localiza un lugar idóneo para la degradación de la cutícula mediante la secreción de enzimas (Gold et al., 2001). El desarrollo del apresorio conlleva el control de la progresión del ciclo celular, la regulación del crecimiento y la reorganización del citoesqueleto, que da lugar a los cambios morfológicos.

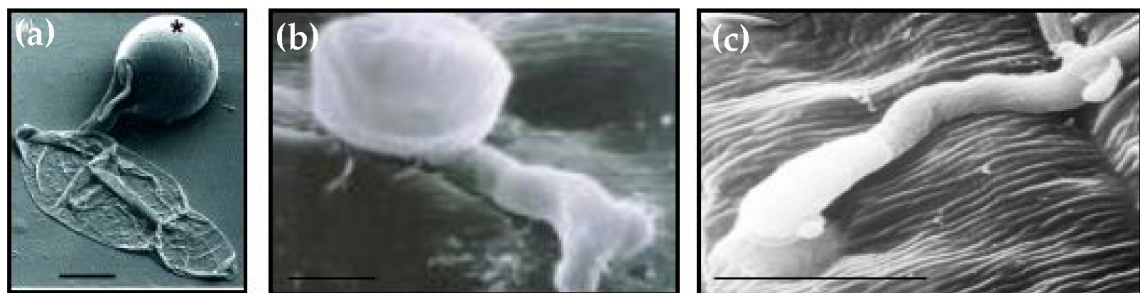


**Fig. I5.** Apresorios de *Magnaporthe grisea* (a), *Colletotrichum graminearum* (b) y *U. maydis* (c).

Una vez vulnerada la protección de la planta y abierto un camino de entrada, el hongo establece un nuevo eje de polaridad para la formación de la hifa que penetrará en el tejido vegetal (Fig. I5). Tras la penetración, se reactiva el ciclo celular supuestamente en respuesta a señales presentes en el interior de la planta, y se desarrolla un micelio multicelular dicarionte. Este altera la fisiología de la planta e induce la formación de tumores (Fig. I6) (Snetselaar y Mims 1993, Banuett y Herskowitz, 1996), en los que crecerá hasta diferenciar las estructuras de resistencia y dispersión denominadas teliosporas, cuyo color negro es responsable del nombre genérico de carbón con el que se conoce la enfermedad (Fig. I6). Las esporas germinarán haciendo meiosis (Fig. I6) y dando como resultado la aparición de cuatro esporidios haploides que crecerán en el medio en forma levaduriforme (Fig. I6) cerrando así el ciclo de vida de este hongo.

Durante las diferentes etapas del proceso tiene lugar una amplia reorganización del organismo a nivel celular, con cambios muy bien definidos de su ciclo de división. De esta forma, los mecanismos que controlan el ciclo celular juegan un papel clave en el desarrollo y en la capacidad infectiva de *U. maydis*, de manera que podemos considerar genes de virulencia a aquellos que controlan el ciclo, antes, durante y después de la infección, siendo por tanto un importante factor a tener en cuenta para controlar su patogénesis.

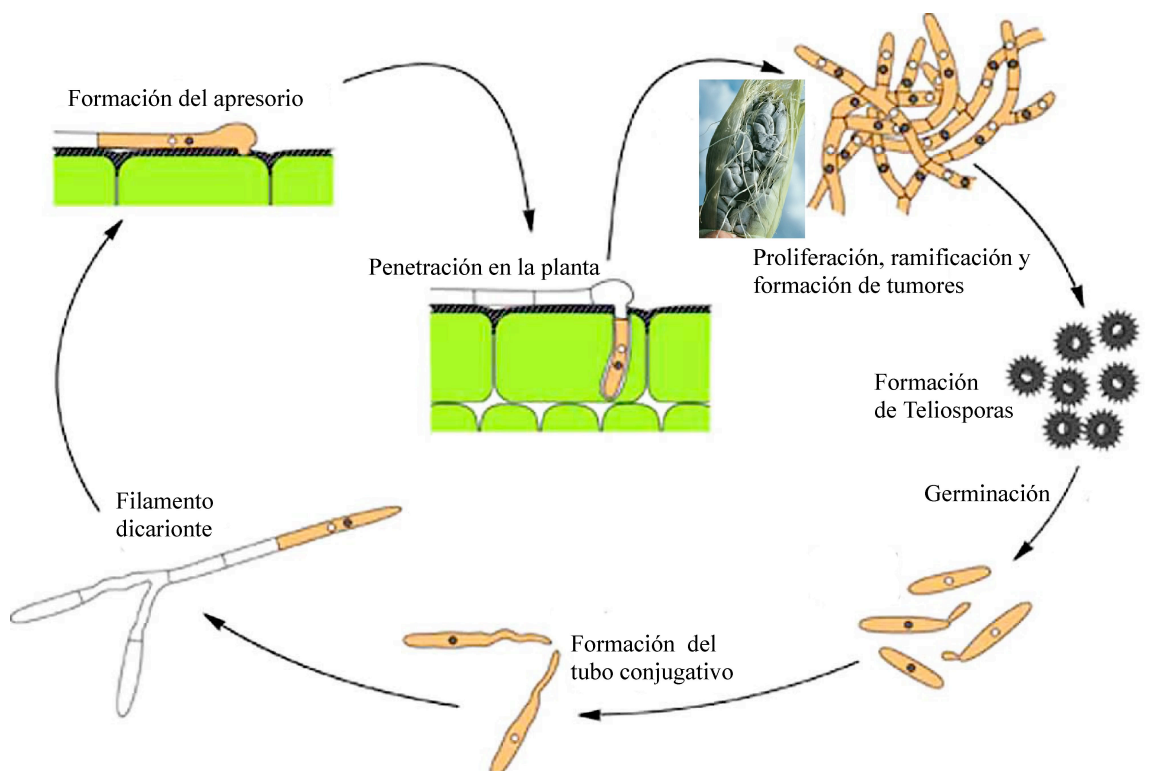


**Fig. I6.** Ciclo de vida de *Ustilago maydis*

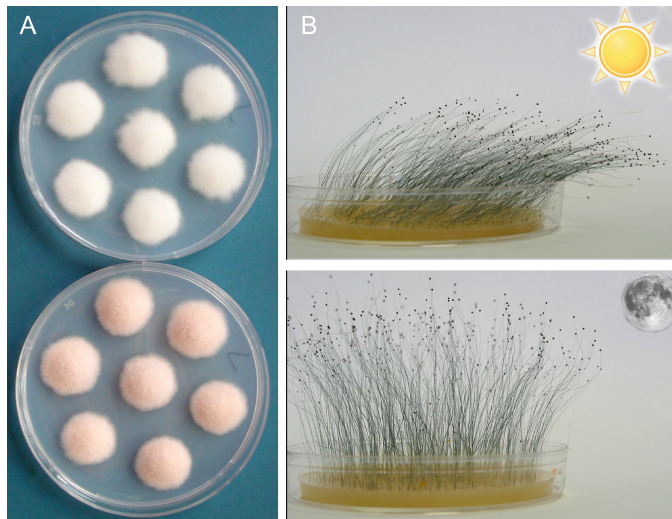


## 2. Fotorreceptores.

Los seres vivos poseen sistemas para detectar y procesar la información que les llega de su entorno. Una de las señales más universalmente utilizadas es la luz. Esta no solo cumple el papel de estímulo o fuente externa de información, sino que además es esencial como fuente de energía, imprescindible para el sostenimiento de la vida en la biosfera. Las plantas perciben la calidad, intensidad y dirección de la luz. Para ello usan proteínas (fotorreceptores) capaces de absorber fotones a través de un grupo prostético (cromóforo). Generalmente la luz recibida provoca un cambio conformacional en el fotorreceptor que se traduce en una señal que genera una respuesta en el organismo. En plantas superiores encontramos fotorreceptores que absorben luz roja (fitocromos) y luz azul (criptocromos y fototropinas) (Briggs, 2007; Christie, 2007; Franklin et al., 2007; Li y Yang, 2007).

### 2.1 Fotorrespuestas en hongos.

La mayoría de los hongos poseen también fotorreceptores que median una gran variedad de respuestas (Corrochano, 2007). Algunas se pueden apreciar a simple vista, como por ejemplo la inducción de la síntesis de carotenoides en *F. fujikuroi* o *N. crassa*, donde la acumulación de un apocarotenoide (neurosporaxantina) confiere al micelio una característica pigmentación anaranjada (Fig. I7A) (Linnemannstöns et al. 2002a, Belozerskaia et al. 1982). Otras fotorrespuestas afectan a la estructura y/o desarrollo de las hifas o la conidiación, como ocurre en *N. crassa* o *P. blakesleanus* (Corrochano, 2007). En algunos casos la respuesta es particularmente llamativa, como el fototropismo de las estructuras de reproducción vegetativa de *P. blakesleanus*, conocidas como esporangióforos (Fig. I7B) (Cerdá-Olmedo, 2001; Linden et al., 1997a). La mayor parte de las respuestas conocidas, como los ejemplos citados, responden a la luz azul del espectro, pero se conocen también respuestas a otras longitudes de onda, como la conidiación en *Aspergillus nidulans*, controlada por luz roja como (Mooney y Yager. 1990), o la conidiación en *Alternaria tomato*, regulada por radiación UV de longitud de onda próxima al visible (UV cercano, Kumagai, 1976). Se ha prestado menos atención a las fotorrespuestas a luz verde, aunque se ha observado que ésta afecta a la producción de esporas en los patógenos de plantas *Tricometasphaeria turcica* y *Alternaria solana*, ya sea por sí sola o en interacción con la luz azul (Klein, 1992).

**Fig. 17.**

A. Fotoinducción de la carotenogénesis en *Fusarium fujikuroi*.

B. Fototropismo en *P. blakesleeana*, arriba iluminado con luz azul desde el lateral derecho, abajo en oscuridad.

## 2.2 *N. crassa* como modelo de fotorreceptores en hongos

*N. crassa* ha sido extensamente utilizado como modelo de fotobiología en hongos. La diversidad de sus fotorrespuestas, abarca además de la fotoinducción de la carotenogénesis (Harding y Turner, 1981), ya mencionada, la inducción de la formación de conidios (Lauter et al., 1992; Ninnemann, 1991) y protoperitecios (Innocenti et al., 1983), el fototropismo de los picos periteciales (Degli-Innocenti et al., 1984; Degli-Innocenti y Russo, 1984; Harding y Melles, 1983), la hiperpolarización de la membrana celular, o la sincronización del ritmo circadiano (Russo, 1988; Dunlap, 2006; Vitalini et al., 2006), lo que ha motivado numerosos estudios (revisados en Dunlap et al., 2007b). Estos llevaron al descubrimiento de los primeros fotorreceptores de hongos, anterior a la disponibilidad de su genoma y proteoma. Entre ellos el complejo destaca el complejo White Collar, elemento clave en la mayoría de sus fotorrespuestas y sobre el cual entramos en detalle en la siguiente sección. Además del complejo White Collar, un heterodímero formado por la flavoproteína WC-1 y su pareja, WC-2, *N. crassa* posee genes para otros fotorreceptores predecibles, como otra flavoproteína (VVD Galagan et al., 2003; Borkovich et al., 2004), un criptocromo (CRY), dos fitocromos (PHY-1 y PHY-2) y una opsina (NOP-1) (Fig. 18).

### 2.2.1 Estructura del sistema fotorreceptor WC.

El primer gen de un fotorreceptor identificado en hongos fue *wc-1* en *N. crassa*. Su descubrimiento tuvo su origen en el estudio de mutantes afectados en la fotoinducción de la carotenogénesis (Degli-Innocenti y Russo, 1984), fácilmente distinguible en los cultivos de este hongo en tubos de agar inclinado.

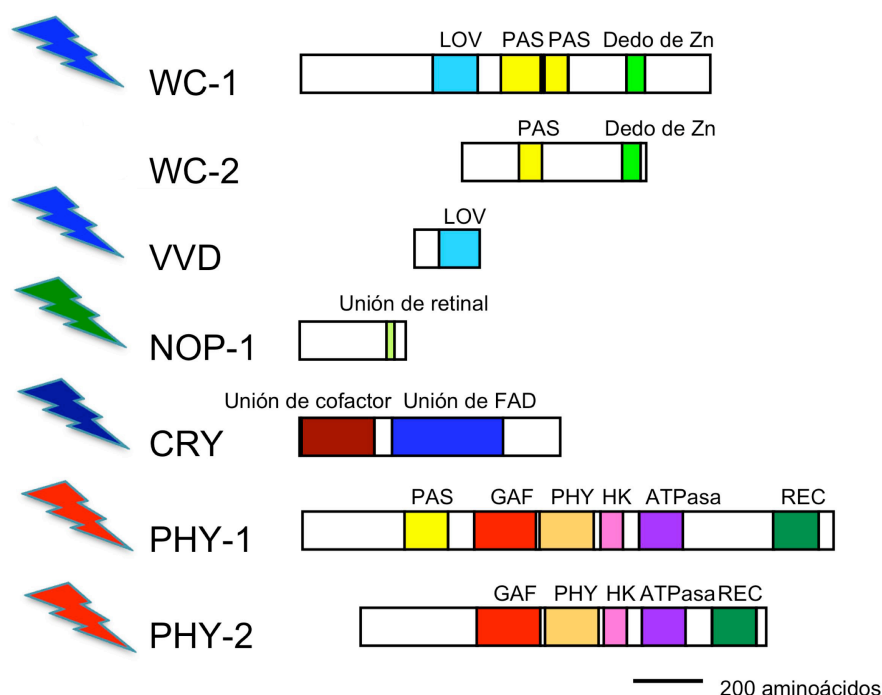


**Fig. 18.** Fotorreceptores de *N. crassa*. WC-1 y VVD poseen dominios LOV, que ligan una flavina responsable de la detección de luz azul. WC-2 no posee cromóforo, pero forma con WC-1 el complejo fotorreceptor WC. Otros fotorreceptores en el genoma de *N. crassa* son la opsina NOP-1, que usa retinal como cromóforo, el criptocromo CRY, que usa flavina, y los fitocromos PHY-1 y PHY-2, que poseen un dominio sensorial en el extremo amino (dominios PAS, GAF y PHY) y un dominio de respuesta (HK, ATPasa y REC).

Su nombre WC (White Collar) se debe al peculiar fenotipo del mutante resultante de la diferente regulación de la carotenogénesis en el micelio y en las esporas. Mientras que en el micelio la síntesis es estrictamente dependiente de la luz, en los conidios se acumulan carotenoides tanto en luz como en oscuridad. En los tubos de agar inclinado se forma una capa de micelio en la base que desarrolla una masa de micelio aéreo dedicada en su gran mayoría a la formación de conidios. El mutante WC presenta la masa aérea pigmentada, mientras que en la base se aprecia un anillo o "collar" albino, dando lugar su denominación. Estos mutantes regulatorios son fácilmente distinguibles de los mutantes albinos alterados en los genes estructurales de la ruta biosintética (*al-1*, *al-2* y *al-3*, ver sección 3.2.3), ya que los conidios en estos mutantes son blancos y por tanto toda la biomasa es albina. Los mutantes *wc* no solo pierden la fotocarotenogénesis sino que además pierden el resto de fotorrespuestas conocidas de este hongo, citadas en la sección anterior, y que aluden a la regulación por luz de la conidiación, el ritmo circadiano, y la formación y comportamiento de los protoperitecios. A pesar de ser mutantes ciegos, no

presentan ninguna alteración en crecimiento, morfología o en genes no regulados por luz.

El análisis genético de los mutantes *wc* dio lugar a la identificación de dos genes, *wc-1* y *wc-2*, cuyas proteínas WC-1 y WC-2 interaccionan formando el complejo WC (Ballario et al., 1998; Talora et al., 1999). El gen *wc-1* posee un promotor complejo, con tres sitios diferentes de inicio de la transcripción (Kaldi et al., 2006). Su marco abierto de lectura determina una proteína, WC-1, de 1167 aminoácidos capaz de unir una molécula de flavina (FAD, *dinucleótido de flavina y adenina*), que actúa como cromóforo y permite que WC-1 funcione como fotorreceptor de luz azul (Froehlich et al., 2002; He et al., 2002).

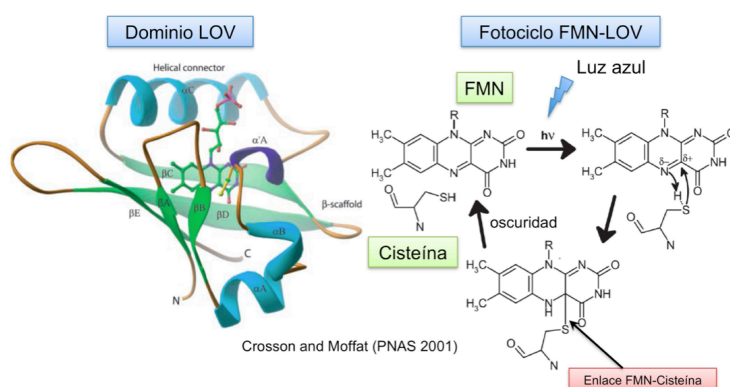


**Fig. 19.** Diagrama de la estructura del dominio LOV representado junto con FMN en el bolsillo interior

En la estructura de la proteína (Fig. 19) destaca el dominio LOV (identificado en proteínas reguladas por **L**uz, **O**xígeno y **V**oltaje) al cual se une una molécula de FAD (Flavin Adenine Dinucleotide) o FMN (Flavin Mononucleotide). El dominio LOV es un tipo especial de dominio PAS (**P**er-**A**rt-**S**im), estudiado en detalle en plantas (Christie et al., 2007). En WC-1 el dominio LOV se denomina PAS-A (Fig. 19), y es uno de los tres dominios PAS de esta proteína. Los otros dos dominios PAS están implicados en interacciones proteína-proteína (PAS-B y PAS-C). El dominio PAS-A/LOV es esencial para la función de WC-1, al igual que ocurre con PAS-B (Cheng et al., 2003), aunque su función no está clara. PAS-C es necesario para la interacción entre WC-1 y WC-2.

La proteína WC-1 posee además un dominio de “dedo de zinc”, implicado en la interacción proteína-ADN, que le confiere la capacidad de unirse a los promotores de sus genes diana (Fig. 18). La unión de WC-1 se lleva a cabo sobre elementos reguladores conservados en los promotores de los genes fotoinducibles, que incluyen una característica secuencia “GATA”, y da lugar a la activación de su transcripción (Ballario et al., 1996; Schwerdtfeger y Linden, 2001). Sin embargo, su acción no se ejerce siempre a través de la unión física a los promotores de sus genes diana: se ha descrito que el dedo de zinc es necesario para el correcto funcionamiento del ritmo circadiano pero no así para la inducción de la carotenogénesis (Cheng et al., 2003). De hecho en algunos hongos, como por ejemplo en *P. blakesleanus*, existen proteínas homólogas a WC-1 que carecen del

dedo de zinc (Idnurm y Heitman, 2005).

La pareja de WC-1, WC-2, es una proteína de 530 aminoácidos que coincide con WC-1 en la presencia de un “dedo de zinc”, pero posee solo un sólo dominio PAS, a través del cual interacciona con WC-1 (Fig. I8) (Linden et al., 1997b; Ballario et al., 1998). La estructura y función de las proteínas WC han sido revisadas recientemente (Dunlap y Loros, 2005; Liu et al., 2003).

### **2.2.2 Funcionamiento del complejo WC**

El micelio de *N. crassa* incubado en oscuridad contiene proteínas WC-1 y WC-2 (Denault et al., 2001; Schwerdtfeger y Linden, 2001; Talora et al., 1999), la primera localizada en el núcleo y la segunda tanto en el núcleo como en el citoplasma (Schafmeier et al., 2006). WC2 es más abundante que WC-1 (Cheng et al., 2001a; Denault et al., 2001; Schafmeier et al., 2006; Schwerdtfeger y Linden, 2001) y por tanto WC-1 es el componente limitante para la formación del complejo (Cheng et al., 2003). A pesar de ello, la sobreexpresión del gen *wc-1* no es suficiente para la activación de la mayoría de los genes fotoinducibles (Lewis et al., 2002).

Cuando la luz incide sobre el micelio de *N. crassa*, la flavina unida a WC-1 capta la luz produciéndose un cambio conformacional en el dominio LOV. Como resultado se forma un enlace covalente entre la flavina y una cisteína altamente conservada en este dominio proteico (Salomon et al., 2000). Consecuentemente, la pérdida de esta cisteína conlleva la pérdida de función de WC-1 (Cheng et al., 2003). La formación del enlace flavina-cisteína da lugar a un cambio de conformación de la proteína y su agregación con otras proteínas WC-1 y WC-2, formando un complejo multimérico denominado L-WCC, y su posterior unión a promotores de genes fotoinducibles. Los elementos reguladores a los que se unen, llamados LRE (**L**ight **R**esponse **E**lements), se encuentran en los promotores de los genes que regula. La activación de estos genes es también facilitada por un aumento en la acetilación de las histonas H3 a través de la proteína NGF1, promovida por la luz, que facilita el acceso de la polimerasa de ARN (Grimaldi et al., 2006).

WC-1 no solo activa numerosos genes uniéndose a sus promotores (He y Liu, 2005), sino que induce además su propia transcripción, provocando un aumento transitorio de sus niveles proteicos. De hecho, su promotor contiene un elemento LRE, ubicado 1179 pb “aguas arriba” de su marco abierto de lectura (Kaldi et al., 2006). Los niveles de ARNm de *wc-1*, que alcanzan su valor máximo aproximadamente a los treinta minutos de iluminación, disminuyen posteriormente hasta recuperar los niveles de oscuridad unas dos horas después. Si persiste la iluminación la cantidad de proteína WC-1 baja también a los niveles de la oscuridad. Esto es debido a que la iluminación prolongada induce la fosforilación de WC-1, su separación del complejo y su degradación o su

reciclado para su posterior uso (Schwerdtfeger y Linden, 2001; Talora et al., 1999). Paradojicamente, su efecto activador sobre el gen al que esta unido es más eficaz en su estado fosforilado (Heintzen et al., 2001). Como consecuencia, tras responder a la luz a través de su complejo WC, *N. crassa* necesita un tiempo de recuperación de al menos una hora en la oscuridad antes de poder responder de nuevo a la luz (Arpaia et al., 1999).

WC-1 y WC-2 se regulan mutuamente. Así, WC-1 reprime la expresión de WC2 (Linden et al., 1997b; Cheng et al., 2003). Por su parte, ciertos mutantes WC-2 muestran alteraciones en el nivel de fosforilación de WC-1, por lo que se cree que WC-2 juega un papel en la transitoriedad y estado de fosforilación de WC-1 (Schwerdtfeger y Linden, 2001; Talora et al., 1999). Se desconoce el mecanismo de fosforilación en WC-1, pero se sabe que posee cinco sitios de fosforilación próximo a su extremo C-terminal, en la región del “dedo de zinc”. El estado de fosforilación de esta región afecta a la regulación del ritmo circadiano, pero no parece jugar ningún papel en su mecanismo de fotoactivación (He et al., 2002). Respecto a la participación de otras proteínas, WC-1 interacciona con una quinasas de proteína (PKC; protein kinase C). PKC actúa como regulador negativo de WC-1, de manera que mutaciones en la regulación de PKC provocan cambios en los niveles de proteína WC-1.

Como WC-1, WC-2 es también fosforilada tras la exposición a luz, siempre en presencia de WC-1 y solo cuando se encuentra en el núcleo (Schwerdtfeger y Linden, 2001). La fosforilación dependiente de luz de WC-2 se pierde mutando el “dedo de zinc”, mientras que lo mismo le ocurre a WC-1 si se muta el dominio de unión al cromóforo (Schwerdtfeger y Linden, 2001).

### 2.2.3 Papel de VIVID en la fotoadaptación del complejo WC

Como ya se ha mencionado, VIVID (VVD) es otro de los fotorreceptores de *N. crassa*. Se trata de una proteína muy pequeña, de sólo 186 aa, dedicados casi exclusivamente a un dominio LOV que une FMN o FAD como cromóforo y que le confiere la capacidad de detectar luz azul (Fig. I8) (Heintzen et al., 2001). Su nombre proviene del color “vívido” que adquieren los mutantes en dicho gen debido a una mayor acumulación de caroteno en el micelio (Heintzen et al., 2001). El dominio LOV es esencial para su función y presenta un fotociclo de aproximadamente 5 h (Zoltowski et al., 2007; Schwerdtfeger y Linden, 2003). VIVID es la proteína encargada de detectar los cambios diarios de intensidad lumínica actuando como represor de los genes fotoinducibles. El papel lo lleva a cabo reprimiendo las fotorrespuestas pasado un cierto tiempo de exposición a la luz, fenómeno conocido como fotoadaptación. La luz induce la transcripción del gen *vvd* a través del complejo WC (Heintzen et al., 2001), pero el propio VIVID ejerce posteriormente un efecto negativo sobre complejo. VIVID posee además

otras funciones en el ritmo circadiano (Elvin et al., 2005).

Resumiendo el proceso, cuando el micelio de *N. crassa* incubado en la oscuridad se expone a la luz, esta es detectada por WC-1 a través de su cromóforo, provocando la unión con WC-2 y otras proteínas WC-1 para formar el complejo WC. El complejo se une transitoriamente a los promotores de los genes fotoinducibles para inducir su expresión. La transitoriedad de la unión es resultado de la inestabilidad del propio complejo, que a su vez dependerá del estado de fosforilación de WC-1. La hiperfosforilación de WC-1 promueve su propia degradación, hasta bajar aproximadamente al 50% de su contenido, y disminuye la eficacia de unión del complejo a los promotores diana (He y Liu, 2005). Sobre dicho estado actúa VIVID, ya que en los mutante *vvd* la hiperfosforilación del complejo se mantiene en el tiempo, lo que hace a WC-1 más activo a pesar de que se reduce su cantidad en la célula (Heintzen et al., 2001; Shrode et al., 2001; Schwerdtfeger y Linden, 2003).

Los niveles de proteína VIVID aumentan rápidamente tras la exposición a la luz alcanzando un máximo a los 30 minutos, mientras que los niveles de WC-1 empiezan a disminuir hasta alcanzar los niveles de oscuridad tras 2 horas de iluminación (He y Liu, 2005). De este modo, el complejo WC no responde a un segundo pulso de luz durante al menos una hora, tiempo suficiente para que haya síntesis de nueva proteína WC-1 (Arpaia et al., 1999; Schwerdtfeger y Linden, 2001). Es interesante resaltar que VIVID es una proteína citoplásmica, mientras que el complejo WC es nuclear. Por tanto, VIVID ejerce su acción sobre el complejo de forma indirecta.

La información disponible sobre el funcionamiento del complejo WC se resume en el modelo representado en la Fig. I10.

#### **2.2.4 Genes fotoinducibles en *N. crassa***

Se estima que la luz azul induce la expresión de un 3% de los genes de *N. crassa* (Lewis et al., 2002). Entre estos se encuentran genes de la biosíntesis de carotenoides, genes de la conidiación y genes controlados por el reloj circadiano (Linden et al., 1997b). Dentro de los genes regulados por la luz se distinguen varios patrones de respuesta. Un grupo de genes responden rápidamente, pudiéndose detectar su ARN mensajero tan solo cinco minutos después del inicio de la iluminación, y alcanzan los niveles máximos a los treinta minutos aproximadamente (Baima et al., 1991; Sommer et al., 1989). Otros genes, sin embargo, requieren al menos una o más horas de iluminación para que los cambios en los niveles de ARNm sean perceptibles (Arpaia et al., 1995a; Arpaia et al., 1993; Arpaia et al., 1995b). Esto permite clasificar los genes fotoinducibles en genes tempranos o tardíos en función del tiempo de respuesta. En otros organismos, como en las plantas, no es infrecuente que la luz provoque la inhibición de la expresión de algunos genes (Gilmartin et al., 1990). Sin embargo, la fotorrepresión parece ser un fenómeno raro en *N. crassa*, ya

que solo se ha descrito para el gen *cut-1*, implicado en la respuesta al estrés osmótico (Youssar y Avalos, 2006).

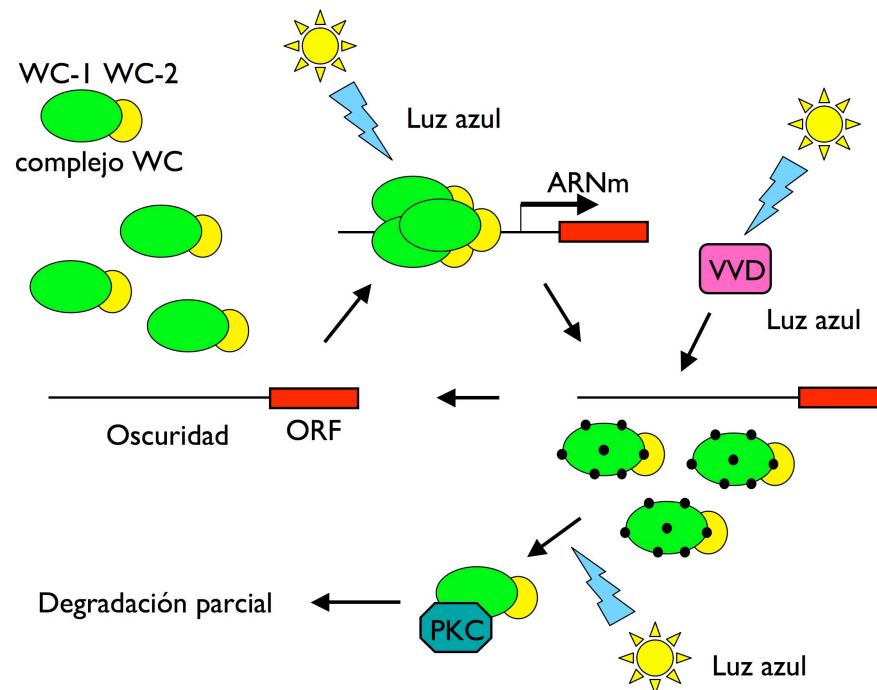


**Fig. I10. Modelo de fotoactivación de la expresión génica por el complejo WC.**

La recepción de luz por el cromóforo FAD unido al dominio LOV de WC-1 provoca la agregación del complejo y la unión a los promotores de los genes fotoinducibles, activando su transcripción. Tras la exposición a la luz, WC-1 es fosforilado (puntos negros) provocando la separación del complejo WC del promotor. La proteína VVD es necesaria para la transitoriedad de la expresión génica. El complejo WC excluido del promotor es desfosforilado y parcialmente degradado, probablemente mediante la interacción con PKC. Modificado de Corrochano, 2007.

## 2.3 Opsinas

Las opsinas son una familia de fotorreceptores de membrana que usan retinal como grupo prostético para la absorción de la luz (revisado por Sharma et al. 2006), y que están involucrados en diferentes procesos relacionados con la luz en gran diversidad de organismos (Zhai et al., 2001). Las opsinas fotoactivas, conocidas también como rodopsinas, fueron descritas por primera vez en arqueas (bacteriorrodopsina) (Bogomolni y Spudich., 1982) donde actúan como bombas de iones. En otros organismos realizan otro tipo de funciones, como fototaxis en algas (Ridge, 2002) o fotoadaptación en bacterias (Jung et al. 2003), denominándose a este grupo Rodopsinas de tipo I. Muy próximas a este



tipo de proteínas están las opsinas humanas, denominadas Rodopsinas de tipo II, responsables de la visión en la retina (Menon et al., 2001). Las opsinas están ampliamente distribuidas en todos los reinos (Spudich, 2006) y se han encontrado incluso en bacterias para las que no se conoce ningún tipo de fotorrespuesta (Handelsman, 2004).

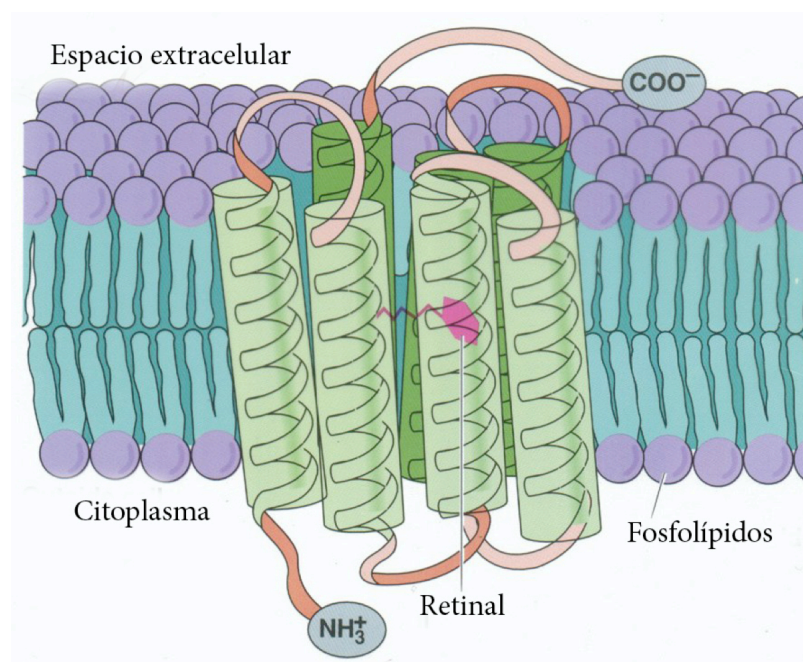


**Fig. I11. Representación esquemática de una opsina genérica embebida en la membrana plasmática.** Los cilindros con hélices en su interior representan los siete dominios transmembrana. En el interior se localiza el bolsillo hidrofóbico, donde se encuentra unido el retinal (en morado).

### 2.3.1 Estructura de las opsinas

Se ha resuelto la estructura tridimensional de varias opsinas (Terakita, 2005; Spudich, 2006). En todos los casos, la estructura incluye una molécula de retinal unida covalentemente a un residuo de lisina, (Fig. I11 y I12) (Neutze 2002, Luecke et al. 2008).

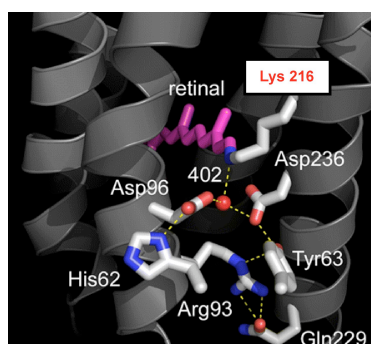


**Fig I12.** Estructura de la base de Schiff unida a retinal.

La opsina estudiada a mayor resolución es la bacteriorrodopsina (BR) de *Halobacterium salinarum*, una proteína de 26 kDa formada por 248 aa. Se trata de una proteína con siete hélices  $\alpha$  transmembrana (nombradas de la I a la VII) y totalmente embebida en una membrana plasmática, de tal manera que solo una pequeña porción de su extremo amino y su extremo carboxilo se encuentran en los espacios intra y extracelular respectivamente (Fig.I11) (Reyes-Martinez et al. 2005). Las siete

hélices  $\alpha$  forman un poro o bolsillo hidrofóbico donde se encuentra la molécula de retinal unida al  $\epsilon$ -amino de la lisina 216 (Lys 216) de la hélice G, formando una base de Schiff. Dentro del bolsillo hidrofóbico hay aminoácidos cuya función es ayudar a la protonización y desprotonización del retinal, siendo residuos claves la asparagina 85 (Asn-85), primer receptor del protón expulsado, y la asparagina 96 (Asn-96), que toma un protón del citoplasma para cedérselo al retinal desprotonado. En *Halobacterium* su función es expulsar protones al espacio extracelular usando la energía de la luz y crear un gradiente de protones, que es aprovechado por una ATPasa para sintetizar ATP.

### 2.3.2 Opsinas en hongos

Los genomas de los hongos contienen genes que codifican secuencias reconocibles como posibles opsinas. Algunas no contienen el residuo conservado de lisina al que se une el retinal. Estas proteínas, presumiblemente no fotorreactivas, se han llamado genéricamente ORPs (de “opsin-related proteins”). Otras poseen el residuo de lisina, pero su fotorreactividad no ha sido investigada, por lo que las abreviaremos como OLPs (de “opsin-like proteins”). Hasta el momento solo hay dos OLPs fúngicas cuya fotobioquímica ha sido investigada y que se ha demostrado que reaccionan a la luz: NOP1 de *N. crassa* (Bieszke et al. 1999a) y OPS de *Leptosphaeria maculans* (Idnurm y Howlett, 2001). NOP-1, descubierta en un análisis de secuencias expresadas (ESTs o “expressed sequence tags”), fue la primera opsina descrita en hongos, antes de la disponibilidad de las secuencias de genomas completos. NOP-1, es capaz de unir retinal (Bieszke et al., 1999b) y presenta un fotociclo típico de estas proteínas (Brown et al., 2001). Sin embargo, su pérdida no produce fenotipo alguno bajo condiciones de laboratorio, aunque se observó una alteración en la morfología de su micelio aéreo cuando crece en iluminación en presencia de oligomicina, un inhibidor de ATPasa (Bieszke et al., 1999a). La función de esta proteína puede estar relacionada de alguna forma con los conidios o con su formación, ya que los niveles de ARNm del gen aumentan al inducirse la conidiación por el contacto del micelio con el aire (Bieszke et al., 2007).

Menos información se dispone de la opsina OPS de *L. maculans*, ya que no se ha investigado su función por mutagénesis dirigida del gen. Su análisis fotoquímico muestra un fotociclo mucho más rápido que el de NOP-1, similar al de la bacteriorrodopsina, por lo que se le atribuye una función como bomba de protones. El reemplazamiento de un residuo de ácido aspártico (Asp-150, equivalente al Asp-96 de la BR), que sirve supuestamente como donador de protones al retinal en *L. maculans*, por ácido glutámico le confiere a la proteína un fotociclo lento, similar al de NOP-1 de *N. crassa* (Brown et al. 2001; Waschuk et al. 2005; Furutani et al. 2006). Su diferente capacidad de reaccionar a la luz sugiere

diferentes funciones para ambas proteínas, pero la similitud de otros aminoácidos conservados no apoya esta hipótesis (Fig. I13).

El análisis de los genomas de otros hongos permite identificar genes en número variable para OLPs y ORPs en ascomicetos y basidiomicetos, pero no en los escasos genomas disponibles de zigomicetos. La levadura *S. cerevisiae* carece de ninguna fotorrespuesta conocida, y en su genoma solo se encuentran dos genes para ORPs y ninguno para OLPs. En otros hongos, como *U. maydis*, se da la circunstancia contraria, ya que no posee ningún gene para ORPs pero posee tres genes para OLPs. Se hace mención a estos en el capítulo 5 de esta Tesis. Con la excepción de NOP-1 de *N. crassa* y OPS de *L. maculans*, los genes de hongos para presuntas opsinas fotoactivas no han sido objeto de atención.

Lm OPS	Y	Y	R	D	W	T	T	L	D	M	Y	A	C	Y	W	Y	W	A	D	E	D	K
Nc NOP-1	Y	F	R	D	W	T	T	L	E	M	Y	G	C	Y	W	Y	W	A	G	E	D	K
Hs BR	Y	Y	R	D	W	T	T	L	D	M	W	S	T	M	W	Y	W	S	E	E	D	K
	57	79	82	85	86	89	90	93	96	118	138	141	142	145	182	185	189	193	194	204	212	216
	II				III					IV		V			VI				VII			

**Fig. I13.** Análisis de la presencia en NOP-1 de *N. crassa* y OPS de *L. maculans* de residuos clave en el fotociclo del retinal y la translocación de protones de la bacteriorodopsina (BR) de *Halobacterium salinarum*. La lisina de unión del retinal y formación de la base de Schiff se destaca en fondo rojo. En fondo verde se resalta el residuo de ácido aspártico, receptor de protones de la base de Schiff. Los residuos recuadrados participan en la transferencia de protones desde la base de Schiff al espacio extracelular. En fondo azul se indican los residuos que rodean la molécula de retinal (distancia mínima de 3,6 Å al anillo de  $\beta$ -ionona o a la cadena de polieno). Los números indican las posiciones de dichos aminoácidos en la bacteriorodopsina. Se señala abajo la ubicación en los dominios transmembrana, indicados con números romanos.

### 2.3.3 Opsinas en *Fusarium*

En el momento de redacción de esta Tesis, se han secuenciado los genomas de tres especies de *Fusarium*: *F. graminearum*, *F. verticillioides*, y *F. oxysporum*. La búsqueda de secuencias con similitud a opsinas mediante la herramienta BLAST muestra la presencia en las tres especies de dos genes para OLPs y un gen para una ORP. Una de las dos OLPs es CarO, anteriormente investigada en *F. fujikuroi* (Prado et al. 2004). El gen *carO* está ligado a genes de la carotenogénesis de este hongo, con los que muestra además un mismo patrón de regulación (ver sección 3.2.2). Al igual que ocurrió con *nop-1* en *N. crassa*, la mutación dirigida del gen *carO* no produjo ningún cambio fenotípico distinguible externamente (Prado et al. 2004).

El gen de la segunda OLP se ha denominado *opsA* y es objeto de investigación en esta Tesis (capítulo 2). El tercer gen, que determina una ORP u opsina presuntamente no

fotoactiva, se ha denominado *hspO* (citado en el capítulo 2). HspO es ortóloga a YRO2 de *N. crassa* y HSP30 de *S. cerevisiae*, llamada así por ser inducible por choque térmico (Zhai et al., 2001). Por esta última característica, se sospecha que puede jugar un papel de chaperona. A este grupo pertenecen también Cvhsp30/1 y Cvhsp30/2 de *Coriolus versicolor* (Iimura y Tatsumi, 2002), aunque los análisis de secuencia descritos en esta Tesis los sitúan más próximos a CarO que a HspO (ver capítulo 2).

### 3. Metabolismo secundario de hongos

#### 3.1 Metabolismo secundario de *Fusarium*.

Las especies del género *Fusarium* se caracterizan por poseer un complejo metabolismo secundario. Muchos de los metabolitos que producen pertenecen a familias, como los terpenoides o los policétidos, que comparten los pasos iniciales de la ruta o el mecanismo inicial de síntesis pero que se diversifican en sus reacciones más tardías para dar lugar a una enorme variedad de compuestos químicos. Algunos de estos metabolitos son importantes por su toxicidad (micotoxinas), ya que las especies de este género infectan muchas plantas cultivadas. Además de las pérdidas que puedan producir en las cosechas, producen micotoxinas cuya presencia en los productos cosechados pueden suponer problemas sanitarios, tanto para los animales domésticos (Uhlinger, 1997) como para la especie humana (Marasas et al., 1988). Entre los numerosos compuestos tóxicos producidos por especies del género *Fusarium* se pueden citar las fumonisinas (Gelderblom et al., 1988), las fusarinas (Barrero et al., 1991), el ácido fusárico (Bacon et al., 1996), las bicaverinas (Giordano et al., 1999a), la moniliformina (Marasas et al., 1986) y la fusaproliferina (Moretti et al., 2007) (Fig. I14). *Fusarium fujikuroi* produce además fusarinas y bicaverinas, descritas en la sección siguiente.

Además de las toxinas, estos hongos producen metabolitos de interés biotecnológico, como los carotenoides (Avalos y Cerdá-Olmedo, 2004), como las giberelinas (Avalos et al., 2007). Éstas son hormonas vegetales estimuladoras del crecimiento, usadas en la agricultura intensiva para mejorar el rendimiento de los cultivos. Se habla en más detalle de estos interesantes metabolitos en la sección 3.1.3 y 3.2. Para otros metabolitos se desconoce su toxicidad o aplicaciones prácticas, como las kaurenolidas (Rojas et al., 2004) o el fujenal (Fernández-Martín et al., 1995), del que existen análogos químicos con propiedades antitumorales (Hanson., 2008).

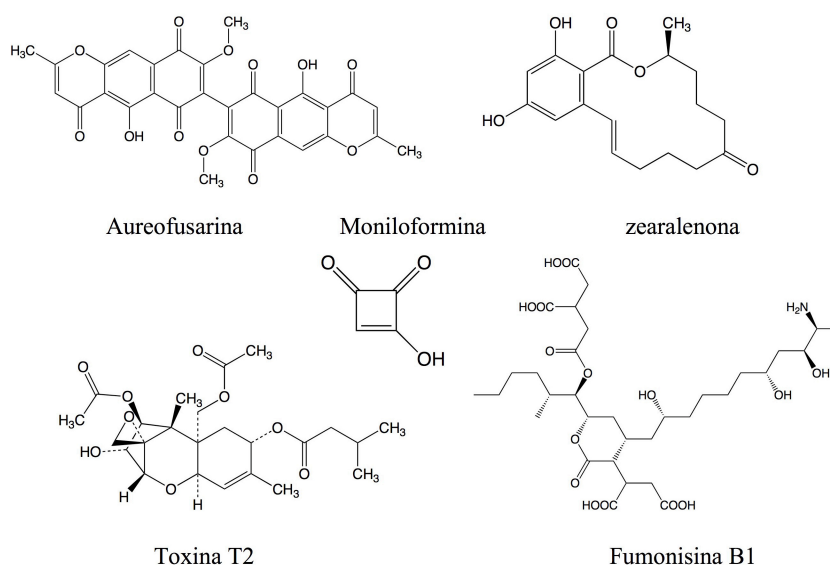


**Fig. I14.** Ejemplos de micotoxinas producidos por especies del género *Fusarium*.

### 3.1.1 Síntesis de policétidos en *Fusarium fujikuroi*: bicaverinas y fusarinas

Los policétidos son metabolitos que tienen en común la síntesis a partir de una enzima multifuncional de gran tamaño, similar a la sintetasa de los ácidos grasos, conocida como sintetasa de los policétidos (Menzella et al., 2005). A partir de ahí las diferentes rutas de policétidos se diversifican con reacciones químicas muy diferentes, que dan lugar a la gran variedad de moléculas de esta familia (O'Hagan, 1993). Las especies del género *Fusarium* producen numerosos policétidos, como indica la presencia en sus genomas de numerosos genes para enzimas de esta familia (Desjardins, 2006; Desjardins y Proctor, 2007). En *F. fujikuroi* se ha investigado al menos la síntesis de dos tipos de policétidos, las bicaverinas (Giordano et al., 1999a), para las que se ha descrito actividad antibiótica frente a los protozoos (Balan et al., 1970), y las fusarinas (Barrero et al. 1991), micotoxinas con propiedades mutagénicas (Fig. I15).

Como las giberelinas (ver sección 3.1.3), las bicaverinas se producen en *F. fujikuroi* solo en ausencia de nitrógeno, aunque están también reguladas por otros factores, como el pH (Giordano et al., 1999a). Mecanismos de regulación similares se han observado en *F. oxysporum*, especie capaz también de producir bicaverinas, habiéndose estudiado en este caso además el efecto de la fuente de carbono o nitrógeno y de la presencia de calcio (Bell et al., 2003). Se conoce el gen de la policétido sintetasa de esta ruta, denominado *pks4* (Linnemannstöns et al., 2002b), haciendo posible la investigación de su regulación a nivel transcripcional. El gen es regulado también por la proteína AreA que controla la asimilación de fuentes alternativas de nitrógeno (Linnemannstöns et al., 2002b). Este

proceso implica la detección de las moléculas nitrogenadas presentes en el medio y la activación selectiva de los genes necesarios para su asimilación (Marzluf, 1997). El hongo en el que se ha investigado más en profundidad este aspecto del metabolismo es *Aspergillus nidulans*, donde se identificó AreA por primera vez (Caddick et al., 1986). Este regulador positivo ejerce su función auxiliado por otras proteínas, como TamA (Small et al., 1999), NmrA (Andrianopoulos et al., 1998) ó el complejo AreB (Conlon et al. 2001). El gen *pks4* forma un “cluster” con otros genes de la ruta, cuya caracterización está siendo llevada a cabo por el grupo de B. Tudzynski (comunicación personal).

Existe escasa información sobre la regulación de la producción de fusarinas en *F. fujikuroi*, donde se ha investigado el efecto del medio de cultivo o la temperatura (Barrero et al., 1991) y donde se ha observado un efecto inhibitor de la aireación (Giordano y Domenech, 1999). Se ha identificado recientemente el gen de la policétido sintetasa para las fusarinas en otras especies de *Fusarium* (Song et al, 2004; Gaffoor et al. 2005), y está actualmente en marcha la caracterización del gen de *F. fujikuroi*. Sin embargo, se desconoce en ésta y en otras especies el resto de los genes necesarios para su síntesis. Finalmente, no se dispone de información sobre la función biológica de estos policétidos en los hongos.

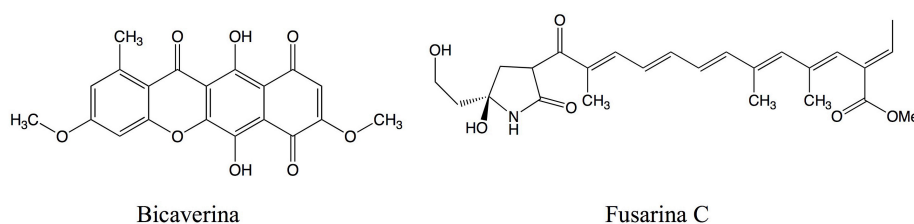


**Fig. I15.**  
Representación esquemática de la estructura de una bicaverina y la fusarina C.

### 3.1.2 Los terpenoides

Los terpenoides son un extenso grupo de compuestos químicos presentes en todos los seres vivos y con funciones muy diversas (Fig. I16). Todos derivan de una misma molécula de cinco átomos de carbono, denominada pirofosfato de isopentenilo (IPP).

Se conocen dos rutas bioquímicas diferentes para la síntesis de IPP. La primera, y más conocida, usa como intermediario mevalonato (Fig. I17). Este compuesto se sintetiza a partir de acetil-CoA, vía acetoacetil-CoA y el 3-hidroxi-3-metilglutaril-CoA (HMG-CoA), que da lugar al mevalonato a través de la actividad de una reductasa (Goodwin y Lijinsky, 1951). Después se producen dos fosforilaciones y una decarboxilación que convierten el mevalonato en IPP.

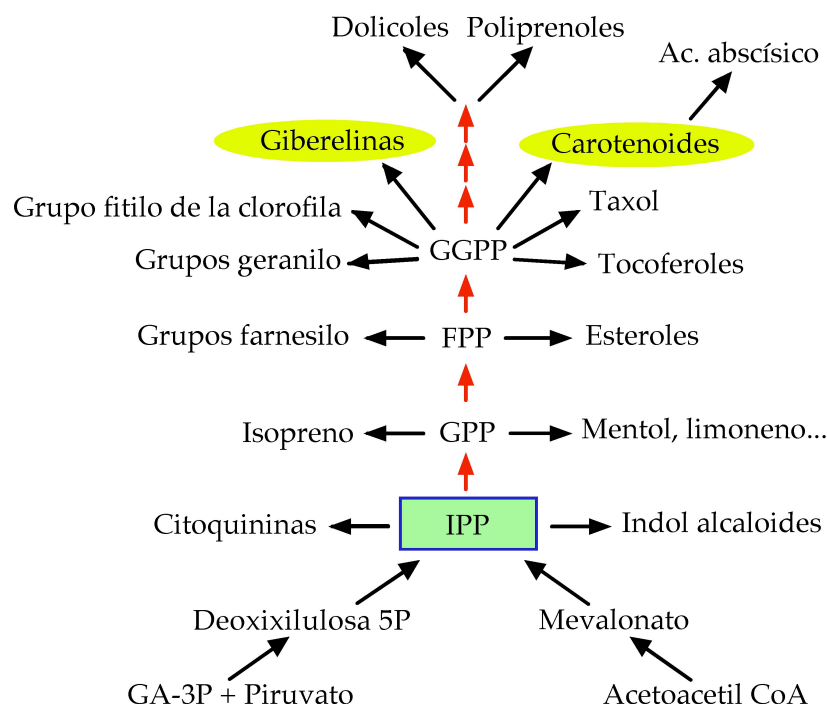


**Fig. I16.** Esquema de la ruta de síntesis de terpenoides. La flecha roja indica la ganancia de una unidad de 5 carbonos. Se muestran una selección de los terpenoides conocidos. Algunos, como el mentol, limoneno, las citoquininas, el ácido abscísico o el grupo fitilo de la clorofila, se han encontrado en plantas.

La segunda ruta, descubierta posteriormente en bacterias (Rohmer et al., 1993; Horbach et al., 1993), comienza con la condensación de gliceraldehído-3-fosfato e hidroxietilamina, producto de la decarboxilación del piruvato. Esta ruta coexiste con la del mevalonato en plantas y otros organismos (Schwender et al., 1996; Eisenreich et al., 1996; Lichtenthaler et al., 1997), pero no se ha descrito en los hongos.

El tronco principal de la ruta, entre IPP y GGPP, consiste en condensaciones sucesivas de una unidad de IPP, elongándose la cadena en cada paso en 5 átomos de carbono (Fig. 16). Así el GPP tiene 10, el FPP 15 y el GGPP 20. El GGPP constituye un terpeno. Los terpenoides se clasifican según el número de moléculas de terpeno que hayan dado origen a su estructura. Así, podemos encontrar los monoterpenos, derivados del GPP, y los sesquiterpenos, derivados del FPP. Los triterpenos a su vez derivan de la condensación de dos moléculas de FPP, como es el caso de los esteroides (Weete y Ghandi, 1997). También podemos encontrar los tetraterpenos, derivados de dos moléculas de GGPP, grupo al que pertenecen los carotenoides.

Algunos terpenoides tienen una especial relevancia biológica. Entre ellos figuran los esteroides, que juegan un papel esencial para la integridad de la membrana plasmática y como diana para antibióticos antifúngicos (Accoceberry y Noël, 2006). El precursor de los esteroides es el escualeno, que se produce por la condensación de dos moléculas de FPP (Weete y Ghandi, 1997). El escualeno sufre posteriormente diversas oxidaciones y ciclaciones que dan lugar a los distintos esteroides. Uno de ellos es el colesterol, de gran



importancia para la salud humana.

También son terpenoides ciertas hormonas vegetales, como el ácido abscísico o las giberelinas. El ácido abscísico es un derivado del metabolismo de los carotenoides, de los cuales se habla en secciones posteriores, mientras que las giberelinas poseen su propia ruta biosintética a partir de GGPP. Ambas hormonas regulan muchos procesos en las plantas. El ácido abscísico controla la apertura estomática, la dormancia de yemas y semillas, la abscisión (de ahí su nombre) de hojas y frutos, y la inhibición del crecimiento de muchas partes de la planta (Addicott, 1983). Las giberelinas estimulan diferentes etapas del desarrollo vegetal, desde la germinación a la elongación del tallo, la floración o la maduración de los frutos. Estas hormonas merecen especial atención por la capacidad de *F. fujikuroi* de llevar a cabo sus síntesis.

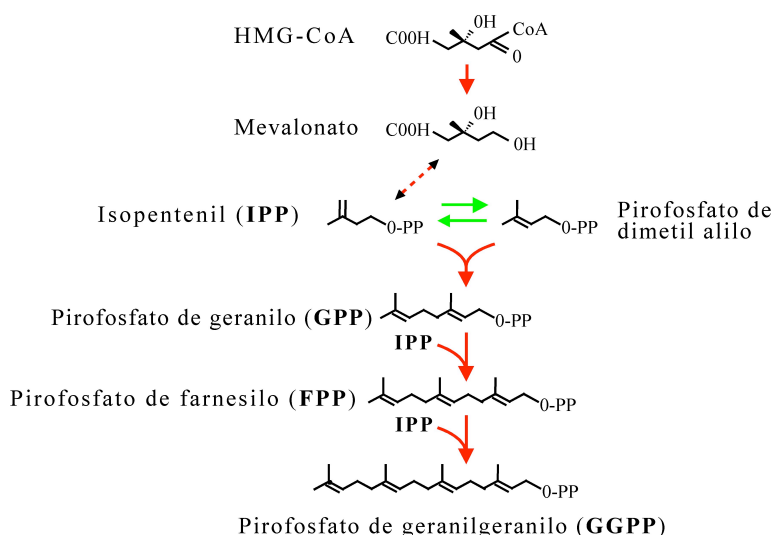


**Fig. I17.** Síntesis de GGPP por la ruta del mevalonato.

### 3.1.3 Síntesis de giberelinas

Las giberelinas tienen en común con los carotenoides los pasos iniciales de la síntesis de terpenoides hasta el GGPP. Sin embargo, ambos procesos biosintéticos tienen lugar en diferentes compartimentos celulares (Domenech et al., 1996) y la conversión de FFPP a GGPP es llevada a cabo por enzimas diferentes (Schwender y Seemann, 1996).

La síntesis de giberelinas arranca con la conversión de GGPP en kaureno, un compuesto tetracíclico sintetizado a través de dos reacciones enzimáticas, llevadas a cabo en las plantas por dos enzimas independientes, pero por una sola enzima en el hongo. Todos las enzimas y genes responsables de la ruta han sido recientemente caracterizados (revisado por Tudzynski, 2005). Los genes están organizados en un cluster (Tudzynski y



Holter, 1998) cuya función en la ruta ha sido objeto de detallada atención. La disponibilidad de los genes ha facilitado el estudio de los mecanismos que controlan su transcripción, reprimida en presencia de fuentes de nitrógeno en el medio. El efecto represor del nitrógeno tiene como consecuencia que la síntesis solo tenga lugar en las fases tardías de los cultivos cuando el nitrógeno es el nutriente limitante (Candau *et al.*, 1992).

Como ocurre con las bicaverinas, la regulación por nitrógeno de la ruta es mediada por la proteína AreA (Tudzynski *et al.*, 1999), que en ausencia de nitrógeno activa la transcripción de la mayoría de los genes estructurales del agrupamiento génico (Mihlan *et al.* 2003). El papel de esta proteína y otras proteínas auxiliares, como TamA o NmrA, en la regulación de la síntesis de giberelinas está siendo investigado en la actualidad por el grupo de la Dra. B. Tudzynski (Universidad de Münster, Alemania). No se han descrito, sin embargo, mutantes desregulados, probablemente por la dificultad de su detección, ya que requiere el escrutinio individual de la producción de giberelinas por números muy elevados de supervivientes a los tratamientos mutagénicos.

La capacidad de sintetizar giberelinas es un carácter infrecuente en los hongos. Dentro del género *Fusarium*, solo las producen *F. fujikuroi* y *F. konzum* (grupo de cruzamiento I). Otras especies del complejo de especies *Gibberella fujikuroi* poseen restos del agrupamiento génico, pero bien por tenerlo incompleto, o por haber acumulado mutaciones, no producen estas hormonas (Malonek *et al.*, 2005). Además de en plantas, fuera de *Fusarium* se ha descrito producción de giberelinas en *Phaeosphaeria sp.* y *Sphaceloma manihoticola*, y en algunas bacterias (McMillan, 2001). Se desconoce el papel de las giberelinas en *Fusarium*, ya que los mutantes que no son capaces de sintetizarlas no poseen ninguna alteración fenotípica en condiciones de laboratorio (Candau *et al.*, 1991; Fernández-Martín *et al.*, 1995). Su posible papel en el proceso de infección del arroz es actualmente objeto de atención en el grupo de investigación .

### 3.2 Los carotenoides

Los carotenoides son pigmentos vitales en plantas y algas por su papel como fotorreceptores y transmisores de energía a los centros de reacción fotosintéticos (Edge *et al.*, 1997). Además están presentes en la gran mayoría de los seres vivos, incluso cuando no son capaces de sintetizarlos, como ocurre con los animales (Maiani *et al.*, 2008; Lu *et al.*, 2008). En el reino vegetal son especialmente abundantes, pero su presencia es enmascarada por el color verde de las clorofilas. Además de su papel como pigmentos accesorios en la fotosíntesis, proporcionan colores llamativos a flores y frutos para atraer a los animales y facilitar la dispersión de las semillas.

En humanos los carotenoides, obtenidos por la dieta, juegan diferentes funciones de importancia para el correcto funcionamiento del organismo (Maiani *et al.*, 2008). El más

importante es el  $\beta$ -caroteno, de propiedades antioxidantes y precursor del retinal (aldehído de la vitamina A o retinol) y del ácido retinoico. Otros carotenos como el licopeno poseen una elevada capacidad antioxidante, y su ingestión reduce el riesgo de cáncer y ciertos problemas cardiovasculares (Hadley et al., 2002). Las propiedades antioxidantes de los carotenoides contribuyen también a la mejora de la respuesta inmunológica (Jyonouchi et al., 1993). Otros carotenoides, como la luteína y zeaxantina, son componentes esenciales del pigmento macular en el ojo, ofreciendo protección frente a la degradación macular, causa principal de la ceguera por edad (Krinsky et al., 2003). En general, está aceptado que la presencia de carotenoides en la dieta confiere numerosos efectos positivos sobre la salud (Mares-Perlman et al., 2002; Giovannucci, 2002).

El retinal es esencial para el correcto desarrollo de la retina. Su carencia puede producir ceguera crepuscular (mal llamada ceguera nocturna), por la cual disminuye la agudeza visual cuando oscurece. También puede dar lugar a sensibilidad a infecciones, como el sarampión, y xeroftalmia (trastornos oculares importantes), generalmente causados con mala absorción, desnutrición crónica y pérdida de peso a causa de una enfermedad debilitante, como el cáncer o la anorexia. Este tipo de enfermedades son comunes donde la dieta se basa principalmente en cereales o arroz y es especialmente pobre en Vitamina A, regiones como el sureste asiático por ejemplo.

Los carotenoides tienen también aplicaciones biotecnológicas derivadas tanto de sus propiedades químicas como de sus llamativos colores, empleándose actualmente como ingredientes activos en las industrias cosmética y alimentaria. Cada vez es más frecuente el uso de carotenoides en productos de belleza, como colorante alimenticio o como reclamo adicional en alimentos pobres en caroteno. Para estos usos hay una creciente preferencia por los carotenoides de origen biológico respecto a los sintetizados por métodos químicos, figurando los hongos entre los organismos preferentes para su obtención biotecnológica (Avalos y Cerdá-Olmedo 2004).

### 3.2.1 Carotenogénesis de hongos

La capacidad de sintetizar carotenoides es un carácter frecuente en los hongos. Por sus facilidades metodológicas, algunos hongos, como *N. crassa*, *P. blakesleeanus*, *Xanthophyllomyces dendrorhous* (anteriormente *Phaffia rhodozyma*) y *F. fujikuroi*, han sido modelos de investigación ampliamente usados para estudiar la bioquímica y genética de este proceso (Sandmann y Misawa 2002; Avalos y Cerdá-Olmedo 2004). Sus rutas biosintéticas son similares en sus primeros pasos, teniendo siempre en común al menos tres reacciones enzimáticas. Las tres enzimas dependen de dos genes: un gen bifuncional que determina una sintasa de fitoeno y una ciclasa, y un segundo gen que determina una desaturasa. El fitoeno, producido por la sintasa de fitoeno a partir de la unión de dos

moléculas de GGPP, es un caroteno incoloro. Los sucesivos intermediarios adquieren la capacidad de absorber luz visible de diferente longitud de onda a causa de la introducción de dobles enlaces conjugados por la actividad enzimática de la desaturasa. La actividad ciclasa cierra los extremos para formar anillos de tipo beta.

Los dos genes responsables de estas reacciones se aislaron primero en *N. crassa* (Schmidhauser et al., 1990, 1994), y posteriormente en otros hongos, incluyendo *F. fujikuroi* (Fernández-Martín et al. 2000; Linnemannstöns et al. 2002a) u hongos más alejados taxonómicamente, como los zigomicetos *P. blakesleeanus* (Ruiz-Hidalgo et al., 1997, Arrach et al., 2001) y *Mucor circinelloides*, (Velayos et al., 2000a, 2000b), o el basidiomiceto *X. dendrorhous*, (Verdoes et al. 1999a, 1999b). En zigomicetos los productos de estos genes conducen a la síntesis de  $\beta$ -caroteno, acumulado mayoritariamente en sus micelios. Sin embargo, las rutas biosintéticas de *N. crassa* y *F. fujikuroi* incluyen reacciones adicionales que conducen a la acumulación de un carotenoide inusual dentro de los hongos, la neurosporaxantina, con un grupo carboxilo en su extremo. El conocimiento sobre esta ruta biosintética en ambos hongos se describe en detalle en las secciones posteriores.

Merece mención aparte por su importancia biotecnológica la ruta biosintética de *X. dendrorhous*. Esta levadura produce astaxantina, un carotenoide responsable de la pigmentación de diferentes animales, desde crustáceos (Goodwin y Srisukh, 1949) hasta flamencos o salmones. Actualmente se usa como aditivo alimentario en piscifactorias de truchas o salmones, necesarios para proporcionar el característico color de su carne. Posteriormente se descubrió la presencia de este carotenoide en *X. dendrorhous*, conocido por entonces como *Phaffia rhodozyma* (Andrewes et al., 1976) y redenominado después de que la observación de su ciclo sexual en el laboratorio permitiera identificarlo como basidiomiceto (Golubev, 1995). Debido a las ventajas de cultivo industrial de los hongos, muy pronto quedó manifiesto su potencial como fuente de astaxantina para alimentación animal (Johnson y Lewis, 1979), siendo utilizado actualmente para su producción a nivel industrial (Johnson, 2003). En los últimos años la biosíntesis de astaxantina se ha descrito también en otros organismos, entre ellos el alga verde *Haematococcus pluvialis* (Bubrick, 1991), o bacterias tanto gram-positivas (*Brevibacterium linens*, Krubasik y Sandmann, 2000) como gram-negativas (*Agrobacterium aurantiacum*, Misawa et al., 1995). La astaxantina se sintetiza a partir de  $\beta$ -caroteno mediante dos actividades enzimáticas que introducen grupos hidroxilo y ceto en los extremos ciclados de la molécula. En bacterias y algas ambas actividades dependen de genes y enzimas independientes, llamadas en las primeras *crtW* (para la cetolasa) y *crtZ* (para la hidroxilasa). En *X. dendrorhous* sin embargo depende de un solo gen, llamado *asy* o *crtS*, que determina una enzima bifuncional con ambas actividades enzimáticas (Ojima et al., 2006; Alvarez et al., 2006).

La regulación de la síntesis de carotenoides tiene rasgos comunes en los diferentes

hongos investigados, aunque se asume que difieren en sus detalles moleculares. Con frecuencia la síntesis es regulada por la luz, respuesta mediada por el sistema WC en los casos investigados (ver sección 2.2.1). En algunos hongos se obtienen con facilidad mutantes desregulados, como en *P. blakesleanus* (Cerdá-Olmedo, 1985), *M. circinelloides* (Navarro et al., 2000) y el propio *F. fujikuroi* (Ávalos y Cerdá-Olmedo, 1987), indicando la mediación de proteínas represoras en la regulación. El análisis genético más detallado se ha llevado a cabo en *P. blakesleanus*, donde se han estudiado mutantes en tres genes diferentes cuyas mutaciones dan lugar a un fenotipo superproductor (Murillo y Cerdá-Olmedo 1976; Salgado y Cerdá-Olmedo, 1992; Mehta et al. 1997). En *N. crassa* no existe tal tipo de mutantes y los que se obtienen en *Blakeslea* producen solo incrementos modestos (Mehta y Cerdá-Olmedo, 1995). Solo se ha identificado a nivel molecular un gen responsable de un represor de la carotenogénesis: *crgA* en *M. circinelloides*, perteneciente a una familia de proteínas con un dedo de zinc de tipo “ring finger” (Navarro et al., 2001). La función del gen homólogo en otros hongos carotenogénicos no ha sido investigada.

### 3.2.2 Carotenogénesis en *Fusarium fujikuroi*

La mayor parte del conocimiento de la síntesis de carotenoides en *F. fujikuroi* se ha generado en el laboratorio donde se ha realizado esta Tesis. El gen responsable de la síntesis de GGPP, llamado *ggs* por sus autores (Mende et al., 1997) y rebautizado *carG* para seguir la terminología genética de *F. fujikuroi* (Rodríguez-Ortiz et al., 2009), es teóricamente compartido por otros terpenoides posteriores a GGPP, excepto las giberelinas (Mende et al., 1997). Como en otros hongos, el primer paso específico de la ruta es la síntesis de fitoeno por condensación de dos moléculas de GGPP, reacción catalizada por el dominio sintasa de la enzima bifuncional CarRA (Linnemannstöns et al 2002a). De acuerdo con los intermediarios encontrados en la estirpe silvestre y en diferentes mutantes, el fitoeno es deshidrogenado en tres posiciones por la desaturasa CarB, para producir neurosporeno, pasando por dos intermediarios parcialmente desaturados, el fitoflueno y el  $\zeta$ -caroteno (Fig. I18). A continuación, la actividad ciclasa introduce un anillo beta en un extremo para dar lugar a  $\beta$ -zeacaroteno (Thewes et al., 2005) y la desaturasa CarB introduce dos nuevas deshidrogenaciones para producir  $\gamma$ -caroteno y toruleno. El  $\gamma$ -caroteno supone un punto de bifurcación en la ruta, ya que es también sustrato de la actividad ciclasa de CarRA para introducir un nuevo anillo beta, dando lugar al  $\beta$ -caroteno. Este caroteno es sustrato de una oxigenasa (CarX) que introduce una rotura oxidativa simétrica y da lugar dos moléculas de retinal (Prado-Cabrero et al., 2007a), usado como grupo prostético por las dos presuntas opsinas fotoactivas del hongo, CarO y OpsA (ver sección 2.3.3). La otra rama de la ruta continua con la rotura oxidativa del toruleno, esta

vez en una posición asimétrica, para producir un apocarotenoide de 35 átomos de carbonos, el  $\beta$ -apo-4'-carotenal. Esta reacción es catalizada por la oxigenasa CarT (Prado-Cabrero et al., 2007b). El grupo aldehído del  $\beta$ -apo-4'-carotenal es oxidado a un grupo ácido para dar lugar a neurosporaxantina (ácido  $\beta$ -apo-4'-carotenoico), producto final de la ruta. La enzima responsable de esta reacción en *F. fujikuroi*, determinada por el gen *carD*, es objeto actualmente de investigación en el mismo grupo de investigación. Como se verá en la siguiente sección, esta Tesis describe el gen y enzima responsable de la misma reacción en *N. crassa*.

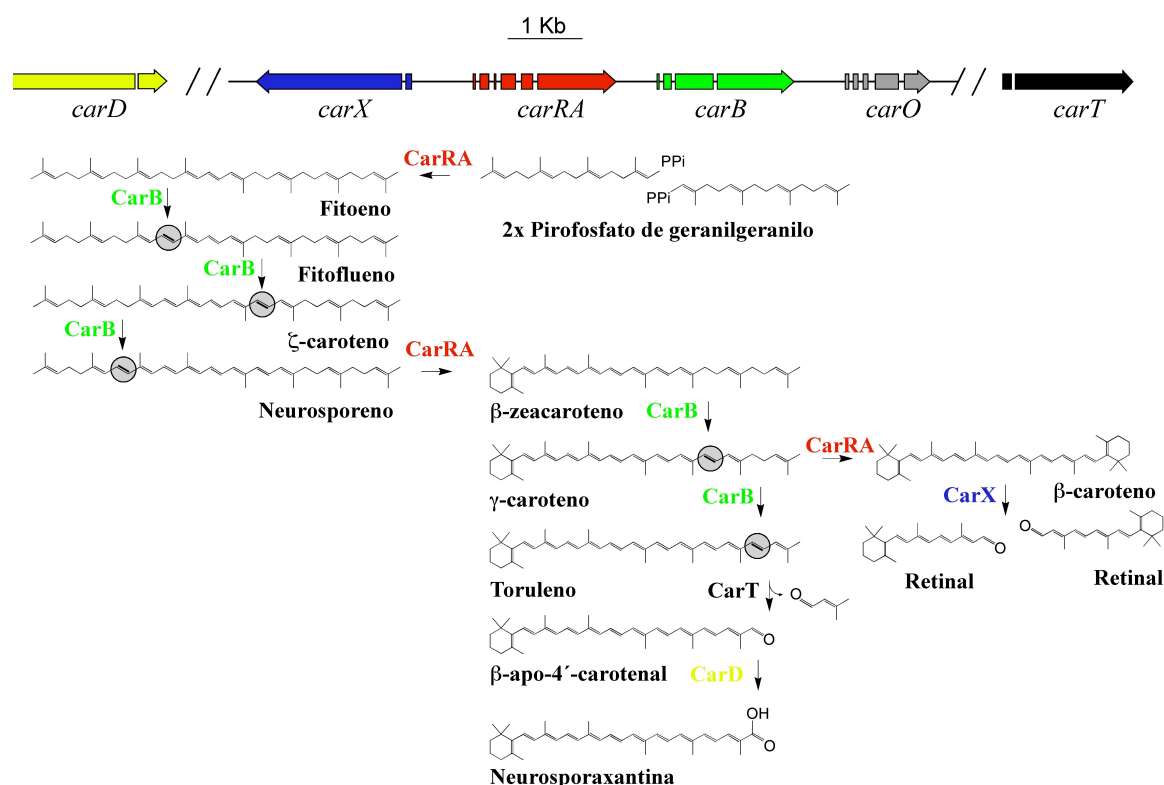


**Fig. I18.** Organización genómica de los genes de la síntesis de carotenoides y ruta biosintética de la Neurosporaxantina en *F. fujikuroi*. Se muestra también la ruta lateral que lleva a la síntesis de retinal. Se indican las enzimas responsables de cada reacción enzimática.

Tres de los genes estructurales de la ruta biosintética, *carX*, *carB*, y *carRA*, se encuentran agrupados en un mismo segmento genómico (Linnemannstöns et al., 2002; Thewes et al., 2005). Junto a ellos se encuentra el gen de una de las dos opsinas presuntamente fotoactivas, *carO* (Prado et al., 2004). Los genes *carT* (Prado-Cabrero et al., 2007b) y *carD* se encuentra en otras regiones del genoma. Los genes investigados hasta ahora, los arriba mencionados menos *carD*, están sujetos a un mismo patrón de regulación. En la estirpe silvestre sus niveles de ARNm son apenas detectables en la oscuridad, y aumentan al exponer el micelio a la luz, alcanzando un máximo aproximadamente tras 30-60 min de iluminación para disminuir posteriormente. Esta disminución indica la existencia en *F.*

*fujikuroi* de un mecanismo de fotoadaptación, ya mencionado en *N. crassa* (ver sección 2.2.3). En consonancia con esta respuesta transcripcional, la síntesis de carotenoides *in vivo* se inicia tras una hora de iluminación y alcanza su máximo aproximadamente a las 12 horas (Avalos y Schrott., 1990).

Los mutantes *carS*, que acumulan altos niveles de carotenoides independientemente de la luz (Avalos y Cerdá-Olmedo, 1987), delatan la existencia de un represor de la carotenogénesis, denominado CarS. Dicho represor actúa a nivel transcripcional, como demuestra los niveles anormalmente altos tanto en luz como en oscuridad de ARNm de los genes *car* ya mencionados (Linnemannstöns et al., 2002; Prado-Cabrero et al., 2007b; Thewes et al., 2005), incluyendo el gen *carO* (Prado et al., 2004) (Fig. I19). Datos no publicados obtenidos en nuestro laboratorio (resultados de V. Díaz-Sánchez), indican ausencia de fotoinducción del gen *carD*, cuyos niveles en la oscuridad son mayores que para los otros genes *car*, y un incremento más modesto en la oscuridad en los mutantes *carS* (cinco veces en comparación de más de cien veces, por ejemplo, en el caso de *carB*). Experimentos recientes muestran un papel más complejo para el gen *carS*, cuyos mutantes están también alterados en la síntesis de otros metabolitos, como las giberelinas o las bicaverinas. Además, el análisis de estos mutantes han permitido poner en evidencia un mecanismo de inducción de la ruta por hambre de nitrógeno (Rodríguez-Ortiz et al., 2009).

En esta tesis se ha investigado la relación de dos fotoreceptores, la proteína ortóloga a WC-1 y la opsina *opsA*, con la carotenogénesis de *F. fujikuroi*. Los resultados se describen en los capítulos 1 y 2.

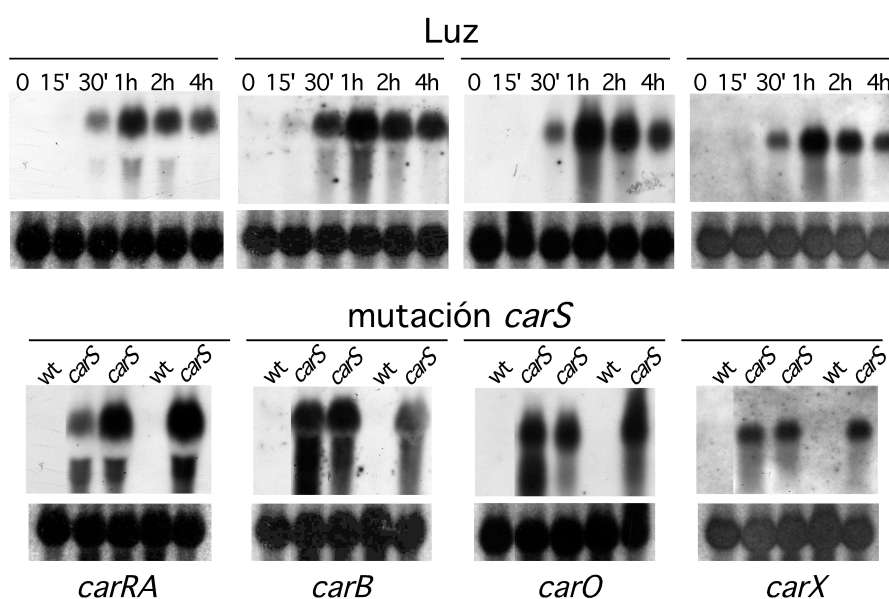


**Fig. I19.** Efecto de la luz y las mutaciones *carS* sobre los niveles de ARNm de cuatro genes *car* de *F. fujikuroi*. Arriba se representa la estirpe silvestre en oscuridad (0) o en distintos tiempos de iluminación, para cada uno de los genes. Abajo se comparan dos estirpes silvestres en oscuridad con tres mutantes *carS* (SG1,

SG22 y A06). Bajo cada carril se muestra se encuentra como control de carga una banda de ARNr.

### 3.2.3 Carotenogénesis en *N. crassa*.

Como *F. fujikuroi*, *N. crassa* posee una ruta biosintética que lleva a la síntesis de Neurosporaxantina, siendo este el organismo donde se describió esta xantofila por primera vez (Aasen y Jensen, 1965). La caracterización de la ruta en este hongo tuvo su origen en la identificación de mutantes albinos, genéricamente llamados *al*, y extensamente usados como marcadores genéticos por el fácil seguimiento de su fenotipo (Arpaia et al., 1995a; Li y Schmidhauser, 1995).

Los pasos de la ruta biosintética en este hongo, propuestos con anterioridad a esta Tesis, coinciden en lo esencial con los ya descritos para *F. fujikuroi* (Fig. I20). La reacción previa de la ruta, la síntesis de GGPP a partir de FPP y una molécula de IPP, la lleva a cabo la enzima AL-3 (albino-3). Los mutantes *al-3* son ligeramente rezumantes y acumulan pequeñas cantidades de caroteno. La interpretación de este hecho es que la pérdida total de función de *al-3* no es viable debido a que participa en la síntesis de terpenoides esenciales para la vida (Sandman et al., 1993a), como pueden ser los grupos geranil-geraniol de proteínas. La enzima bifuncional responsable de la síntesis de fitoeno se denomina AL-2. y la desaturasa de fitoeno AL-1 (Schmidhauser et al., 1990) a diferencia de *carB* en *F. fujikuroi* (Fernández-Martín et al., 2000). AL-1 lleva a cabo cinco desaturaciones consecutivas, que convierten al fitoeno en 3,4-didehidrolicopeno, pasando por fitoflueno,  $\zeta$ -caroteno, neurosporeno y licopeno. El dominio ciclasa de AL-2 es capaz de reconocer el licopeno como sustrato, compitiendo por tanto con la desaturasa AL-1, e introducir dos ciclaciones para dar lugar a  $\gamma$ -caroteno y  $\beta$ -caroteno.

En competición con la actividad ciclasa, a diferencia de *F. fujikuroi*, la desaturasa AL-1 no reconoce el  $\gamma$ -caroteno como sustrato (Hausmann y Sandmann, 2000), por lo que este caroteno se acumula o es convertido a  $\beta$ -caroteno por la actividad ciclasa de AL-2. Esta vía lateral de la ruta, puesta en evidencia por la acumulación de pequeñas cantidades de  $\gamma$ -caroteno y  $\beta$ -caroteno en este hongo (De Fabo et al., 1976), parece ser muy minoritaria, conduciendo la mayor parte de la ruta a 3,4-didehidrolicopeno.

Una vez producido el 3,4-didehidrolicopeno, la síntesis de neurosporaxantina requiere una reacción de ciclación, llevada a cabo por AL-2, capaz de actuar solo en el extremo no desaturado de la molécula, para dar lugar al toruleno. Este sufre finalmente un corte oxidativo para eliminar un fragmento de 5 átomos de carbono y dar lugar a  $\beta$ -apo-4'-carotenal, reacción catalizada por CAO-2 (Saelices et al. 2007), enzima ortóloga al CarT de *F. fujikuroi* (Prado-Cabrero et al 2007b). Finalmente, el extremo aldehído de este apocarotenoide es oxidado por una última enzima, caracterizada en esta Tesis, para producir la Neurosporaxantina. Los mutantes carentes de actividad ciclasa presentan una

pigmentación rojo pálida, y se ha propuesto que acumulan la versión no ciclada de la neurosporaxantina (Arrach et al. 2002).

La demostración de que la opsina NOP-1 liga retinal y es fotoreactiva (Bieszke et al., 1999a; Bieszke et al., 2007) sugiere fuertemente la capacidad de este hongo para sintetizar este apocarotenoide. *N. crassa* carece de un ortólogo evidente de CarX para desarrollar esta función, siendo la identificación de la actividad enzimática responsable uno de los objetivos actuales del grupo en el que se ha desarrollado este trabajo.

La carotenogénesis en *N. crassa* es constitutiva en los conidios (Baima et al., 1992), pero es dependiente de la luz en el micelio. La regulación de la carotenogénesis en las hifas por la luz es mediada por el complejo WC, descrito en la sección 2.2.2. Como ocurre con sus ortólogos en *F. fujikuroi*, los genes *al-1*, *al-2*, *al-3* y *cao-2* son fotoinducibles y presentan niveles máximos de ARNm aproximadamente a los treinta minutos de exposición a la luz (Arpaia et al., 1993; Saelices et al., 2007). La fotoinducción desaparece en los mutantes nulos de los genes *wc-1* o *wc-2*. En *N. crassa* no existen estirpes equivalentes a los mutantes *carS* de *F. fujikuroi*, pero existen dos mutantes que acumulan niveles mayores que la estirpe silvestre en la luz. El mutante *vvd* (*vivid*) acumula aproximadamente cinco veces más carotenoides que la estirpe silvestre (Schwerdtfeger y Linden, 2001), mientras que el mutante *ovc* (de “over carotenoid”) acumula aproximadamente el doble (Youssar et al., 2007). Ninguno de los dos mutantes produce más carotenoides que la estirpe silvestre en la oscuridad, lo que evidencia las diferencias a nivel de regulación entre *N. crassa* y *F. fujikuroi* a pesar de la similitud de sus rutas biosintéticas. Al contrario que *vvd*, el mutante *ovc* tiene una base molecular más compleja, ya que debe su fenotipo a una delección de 77 kb que ha provocado la pérdida de 21 genes (Youssar et al., 2007). El fenotipo *ovc* es además sensible a estrés osmótico debido a que uno de los genes delecionados es *cut-1*, cuya mutación confiere dicho fenotipo. La pérdida de función de *cut-1* no altera la síntesis de carotenoides, pero su introducción en el mutante *ovc* restaura la fotoinducción normal de la carotenogénesis, lo que le vincula al fenotipo *ovc*. En *N. crassa* el oxígeno y el agua oxigenada estimulan la acumulación de carotenoides (Iigusa et al., 2005). Este resultado, junto con el incremento en la concentración de carotenoides en mutantes de una catalasa (Michán et al. 2003) o de una superóxido dismutasa (Yoshida y Hasunuma, 2004), supuestamente sometidos a mayor estrés oxidativo, indican una regulación de la ruta por dicho estrés, presumiblemente asociado a las propiedades antioxidante de los carotenoides (Edge et al., 1997).



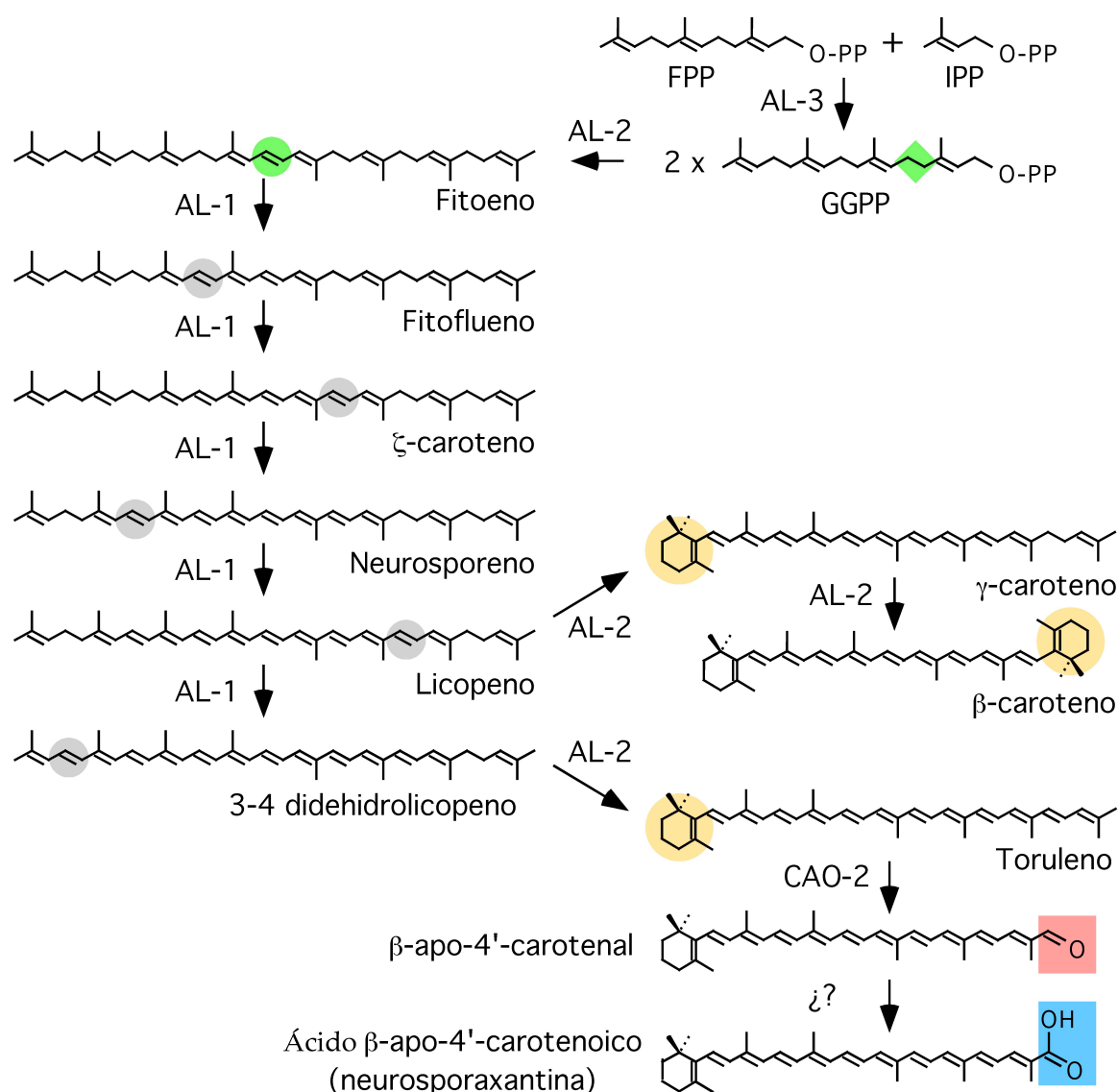


**Fig. I20.** Ruta biosintética de la carotenogénesis en *N. crassa*. Los productos de los tres genes *al* se conocían anteriormente. La enzima CAO-2 se descubrió durante el desarrollo de este trabajo. Se resaltan en distintos colores los lugares donde se ha generado una modificación química.

Esta Tesis ha contribuido al conocimiento de la síntesis de carotenoides en *N. crassa* mediante la caracterización de la última enzima de la ruta, responsable de la conversión de β-apo-4'-carotenal en Neurosporaxantina, determinada por el gen *ylo-1*, descrito en el capítulo 3. Además, mediante el análisis bioquímico de los intermediarios acumulados por distintos mutantes, incluyendo el propio mutante *ylo-1*, se ha propuesto un nuevo orden de reacciones enzimáticas para la ruta de la carotenogénesis en este hongo viene, descrito en el capítulo 4.

### 3.2.4 Síntesis de carotenoides en *Ustilago*

Con el objetivo de explorar un modelo fúngico alternativo, esta Tesis aborda por primera vez la síntesis de carotenoides en el hongo *U. maydis*. El inicio de este estudio se basa en la presencia en su genoma de genes ortólogos para *carRA/al-2* y *carB/al-1* de otros hongos y de tres genes para opsinas previsiblemente fotoactivas.

Anteriormente se ha analizado la síntesis de carotenoides en otras especie de *Ustilago*, *U. violacea*, patógeno de *Silene alba*. Diferentes estirpes de esta especie presentan diversos colores, desde tonalidades amarillentas a más rojizas, y acumulan diferentes mezclas de carotenos en la ruta desde fitoeno a  $\beta$ -caroteno (Will et al. 1984). Los resultados descritos en el capítulo 5 de esta Tesis son consistentes con los descritos en *U. violacea* y abren el camino a futuras investigaciones sobre esta ruta biosintética.



# Objetivos



## Objetivos

Esta Tesis se plantea cuatro objetivos relacionados con diferentes aspectos del metabolismo y la función de los carotenoides en los hongos.

1. Completar el conocimiento sobre la ruta biosintética de neurosporaxantina en el hongo *Neurospora crassa* mediante la caracterización de la alteración enzimática del mutante amarillo *ylo-1* y la base bioquímica de su patrón de carotenoides, así como la del pigmento acumulado por los mutante carentes de actividad ciclasa AL-2.
2. Investigar la función del gen *wcoA* de *Fusarium fujikuroi*, que determina la proteína ortóloga de White Collar 1 de *Neurospora crassa*, como posible fotoreceptor de la fotoinducción de la síntesis de neurosporaxantina.
3. Estudiar la función de la opsina presuntamente fotoactiva de *Fusarium fujikuroi* OpsA, mediante el análisis de la expresión de su gen y las consecuencias fenotípicas de su mutación.
4. Explorar el potencial de la levadura *Ustilago maydis* como nuevo modelo de estudio del metabolismo de los carotenoides en hongos basidiomicetos y analizar la función de un gen para una oxigenasa de carotenoides ortóloga a CarX de *Fusarium fujikuroi*, candidata a enzima productora del retinal para tres opsinas supuestamente fotoactivas predichas en su proteoma.



# Capítulos





## CAPÍTULO 1

El gen *ylo-1* determina una aldehído deshidrogenasa responsable de la última reacción de la ruta de la carotenogénesis en *Neurospora*

The *ylo-1* gene encodes an aldehyde dehydrogenase responsible for the last reaction in the *Neurospora* carotenoid pathway

Alejandro F. Estrada<sup>1</sup>, Loubna Youssar<sup>1</sup>, Daniel Scherzinger<sup>2</sup>, Salim Al-Babili<sup>2</sup>, and Javier Avalos<sup>1\*</sup>

<sup>1</sup> *Department of Genetics, Faculty of Biology, University of Seville, E-41012 Seville, Spain.*

<sup>2</sup> *Faculty of Biology, Albert-Ludwigs University of Freiburg, Schaezlestr. 1, D79104 Freiburg, Germany.*



---

**Abstract**

The accumulation of the apocarotenoid neurosporaxanthin and its carotene precursors explains the orange pigmentation of the *Neurospora* surface cultures. Neurosporaxanthin biosynthesis requires the activity of the *albino* gene products (AL-1, AL-2 and AL3), which yield the precursor torulene. Recently, we identified the carotenoid oxygenase CAO-2, which cleaves torulene to produce the aldehyde  $\beta$ -apo-4' carotenal. This revealed a last missing step in *Neurospora* carotenogenesis, namely the oxidation of the CAO2-product to the corresponding acid neurosporaxanthin. The mutant *ylo1*, which exhibits a yellow color, lacks neurosporaxanthin and accumulates several carotenes, but its biochemical basis is unknown. Based on available genetic data, we identified *ylo-1* in the *Neurospora* genome, which encodes an enzyme representing a novel subfamily of aldehyde dehydrogenases, and demonstrated that it is responsible for the yellow phenotype, by sequencing and complementation of mutant alleles. In contrast to the precedent structural genes in the carotenoid pathway, light does not induce the synthesis of *ylo-1* mRNA. *In vitro* incubation of purified YLO-1 protein with  $\beta$ -apo-4' carotenal produced neurosporaxanthin through the oxidation of the terminal aldehyde into a carboxyl group. We conclude that YLO-1 completes the set of enzymes needed for the synthesis of this major *Neurospora* pigment.

**Keywords:** ALDH Superfamily,  $\beta$ -apo-4' Carotenal, Apocarotenoid Acids, Neurosporaxanthin, Retinoic Acid

## 1. Introduction

Carotenoids are widespread terpenoid pigments (Britton et al., 2004) synthesized by all photosynthetic organisms (Hirschberg, 2001) and some heterotrophic bacteria (Armstrong, 1997) and fungi (Sandmann y Misawa, 2002; Avalos and Cerdá-Olmedo, 2004). Carotenoids protect the photosynthetic apparatus from photooxidation and represent structural components of light-harvesting antenna and reaction center complexes in plants. These pigments fulfill also a more general function as precursors for apocarotenoids, physiologically important compounds found in all taxa. Examples of these are represented by the ubiquitous chromophore retinal, the plant hormone abscisic acid, the fungal pheromone trisporic acid, and the key regulator of differentiation of vertebrate embryogenesis retinoic acid (Giuliano et al., 2003; Moise et al., 2005; Bouvier et al., 2005; Auldridge et al., 2006; Blomhoff, 2006). However, like other animals, vertebrates do not synthesize carotenoids *de novo*, and rely, therefore, on nutritional sources to meet their needs. Carotenoids confer their color to many flowers and fruits contributing substantially to plant-animal communication (Cunningham and Gantt, 1998; Hirschberg, 2001; Fraser and Bramley, 2004). Moreover, the bright colors of some animals, e.g. flamingos, some fungi, like the ascomycete *Neurospora crassa*, and some bacteria, e.g. *Erwinia*, are the visible results of carotenoid accumulation.

Because of methodological advantages, microorganisms have been major research objects in the analysis of carotenoid biosynthetic pathways (Johnson and Schroeder, 1996; Sieiro *et al.*, 2003). A well known example is *Neurospora crassa*, an outstanding genetic model for different biological phenomena (Davis, 2000), particularly fruitful in the area of fungal photobiology and circadian regulation (Linden, 2002; Vitalini *et al.*, 2006). A characteristic trait of this fungus is the orange pigmentation of its mycelial masses, caused by the accumulation of the xanthophyll neurosporaxanthin and variable amounts of its carotene precursors. Carotenoids also accumulate in the asexual spores, the conidia (Li and Schmidhauser, 1995), abundantly produced by illuminated, airborne mycelia (Lauter *et al.*, 1997).

The occurrence of albino strains, *al-1* to *-3*, enabled the elucidation of the first three steps in the carotenoid pathway of *Neurospora*. The initial reaction in the synthesis of these pigments is catalyzed by the prenyl transferase AL-3 (Sandmann *et al.*, 1993) mediating the formation of the precursor geranylgeranyl diphosphate (GGPP). Two molecules of GGPP are then condensated by the enzyme AL-2 to yield phytoene (Schmidhauser *et al.*, 1994), the first molecule with the characteristic C<sub>40</sub> carotene structure (Fig. C1.1). AL-2 is a bifunctional enzyme with  $\beta$ -cyclase activity in its amino domain (Arrach *et al.*, 2002), used in later steps. The colorless phytoene is subject to five desaturation reactions (Fig. C. 1), catalyzed by the desaturase AL-1, leading to 3,4-didehydro-lycopene via phytofluene,

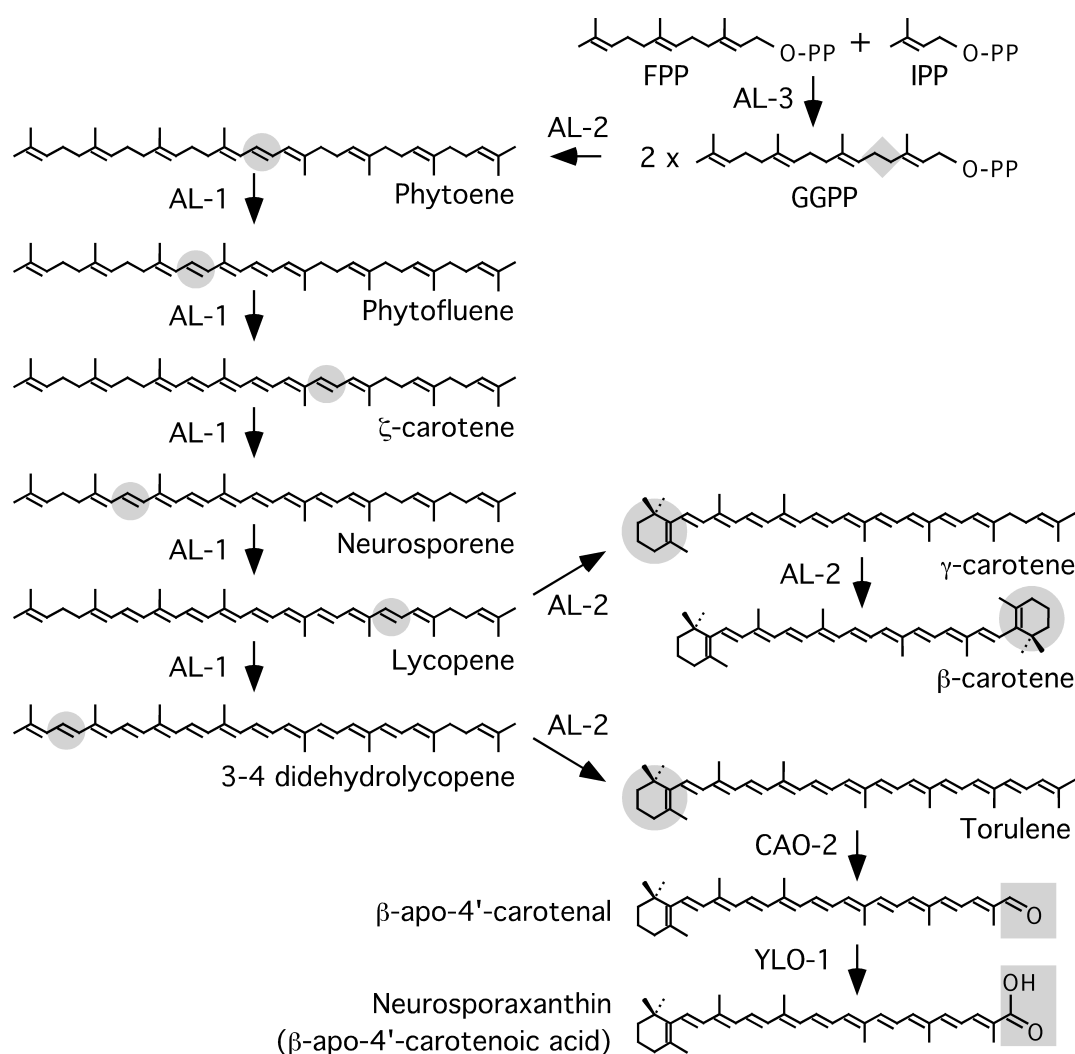


**Fig. C1.1 Carotenoid biosynthetic pathway of *Neurospora*.** The gene products responsible for each enzymatic reaction are indicated. Chemical changes from precursor molecules are highlighted as shaded areas. Attribution of the YLO-1 gene product to β-apo-4' carotenal oxidation derives from results of this work.

ζ-carotene, neurosporene and lycopene (Schmidhauser *et al.*, 1990; Hausmann and Sandmann, 2000).

The progressive introduction of conjugated double bonds shifts the absorption maxima towards longer wavelengths, resulting in the typical yellow to red colors of the desaturation products. The red compounds lycopene and 3,4-didehydro-lycopene are substrates of the β-cyclase activity of AL-2, converting the former into γ-carotene and β-carotene and the latter into torulene (Fig. C1.1). It was assumed that torulene was the precursor of the *Neurospora* end-product, the acidic C<sub>35</sub> apocarotenoid neurosporaxanthin. This was supported by the occurrence of a torulene-accumulating and neurosporaxanthin-lacking mutant of the closely related ascomycete *Fusarium* (*Gibberella fujikuroi*, Avalos and Cerdá-Olmedo, 1987). The identification of the responsible gene (*carT*) and the

enzymatic characterization of the encoded enzyme revealed the involvement of a carotenoid oxygenase mediating the cleavage of torulene into  $\beta$ -apo-4'carotenal (Prado-Cabrero *et al.*, 2007a). This indicated that  $\beta$ -apo-4'carotenal, the aldehyde form of the carboxylic neurosporaxanthin, was an intermediate of the carotenoid pathway in *Fusarium*. Recently, we characterized similar mutants in *Neurospora* showing that neurosporaxanthin synthesis employs, as in *Fusarium*, a carotenoid oxygenase, CAO-2, mediating the formation of  $\beta$ -apo-4'carotenal from torulene (Saelices *et al.*, 2007; Fig. C.1). Based on these data, we postulated an oxidizing enzyme which converts  $\beta$ -apo-4'carotenal into neurosporaxanthin, and, thus, catalyzes the last step in the *Neurospora* carotenoid pathway. The oxidation of apocarotenals into the corresponding acids is a common reaction utilized in both vertebrates and plants to produce the signaling molecules retinoic acid and abscisic acid, respectively. However, plants and vertebrates employ unrelated enzymes to perform this reaction. In plants, the abscisic aldehyde is converted by an aldehyde oxidase containing a molybdenum cofactor (MoCo) activated by a corresponding sulfurase (for review, see Nambara and Marion-Poll, 2005). In contrast, retinoic acid is produced by aldehyde dehydrogenases (ALDHs) with active sites containing a catalytic cysteine (for review, see Duester, 2000). Aldehyde dehydrogenases are also used by plants in carotenoid metabolism, as found for norbixin and bixin production from bixin aldehyde in *Bixa orellana* (Bouvier *et al.*, 2004).

Based on their different colors, three major mutant classes with qualitative alterations in the carotenoid content have been described in *Neurospora*: (1) *albino* (*al*) strains, missing either *al-1*, *al-2* or *al-3* functional alleles; (2) pale reddish mutants, lacking either AL-2 cyclase activity (Arrach *et al.*, 2002) or a *cao-2* functional allele (Saelices *et al.*, 2007); and (3) yellow (*ylo*) mutants. The yellowish appearance of the latter is presumably caused by differences in carotenoid content, as found with *ylo-1*, but it might be also associated with developmental alterations in other mutants, such as *ylo-2* or *ylo-3* (Perkins *et al.*, 2001). In contrast to the well characterized classes (1) and (2), the biochemical basis of the *ylo-1* mutants remained obscure. The two reports available on the carotenoid content of this mutant provided inconsistent data. Colored carotenoids represented less than 10% of the total carotenoid content in one case, with lycopene and  $\gamma$ -carotene as the predominant components (Goldie and Subden, 1973), and up to 50% in the second case, mainly constituted by  $\zeta$ -carotene and  $\gamma$ -carotene (Sandmann, 1993). In the first report, acidic carotenoids (namely neurosporaxanthin) were not detected, while these compounds were not investigated in the second one. The *ylo-1* mutation was genetically mapped on the left arm of linkage group VI (Wan *et al.*, 1997).

To clarify the *ylo-1* phenotype, we analyzed the carotenoid pattern of this mutant under growth conditions optimal for neurosporaxanthin biosynthesis. Based on enzymatic predictions and available genetic data, we identified the *ylo-1* gene in the *Neurospora*

genome, encoding a member of the widespread aldehyde dehydrogenase superfamily. Gene assignment was confirmed by the finding of mutated *ylo-1* alleles in two yellow mutants and the complementation of the yellow phenotype with the wild-type allele. The biochemical activity of heterologously expressed and purified YLO-1 protein suggested that this enzyme catalyzes the postulated  $\beta$ -apo-4'-carotenal oxidation step to yield neurosporaxanthin. The identification of YLO-1 and the elucidation of its enzymatic function complete the enzymatic scenario for neurosporaxanthin biosynthesis in this model fungus.

## 2. Results

### 2.1 Carotenoid pattern of the *ylo-1* mutant

Earlier analyses of the carotenoid pattern of the *ylo-1* mutant did not throw light on the underlying biochemical defect (Goldie and Subden, 1973; Sandmann, 1993). The lack of neurosporaxanthin and the presence of different intermediate carotenoids suggested a block in a late step of the carotenoid pathway. However, the complex carotenoid mixtures found under the experimental conditions tested hindered a more detailed interpretation. Illumination of *Neurospora* mycelia at low temperature results in a high neurosporaxanthin content in the wild type (Harding *et al.*, 1969) and, therefore, makes the identification of missing biosynthetic steps in carotenogenic mutants easier. Thus, submerged cultures of *cao-2* mutants, grown on Petri dishes and illuminated at 16°C, accumulated torulene as the major pigment and minor amounts of other carotenes, while neurosporaxanthin accounted for at least 75% of the carotenoids accumulated by the wild type (Saelices *et al.*, 2007). The proportion of this xanthophyll in the wild type increased to more than 95% upon introduction of three variations to our earlier experimental procedure, which we applied here to investigate the *ylo-1* phenotype: (a) shake cultures were used instead of Petri dishes, (b) the cultures were precooled for one hour at 4°C after the incubation at 30°C, and (c) illumination was done at 8°C instead of 16°C.

HPLC analyses of the carotenoids accumulated by the wild type under these improved experimental conditions showed a single major peak, with the typical absorption spectrum of neurosporaxanthin, and only traces of other carotenoids (Fig. C1.2A). Unexpectedly, the HPLC chromatogram from the *ylo-1* strain grown under the same conditions was more complex, with at least six prominent peaks. The amounts of two of them (peaks c and d) varied between different repetitions of the experiment, while the others were more regularly found. One of them (peak e) corresponds to all-*trans*-lycopene, as suggested by comparison with the authentic standard. Two minor surrounding peaks (e' and e'') exhibited a similar absorption spectrum and are likely lycopene derivatives. The UV-Vis-spectra of



the compound corresponding to peak d resembled the one of  $\beta$ -apo-4'-carotenal, but exhibited a longer maximal absorption wavelength (488 nm instead of 485 nm, see peak b in Fig. C1.5B). Also, it eluted later than  $\beta$ -apo-4'-carotenal (42.5 min against 40 min in Fig. C1.5B), suggesting a less polar isomer. Supportingly, LC-MS analyses revealed a molecular ion of  $m/z = 483.85 [M+H]^+$  (results not shown) which is consistent with that of  $\beta$ -apo-4'-carotenal. According to these data, this compound could be apo-4'-lycopenal. The carotenoids corresponding to peaks b and c could not be identified clearly. UV-Vis-spectra of peaks b and c resemble that of  $\gamma$ -carotene but show a different elution time. In agreement with Goldie and Subden (1973), neurosporaxanthin was not detected in our samples from this mutant.

Illumination of the wild type at 30°C instead of 8°C under otherwise identical culture conditions resulted in a drastic reduction of the carotenoid content (about 25-fold less than at 8°C) and the accumulation of a complex carotenoid mixture (Fig. C1.2B), which included phytofluene,  $\zeta$ -carotene, neurosporene,  $\beta$ -zeacarotene,  $\gamma$ -carotene,  $\beta$ -carotene and neurosporaxanthin. HPLC analyses of the *ylo-1* mutant showed a very similar mixture except that no neurosporaxanthin was detected (supplementary material 1). Similar results were obtained with another yellow mutant, called JA18 (results not shown), obtained by UV mutagenesis

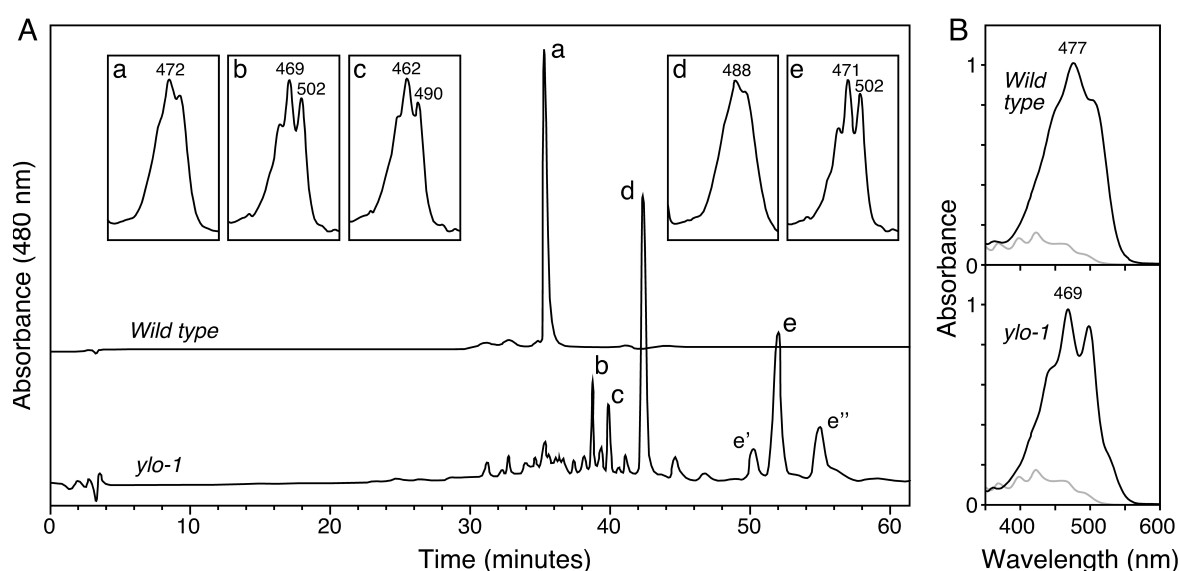


**Fig. C1.2 Phenotype of the *ylo-1* mutant.**

A. HPLC profiles of the carotenoid samples from submerged cultures of the wild type and *ylo-1* strains grown for 48 h in the dark at 30°C and 24h in the light at 8°C. Absorption spectra of major peaks are shown in inner boxes. Peaks a, and e were identified from standards as neurosporaxanthin and lycopene respectively.

B. Absorption spectra of the crude carotenoid samples from the cultures indicated above illuminated at either 8°C (black line) or 30°C (grey line). The 30°C samples were concentrated four-fold for better comparison.

## 2.2 Identification of the putative *ylo-1* gene in the *Neurospora* genome

The *ylo-1* mutation was mapped to the left arm of linkage group VI, between *cys-1* (8%) and *un-13* (2%; 38 kb) (Wan *et al.*, 1997). Analysis of the genomic region fitting these data pointed to the predicted genes NCU04008 and NCU04009. However, the encoded enzymes do not show significant similarities to aldehyde dehydrogenases (ALDHs) or aldehyde oxidases (AOs), known to convert apocarotenals into the corresponding acids (see introduction). Therefore, we searched for predicted ALDHs or AOs among neighboring genes. About 8 kb from NCU04009 we found the ORF NCU04013, which encodes an enzyme from the ALDH family. This fits unpublished data by T. J. Schmidhauser, who associated *ylo-1* to this class of enzymes (Perkins, 2001). The NCU04013 gene, that we have identified as *ylo-1* (see following section), extends along 1,685 bp in contig 7.12 in the *Neurospora* genome assembly, interrupted by an 84 bp intron, and encodes a presumptive 533 aa polypeptide. Structural analysis of the predicted YLO-1 protein revealed a highly conserved ALDH domain (Aldedh in the PFAM domain database, E-value below  $6.10^{-52}$ ) extending along 83% of the protein (residues 4-446), followed by a predicted unstructured segment (474-490) and a transmembrane segment (510-527) close to the carboxy end (Fig. C.3A). Closest matches obtained by Blast comparison of YLO-1 against the SwissProt data base were the dimeric aldehyde dehydrogenase 3A1 (ALDH class 3, member A1, human protein No. P30838) and fatty aldehyde dehydrogenase (ALDH class 3, member A2, human protein No. P51648), with 39% and 38% identities along 449 and 463 aa, respectively.

ALDHs compose a superfamily of NAD(P)<sup>+</sup>-dependent oxidoreductases, widely distributed from bacteria to humans, which catalyze the conversion of a wide spectrum of aldehydes into the corresponding acids. The eukaryotic ALDHs are divided into at least 22 families, based on specific homology criteria established by the ALDH Gene Nomenclature Committee (AGNC). According to the AGNC, protein sequences that are more than 40% identical to other previously identified ALDH sequence define a family, and sequences more than 60% identical are members of a protein subfamily. Protein sequences that are less than 40% identical would describe a new ALDH protein family (Vasiliou *et al.*, 1999; Kirch *et al.*, 2004). The highest identity of NCU04013 to already characterized class 3 ALDHs is 39%, which rises to 40% if the alignment is restricted to the ALDH segment. This indicates that this *Neurospora* enzyme represents a new subfamily in the ALDH3 group. A phylogenetic analysis of YLO-1 with representative proteins from these families confirms the ascription of this protein to ALDH class 3 (supplementary material 2). Other ALDH proteins found in the *Neurospora* genome, included in this analysis, belong to other families and are as dissimilar to YLO1 as to ALDHs from other taxa.

Aldehyde dehydrogenases share a conserved ALDH domain and differ in the presence of variable amino and carboxy extensions (see comparison of YLO1 with three representative examples in Fig. C1.3B), that include in some cases short organelle transit signals. Computational predictions rarely find transmembrane (TM) domains in these extensions; besides YLO1, only two proteins displayed in the phylogram (P38694 and P47740, supplementary material 2) contain a bona fide TM segment. P38694 is a yeast protein of unknown function with a 23 aa TM segment in its amino extension. The mouse protein P47740, phylogenetically closer to YLO1, contains a TM domain in a similar position in the carboxy extension (human counterpart P51648 displayed in Fig. C1.3B). P47740 and P51648 are fatty acid dehydrogenases (FALDHs), a subfamily of ALDHs that oxidize long-chain aliphatic aldehydes to fatty acids. The carboxy extensions of FALDH and YLO1 are less conserved than the ALDH domain, although some similarity is found between their respective TM segments (Fig. C1.3B). One of the proteins compared in Fig. C1.3B is a retinal dehydrogenase (RALDH-3, from the ALDH1 family), a subgroup of ALDH enzymes that recognizes a carotenoid substrate. YLO1 is less similar to retinal dehydrogenases (20%, 21% and 22% along 501, 518 and 512 aa for mouse RALDH-1, RALDH-2 and RALD-3 proteins, respectively) than to the ALDH3 family (39%), as confirmed by the greater distance exhibited in the phylogenetic tree (supplementary material 2). A low similarity (20%) is also found with bixin aldehyde dehydrogenase (AJ548846). Additionally, this enzyme and RALDHs contain very short carboxy extensions and lack putative TM domains.

### 2.3 Genetic identification of NCU04013 as the *ylo-1* gene

To confirm that NCU04013 is the *ylo-1* gene, we amplified by PCR, cloned and sequenced the alleles from the *ylo-1* mutants FGSC4100 and JA18. Comparison against the wild type NCU04013 sequence revealed the occurrence of a single mutation in each allele. The *ylo-1* FGSC4100 mutant exhibited a frameshift mutation (T insertion at position 349, Fig. C1.3B) before reaching a premature stop codon. The *ylo-1* JA18 allele encodes a premature stop codon at amino acid 113 (AAA->TAA), resulting in a truncated protein with only 21% of the native protein size (Fig. C.3B). These data indicated that the ORF NCU04013 is the sought-after *YLO-1* gene.

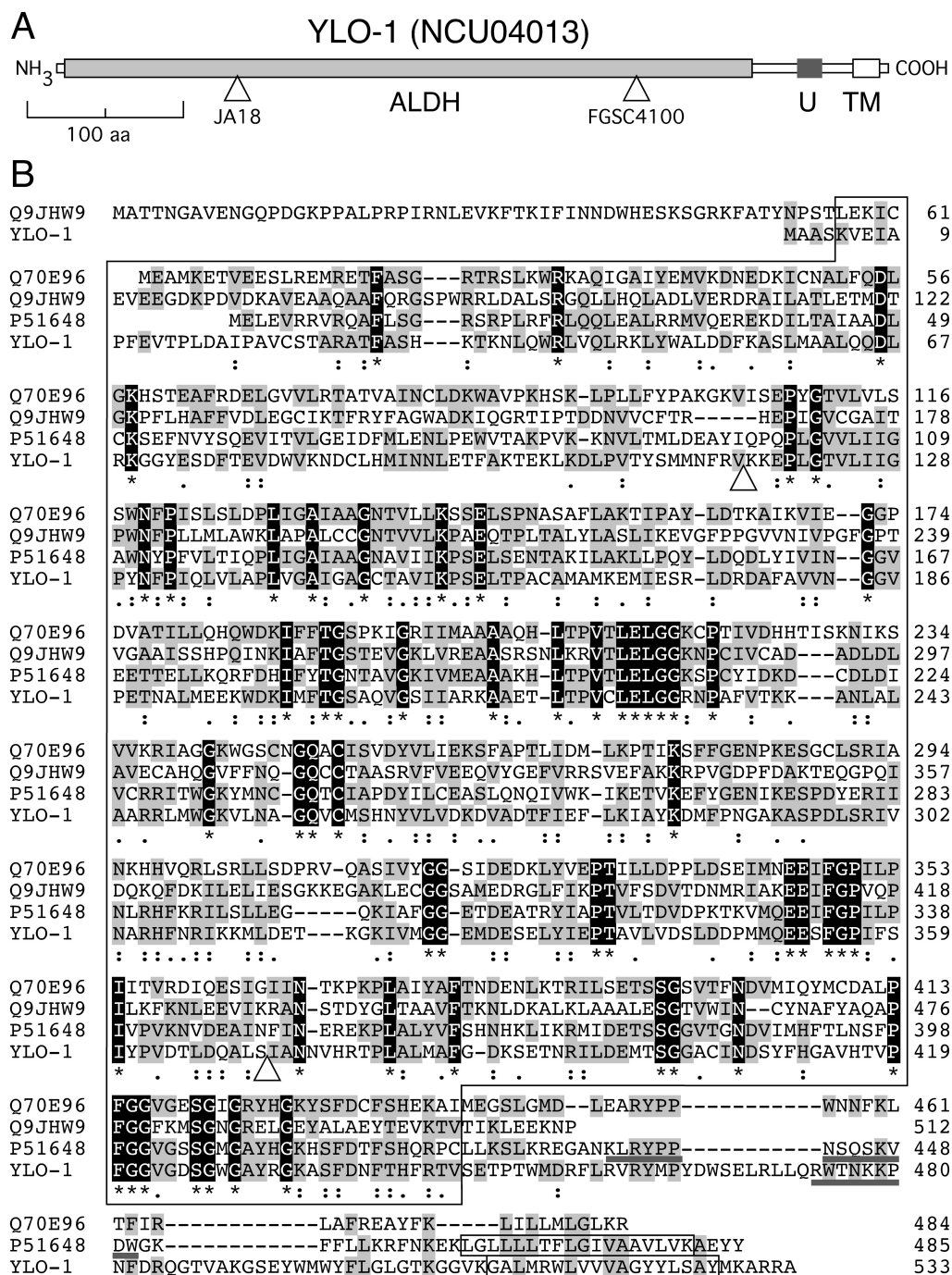


**Fig. C1.3** Sequence analysis of the predicted YLO-1 protein from *Neurospora*.

A. Schematic representation of the YLO-1 domain architecture. U and TM: predicted unstructured and transmembrane domains, respectively. The white arrowheads indicate the locations of the mutations on the *ylo-1* alleles of the FGSC4100 and JA18 mutants.

B. Clustal alignment of YLO-1 with three proteins from the ALDH family (Q70E96: Aldehyde dehydrogenase 3F1 from *Arabidopsis thaliana*; Q9JHW9: Retinal aldehyde dehydrogenase RALDH-3 from *Mus musculus*; P51648: human fatty aldehyde dehydrogenase). Residues present at the same position in at least two of the proteins are shaded in grey, and a black background is used for those conserved in the four proteins. The large box indicates the ALDH domain. The predicted unstructured and transmembrane domains found in the carboxy regions of YLO-1 and P51648 are underlined (grey line) and boxed, respectively.

To further confirm NCU04013 as *ylo-1*, spheroplasts from the *ylo1* FGSC4100 mutant were cotransformed with two plasmids harboring a *hygR* resistance cassette and the wild-type NCU04013 ORF equipped with 5' and 3' regulatory sequences. Following hygromycin selection, transformants were placed into individual slant tubes and checked for color. Among 74 transformants investigated, 62 exhibited the same yellow pigmentation as the *ylo-1* mutant, while 12 were orange resembling the wild type. Examples of two strains from each class are shown in Fig. C1.4A. Six orange transformants were randomly chosen for further molecular characterization. Southern blot analysis with an *ylo1* probe showed additional bands in the six transformants compared to the control strains, indicating the integration of at least one copy of the wild type *ylo-1* gene. Two examples, represented by T1 and T2, are shown in Fig. C1.4B. Carotenoid analyses of T1 and T2 mycelia grown at low temperature in parallel with the *ylo1* mutant and the wild type showed the recovery of neurosporaxanthin biosynthesis in both transformants (Fig. C1.4C), confirming the complementation of the *ylo1* phenotype.

#### 2.4 Characterization of YLO-1 enzymatic activity

The absence of neurosporaxanthin in the *ylo-1* mutant suggests that the YLO-1 enzyme is responsible for the oxidation of  $\beta$ -apo-4'carotenal to neurosporaxanthin. To confirm this hypothesis, we performed *in vitro* assays using  $\beta$ -apo-4'carotenal as a substrate. For this purpose, the *ylo-1* gene was expressed in *E. coli* as a Glutathione S-transferase (GST) fusion protein and purified using glutathione sepharose. The purified YLO-1 protein was then incubated with  $\beta$ -apo-4'carotenal. The reaction resulted in the formation of a product of identical chromatographic and spectrophotometric properties as neurosporaxanthin obtained from *Neurospora* wild type (Fig. C1.5A). As further confirmation, the substrate and the products were analyzed by LC-MS. The masses of the analyzed samples were consistent with the predicted molecular masses for  $\beta$ -apo-4'carotenal and neurosporaxanthin (Fig. C1.5B).

Members of the ALDH superfamily act on a diversity of aldehyde substrates such as acetaldehyde (EC:1.2.1.10), succinate-semialdehyde (EC:1.2.1.16), lactaldehyde (EC:1.2.1.22), benzaldehyde (EC:1.2.1.28,) methylmalonate-semialdehyde (EC:1.2.1.27), glyceraldehyde-3-phosphate (EC:1.2.1.9), delta-1-pyrroline-5-carboxylate (EC:1.5.1.12) or glutamate-5-semialdehyde (EC:1.2.1.41). The homology of YLO-1 to the members of the ALDH3-family pointed to a substrate specificity towards medium chain fatty aldehydes.

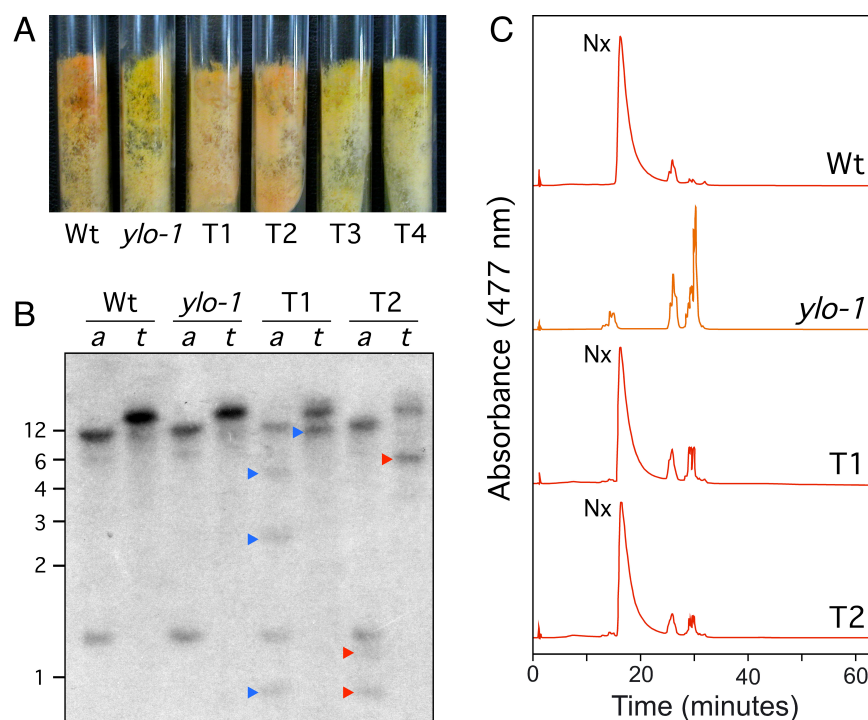


**Fig. C1.4 Complementation of the *ylo-1* mutation.**

A. Slant cultures of the wild type and two representative transformants from each of the two classes identified by visual screening.

B. Southern blot of genomic DNA from the wild type (WT), the *ylo-1* mutant and two selected transformants digested with *SacI* (*a*) or *StuI* (*t*) and hybridized with the *ylo-1* probe (see material and methods). The probed sequence contains a *SacI* restriction site (370 and 233 bp from the probe ends) and no *StuI* sites. Numbers on the left show size markers (kb). Red and blue arrowheads indicate additional bands in each transformant.

C. HPLC analyses of the carotenoid samples from the same four strains. The peak marked as Nx is neurosporaxanthin.

However, we did not detect significant activities upon the incubation of the enzyme with C<sub>9</sub> aldehyde nonanal (data not shown) which is converted readily by the human ALDH3A1 (Pappa *et al.*, 2003). Similarly, we did not detect any conversion of the shorter acetaldehyde and the cyclic benzaldehyde. These results pointed to a specificity for apocarotenals. To check whether it converts apocarotenals other than β-apo-4'-carotenal (C<sub>35</sub>), purified YLO-1 was incubated with β-apo-8'-carotenal (C<sub>30</sub>), β-apo-10'-carotenal (C<sub>27</sub>) and the acyclic apo-8'-lycopenal (C<sub>30</sub>). As shown in HPLC analyses (Fig. C1.6), the incubations with these apocarotenals resulted in the formation of compounds whose respective absorption spectra and elution patterns were consistent with their conversion to the corresponding carboxylic products. Indeed, in all cases, their absorption spectra acquired a secondary peak on the right and exhibited a maximal absorption at a shorter wavelength. The same features distinguish neurosporaxanthin when compared to β-apo-4'-carotenal. Accordingly, their molecular masses determined by LC-MS analyses increased as expected from the oxidative reaction (results not shown). The efficient activity on a non-cycled substrate, apo-8'-lycopenal, and the recognition of substrates of different chain

lengths indicate that the enzyme recognizes the end of the molecule with the aldehyde group and a partial segment of the aliphatic chain. To check the impact of the apocarotenal chain length on the enzymatic activity, purified YLO-1 was incubated with the C<sub>20</sub>-apocarotenal, retinal. In contrast to the longer substrates, we did not detect significant conversion of retinal (results not shown).

## 2.5 Expression of *ylo-1*

All the structural genes of the carotenoid pathway, *al-1*, *al-2*, *al-3* and *cao-2*, are transcriptionally induced by light (Li and Schmidhauser, 1995; Nelson *et al.*, 1989; Schmidhauser *et al.*, 1994; Saelices *et al.*, 2007). However, we did not detect significant changes of the *ylo-1* transcript level using Real-time RT-PCR after 30 min illumination,

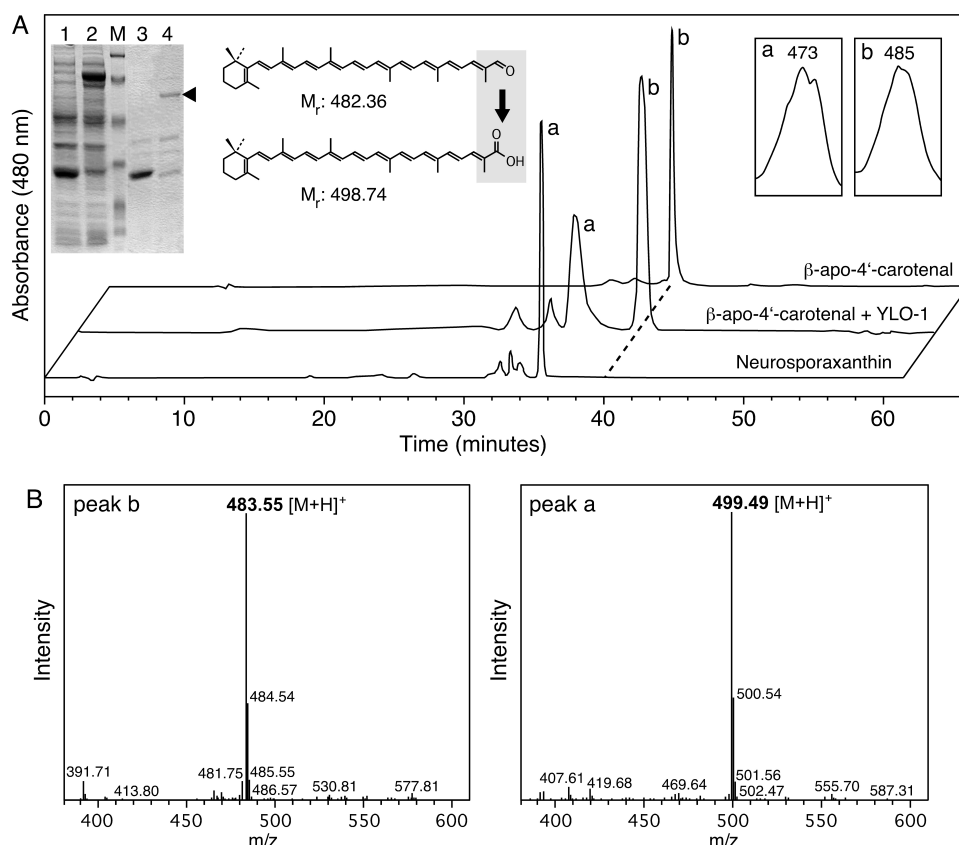


**Fig. C1.5** *In vitro* activity of YLO-1 on β-apo-4'-carotenal.

**A.** HPLC analyses of the *in vitro* assays with YLO-1 protein incubated with β-apo-4'-carotenal (peak b). Absorption spectrum and elution time of the generated product coincided with those of a neurosporaxanthin standard (peak a). The inner picture shows the SDS-PAGE of total *E. coli* extracts expressing either pGEXylo1 (lane 2) or the control plasmid pGEX5X1 (lane 1), and glutathionsepharose samples purified and digested with factor Xa from the former extracts (lane 3: from pGEX5X1, lane 4: from pGEXylo1). The YLO1 protein (59.5 kDa) is indicated with an arrowhead. The interpreted enzymatic reaction is depicted. Incubation with the control protein sample without YLO-1 (lane 3) gave the same chromatogram than β-apo-4'-carotenal standard (data not shown).

B. LC-MS analyses of peaks a and b from the chromatogram.

which is an optimal time for light induction of other genes along the pathway, such as *al-1* or *cao-2* (Li and Schmidhauser, 1995; Saelices *et al.*, 2007). Time courses of the light responses in *Neurospora* are known to be variable (Lewis *et al.*, 2002).

Therefore, we measured *ylo-1* transcript levels after different illumination times covering a range from 15 min to 4 hours (Fig. C1.7), but we did not observe any significant induction of *ylo-1* over this wide range. As expected, the genes *al-1* or *cao-2*, used here as a control, exhibited a fast induction followed by a characteristic photoadaptation after one hour exposure. These results indicate that *ylo-1* is not co-regulated by light with the genes responsible for the preceding reactions in the carotenoid pathway.

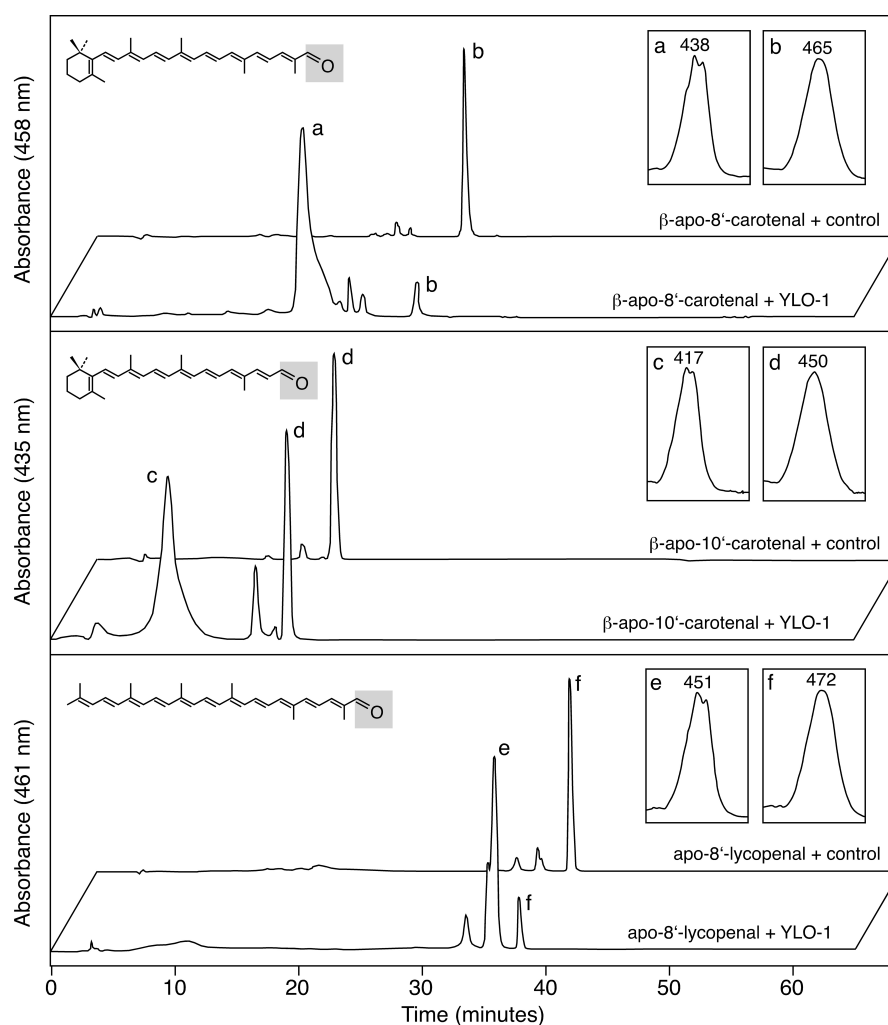


**Fig. C1.6. *In vitro* activity of YLO-1 on alternative carotenoid aldehydes.** HPLC-analyses of the *in vitro* assays with purified YLO-1 protein incubated with  $\beta$ -apo-8'-carotenal (above),  $\beta$ -apo-10'-carotenal (medium) and apo-8'-lycopenal (below). Chromatograms behind show the corresponding incubations with the control protein sample without YLO-1 (lane 3 in SDS-PAGE picture, Fig. 5). Absorption spectra of the relevant peaks are shown in inner boxes.



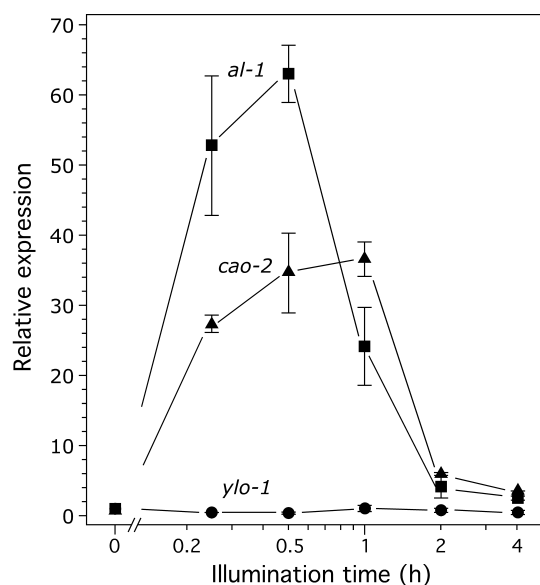


**Fig. C1.7. Expression of the gene *ylo-1*.** Real-time RT-PCR analyses of the genes *ylo1*, *al-1* and *cao-2* from RNA samples of the wild type strain grown in the dark and exposed to light for the times indicated (hours). Relative expression was referred to the value for each gene in the dark. The bars represent the standard deviation for 4 determinations from two independent experiments.

### 3. Discussion

The *yellow* (*ylo*) group of *Neurospora* mutants comprises several strains distinguished by their color (Perkins *et al.*, 2001). Earlier reports on the *ylo1* mutant described the absence of neurosporaxanthin (Goldie and Subden, 1973) and the presence of a complex carotenoid mixture, with  $\gamma$ -carotene and  $\zeta$ -carotene as the major components (Sandmann, 1993).

This phenotype suggested a defect in a late step of neurosporaxanthin biosynthesis, but the carotenoids accumulated by the mutant did not fit any simple hypothesis or specific block of the carotenoid pathway. Possible roles for YLO-1 on lycopene C3C4 desaturation or on torulene carboxylation were tentatively proposed (Goldie and Subden, 1973), but the absence of 3,4-didehydrolycopene or torulene in the *ylo-1* mutant contradicted these hypotheses. The recent discovery of the carotene oxygenase CAO-2 and the predicted formation of  $\beta$ -apo-4' carotenal (Saelices *et al.*, 2007) suggests *Neurospora* encodes an enzyme oxidizing this aldehyde to produce neurosporaxanthin. Our results demonstrate that *ylo-1* codes for the enzyme responsible for this reaction. This was supported genetically, by identification of mutations in two independent *ylo* strains and complementation of one of them, and biochemically, by the catalytic activities of the YLO-1 enzyme demonstrated *in vitro*.

The phenotype of the *ylo-1* mutant seemingly does not conform to the function imputed to YLO-1 in *Neurospora* carotenogenesis: the loss of this enzyme is not expected to cause an increase in the content of yellow carotenoids; actually, the neurosporaxanthin

precursors torulene and  $\beta$ -apo-4'carotenal are reddish. This should be especially true under culture conditions leading to the accumulation of neurosporaxanthin as the almost sole component in the wild type, and therefore, to the accumulation of the corresponding intermediates in the mutants (Arrach *et al.*, 2002; Saelices *et al.*, 2007). According to this scenario, the *ylo-1* mutant should accumulate  $\beta$ -apo-4'carotenal, the cleavage product of torulene and the substrate of YLO-1. However, we detected a more complex mixture composed of lycopene beside other compounds. The major one (peak d, Fig. C1.2A) is likely to be apo-4'lycopenal, the acyclic, less polar isomer of  $\beta$ -apo-4'carotenal. Other compounds (peaks b and c) could be  $\beta$ -apo-4'carotenal degradation products, a hypothesis that would explain the lack of this molecule in the *ylo-1* strain. Earlier analyses found polar "residual carotenoids" in the *ylo-1* mutant in higher amounts than in the wild type, tentatively interpreted as epoxy-carotenoids (Goldie and Subden, 1973). The high similarity of the UV-Vis-spectra of the compound c to  $\gamma$ -carotene may explain the earlier misidentification of this carotenoid in the *ylo-1* mutant. Detailed chemical analyses will be needed for the identification of these carotenoids and to explain their putative origin.

The eventual degradation of  $\beta$ -apo-4'carotenal would not explain the high concentration of lycopene and the assumed occurrence of apo-4'lycopenal in the *ylo-1* mutant. This is not an allele-specific effect, since the same result was obtained with an independent yellow mutant. Rather, this effect suggests the need of functional YLO-1 for proper function of enzymes further upstream in the pathway. YLO-1 could possibly interact with the cyclase domain of AL-2 for its efficient function; thus, lack of YLO-1 would result in lycopene abundance in the mutant (Fig. C1.2). A less efficient desaturation of lycopene by the AL-1 enzyme is also apparent in the absence of YLO-1, as judged by the lack of 3,4-didehydro-lycopene. The specific alterations of such enzymatic activities could be also related to changes in the physical properties of the membranes produced by the accumulation of different carotenoids, as shown to happen on *in vitro* generated liposomes (Wisniewska *et al.*, 2006).

In contrast to the results found under illumination at low temperature, the wild type and the *ylo1* mutant accumulated similar carotenoid mixtures upon illumination at 30°C, with the exception of the lack of neurosporaxanthin in the mutant strain. Although these experimental conditions are close to the optimal for *Neurospora* growth, the amount of carotenoids was much lower than upon illumination at 8°C. Moreover, different intermediates accumulated and neurosporaxanthin was a minor component, implying a very low efficiency of the carotenogenic machinery at 30°C. No reports are available on the effect of temperature on the expression of the carotenogenic genes or on the corresponding enzymatic activities, but a higher efficiency at optimal growth could be presumed. The reasons for the unexpected efficacy of carotenoid biosynthesis at low

temperature, earlier described (Harding, 1974), remain a fascinating biochemical challenge.

The *ylo-1* gene was identified thanks to available genetic data, unpublished information from T.J. Schmidhauser (cited by Perkins *et al.*, 2001), and our own biochemical predictions. ALDHs possess a similar enzymatic function on a large diversity of organic compounds. All of them have in common the oxidation of an aldehyde to a carboxy group, i.e., as in the case of the production of neurosporaxanthin ( $\beta$ apo-4'carotenoic acid) from  $\beta$ -apo-4'carotenal. YLO-1 shares common structural features with most ALDHs: 5643 of the 6798 proteins from this superfamily in the Pfam database (<http://pfam.sanger.ac.uk/>) consist of a single ALDH domain (called Aldeh in the database), surrounded by short amino and carboxy end segments, while the rest have a more complex architecture in combination with other functional domains. In YLO-1, the ALDH domain is combined with a short carboxy extension that includes a TM domain, pointing to a membrane-anchored enzyme. This is not surprising: differential centrifugation of *Neurospora* cell extracts located the carotenoids in membranes fractions (MitzkaSchnabel and Rau, 1980). Enzymes further upstream in the pathway are also membrane bound (MitzkaSchnabel, 1985), and similarly, the high hydrophobicity of the lycopene cyclase domain of AL-2 implies its physical integration in the membrane (Arrach *et al.*, 2001, 2002).

By functional similarity, we might expect YLO-1 to be related to retinal dehydrogenases, which oxidize either 9-*cis*- or all-*trans*-retinal to retinoic acid. Retinal is very similar to the YLO-1 substrate,  $\beta$ -apo-4'carotenal, from which it differs only in the length of the aliphatic hydrocarbon chain (20 against 35 carbon atoms, respectively). In chordates, these reactions are catalyzed by at least three different ALDHs (RALDH-1 to 3), representing some of the proteins involved in vitamin A metabolism, together with alcohol dehydrogenases and retinoid-binding proteins (Duester, 2000). Retinal dehydrogenases probably originated independently from YLO-1 in evolution, as suggested by the lack of a particularly high similarity and the absence of a TM domain. The later is not unexpected, considering the different physiological context of retinoids metabolism in animal tissues, which includes the use of specialized proteins for retinoid binding and transport (Napoli, 1996). Retinal dehydrogenases interact with retinal-bound RBP (retinol-binding protein) (Posch *et al.*, 1992), while YLO-1 probably recognizes  $\beta$ -apo-4'carotenal bound to a plasma membrane.

The occurrence of a TM domain in an ALDH protein is rare in this enzyme family but not unique to YLO-1. It is also found in mammal fatty ALDH (EC 1.2.1.3, human protein P51648), an enzyme that catalyzes the oxidation of long-chain aliphatic aldehydes to fatty acids (Chang and Yoshida, 1997), and where mutants thereof produce the Sjögren-Larsson syndrome (Haug and Braun-Falco, 2006). Like YLO1, fatty ALDH is active on a variety of

substrates, in this case either saturated or unsaturated, and between 6 and 24 carbons in length. Both enzymes have in common the oxidation of hydrophobic membrane-embedded compounds and apparently are membrane-anchored proteins. Linkage to the membrane provides access to the substrate and the unstructured domain may act as a hinge allowing a free interaction of the enzyme on the membrane surface. In both cases, the enzyme recognizes a part of the hydrophobic chain, suggesting that their active centers include a hydrophobic surface able to insert partially into the membrane. In the case of YLO-1, a minimal length for the hydrophobic chain was required for efficient substrate recognition *in vitro*.

The conversion of apocarotenals, other than retinal or bixin aldehyde, into the corresponding acids is novel and has not been described for any aldehyde dehydrogenase so far. In rats, an alternative retinoic acid formation was proposed, which is initiated by the oxidization of apocarotenals into apocarotenoic acids which are then shortened to retinoic acid by a mechanism similar to the  $\beta$ -oxidation of fatty acids (Barua and Olson, 2000). However, none of the characterized animal ALDHs was shown to catalyze such an activity. Indeed, the YLO1 enzyme represents a new subfamily of ALDHs, as indicated by phylogenetic analyses (supplementary material 2). Moreover, the absence of neurosporaxanthin in the *ylo1* mutant suggests that the oxidization of  $\beta$ -apo-4'-carotenal is unique to YLO1, which could not be replaced by any of the other 12 ALDHs occurring in *Neurospora* (supplementary material 2).

Light stimulates the biosynthesis of carotenoids in *Neurospora* (Harding *et al.*, 1969; Harding and Turner, 1981). This activation is achieved by the White Collar complex at the level of transcription of the four structural genes identified for the carotenoid pathway, *all*, *al2*, *al3* and *cao2* (Li and Schmidhauser, 1995; Nelson *et al.*, 1989; Schmidhauser *et al.*, 1994; Saelices *et al.*, 2007). The light induction is transient, a phenomenon known as photoadaptation and exhibited also by other WC-controlled genes (Schwerdtfeger and Linden, 2001; He and Liu, 2005). In contrast to the other structural genes of the carotenoid pathway, *ylo1* is not induced by light, a feature that could explain the low efficiency of neurosporaxanthin formation by the wild type at 30°C. Irrespective of light, the *ylo1* mutants do not exhibit alterations in growth or morphology under laboratory conditions, suggesting lack of relevant roles for YLO-1 aside from *Neurospora* carotenogenesis.

YLO-1 completes the set of enzymes needed for neurosporaxanthin biosynthesis in *Neurospora*. A similar enzyme is expected to achieve the same reaction in other neurosporaxanthin producing fungi, such as those of the genus *Fusarium* (Bindl *et al.*, 1970; Avalos and Cerdá-Olmedo, 1987; Sakaki *et al.*, 2002). Experiments in progress to characterize the orthologous *ylo-1* gene in *Fusarium fujikuroi* are expected to confirm and complement our data in *Neurospora*. However, organisms from other taxa have adapted different aldehyde dehydrogenases for the synthesis of other carboxylic apocarotenoids, as

found for retinoic acid in animals or bixin in plants. Carboxylic apocarotenoids are rare in fungi, and YLO-1-like proteins may represent a singular group of ALDH enzymes, lately developed by some fungal groups, whose evolutionary relevance remains to be elucidated.

## 4. Experimental Procedures

### 4.1 *Neurospora* strains and culture conditions

The Wild-type 74-OR23-1 A, and the mutant FGSC4100 (*ylo-1* a, allele *Y30539y*) are deposited in the Fungal Genetic Stock Center (McCluskey, 2003). The mutant JA18 was identified as a yellow strain after a UV search as described by Arrach *et al.* (2002).

For carotenoid analyses, the strains were grown in 500-ml Erlenmeyer flasks with 200 ml Vogel's broth (Davis and de Serres, 1970) inoculated with  $10^5$  conidia and shaken at 150 rpm. Incubations were done for two days in the dark at 30°C, followed by one day in the light at the same temperature or at 8°C under 4 Wm<sup>-2</sup> white light obtained with two fluorescent tubes. In the case of 8°C incubation, the flasks were placed in a 4°C chamber for one hour before incubation under light.

For genomic DNA and total RNA extractions, the strains were grown for two days in Petri dishes at 30°C in 25 ml liquid Vogel's media.

Liquid cultures were supplemented with 0.2% Tween 80 to suppress aerial development and subsequent conidia formation.

### 4.2 Transformation and southern blot analysis

Spheroplasts of the *ylo-1* strain FGSC4100 were prepared as described by Royer and Yamashiro (1992), using Glucanex (Novozymes Switzerland AG, Dittingen, Switzerland) as cell-wall-lysing enzymes. A spheroplast sample was transformed with 0.5 µg of plasmid pHJA2 (Fernández-Martín *et al.*, 2000) and 1 µg of plasmid pGEM-YLO following the protocol of Vollmer and Yanofsky (1986). Transformants were selected on hygromycin B-supplemented medium (250 mg l<sup>-1</sup>). pHJA2 contains a hygromycin resistance cassette and pGEMYLO contains the *ylo-1* gene. The latter is the result of introducing in the pGem®-T vector (Promega, Mannheim, Germany) a 3,815 bp PCR product obtained from wild-type genomic DNA with primers 5'-GATGATCAGTTGAGCTTCGCGG-3' and 5'-GTTGAATCGTGCTCACGTAGC-3'. This DNA segment contains the NCU04013 ORF surrounded by 1,446 bp and 683 bp of upstream and downstream regulatory sequences, respectively. PCR amplifications were achieved with the Triplmaster PCR system (Eppendorf AG, Hamburg, Germany) to maximize replication fidelity.

DNA samples were obtained with the GenElute Plant Genomic DNA Miniprep Kit (Sigma). Southern blot hybridization was performed as described by Sambrook and Russell (2001). A nylon membrane was probed at 68°C with a <sup>32</sup>P-labeled 603 bp segment from the *ylo-1* gene obtained by PCR with primers 5'-CAATAACGTGCACCGGACGC-3' and 5'-CGAGGTAATGTGCAAGTGAC-3'.

#### 4.3 Real-time RT-PCR analyses

Real-time RT-PCR expression analyses were performed with DNase I-treated total RNA samples obtained with the Perfect RNA Eukaryotic Kit (Eppendorf). The reactions, carried out in 25 µl volumes in an ABI 7500 equipment (Applied Biosystems), started with 30 min retrotranscription step at 48°C, and were followed by 10 min at 95°C and 40 cycles of 95°C denaturation for 15 s and 60°C polymerization for 1 min. Dissociation steps were achieved afterwards. Optimization of MgCl<sub>2</sub> and primer concentrations and annealing temperatures were done as described by Estrada and Avalos (2008) using 50 ng of RNA and 5 µM of each primer. The primers used for the reactions were 5'-CGGTGGTGGGCGAGAA-3' and 5'-TCCAATGTTTCCCCAACTACAAC-3' (*all*), 5'-TCAAGGGACTGAGAGAGCCG-3' and 5'-CGTTGACGTTGTTGTGCCAC-3' (*cao2*), and 5'-ACTGCCTGCACATGATCAACA-3' and 5'-CGGGCAGATCCTTG AGCTT-3' (*ylo1*). The β-tubulin gene of *N. crassa* NCU04054 (primers 5'-CGTCCATCAGCTCGTTGAGA-3' and 5'-CGCCTCGTTGTCAATGCA-3') was used as endogenous control for constitutive expression. The primers were designed with the software Primer Express™ v2.0.0 (Applied Biosystems) from intronless sequences of each gene and synthesized (HPLC grade) by StabVida (Oeiras, Portugal). Relative gene expression was calculated with the 2<sup>-ΔΔCT</sup> method (Sequence Detection Software v1.2.2, Applied Biosystems). Each RT-PCR analysis was performed four times (duplicated samples from two independent experiments) and standard deviations calculated to ensure statistical accuracy.

#### 4.4 In vitro protein expression and enzyme assays

For in vitro analysis, the *ylo-1* coding sequence was amplified with primers 5'-ATGGCCGCATCCAAAGTCG-3', and 5'-CGAGGTAATGTGCAAGTGAC-3' from cDNA obtained from a total RNA sample of the wild-type strain using the SuperScript III First-Strand Synthesis System for RT-PCR (Invitrogen, Paisley, UK). The PCR product was cloned into pSC (Strataclone) leading to plasmid pSCylo1, and the inserted cDNA was sequenced to confirm integrity and orientation. The inserted sequence was then removed from pSC-ylo1 by *EcoRI* digestion and subcloned into *EcoRI*-treated pGEX-5X-1 (Amersham Biosciences, NJ, USA). The resulting plasmid, pGEX-ylo1, was introduced

into JM109 *E. coli* cells. The transformed cells were grown, induced with 0.1 mM IPTG, and the protein was purified as described by Prado-Cabrero *et al.* (2007b).

Carotenoids used for enzyme assays ( $\beta$ -apo-4'-carotenal,  $\beta$ -apo-8'-carotenal,  $\beta$ -apo-10'-carotenal and apo-8'-lycopenal) were kindly provided by BASF (Ludwigshafen, Germany). These substrates were purified on TLC silica gel plates (Merck, Darmstadt, Germany) run in petroleum benzene/diethylether/acetone (40:10:7, v/v/v). The substrates were scraped off under dim light and eluted with acetone. To produce micelles, the substrates were mixed with 150  $\mu$ l of 4% (v/v) octyl- $\beta$ -glucoside in ethanol and dried in a vacuum centrifuge. The resulting gel was carefully resuspended in 100  $\mu$ l of 200 mM pyrophosphate (anhydride), pH 7.5, 200 mM NaCl and mixed with 25  $\mu$ g of purified protein in 100  $\mu$ l distilled water, to yield a final substrate concentration of 50 mM. NAD was used as cofactor at a final concentration of 1 mM. Incubations were done at 27°C for 30 min, stopped by addition of 1 vol acetone, extracted with petroleum benzene/diethylether (1:4, v/v) and subjected to HPLC analyses. The products obtained from the assay were purified directly from the HPLC, dried and dissolved again in chloroform for LC-MS analysis.

#### 4.5 Analytical methods

Substrates were quantified spectrophotometrically from their absorption spectra using  $\lambda_{\max}$  extinction coefficients calculated from E1% as given by Barua and Olson (2000) or as determined from synthetic standards (BASF, Ludwigshafen, Germany). Protein concentration was determined with the Bio-Rad protein assay kit (Bio-Rad, CA, USA). HPLC analyses of carotenoids were done using a Waters system (Eschborn, Germany) equipped with a photodiode array detector (model 996) and a C30-reversed phase column (YMC Europe, Schermbeck, Germany) or a Hewlett Packard 1100 series system (Waldbronn, Germany), equipped with a photodiode array detector and a C30-reversed phase column (Waters, hypersil ODS). The separations were performed using the solvent systems A (MeOH/ tert-butylmethylether, 500:500, v/v), and B (MeOH/ tertbutylmethylether/ water, 600:120:120, v/v/v). In both HPLC equipments, the C30 column was developed at a flow rate of 1 ml min<sup>-1</sup> with a linear gradient from 100% B to 57% A 43% B within 25 min, followed by a linear gradient to 100% A with a flow rate of 1.5 ml within 7 min. The flow was then increased to 2 ml min<sup>-1</sup> of 100% A maintaining these conditions for 32 min. Carotenoids from wild type, mutants *ylo-1* and JA18, and transformants T1 and T2 were extracted following Youssar and Avalos (2007) and analyzed as described above.

LC-MS analyses of HPLC-purified compounds were performed using a Thermo Finnigan LTQ mass spectrometer coupled to a Surveyor HPLC system consisting of a

Surveyor Pump Plus, Surveyor PDA Plus and Surveyor Autosampler Plus (Thermo Electron, Waltham, MA). Separations were carried out using a YMC-Pack C30-reversed phase column (150 x 3 mm i.d., 3  $\mu$ m) with the solvent system A: MeOH/water/tert-butylmethyl ether (50:45:5, v/v/v) and B: MeOH/water/tert-butylmethyl ether (27:3:70, v/v/v) with the water containing 0.1 g l<sup>-1</sup> ammonium acetate. The column was developed at a flow rate of 450  $\mu$ l min<sup>-1</sup> with 90% A and 10 % B for 5 min, to 5% A and 95% B in 10 min, then increasing the flow to 900  $\mu$ l min<sup>-1</sup> within 4 min and maintaining these final conditions for 5 min. The identification of  $\beta$ -apo-4'-carotenal and neurosporaxanthin were carried out using APCI in positive mode. Nitrogen was used as sheath and auxiliary gas and set to 20 and 5 units, respectively. The vaporizer temperature was 350°C and capillary temperature 150°C. The source current was set at 5  $\mu$ A, and the capillary and tube lens voltages were set at 49 V and 125 V, respectively.

### Acknowledgements

We thank Prof. Peter Beyer and Dr. Jorge Mayer for valuable discussions of the manuscript. We are indebted to Dr. Hansgeorg Ernst for providing the apocarotenals. This work was supported by Deutsche Forschungsgemeinschaft (DFG) Grant 892/1-3 and the Spanish Government (Ministerio de Ciencia y Tecnología, projects BIO2003-01548 and BIO2006-01323, and Acciones Integradas Hispano-Alemanas). We are grateful to Dr. T.J. Schmidhauser for unpublished work on *ylo-I* identification.





## CAPÍTULO 2

La identificación de nuevos apocarotenoides intermediarios en mutantes de *Neurospora crassa*, implican un nuevo orden de reacciones para la formación de neurosporaxantina

Novel apocarotenoid intermediates in *Neurospora crassa* mutants imply a new biosynthetic reaction sequence leading to neurosporaxanthin formation

Alejandro F. Estrada<sup>a</sup>, Dominic Maier<sup>b,c</sup>, Daniel Scherzinger<sup>b</sup>, Javier Avalos<sup>a</sup>, Salim Al-Babili<sup>b\*</sup>

<sup>a</sup> Department of Genetics, Faculty of Biology, University of Seville, E-41012 Seville, Spain

<sup>b</sup> Cell Biology, Institute for Biology II, Faculty of Biology, Albert-Ludwigs University of Freiburg, Schaenzlestr. 1, D-79104 Freiburg, Germany

<sup>c</sup> Current address: Laboratory of Epithelial Cell Biology, Institut de recherches cliniques de Montréal (IRCM) 110, avenue des Pins Ouest, Montréal (Québec) H2W 1R7, Canada



**Abstract**

Neurosporaxanthin,  $\beta$ -apo-4'-carotenoic acid ( $C_{35}$ ), represents the end-product of the carotenoid pathway in *Neurospora crassa*. It is supposed to be synthesized in three steps catalyzed by sequential AL-2, CAO-2 and YLO-1 activities: (i) cyclization of 3,4-didehydrolycopene ( $C_{40}$ ); (ii) cleavage of torulene into  $\beta$ -apo-4'-carotenal ( $C_{35}$ ); and finally (iii) oxidation of  $\beta$ -apo-4'-carotenal. However, analyses of the *ylo-1* mutant revealed the accumulation of intermediates other than  $\beta$ -apo-4'-carotenal. Here, we generated a 3,4-didehydrolycopene accumulating *E. coli* strain and showed that CAO-2 cleaves this acyclic carotene *in vivo* and *in vitro* yielding apo-4'-lycopenal. The apocarotenoids accumulated in the *ylo-1* mutant were then identified as apo-4'-lycopenal and apo-4'-lycopenol, pointing to the former as the YLO-1 substrate and indicating that cyclization is the last step in neurosporaxanthin biosynthesis. This was further substantiated by analyses of a cyclase-deficient *al-2* mutant, revealing the accumulation of apo-4'-lycopenoic acid. The three acyclic apocarotenoids presented here have not been found naturally before.

**Index Descriptors:** Apocarotenoids, Carotenoid Biosynthesis, Carotenoid Cleavage, *Neurospora crassa*, Fungi, Neurosporaxanthin

## 1. Introduction

Carotenoids are widely distributed isoprenoid pigments fulfilling diverse functions in all taxa (Britton *et al.*, 2004). Due to their vital role in protecting the photosynthetic apparatus from photooxidation, carotenoids are synthesized in all photosynthetic organisms. Moreover, carotenoids represent essential structural components of the light-harvesting antenna and reaction center complexes and are accumulated in many flowers and fruits, contributing substantially to plant-animal communication (for review see Cunningham and Gantt, 1998; Hirschberg, 2001; Fraser and Bramley, 2004; DellaPenna and Pogson, 2006). In addition, many heterotrophic bacteria (Armstrong, 1997) and fungi (Sandmann and Misawa, 2002; Avalos and Cerdá-Olmedo, 2004) produce these pigments, responsible for their typical bright yellow to red appearance (Sandmann and Misawa, 2002; Avalos and Cerdá-Olmedo, 2004). Carotenoids confer also their color to some crustaceans, fish and birds. However, animals do not synthesize carotenoids *de novo* and rely, therefore, on nutritional sources to meet their needs.

Apart from these functions, carotenoids serve as precursors of several physiologically important compounds, synthesized through oxidative cleavage and generally known as apocarotenoids. Representative examples are the ubiquitous chromophore retinal, the chordate morphogen retinoic acid, the phytohormone abscisic acid, and the fungal pheromone trisporic acid. In addition, a group of C<sub>15</sub>-apocarotenoids, the strigolactones, are essential signalling molecules attracting both symbiotic arbuscular mycorrhizal fungi and parasitic plants (Akiyama, 2007; Bouwmeester *et al.*, 2007). Moreover, it was recently shown that strigolactone functions as a novel plant hormone regulating shoot branching (Gomez-Roldan *et al.*, 2008; Umehara *et al.*, 2008). Biochemical characterization of the Arabidopsis, rice and pea carotenoid cleaving dioxygenase 8 (CCD8) supposed to be involved in the strigolactone biosynthesis (Gomez-Roldan *et al.*, 2008), revealed a highly conserved cleaving reaction leading to the presumed precursor  $\beta$ -apo-13-carotenone (Alder *et al.*, 2008). In addition,  $\beta$ -apo-13-carotenone, designated as d'orenone, is a biologically active compound shown to inhibit the growth of root hairs by interfering with PIN2-mediated auxin transport (Schlicht *et al.*, 2008). The development of arbuscular mycorrhiza is accompanied by accumulation of cyclohexenone (C<sub>13</sub>) and mycorradicin (C<sub>14</sub>) derivatives (Schliemann *et al.*, 2008), apocarotenoids arising from the cleavage of xanthophylls and leading to yellow pigmentation of the roots (Walter *et al.*, 2000). In addition, C<sub>13</sub>-apocarotenoids, such as  $\beta$ -ionone, constitute an essential aroma note in tea, grapes, roses, tobacco and wine (Rodriguez-Bustamante and Sanchez, 2007). These volatile compounds are also synthesized and released by cyanobacteria (Scherzinger & Al-Babili, 2008; Jüttner, 1984).

Some apocarotenoids, such as saffron and bixin, represent plant pigments of economical value (for review, see Bouvier *et al.*, 2005).

The cleavage reactions in the biosynthesis of apocarotenoids are usually catalyzed by carotenoid oxygenases, non-heme iron enzymes common in all taxa (for review see, Moise *et al.*, 2005; Bouvier *et al.*, 2005; Auldridge *et al.*, 2006; Kloer and Schulz, 2006). The crystal structure of a member of this family, the *Synechocystis* apocarotenoid oxygenase (Ruch *et al.*, 2005), was elucidated at 2.4 Å resolution. The enzyme contains a Fe<sup>2+</sup>-4-His arrangement at the axis of a seven-bladed  $\beta$ -propeller chain fold covered by a dome formed by six large loops (Kloer *et al.*, 2005). The oxidative cleavage of a double bond in the carotenoid backbone results in two products carrying an aldehyde or a ketone function at the reaction site. The apocarotenals formed are frequently converted into the corresponding acids. This oxidation is a common reaction utilized in both vertebrates and plants to produce the signalling molecules retinoic acid and abscisic acid, respectively. However, different enzymes are employed to perform this oxidation step. In plants, abscisic aldehyde is converted by an aldehyde oxidase containing a **m**olybdenum **c**ofactor (MoCo) activated by a corresponding sulfurase (for review, see Nambara and Marion-Poll, 2005). In contrast, retinoic acid is produced by aldehyde dehydrogenases (ALDHs) with active sites containing a catalytic cystein (for review, see Duester, 2000).

Research on microorganisms has contributed substantially to our knowledge on carotenoid biosynthetic pathways (Johnson and Schroeder, 1996; Sieiro *et al.*, 2003). A well-known example is represented by the ascomycete fungus *Neurospora crassa*, extensively employed to investigate various biological phenomena (Davis, 2000), including the biosynthesis of carotenoids and its regulation. Surface cultures of *Neurospora* exhibit a typical orange color due to the accumulation of a complex carotenoid mixture (Zalokar, 1954) that includes the C<sub>35</sub>-apocarotenoid acid neurosporaxanthin (Aasen and Jensen, 1965). The elucidation of the carotenoid biosynthetic pathway in *Neurospora* was paved by the identification of the albino strains *al-1* to *-3* and the characterization of the responsible genes. AL-3 is a prenyl transferase mediating the formation of the carotenoid precursor geranylgeranyl diphosphate (GGPP; Sandmann *et al.*, 1993). The colorless carotene phytoene is then synthesized by AL-2 through condensation of two GGPP molecules (Schmidhauser *et al.*, 1994). AL-2 is a bifunctional enzyme constituted of two domains catalyzing phytoene synthesis and the formation of  $\beta$ -ionone rings in several AL-1 products (Arrach *et al.*, 2001; Arrach *et al.*, 2002). AL-1 is a desaturase mediating the introduction of up to five conjugated double bonds into phytoene, leading to 3,4-didehydrolycopene via phytofluene,  $\zeta$ -carotene, neurosporene and lycopene (Schmidhauser *et al.*, 1990; Hausmann and Sandmann, 2000). These reactions shift the absorption maxima towards longer wavelengths, resulting in the typical yellow to red colors of the desaturation products. According to the carotenoid mixture accumulated by

the wild type, the red compounds lycopene and 3,4-didehydrolycopene are substrates of the  $\beta$ -cyclase activity of AL-2, converting the former into  $\gamma$ -carotene and  $\beta$ -carotene and the latter into torulene.

The C<sub>40</sub>-compound torulene is supposed to be the precursor of the *Neurospora* carotenoid end-product, the C<sub>35</sub> apocarotenoid acid neurosporaxanthin. This was indicated by the occurrence of a torulene-accumulating and neurosporaxanthin-lacking mutant of the closely related ascomycete *Fusarium fujikuroi*, known to produce the same apocarotenoid (Avalos and Cerdá-Olmedo, 1987), and more recently by the identification of corresponding *Neurospora* strains (Saelices *et al.*, 2007). However, the torulene-accumulating phenotype of the *Neurospora* mutants was only observed upon illumination of the culture at low temperature, experimental conditions under which the wild type exhibits a particularly efficient neurosporaxanthin biosynthesis (Harding 1974; Harding *et al.* 1984). Further confirmation of the role of torulene as precursor was then provided by the characterization of the carotenoid oxygenases CarT from *F. fujikuroi* (Prado-Cabrero *et al.*, 2007) and CAO-2 from *Neurospora* (Saelices *et al.*, 2007), both catalyzing the cleavage of torulene at the C3'-C4' double bond leading to the cyclic C<sub>35</sub> compound  $\beta$ -apo-4'-carotenal. Therefore, it was assumed that this aldehyde is an intermediate representing the direct precursor of its corresponding acid neurosporaxanthin. Recently, we characterized the enzyme YLO-1, an aldehyde dehydrogenase catalyzing the oxidation of apocarotenals *in vitro*, and showed that *ylo-1* mutants do not accumulate neurosporaxanthin (Estrada *et al.*, 2008). However, the proposed intermediate  $\beta$ -apo-4'-carotenal was not detected in the *ylo-1* mutant, even under conditions for efficient neurosporaxanthin production. Instead, lycopene and unidentified carotenoids were accumulated, including a compound tentatively identified as apo-4'-lycopenal. The carotenoid pattern of the *ylo-1* mutant indicated that acyclic apocarotenoids may be precursors of neurosporaxanthin.

To determine the order of the late reactions in the neurosporaxanthin pathway in *Neurospora*, we generated a 3,4-didehydrolycopene accumulating *E. coli* strain that allowed us to show that this carotene can be metabolized by sequential actions of CAO-2 and YLO-1. The products obtained were then employed as standards to clarify the carotenoid pattern of the *ylo-1* and an *al-2* mutant lacking carotene cyclization activity. Our results revealed an alternative order in the pathway for neurosporaxanthin biosynthesis and allowed the identification of three novel natural apocarotenoids.

## 2. Materials and Methods

### 2.1. Strains and growth conditions

The *Neurospora crassa* wild-type Oak Ridge 74-OR23-1A strain and the mutant FGSC4100 (*ylo-1 a*) were obtained from the Fungal Genetic Stock Center (McCluskey, 2003). The *al-2* mutants JA26 and JA28 have been described earlier (Arrach *et al.* 2002). For carotenoid extractions, the strains were grown at 30°C for two days in the dark, cooled at 8°C for 1 h and illuminated for 24 h at this temperature, following the incubation protocol described by (Estrada *et al.*, 2008). Mycelial samples were filtered, frozen, and lyophilized before carotenoid extraction.

### 2.2. Construction of plasmids

A DNA fragment encoding the lycopene biosynthesis cassette containing the genes *CrtE*, *ORF6*, *CrtB* and *CrtI* from *Erwinia herbicola* (Hundle *et al.*, 1994) was isolated from the plasmid pLycopene (unpublished data) using the restriction enzymes *ApaI* and *EcoRI*. After treatment with T4-DNA polymerase, the fragment was then ligated into the *Ecl136II* site of pFDY297, a pACYC (Fermentas GmbH; St. Leon-Rot, Germany) derivative carrying the pBluescript SK polylinker, to yield pFarbeR. For the cloning of *al-1* from *Neurospora crassa*, total RNA was extracted from mycelial samples grown for two days in Petri dishes at 30°C in 25 ml liquid Vogel's media. Five micrograms of total RNA was subjected to cDNA synthesis using SuperScript™ RNaseH<sup>-</sup> reverse transcriptase (Invitrogen, Paisley, UK) following the instructions of the manufacturer. Two microliters of the obtained cDNA was then used for the amplification of *al-1* using the primers 5'-ACCAGACTTACAGACAAAATGGCT -3' and 5'-ACAGAACCCTACCT-CACAAATTAGC-3' deduced from the public sequence database (accession no.: [M57465](#)). The obtained PCR product was purified using the GFX™ PCR DNA and Gel Band Purification Kit (Amersham Biosciences, NJ, USA) and cloned into pSC (Stratagene Europe; Amsterdam, Netherlands) leading to the plasmid pSC-AL1. The plasmid pPhytoene-AL-1 was generated by amplification of *al-1* from the plasmid pSC-AL-1 using the primers AL1-Ret A1: 5'-AGCGGGCCCTGAGCGCAACGCAATTAATGT-3' and AL-Ret B: 5'-GATGGTACCCTACCTCACAAATAGCAAGAA-3', carrying an *ApaI* and a *KpnI* restriction site, respectively. The obtained product was purified as described above, digested with *ApaI* and *KpnI*, and cloned into pPhytoene, a pFDY297 derivative carrying an *Erwinia* phytoene synthesis cassette, including *CrtE*, *ORF6*, *CrtB* (unpublished data), and pFarbeR, yielding pPhytoene-AL1 and pFarbeR-AL1, respectively. The *lac* promoter was amplified from pSC-AL1 using the primers LacAscI: 5'-GACTAGTAAGGCGCGCC-



GTGAGCGCAACGCAACGC–3′ and Lac2: 5′-AACTAGTCATAGCTGTT-TCCTGTGTGAAAT–3′ both carrying a *SpeI* restriction site. The PCR product was purified as described above, digested with *SpeI* and ligated into pFarbeR-AL1 to generate pFarbeR-AL1-ind. PCR reactions were performed using the enzyme Accu™ *Pfx* DNA polymerase (Invitrogen, Paisley, UK), and the nature of the products was verified by sequencing.

### 2.3. *In vivo* and *in vitro* analyses

To produce 3,4-didehydrolycopene, TOP 10 *E. coli* cells were transformed with pFarbeR-AL1-ind. An overnight culture was then inoculated into 50 ml LB medium containing kanamycin (50 µg ml<sup>-1</sup>) and 0.2 mM isopropyl-β-D-thiogalactopyranoside (IPTG) and grown at 24°C for 24 h. Cells were then harvested and pellets were extracted with chloroform-methanol (2:1, vol/vol). The extraction was then repeated using acetone and the obtained organic extracts were vacuum-dried, redissolved in chloroform and combined prior to high-performance liquid chromatography (HPLC) analyses. For liquid chromatography–mass spectrometry (LC-MS) analyses, 3,4-didehydrolycopene was collected from HPLC. To check CAO-2 activity *in vivo*, TOP 10 *E. coli* cells were cotransformed with pFarbeR-AL1-ind and pGEX-Cao2 (Saelices *et al.*, 2007). The cells were grown in LB medium containing kanamycin (50 µg ml<sup>-1</sup>) and ampicillin (100 µg ml<sup>-1</sup>), induced and extracted as described above. Apo-4′-lycopenal was produced *in vivo* using 3,4-didehydrolycopene and CAO-2 as described above, collected from HPLC and employed as standard for pigment analyses of the mutants. Apo-4′-lycopenol was prepared by reducing the corresponding aldehyde with NaBH<sub>4</sub> in an EtOH solution. YLO-1 *in vitro* assays were performed according to Estrada *et al.* (2008). Expression, purification and incubation of CAO-2 were performed according to Saelices *et al.* (2007).

### 2.4. Analytical methods

Substrates were quantified spectrophotometrically at their individual  $\lambda_{\max}$  using extinction coefficients as given by Barua and Olson (2000) or Davies (1976). Protein concentration was determined using the BioRad protein assay kit (BioRad, Hercules, CA). HPLC analyses were performed using a Waters system (Eschborn, Germany) equipped with a photodiode array detector (model 996) and a YMC-Pack C<sub>30</sub>-reversed phase column (250 x 4.6 mm i.d., 5 µm; YMC Europe, Schermbeck, Germany). HPLC analyses of carotenoids from *E. coli* cells and CAO-2 *in vitro* assays were run with the solvent systems B: MeOH-*tert*-butylmethyl ether-water (120:24:24, vol/vol/vol) and A: MeOH-*tert*-butylmethyl ether (350:650, vol/vol). The column was developed at a flow rate of 1 ml

min<sup>-1</sup> with a linear gradient from 100% B to 50% B within 5 min, then to 100% A and a flow rate of 2 ml min<sup>-1</sup> within 1 min, maintaining the final conditions for another 19 min. For HPLC analyses of *ylo-1* and *al-2* mutants, carotenoid extractions were performed by homogenizing about 0.1 g of the dry mycelium with sand in a mortar and extracted with acetone until sample bleaching. Samples were then centrifuged and the supernatants were collected and vacuum-dried. In the case of the *ylo-1* mutant, the column was developed with the solvent systems B: MeOH-*tert*-butylmethyl ether-water (120:24:24, vol/vol/vol) and A: MeOH-*tert*-butylmethyl ether (50:50, vol/vol). The column was developed at a flow rate of 1 ml min<sup>-1</sup> with a linear gradient from 100% B to 43% B within 45 min, then to 100% A and a flow rate of 2 ml min<sup>-1</sup> within 1 min, maintaining the final conditions for another 25 min at a flow rate of 2 ml min<sup>-1</sup>. For analysis of the reddish *al-2* mutant JA26, the column was developed with solvent systems B: MeOH-*tert*-butylmethyl ether-water (120:24:24, vol/vol/vol) and A: MeOH-*tert*-butylmethyl ether (50:50, vol/vol) at a flow rate of 1 ml min<sup>-1</sup> with a linear gradient from 100% B to 43% B within 25 min, then to 100% A within 7 min. The flow rate was then increased to 1.5 ml min<sup>-1</sup> and maintained for another 19 min.

LC-MS analyses of HPLC-purified compounds were performed using a Thermo Finnigan LTQ mass spectrometer coupled to a Surveyor HPLC system consisting of a Surveyor Pump Plus, Surveyor PDA Plus and Surveyor Autosampler Plus (Thermo Electron, Waltham, MA). Separations were carried out using a YMC-Pack C<sub>30</sub>-reversed phase column (150 x 3 mm i.d., 3 µm) with the solvent system A: MeOH-water-*tert*-butylmethyl ether (50:45:5, vol/vol/vol) and B: MeOH-water-*tert*-butylmethyl ether (27:3:70, vol/vol/vol) with the water containing 0.1 g l<sup>-1</sup> ammonium acetate. The column was developed at a flow rate of 450 µl min<sup>-1</sup> with 90% A and 10 % B for 5 min, to 5% A and 95% B in 10 min, then increasing the flow to 900 µl min<sup>-1</sup> within 4 min and maintaining these final conditions for 5 min. The identification of apo-4'-lycopenal, apo-4'-lycopenol, apo-4'-lycopenoic acid and 3,4-didehydrolycopene were carried out using APCI in positive mode. Nitrogen was used as sheath and auxiliary gas and set to 20 and 5 units, respectively. The vaporizer temperature was 350°C and capillary temperature 150°C. The source current was set at 5 µA, and the capillary and tube lens voltages were set at 49 V and 125 V, respectively.

### 3. Results

#### 3.1. Generation of a 3,4-didehydrolycopene accumulating *E. coli* strain

To generate a 3,4-didehydrolycopene accumulating *E. coli* strain, the plasmid pPhytoene-AL-1, encoding the *Neurospora* desaturase AL-1 and the three *Erwinia*

enzymes, IPP/DMAPP isomerase (*ORF6*), geranylgeranyl-diphosphate synthase (CrtE) and phytoene synthase (CrtB), needed for phytoene formation was constructed and transformed into *E. coli* TOP10 cells, expecting the accumulation 3,4-didehydrolycopene. However, HPLC analyses revealed only traces of this compound beside high amounts of phytoene and desaturation intermediates (data not shown). This indicated a low desaturation efficiency of AL-1. Previous investigation of the AL-1 activity showed that the enzyme converts also desaturation intermediates like lycopene or neurosporene (Hausmann and Sandmann, 2000). Therefore, we combined the *Erwinia* lycopene synthesis activity with AL-1, which should then only perform the last desaturation step to produce 3,4-didehydrolycopene. For this purpose, a second plasmid, pFarbeR-AL1, was generated encoding AL-1 and the *Erwinia* enzymes IPP/DMAPP isomerase (*ORF6*), CrtE, CrtB and CrtI (carotene desaturase). Here again, only traces of 3,4-didehydrolycopene were detected, and the transformed *E. coli* cells accumulated mainly lycopene, likely to be produced by the bacterial enzyme CrtI.

Assuming that the weak activity of AL-1 may be a result of low protein amounts, we constructed the plasmid pFarbeR-AL1-ind, harbouring the *Erwinia* lycopene synthesis cassette and *al-1* under the control of the strong *lacZ* promoter. As shown by HPLC analyses (Fig. C2.1-I, *Con*), the transformation of *E. coli* cells with this plasmid resulted in the accumulation of lycopene (compound B) together with a novel compound (C) resembling the desired 3,4-didehydrolycopene in its UV-Vis spectrum and elution pattern. To prove its identity, compound C was purified and subjected to LC-MS analysis. The product exhibited a molecular ion  $[M+H]^+$  of 535.29, consistent with its identity as 3,4-didehydrolycopene (Fig. C2.1; IIC).

### 3.2. CAO-2 converted 3,4-didehydrolycopene into apo-4'-lycopenal

Previous work suggested the specificity of CAO-2 in cleaving the C3'-C4' double bond of torulene (Saelices *et al.*, 2007). To determine if 3,4-didehydrolycopene, an acyclic isomer of torulene, is also cleaved by CAO-2, *E. coli* cells were cotransformed with the plasmids pFarbeR-AL1-ind and pGEX-Cao2 that encodes CAO-2 in fusion with GST (Saelices *et al.*, 2007). Cultures were grown, induced by IPTG and analysed by HPLC. The results (Fig. C2.1-I) revealed the conversion of 3,4-didehydrolycopene (compound C) into a novel product (compound A), the UV-Vis spectrum of which was very similar to that of  $\beta$ -apo-4'-carotenal (not shown) but exhibited, as expected for an acyclic isomer, a higher absorption maximum (493 nm) and a longer retention time.

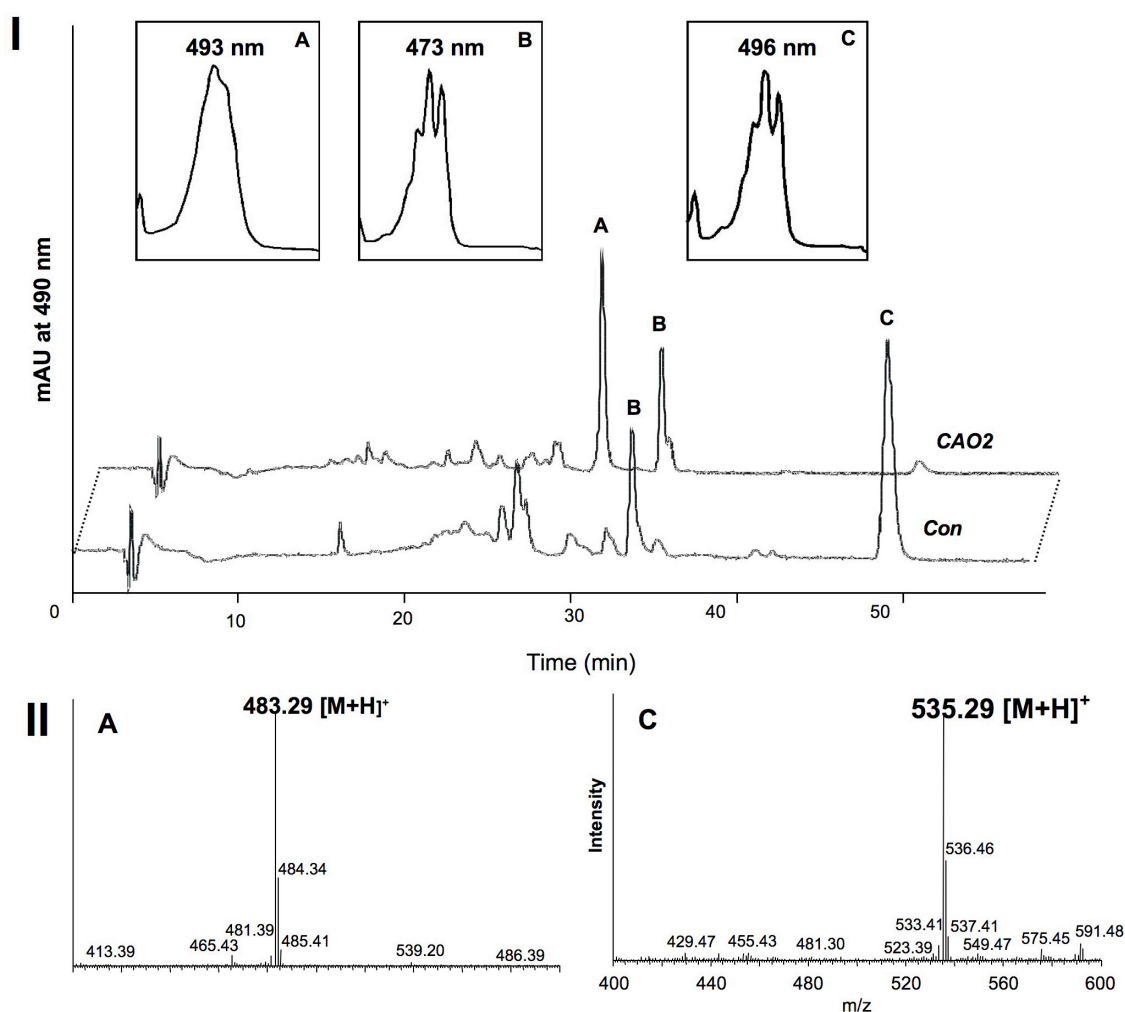


**Fig. C2.1. Characterization of a 3,4-didehydrolycopene accumulating *E. coli* strain and CAO-2 cleavage activity *in vivo*.** (I) HPLC analyses of a TOP 10 *E. coli* strain transformed either with pFarbeR-AL1-ind alone (*Con*) or together with pGEX-Cao2 (*CAO-2*). After induction, the *Con* cells accumulated lycopene (peak B) and 3,4-didehydrolycopene (peak C). The introduction of CAO-2 resulted in the cleavage of 3,4-didehydrolycopene into apo-4'-lycopenal (peak A). The three products were identified by their elution patterns and UV-Vis spectra, shown in the insets. To confirm their nature, the compounds A and C were purified and subjected to LC-MS analysis (II). The compounds exhibited [M+H]<sup>+</sup> molecular ions of 535.29 (C) and 483.29 (A) suggesting their identities as 3,4-didehydrolycopene and apo-4'-lycopenal, respectively. The structures are shown in the insets.

To confirm its identity, the product was purified and subjected to LC-MS analysis. The determined molecular ion [M+H]<sup>+</sup> of 483.29 (Fig. C2.1-II, compound A) was identical to the one expected for apo-4'-lycopenal, proving the cleavage of 3,4-didehydrolycopene at the C3-C4 double bond. To further confirm this cleavage activity, *in vitro* assays were performed using purified CAO-2. HPLC analyses of these incubations (Fig. C2.2) revealed a clear conversion of the substrate 3,4-didehydrolycopene (S) into apo-4'-lycopenal (P), as determined by UV-Vis spectrum, elution pattern and LC-MS analysis (data not shown).

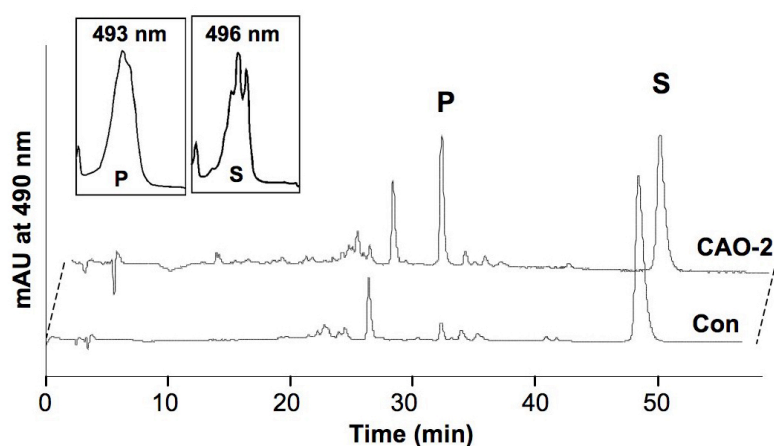


**Fig. C2.2. HPLC analysis of the incubation of CAO-2 with 3,4-didehydrolycopene.** The *in vitro* assay was performed using purified CAO-2 in a total volume of 200  $\mu$ l. The enzyme cleaved 3,4-didehydrolycopene (peak S) into apo-4'-lycopenal (peak P), as suggested by elution pattern and UV-Vis spectrum (inset).

### 3.3. Analyses of the *ylo-1* mutant

Recently, the growth of an *ylo-1* mutant under conditions optimized for neurosporaxanthin accumulation (Arrach *et al.*, 2002) enabled the determination of its carotenoid pattern, indicating the accumulation of apo-4'-lycopenal and  $\beta$ -apo-4'-carotenal-derivatives (Estrada *et al.*, 2008). However, a clear identification of these compounds was hindered by lack of appropriate standards. Taking advantage of the CAO-2 *in vivo* activity described above, apo-4'-lycopenal was produced and used as a standard for the analyses of the *ylo-1* strain. As shown in Fig. C2.3, the *ylo-1* mutant accumulated three major pigments. The first one (C) represented lycopene, as indicated by comparison with the authentic standard. The second pigment (B) corresponded to apo-4'-lycopenal as suggested by the identical elution pattern and UV-Vis of the standard produced by CAO-2. The nature of compound B was also confirmed by LC-MS analysis (data not shown). The third pigment (A) exhibited an UV-Vis spectrum similar to that of  $\gamma$ -carotene or of an apocarotenol. However, the retention time observed was consistent with an alcohol rather than with a carotene. Based on the accumulation of apo-4'-lycopenal, we assumed that compound A may represent the corresponding alcohol. Therefore, apo-4'-lycopenol obtained by chemical reduction of the CAO-2 product was used as standard. As shown in Fig. C2.3, compound A was identical to apo-4'-lycopenol in the HPLC analyses. To confirm this data, standard apo-4'-lycopenol and purified compound A were subjected to LC-MS analysis. The mass spectra of both apocarotenoids were identical (Fig. C2.4),

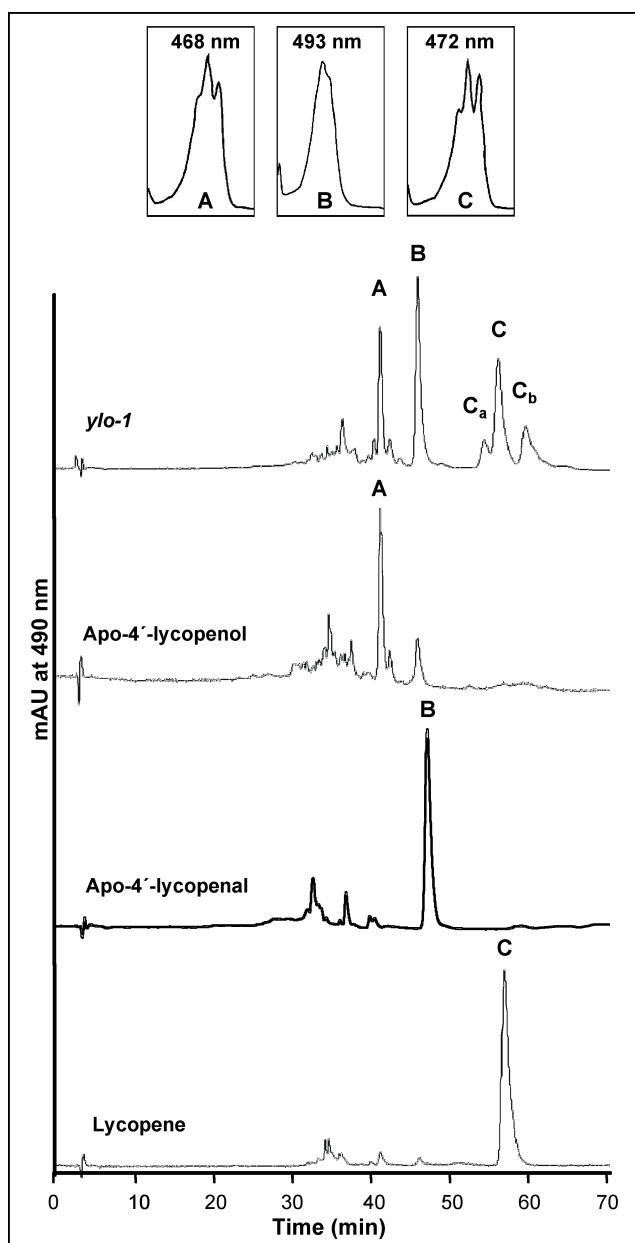


**Fig. C2.3. Elucidation of the *ylo-1* carotenoid pattern.** The HPLC analysis showed the accumulation of lycopene (peak C, C<sub>a</sub>, C<sub>b</sub>), apo-4'-lycopenal (peak B) and apo-4'-lycopenol (peak A). The three compounds were identified by their UV-Vis spectra (shown in the insets) and by comparison to HPLC chromatograms of authentic standards. The nature of compound B and C was further confirmed by LC-MS analysis (data not shown). LC-MS analysis of compound A is presented in Fig. C2.4.

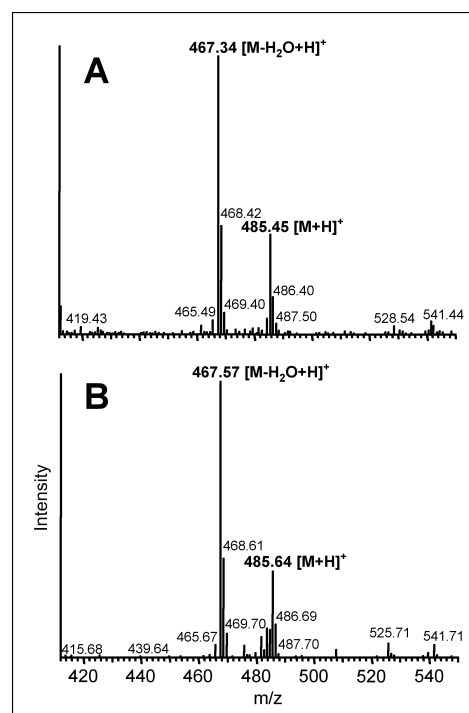


**Fig. C2.4. LC-MS determination of apo-4'-lycopenol accumulated in *ylo-1*.** The compound A (Fig. C2.3) was purified and compared to apo-4'-lycopenol standard in LC-MS analyses. The mass spectrum of the *ylo-1* compound (A) was identical to that of the standard (B), including the [M+H]<sup>+</sup> and [M-H<sub>2</sub>O+H]<sup>+</sup> molecular ions of 485 and 467, respectively

including the molecular ion [M+H]<sup>+</sup> of 485 and the molecular ion [M-H<sub>2</sub>O+H]<sup>+</sup> of 467. In addition to lycopene, apo-4'-lycopenal and apo-4'-lycopenol, we detected in some *ylo-1* samples an ester of apo-4'-lycopenol (data not shown) that corresponds to one of the apocarotenoids described by (Estrada *et al.*, 2008). Taken together, the pigments accumulated in the *ylo-1* mutant are non-cyclic and represent lycopene and apolycopenoids. These data indicate that the *in vivo* substrate of YLO-1 is apo-4'-lycopenal rather than its cyclic isomer β-apo-4'-carotenal.

### 3.4. Analyses of the reddish *al-2* mutant JA26

The synthesis of neurosporaxanthin from apo-4'-lycopenal requires two sequential reactions, the introduction of a  $\beta$ -ionone ring and the conversion of the aldehyde into the corresponding acid. To determine the sequence of these reactions in *Neurospora*, we analysed the carotenoid pattern of the JA26 mutant, lacking the AL-2 cyclization activity (Arrach *et al.*, 2002). For this purpose, we used again experimental conditions that lead to optimal neurosporaxanthin production in the wild type. As shown in Fig. C2.5-I, the JA26 mutant accumulated one major pigment (B) exhibiting an UV-Vis spectrum similar to that of neurosporaxanthin (A), but showing a longer maximal absorption wavelength (479 nm instead of 472 nm, see peak A and B in Fig. C2.5). Compound B eluted also later than neurosporaxanthin, indicating a less polar isomer. Both properties are expected if the compound accumulating in the JA26 mutant is apo-4'-lycopenoic acid. Indeed, the elution pattern and UV-Vis spectrum of compound B were identical to those of the product obtained from the incubation of purified YLO-1 with apo-4'-lycopenal (Fig. C2.5-I). To further confirm its identity, the JA26 compound was purified and analysed by LC-MS (Fig. C2.5-II). The determined  $[M+H]^+$  molecular ion of 499.69 supported the HPLC results. Moreover, the obtained MS<sup>2</sup> spectrum was identical to that of apo-4'-lycopenoic acid purified from the incubation of YLO-1 with apo-4'-lycopenal. Analyses of a similar *al-2* mutant, JA28 (Arrach *et al.*, 2002), led to similar results (data not shown).

## 4. Discussion

The identification of the enzymes catalyzing the synthesis of neurosporaxanthin has become possible through the occurrence of the corresponding *Neurospora* color mutants. Based on these alterations, such carotenoid mutants can be divided into three classes: (i) *albino* (*al*) strains, missing either *al-1*, *al-2* or *al-3* functional alleles mediating the initial steps in the carotenoid pathway; (ii) reddish mutants, lacking either AL-2 cyclase (Arrach *et al.*, 2002) or the CAO-2 carotene cleavage activity (Saelices *et al.*, 2007); and (iii) yellow (*ylo*) mutants. Due to the accumulation of the cyclic torulene in the *cao-2* mutant and the activity of the corresponding enzyme, which converted torulene into  $\beta$ -apo-4'-carotenal *in vitro* (Saelices *et al.*, 2007), it was assumed that neurosporaxanthin is synthesized from  $\beta$ -apo-4'-carotenal via an oxidation reaction (Fig. C2.6). Genetic mapping of an *ylo-1* mutant led to the identification of the responsible gene, which encodes a member of the widespread aldehyde dehydrogenase family. The genetic findings were confirmed by the *in vitro* characterization of purified YLO-1, that revealed its activity in converting  $\beta$ -apo-4'-carotenal to neurosporaxanthin (Estrada *et al.*, 2008).

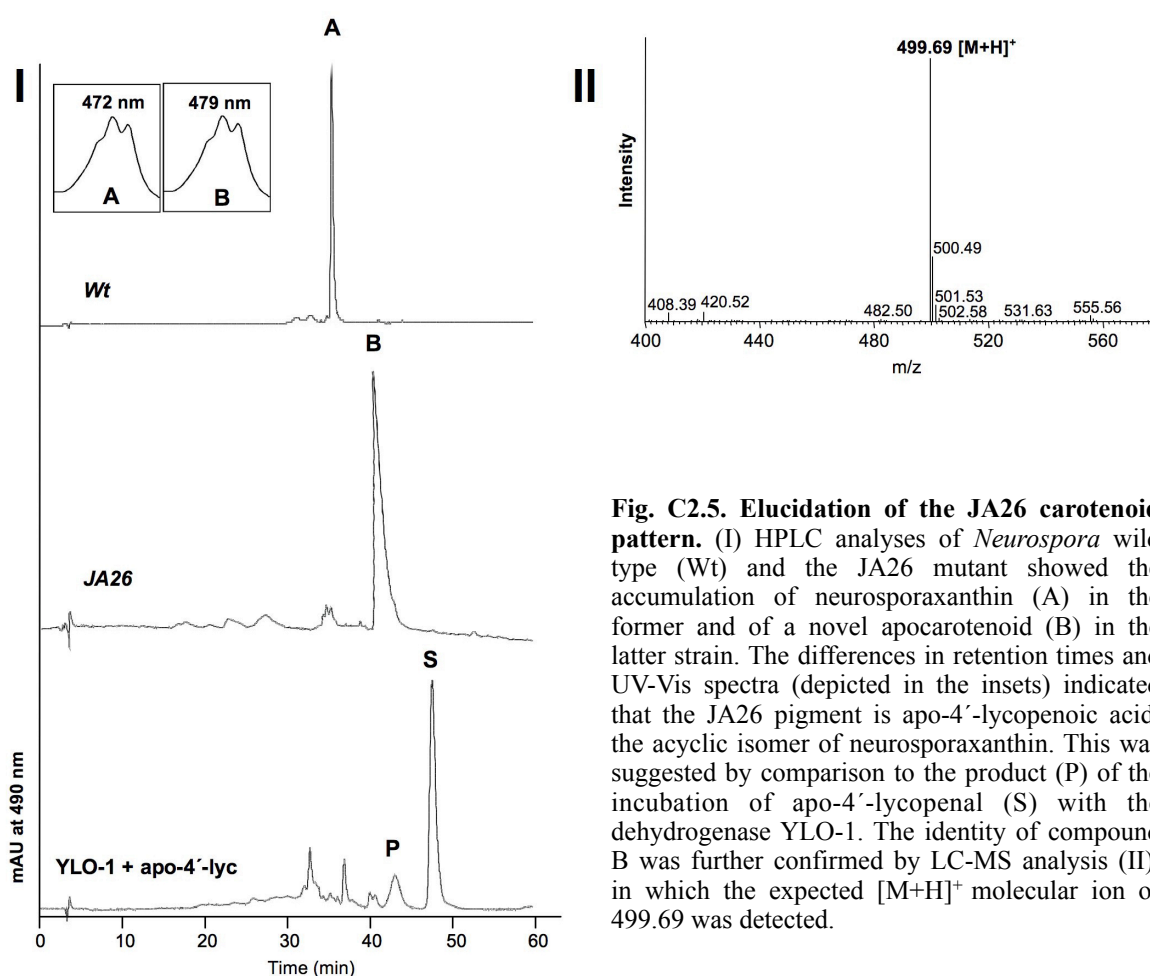


**Fig. C2.5. Elucidation of the JA26 carotenoid pattern.** (I) HPLC analyses of *Neurospora* wild type (Wt) and the JA26 mutant showed the accumulation of neurosporaxanthin (A) in the former and of a novel apocarotenoid (B) in the latter strain. The differences in retention times and UV-Vis spectra (depicted in the insets) indicated that the JA26 pigment is apo-4'-lycopenoic acid, the acyclic isomer of neurosporaxanthin. This was suggested by comparison to the product (P) of the incubation of apo-4'-lycopenal (S) with the dehydrogenase YLO-1. The identity of compound B was further confirmed by LC-MS analysis (II), in which the expected [M+H]<sup>+</sup> molecular ion of 499.69 was detected.

The biological function of this enzyme was substantiated by the absence of neurosporaxanthin in the *ylo-1* mutant under growth conditions in which this xanthophyll represents more than 90% of the carotenoids produced by the wild type. However,  $\beta$ -apo-4'-carotenal was not detected either. Instead, the HPLC analysis revealed the accumulation of the acyclic lycopene and unidentified apocarotenoids, including a presumed apo-4'-lycopenal (Estrada *et al.*, 2008). This pattern was unexpected, because of the presence of a functional AL-2 cyclization activity. Therefore, we inferred that neurosporaxanthin is synthesized from apo-4'-lycopenal *in vivo*. This hypothesis implies that 3,4-didehydrolycopene is cleaved by CAO-2, leading to apo-4'-lycopenal that is then oxidized by YLO-1 to yield apo-4'-lycopenoic acid. Neurosporaxanthin is then synthesized from its acyclic isomer by the AL-2 cyclization activity. Following this scenario (Fig. C2.6), a lack of the AL-2 cyclization activity would then lead to accumulation of apo-4'-lycopenoic acid. Indeed, previous analyses of the JA26 and JA28 mutants missing the AL-2 cyclase activity revealed the accumulation of a carotenoid whose UV-Vis spectrum resembled neurosporaxanthin, but exhibited a longer maximal absorption wavelength and less polarity in the HPLC analyses (Arrach *et al.*, 2002). Based on these data, the authors proposed that



the polar compound accumulated in these cyclase-defective mutants could be apo-4'-lycopenoic acid, the acyclic isomer of neurosporaxanthin. However, no biochemical evidence was provided to support this hypothesis.

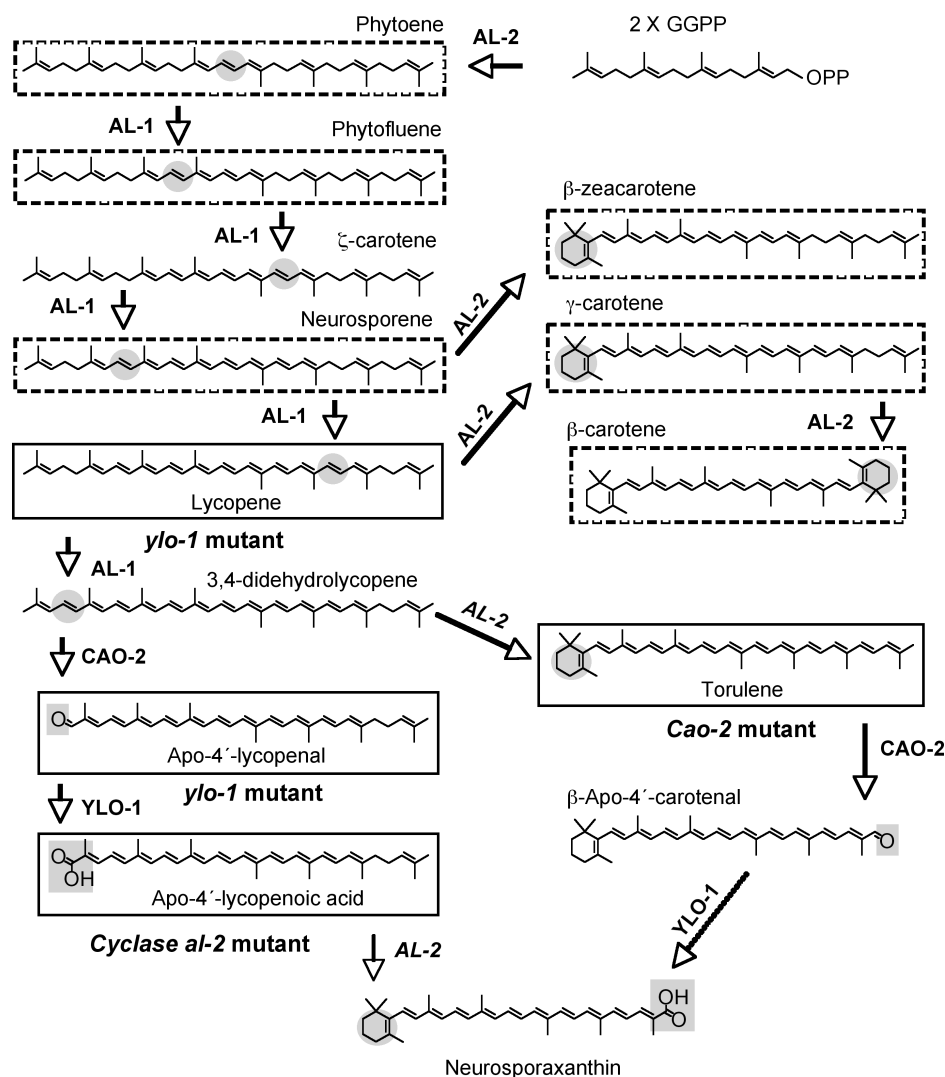


**Fig. C2.6. Two possible pathways for neurosporaxanthin synthesis.** Carotenoid biosynthetic pathway of *Neurospora*. Enzymes are indicated in bold, and chemical changes from precursor molecules are highlighted as shaded areas. Neurosporaxanthin is highly accumulated upon illumination at 8°C and is present at lower levels beside desaturation intermediates (dashed boxes) upon illumination at 30°C. It is synthesized from 3,4-didehydrolycopene via sequential cyclization, cleavage and desaturation reactions. According to the former hypothesis, 3,4-didehydrolycopene is first converted by AL-2 into torulene, which is then cleaved by CAO-2 to yield β-apo-4'-carotenal. The latter is then oxidized by YLO-1 leading to neurosporaxanthin. However, the accumulation of apo-4'-lycopenal in the *ylo-1* and apo-4'-lycopenoic acid in the cyclase *al-2* mutant (JA26) indicates the occurrence of an alternative sequence, in which the first step is the cleavage of 3,4-didehydrolycopene into apo-4'-lycopenal, which is then oxidized by YLO-1 to yield apo-4'-lycopenoic acid, the last intermediate in the pathway. The final step is then catalyzed by the cyclase activity of AL-2. The new sequence indicates a competition between AL-2 and CAO-2 on the conversion of 3,4-didehydrolycopene. Pigments accumulated in the mutants are presented in boxes.

Acyclic carotenoids cannot be easily distinguished from their cyclic isomers by mass spectrometry. Therefore, acyclic standards are required for discrimination by HPLC. Making use of such standards, obtained either by appropriate, engineered *E. coli* strains or by chemical modification, a clear identification of the intermediates present in different *Neurospora* mutants could be carried out. Using a combination of HPLC and LC-MS analyses, we demonstrated the occurrence of three novel apocarotenoids in *Neurospora*, apo-4'-lycopenal, apo-4'-lycopenol and apo-4'-lycopenoic acid. The identification of these intermediates provides indeed a solid evidence for a novel sequence of reactions in *Neurospora*. Against former beliefs, our data suggest that neurosporaxanthin is synthesized from its acyclic isomer apo-4'-lycopenoic acid *in vivo*.

Using *in vivo* and *in vitro* assays, we showed that CAO-2 is able to cleave 3,4-didehydrolycopene, like its cyclic isomer torulene, at the C3-C4 double bond. Thus, in contrast to the cleavage reaction mediated by the *Fusarium* retinal-forming enzyme CarX (Prado-Cabrero *et al.*, 2007b), the occurrence of the  $\beta$ -ionone ring is not necessary for the recognition of the substrate. Moreover, the identical cleavage sites determined for the cyclic torulene and the acyclic 3,4-didehydrolycopene indicate that both substrates enter the enzyme cavity with their identical acyclic moiety. The cleavage site would be then determined by the distance to this end, which is equal in both substrates. Taken together, the cleavage at the same site implies structural determinants different from  $\beta$ -ionone responsible for the accurate conversion of different  $\beta$ -apocarotenoids at the C15-C15' double bond by the cyanobacterial enzymes SynACO (Ruch *et al.*, 2005; Kloer *et al.*, 2005) and NosACO (Scherzinger *et al.*, 2006).

The conversion of 3,4-didehydrolycopene into apo-4'-lycopenal indicates that this carotene is a substrate for two different, competing enzymes in *Neurospora*, CAO-2 and AL-2. This competition provides an explanation for the accumulation of the cyclization product torulene in the *cao-2* mutant (Saelices *et al.*, 2007) and the presence of the acyclic apo-4'-lycopenoic acid in the JA26 strain lacking the AL-2 cyclization activity. However, it is reasonable to assume that the cleavage of 3,4-didehydrolycopene into apo-4'-lycopenal is the predominant reaction in the wild type. This is supported by the carotenoid pattern of the *ylo-1* mutant in which the pathway is apparently blocked downstream of the cleavage step of 3,4-didehydrolycopene, but also upstream of the cyclization reaction. As shown here, the *ylo-1* mutant did not accumulate cyclic carotenoids, neither torulene nor  $\beta$ -apo-4'-carotenal were detected. Instead, the *ylo-1* mutant accumulated only the acyclic compounds lycopene, apo-4'-lycopenal and apo-4'-lycopenol.

The hypothesis that apo-4'-lycopenoic acid is the direct precursor of neurosporaxanthin implies that YLO-1 converts apo-4'-lycopenal into its corresponding acid. In our recent work, we showed that YLO-1 is active on both cyclic and acyclic apocarotenals. Indeed, YLO-1 oxidized  $\beta$ -apo-4'-,  $\beta$ -apo-8'-,  $\beta$ -apo-10'-carotenal and

apo-8'-lycopenal *in vitro* (Estrada *et al.*, 2008). Here, we checked the activity of YLO-1 on apo-4'-lycopenal and showed its conversion into the corresponding acid, thus, confirming its nature as an intermediate and explaining its accumulation in the *ylo-1* mutant. The new order in the neurosporaxanthin synthesis indicates that the last step is the cyclization of apo-4'-lycopenoic acid by the bifunctional enzyme AL-2, which is now under investigation. A conversion of acyclic apocarotenoids into their cyclic isomers has not been reported for any carotene cyclase so far.

The mycelia used for our experiments were grown under illumination at 8°C, conditions causing particularly efficient neurosporaxanthin accumulation in the wild type (Harding, 1974; Harding *et al.*, 1984), and allowing the *cao-2*, *ylo-1* and reddish *al-2* mutants to exhibit visible phenotypes due to the accumulation of torulene (Saelices *et al.*, 2007), apo-4'-lycopenal and apo-4'-lycopenoic acid, respectively (Fig. C2.6). These phenotypes are not apparent upon illumination at 30°C, conditions which lead to a complex carotenoid mixture (Fig. C2.6), including phytofluene, neurosporene,  $\beta$ -zeacarotene,  $\gamma$ -carotene and  $\beta$ -carotene (Estrada *et al.*, 2008).

This carotenoid pattern can be explained by a reduced AL-1 activity at 30°C, as further suggested by a higher phytoene content and a severe reduction in the total amount of colored carotenoids compared to the ones accumulated upon illumination at 8°C (Estrada *et al.*, 2008). Furthermore, it demonstrates that the AL-2 cyclase is also active on earlier precursors of the pathway. Unsaturated intermediates, presumably accumulated because of the inefficient desaturase activity, are now available for AL-2, resulting in premature substrate cyclization and a partial deviation of the pathway towards  $\gamma$ -carotene and  $\beta$ -carotene. In contrast, under low temperature phytoene is efficiently desaturated to 3,4-didehydrolycopene, cleaved by CAO-2, or at least to lycopene, which does not represent a suitable substrate for CAO-2 due to the absence of the specific cleaving site, the C3-C4 double bond. The weak activity of AL-1 was also observed in *E. coli* cells grown at 24°C. Hence, we had to combine it with the bacterial desaturase CrtI to accumulate 3,4-didehydrolycopene in the heterologous *E. coli* system. The biochemical basis of this temperature effect remains to be investigated.

Taken together, the combined mutant analyses and enzymatic studies presented here suggest a new sequence in the biosynthetic pathway leading from 3,4-didehydrolycopene to neurosporaxanthin in *Neurospora* and provide consistent interpretations of the mutant phenotypes. The sequence is presumably governed by protein-protein interactions determining substrate accessibility rather than by narrow substrate specificities of the involved enzymes CAO-2 and YLO-1 that convert both cyclic and acyclic substrates. Lack of precedents on the carotenoids accumulated by the *ylo-1* and reddish *al-2* mutants hindered its appropriate characterization, and delayed the elucidation of the final steps of the pathway. Our findings complete the knowledge on the neurosporaxanthin biosynthetic

pathway in this model fungus and complement the genetic information on the responsible genes.

### **Acknowledgments**

This work was supported by the Deutsche Forschungsgemeinschaft (DFG) Grant AL 892/1-3 and by the Spanish Government (Ministerio de Ciencia y Tecnología, projects BIO2003-01548 and BIO2006-01323, and Acciones Integradas Hispano-Alemanas). We are indebted to Dr. Peter Beyer and Dr. Jorge Mayer for valuable discussions. We would like to thank Erdmann Scheffer for skilful technical assistance.



### CAPÍTULO 3

La proteína White Collar WcoA de *Fusarium fujikuroi* no es necesaria para la fotocarotenogénesis, pero juega un papel en la regulación del metabolismo secundario y la conidiación.

The White Collar protein WcoA of *Fusarium fujikuroi* is not required for photocarotenogenesis, but plays a role in the regulation of secondary metabolism and conidiation

Alejandro F. Estrada and Javier Avalos \*

*Department of Genetics, Faculty of Biology, University of Seville, E-41012 Seville, Spain*



---

**Abstract**

The fungal proteins of the White Collar photoreceptor family, represented by WC-1 from the *Neurospora crassa*, mediate the control by light of different biochemical and developmental processes, such as carotenogenesis or sporulation. Carotenoid biosynthesis is induced by light in the gibberellin-producing fungus *Fusarium fujikuroi*. In an attempt to identify the photoreceptor for this response, we cloned the only WC-1-like gene present in *Fusarium* genomes, that we called *wcoA*. The predicted WcoA polypeptide is highly similar to WC-1 and contains the relevant functional domains of this protein. In contrast to the *Neurospora* counterpart, *wcoA* expression is not affected by light. Unexpectedly, targeted *wcoA* disruptant strains maintain the regulation of carotenogenesis by light. Furthermore, the *wcoA* mutants show a drastic reduction of fusarin production in the light, and produce less gibberellins and more bikaverins than the parental strain under nitrogen-limiting conditions. The changes in the production of the different products indicate a key regulatory role for WcoA in secondary metabolism of this fungus. Additionally, the mutants are severely affected in conidiation rates under different culture conditions, indicating a more general regulatory role for this protein.

**Keywords:** *Gibberella*; WC proteins; Nitrogen regulation, Carotenoid; Gibberellin, Bikaverin, Fusarin



## 1. Introduction

The genus *Fusarium* groups a large number of phytopathogenic fungi characterized by the production of fusiform asexual spores, called conidia. The *Fusarium* species usually display a complex secondary metabolism, which includes the production of different mycotoxins (Desjardins, 2006). Some secondary metabolites produced by these fungi have found commercial applications. A representative example are the gibberellins, a group of tetracyclic terpenoids synthesized by *Fusarium fujikuroi* (Tudzynski, 2005; Avalos et al., 2007), formerly known as the mating population C of the *Gibberella fujikuroi* species complex. The gibberellins are growth-promoting plant hormones (MacMillan, 1997), rarely produced by microorganisms (MacMillan, 2001), whose beneficial effects on plant development have found applications in agriculture and brewing industry. The high gibberellin biosynthetic activity of *F. fujikuroi* has made this fungus a major source for biochemical information on the pathway and the obvious choice for large-scale gibberellin production (Tudzynski, 1999; Avalos et al., 1999).

In addition to gibberellins, *F. fujikuroi* produces other secondary metabolites, which include carotenoids, (Avalos and Cerdá-Olmedo, 1986, 1987), bikaverins (Giordano et al., 1999) and fusarins (Barrero et al., 1991). Carotenoids are terpenoid pigments widely spread in nature, where they are synthesized by all plants and algae, and by many bacteria and fungi (Britton et al., 1998; Sandmann and Misawa, 2002). As terpenoids, carotenoids and gibberellins share their first biosynthetic steps up to geranylgeranyl pyrophosphate, from which both pathways bifurcate as independent branches. Bikaverins and fusarins are polyketides, and their syntheses start from acetate units via a multifunctional enzyme called polyketide synthase. The genes responsible for the biosynthesis of these compounds are well known for the carotenoid (Linnemanstöns et al., 2002a, Prado-Cabrero et al., 2007a) and gibberellin pathways (Tudzynski, 2005), and only partially for the ones of bikaverins and fusarins. The major polyketide synthase gene for bikaverin has been identified in *F. fujikuroi* (Linnemanstöns et al., 2002b) but not the one for fusarins, although it is known in other *Fusarium* species (Song et al., 2004).

The synthesis of these secondary metabolites is subject to different regulations. Thus, gibberellin and bikaverin productions are induced by the absence of nitrogen in the medium, mainly through the activation by the key nitrogen regulator AreA (Mihlan et al., 2003). Additionally, bikaverin biosynthesis is regulated by pH (Giordano et al., 1999). Fusarin production depends on temperature (Barrero et al., 1991), but the effects of nitrogen limitation and pH have not been investigated. In contrast, carotenoid biosynthesis of *F. fujikuroi* is mostly dependent on illumination. The surface cultures of this fungus acquire an orange pigmentation when grown under light because of the accumulation of a mixture of carotenoids, that includes neutral intermediates, like gamma-carotene and

torulene, and an acidic apocarotenoid, neurosporaxanthin, end product of the pathway (Avalos and Cerdá-Olmedo, 1987).

Light is a key environmental signal that controls many aspects of the life of microorganisms (Herrera-Estrella and Horwitz, 2007). The fungi *Neurospora crassa* and *Phycomyces blakesleeanus* (Linden, 2002; Cerdá-Olmedo, 2001) stand out as models for photobiology research. These fungi exhibit a variety of responses to light, which include the modulation of different developmental processes and the stimulation of carotenoid biosynthesis (Corrochano and Cerdá-Olmedo, 1992; Linden et al., 1997). In both cases, the control is carried out through the transcriptional induction of relevant sets of genes. This activation is achieved in *N. crassa* by the White Collar proteins (Talora et al., 1999), identified because of the lack of carotenoids in light-grown mycelia in the mutants of the genes *wc1* and *wc2* (Harding and Turner, 1981). Both proteins contain a PAS domain, that mediates their interaction to form a heterodimer known as WC complex (Ballario et al., 1996), and a DNA-binding zinc-finger domain. The WC complex is transiently activated by light and binds regulatory elements of light-regulated target genes to activate their transcription (Liu et al., 2003). The photoreceptor of the complex is WC-1, which contains a special PAS domain, called LOV from “light, oxygen and voltage” (Cheng et al., 2003), that binds a light-absorbing FAD molecule (He et al., 2002).

The WC complex is responsible for the regulation of all known photoresponses in *N. crassa*. The identification of these proteins led to find similar light regulatory systems in other fungi (Corrochano, 2007), as the ones from the ascomycete *Trichoderma atroviride* (Casas-Flores et al., 2004) or the basidiomycete *Cryptococcus neoformans* (Idnurm and Heitman, 2005). The photoresponses vary between different species, e.g., the WC system controls light induction of conidiation in the first case (Casas-Flores et al., 2004), and light repression of sexual cell fusion and its subsequent filamentation in the second (Idnurm and Heitman, 2005; Lu et al., 2005). The number of examples is currently increasing and putative WC orthologues are found in the fungal genome sequences that are becoming available. Recently, WC proteins have also been described in zygomycetes. The *madA* mutants of *P. blakesleeanus*, identified many years ago by genetic analyses and affected in most of the photoresponses of this fungus, turned out to lack a functional WC-1-like protein (Idnurm et al., 2006). Moreover, this group of fungi displays a unique diversification of these regulatory proteins: three WC genes have been described in *Mucor circinelloides* (Silva et al., 2006), and a second orthologue has been found in *P. blakesleeanus* (Idnurm et al., 2006).

The similar light-regulatory mechanisms found in taxonomically distant species point to the WC proteins as universal photoreceptor systems in fungi, already present in early ancestors common to ascomycetes, basidiomycetes and zygomycetes. To extend the knowledge of this regulation to the fungus *F. fujikuroi*, we cloned the only *wc-1* orthologue

found in the available *Fusarium* genomes, that we called *wcoA*, and we obtained targeted disruptant strains for this gene. Unexpectedly, the *wcoA* mutants conserve the photoinduction of carotenoid biosynthesis but exhibit a pleiotropic phenotype. This includes alterations in the patterns of gibberellin, bikaverin and fusarin productions, as well as in conidia formation, pointing to an unusually complex regulatory role for the WcoA protein in *F. fujikuroi*.

## 2. Materials and methods

### 2.1. Strains and culture conditions

FKMC1995 is a wild-type strain of *F. Fujikuroi* (*Gibberella fujikuroi* mating population C; O'Donnell et al., 1998). SF4 is a carotenoid overproducing strain obtained by exposition to N-methyl-N'-nitro-N-nitrosoguanidine (Prado-Cabrero et al., 2007a). Unless otherwise stated, experiments were done on DG minimal medium (Avalos et al., 1985) with L-asparagine instead of sodium nitrate as the nitrogen source. When required, the medium was supplemented with 200 mg hygromycin /ml. For analysis of carotenoids and fusarins in the mycelia, the strains were grown on DG minimal agar for 7 days as described by Prado et al. (2004). Incubations were at 22°C or 30°C, either in the dark or under illumination (5 W/m<sup>2</sup> white light at 22°C and 25 W/m<sup>2</sup> at 30°C). For gibberellin and bikaverin analyses, the strains were grown as submerged shaken cultures in 500 ml flasks with 250 ml of high nitrogen broth (ICI medium, Geissman et al., 1966) or low nitrogen broth (the same medium with 10% of the nitrogen source, called 10% ICI medium by the same authors). The flasks were inoculated with 10<sup>6</sup> conidia and grown for 7 days on a rotary shaker at 30°C.

For RNA extractions, 14 cm wide Petri dishes with 80 ml DG minimal medium were inoculated with 10<sup>6</sup> conidia and incubated in the dark at 30°C for 3 days. When indicated, the dish was illuminated under 25 W/m<sup>2</sup> for the times indicated before mycelia filtration. Heat-shock incubations were done as described by Youssar et al. (2005). For large-scale DNA extraction, 250 ml Erlenmeyer flasks with 50 ml of minimal medium were inoculated with 10<sup>6</sup> conidia and incubated for 3 days at 30°C before filtration. In all cases, the mycelial samples were separated from the media with filter paper, frozen in liquid nitrogen and stored at -80°C before DNA or RNA extraction.

### 2.2. Cloning of *wcoA*

Two degenerate oligonucleotides, 5'-GA(TC)ATG(TA)(CG)(TC)TG(TC)GC(TC)TT(TC) GT-3' and 5'-(GC)(TA)(TC)TC(AG)AACCA(AG)-GT(AG)TA(AG)CC-3', were deduced from the aminoacid sequences DMSCAFV and

GYTWFES from the *F. graminearum* FG07941.1 predicted polypeptide, and used for PCR amplification on cDNA from the wild type strain FKMC1995, resulting in the amplification of a 829 bp PCR product. The conserved segments were chosen upon comparison with the WC-1 protein of *N. crassa*. To reduce the chance of point mutations, the PCR reaction was carried out with the proofreading Triplmaster® PCR system (Eppendorf, Hamburg, Germany). The sequence of the obtained PCR product confirmed that we cloned an internal segment of the WC-1 orthologue of *F. fujikuroi*. Based on this sequence, two new oligonucleotides, 5'-GACTCTGCTGAACCTCCCTGCCTTCGTGAACCATCTTCTTC-3' and 5'-GAAGAAGAT GGTTCACGAAGGCAGGGAGGTTTCAGCAGAGTCGC-3', were chosen to obtain the DNA fragments corresponding to the sequences from each primer to the 5' and 3' ends of *F. fujikuroi wcoA* cDNA, respectively, using the BD Smart™ RACE cDNA amplification kit (BD Biosciences Clontech, San Jose, CA, USA). The complete *wcoA* gene sequence was obtained from five overlapping DNA segments obtained from FKMC1995 DNA with the following primer pairs (product size in parenthesis): 5'-CCGCTGCAGCTAGGGTCTTC-3' / 5'-TACCTCCATCGGCATGGACC-3' (563 bp), 5'-ACATGTCCTGCGCCTTTGTC-3' / 5'-GAGGCTGCGGATTTGGTTGG-3' (691 bp), 5'-CGAAAACCACGCCACGGGTC-3' / 5'-GGTAGAGGGCATCATAGAAC-3' (602 bp), 5'-TGACGACTATAACCGGTGAG-3', 5'-TGTTGTGTCCTTCAGCTCGC-3' (681 bp), and 5'-GTTGTCCTCTGAGGCTAAAG-3', 5'-GCACCACGCTCCGTAAATCC -3' (704 bp). PCR reactions were performed using the Triplmaster PCR system (Eppendorf AG, Hamburg, Germany) to enhance the fidelity of the amplification. The sequences from each segment were determined from both DNA strands of at least two independent PCR products using an ABI Prism® 3100 Genetic Analyzer (Applied Biosystems, Foster City, CA, USA).

### 2.3. Transformation

Protoplasts were obtained from FKMC1995 as described by Prado-Cabrero et al. (2007a). 10<sup>8</sup> protoplasts were transformed with plasmid pALEX7 linearized with *NotI*, containing the *wcoA* gene interrupted by the *hph* gene (hygromycin resistant cassette). The *wcoA* gene was obtained by PCR from genomic DNA with primers 5'-ACGACATAGCGGATCCTCCC-3' and 5'-TTTATTAGACCATGCTTCGCCTCGC-3'. The resulting 4.3 kb DNA product, which includes 0,56 and 0,65 kb of upstream and downstream untranslated sequences, respectively, was cloned into the pGem®-T vector (Promega, Mannheim, Germany). A 3,8 kb DNA segment containing the *hph* gene was obtained from the plasmid pHJA2 (Fernández-Martín et al., 2000) by amplification with primers 5'-ATCGTCCCAAAGCTTTTGGCGG-3' and 5'-GTCCTGTAAGCTTGAGAG

TTCA-3' and introduced into the *Hind*III restriction site of the *wcoA* gene to yield plasmid pALEX7. The orientation of the insert was determined by restriction analysis. Transformation was done following Proctor et al. (1997).

#### 2.4. Molecular techniques

DNA and RNA samples for southern and northern analyses were obtained with the GenElute Plant Genomic DNA Miniprep Kit (Sigma) and the Perfect RNA Eukaryotic Kit (Eppendorf), respectively. Southern and northern blot hybridizations were performed as described Sambrook and Russell (2001). In both cases, nylon membranes were probed with an internal 765 bp segment from the *wcoA* gene obtained by PCR with primers 5'-TACCTCCATCGGCATGGACC-3' and 5'-TGACGACTATAACCGGTGAG-3'. The *carB* probe used in the northern analysis was obtained with primers 5'-TGGGCGA GCTCATGAGCGACATTAAGAAATCTG-3' and 5'-CTTAATGTCGC-CCATGGTGGCTG-3'. After transfer, RNA on the membranes were stained during 30 min in a 0.02% methylene blue solution in 0.3 M sodium acetate, pH 5.2, and washed with distilled water for 2 h. Stained rRNA bands were used as load controls. Primer extension was performed as described by Sambrook and Russell (2001) from primers 5'-CAAACCTCTA TCAGGGAGGA-3' and 5'-CGACCAAGCACGAAATACC-3', 23 bp downstream and 401 bp upstream of the translation start codon, respectively. For PCR analyses, DNA samples from the transformant strains were obtained from a small mycelial fragment following the method described by Hoffman and Winston (1987).

Real time PCR (RT-PCR) expression analyses were performed using total RNA samples as template. The reactions, carried out in 25 µl volumes on an ABI 7500 (Applied biosystems), consisted of a 30 min retrotranscription step at 48°C, 10 min at 95°C and 40 cycles of 95°C denaturation for 15 s and 60°C polymerization for 1 min. Dissociation curves were achieved afterwards. The genes investigated and their corresponding primers sets for the RT-PCR reactions were: *carB* (5'-TCGGTGTCGAGTACCGTCTCT-3' and 5'-TGCCTTGCCGGTTGCTT-3'), *carT* (5'-CGGCACCAACACCAGACA-3' and 5'-TGGACTAGGAATGGCAAGGACTT-3'), and *wcoA* (5'-GGGCAAAGGCGGATGTCT-3' and 5'-CGGCGTTATCGGTTCCAA-3'). The indicated primers were chosen with the software Primer Express™ v2.0.0 (Applied Biosystems) from intronless sequences from each gene and synthesized (HPLC grade) either by Thermo Electron Corporation (Waltham, USA) or by StabVida (Oeiras, Portugal). The RT-PCR conditions were optimized as recommended by the manufacturer. This included optimization of MgCl<sub>2</sub> and primer concentrations and annealing temperatures. The optimized conditions for all the genes investigated were 12 µl Power SYBR® Green PCR Master Mix 2X (Applied Biosystems), 0.125 µl MultiScribe™ Reverse Transcriptase (50

U/ml), 0.125 µl RNase Inhibitor (10 U/ml), 50 ng of RNA and 5 mM of each primer, in a total volume of 25 µl. As a control for constitutive expression it was used the  $\beta$ -tubulin gene of *F. fujikuroi* (5'-CCGGTGCTGGAAACAAGT-3' and 5'-CGAGGACCTGGTCGACAAGT-3'). Relative gene expression was calculated with the  $2^{-\Delta\Delta CT}$  method with Sequence Detection Software v1.2.2 (Applied Biosystems). Each RT-PCR analysis was performed four times (duplicated samples from two independent experiments) and standard deviations calculated to ensure statistical accuracy.

## 2.5. Chemical analyses and conidia production

Carotenoid extractions were performed from lyophilized mycelial samples as described by Saelices et al. (2007). The polar and neutral carotenoid fractions were obtained as described by Thewes et al. (2005). Thin layer chromatography was done on silica gel (Merck, Darmstadt, Germany) run with a mixture of 40 ml light petroleum, 10 ml diethyl ether and 7 ml acetone. For HPLC analysis, a Waters system (Eschborn, Germany) equipped with a C30-reversed phase column (YMC Europe, Schermbach, Germany) and a photodiode array detector (model 996) was used. The column was developed with two solvents, A (MeOH:tert-butylmethylether, 500:500, v/v), and B (MeOH:tertbutylmethylether :water, 120:4:40, v/v/v). Each run consisted of 25 min with solvent A (1 ml min<sup>-1</sup>), 7 min with 57% solvent A 43% solvent B (1 ml min<sup>-1</sup>), and 40 min with solvent B (1,5 ml min<sup>-1</sup>).

Bikaverin concentrations were determined spectrophotometrically. The bikaverins were separated from carotenoids by adding 50 µl of NaOH 10 N to 500 µl of the crude acetone sample and centrifuged 2 min at 13,200 r.p.m. The supernatant, containing the carotenoid fraction, was removed and the precipitated fraction, containing the bikaverins, was dissolved again by adding 500 µl of chloroform and 200 µl of HCl 10 N. Bikaverin concentrations were calculated following Balan et al. (1970). Fusarin concentrations were calculated as described by Barrero et al. (1991), assuming that the major fusarin accumulated is 8Z-fusarin. Gibberellic acid (GA3) was analyzed by HPLC according to Barendse et al. (1980) using a Hewlett Packard HPLC system (Hewlett Packard, USA).

Conidia production on agar cultures was quantified as described by Prado et al. (2004). Conidia in submerged cultures were quantified by direct counting on a hemocytometer.

## 2.6. Sequence analyses

Blast analyses were done through the NCBI server ([www.ncbi.nlm.nih.gov/blast/](http://www.ncbi.nlm.nih.gov/blast/)). BlastP was carried out against the non-redundant Swissprot database. Alignments were achieved with the Clustal W program (EMBL-EBI European Bioinformatics Institute,

<http://www.ebi.ac.uk/clustalw/>). Corrections for multiple substitutions were applied for phylogenetic analyses. DNA sequences were obtained through the server [www.broad.mit.edu/annotation/fungi/](http://www.broad.mit.edu/annotation/fungi/) of the Broad Institute (Cambridge, MA. USA).

### 3. Results

#### 3.1. Cloning and sequence of the *wc-1* orthologue of *F. fujikuroi*, *wcoA*

The presence of *wc-1*-like genes in *Fusarium* species was checked by blast analysis against the sequence of the *F. graminearum* genome. Only one annotated gene, FG07941.1, was found with significant similarity to *wc-1* of *N. crassa*. Further Blast analyses against new *Fusarium* genomes, becoming available during execution of this work, confirmed the occurrence of a single gene. Taking into account the close phylogenetic relationship between *F. fujikuroi* and *F. graminearum*, degenerate oligonucleotides were designed from highly conserved domains in this protein family and used for PCR amplification on *F. fujikuroi* cDNA samples. As a result, an 800 bp PCR product was obtained whose sequence confirmed the amplification of the FG07941.1 *F. fujikuroi* counterpart for this DNA segment. The use of two new oligonucleotides from the ends of the 800 bp sequence, oriented outwards, allowed the cloning by a RACE cDNA technique of the missing 5' and 3' DNA segments of the gene, leading to the completion of the whole coding sequence. Comparison with the *wc-1* gene indicated that the cloned DNA segments included 555 and 241 bp of 5' and 3' presumable untranslated sequences. The sequence of this *F. fujikuroi* gene, that we called *wcoA*, was deposited in the EMBL database under accession number AM778551.

The gene *wcoA* of *F. fujikuroi* extends along 3,128 bp from the start to the stop codons, including a single 53 bp intron as deduced from the comparison of genomic and cDNA sequences. The open reading frame codes for a predicted 1,024 aa polypeptide, that is, 143 aa less than the *N. crassa* WC-1 protein. Comparison between both proteins revealed identical aminoacids in 578 positions, that is, a 56% of the WcoA protein, an identity percentage that rises to 83% when compared to the *F. graminearum* orthologue FG07941.1. A detailed comparison of the predicted WcoA protein with WC-1 (Fig. C3.1a) showed the presence of most of the relevant functional regions, i.e., the three PAS domains, the zinc-finger domain, and a shorter version of one of the two poly-glutamine domains, separated here in two sub-domains (18 and 8 glutamine residues in two segments of 28 and 12 aa, respectively, separated by 41 aa, against 37 glutamine residues in a single segment of 46 aa in the *N. crassa* protein). The major difference between WcoA and WC-1 is the lack in the former of some protein segments close to the carboxy end of the protein (Fig. C3.1b), that include the second poly-glutamine domain of WC-1.

A Clustal comparison between WcoA and a selection of proteins from this family (Fig.

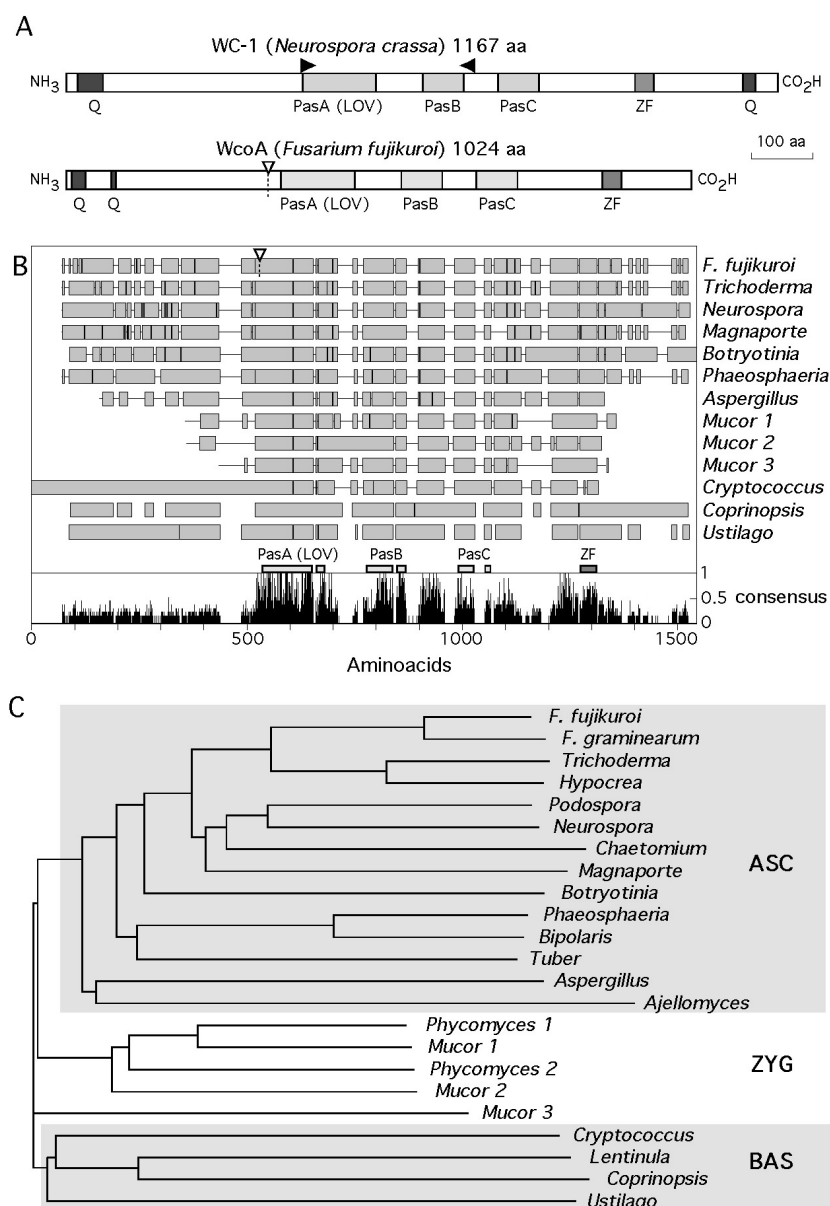


**Fig. C3.1. Sequence analysis of WcoA and other fungal proteins of the Wc-1 family.** (a) Schematic representation of the WcoA (AM778551) and Wc-1 polypeptides (Q01371). The inner boxes indicate relevant functional domains (Q: poly-glutamine domain; ZF: Zinc finger). The black arrowheads indicate the positions of the primers used for the cloning of the first *wcoA* DNA segment. The white arrowhead indicates the insertion site of the *hph* cassette in the *wcoA* disruption mutants (also shown in b). (b) Simplified representation of the Clustal comparison between WcoA and a selection of proteins from the WC-1 family (see below). The breaks between the boxes represent the gaps introduced by the Clustal program to facilitate alignment. The diagram below plots the presence of the consensus aminoacid. Locations of the PAS and zinc finger domains are represented over the plot. The dotted line indicates the interruption point in the *wcoA* mutants described in the next sections. (c) Phylogram of 23 fungal proteins from the WC-1 family. Species and accession numbers: *Fusarium fujikuroi* (WcoA, AM778551); *Fusarium graminearum* (FGSG\_07941); *Trichoderma atroviride* (BLR-1, AAU14171); *Hypocrea jecorina* (AAV80185); *Podospora anserina* (CAD60767); *Neurospora crassa* (WC-1, Q01371); *Chaetomium globosum* (XP\_001219613); *Magnaporthe grisea* (MGWC-1, XP\_360995); *Botryotinia fuckeliana* (EDN19381); *Phaeosphaeria nodorum* (EAT80456); *Bipolaris oryzae* (BAF35570); *Tuber borchii* (TBWC-1, CAE01390); *Aspergillus nidulans* (XP\_661040); *Ajellomyces capsulatus* (EDN06969); *Phycomyces blakesleeanus* (1: MadA, ABB77846; 2: WcoA, ABB77844); *Mucor circinelloides* (1: MCWC-1a, CAJ13843; 2: MCWC-1b, CAJ13844; 3: MCWC-1c CAJ13845); *Cryptococcus neoformans* (Bwc-1, AAT73612); *Lentinula edodes* (BAF56991); *Coprinopsis cinerea* (Dst1, AB195817); *Ustilago maydis* (XP\_759327). Shaded areas stand out ascomycete (ASC) and basidiomycete (BAS) species. Non-shaded area, zygomycete species (ZYG).



C3.1b) showed a high conservation of several protein domains, that includes the three PAS domains, and a high divergence in other regions of the protein. Out of 23 proteins investigated (13 of them depicted in Fig. C3.1b), only the ones from the *Fusarium* species, and *Magnaporthe grisea*, besides *N. crassa*, contain clear poly-glutamine domains, and very short versions of this motif are also found in the amino domains of the proteins from *Botryotinia fuckeliana* and MCWC-1a from *M. circinelloides*. Additionally, the zinc-finger motif is missing in the four WC-1 like proteins from basidiomycetes included in our analysis and incomplete in MCWC-1b from *M. circinelloides*. The phylogenetic comparison of the 23 fungal WC-1 protein sequences (Fig. C3.1c) fits the taxonomic separation of ascomycetes, zygomycetes and basidiomycetes, and a presumed common origin from an ancestor WC protein in an ancient fungal group.

### 3.2. *wcoA* expression

The presence of 555 bp untranslated sequence in the *wcoA* DNA obtained from a *F. fujikuroi* cDNA sample indicates a considerable distance from the transcription start point to the presumed start codon of the gene. To confirm this, primer extension experiments were carried out from two different primers along the *wcoA* 5' region. The analysis from a primer 24 bp downstream of the start codon gave no clear signal in the gel (result not shown), suggesting the lack of transcription start close to the coding sequence. The analysis from a second primer covering a farther upstream region resulted in several clear bands in samples either from dark or light-grown mycelia (Fig. C3.2). This result indicates different alternative transcription start points at variable distances, ranging from 400 to 600 bp upstream of the predicted start codon. With any of these start points, a long 5' UTR is expected in the *wcoA* mRNA, probably involved in post-transcriptional regulation. A complex transcriptional regulation has also been described for *wc-1* in *N. crassa*, that include transcription initiation sites leading to even longer 5' UTR segments for this gene (Káldi et al., 2006).

The *wc-1* mRNA levels are induced by light in *N. crassa*, a stimulation mediated by the own WC-1 protein (Ballario et al., 1996). Northern blot experiments were carried out with a *wcoA* probe on total RNA from *F. fujikuroi* mycelia incubated in the dark or exposed

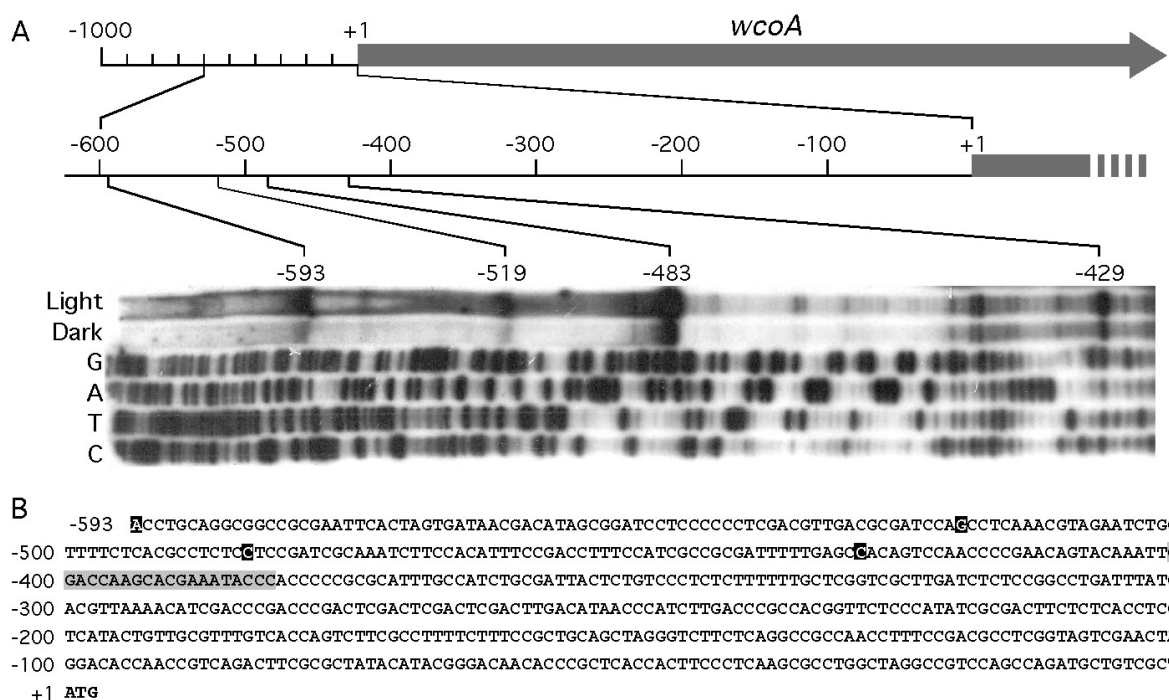


**Fig. C3.2. Transcription start points for *wcoA*.** Primer extension analysis of *wcoA* from total RNA samples from the wild type strain grown in the light or in the dark and schematic representation of the relevant regions of the gene. The tentative sites for transcription start are marked in black in the promoter sequence shown below. The grey box indicates the  $^{32}\text{P}$ -end-labeled primer used in the analysis.

to different light pulses. The amounts of *wcoA* mRNA levels suffered no significant changes following different times of illumination either in the wild type or in a carotenoid overproducing strain (Fig. C3.3a). As a control, the membrane was also probed with the *carB* gene. As expected, this gene showed a light-dependent expression in the wild type, and a derepression in the dark in the carotenoid overproducing strain.

Further northern blot experiments on total RNA from the wild type strain showed similar levels of *wcoA* mRNA in mycelial samples of different ages (Fig. C3.3b). In addition to light-regulation, a mild heat-shock activation was reported for the gene *carB* (Prado et al., 2004). To check a possible occurrence of heat-shock regulation of *wcoA*, the cultures were incubated for 1h or 2h at 38°C or 42°C before RNA extraction. The amounts of *wcoA* mRNA were similar to the ones under control conditions (Fig. C3.3b), suggesting the lack of such regulation. In summary, the *wcoA* gene appeared to be constitutively expressed under the different culture conditions tested, and showed no correlation with the regulation of a structural gene for the carotenoid pathway.

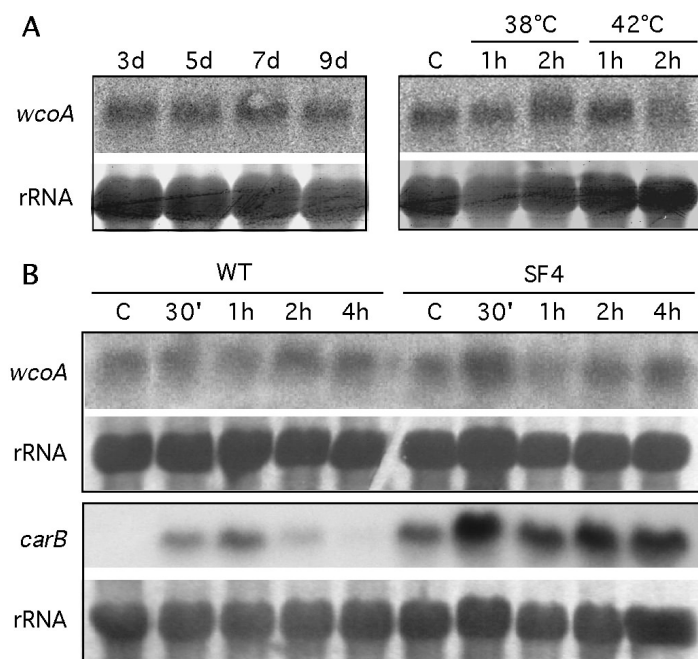


**Fig. C3.3. Expression of the gene *wcoA*.** (a) Effect of Light. Northern blots of total RNA isolated from the wild type FKMC1995 or the carotenoid overproducing strain SF4 in the dark or following incubation in the light for the indicated times in hours (D: dark control). Expression of the gene *carB* is shown below for comparison. rRNA bands are shown below each panel as load controls. (b) Effect of age and heat-shock. Northern blots of total RNA isolated from the wild type FKMC1995 grown for the indicated days (left panel) or incubated 3 days followed by 1 or 2 hours at the indicated temperature (right panel; C: non-heated control).

### 3.3. Gene disruption of *wcoA*

A gene disruption vector was constructed containing the *wcoA* sequence interrupted with a hygromycin-resistant cassette (Fig. C3.4a). The interruption point precedes the relevant PAS domains of the protein (Fig. C3.1a); thus, the production of a severely truncated non-functional WcoA polypeptide is expected. Upon transformation of wild-type protoplasts with a linear fragment of the interrupted gene, 56 hygromycin-resistant transformants were obtained. To identify those that replaced the wild type gene by the interrupted version through homologous recombination events (Fig. C3.4a), DNA samples were obtained from each transformant after subculture on hygromycin-supplemented medium and growth from uninucleate conidia to ensure homokaryosis. A PCR screening using primers located at both sides of the *hph* inserted DNA segment indicated the absence of the wild type *wcoA* gene in 12 out of 56 transformants tested. Six of these transformants were chosen for detailed southern blot analysis using an internal segment of the *wcoA* gene as a probe (Fig. C3.4b). Five of them (M5, M6, M15, M42 and M50) exhibited two bands upon digestion with either *Bgl*II (6,1 and 2,6 kb) or *Pvu*I (2,9 and 3 kb), compared to the expected single band obtained with the wild type DNA with the same restriction enzymes (5 and 1,9 kb, respectively). The sizes of the bands were consistent with the replacement by homologous recombination of the wild type *wcoA* allele with the one disrupted with the 3.8 kb *hph* cassette, which contains single *Bgl*II and *Pvu*I restriction sites (Fig. C3.4a). As further support, one of the bands showed a weaker signal in the transformants (Fig. C3.4b), as expected from the short length of the DNA segment covered by the probe in one of the

bands because of the *hph* insertion (Fig. C3.4a). One of the transformants (M16) showed the wild type band plus additional bands of different sizes than the ones expected from homologous recombination. This could be a false positive from the PCR screening. The transformant M16 was probably originated by the integration of the *hph* gene in an unrelated location at the genome through non-homologous recombination.

The single band found in the wild type and the loss of this band in the transformants on the southern blot (Fig. C3.4b) supports the presence of a single copy of the *wcoA* gene in *F. fujikuroi* and confirms the haploid nature of this fungus.

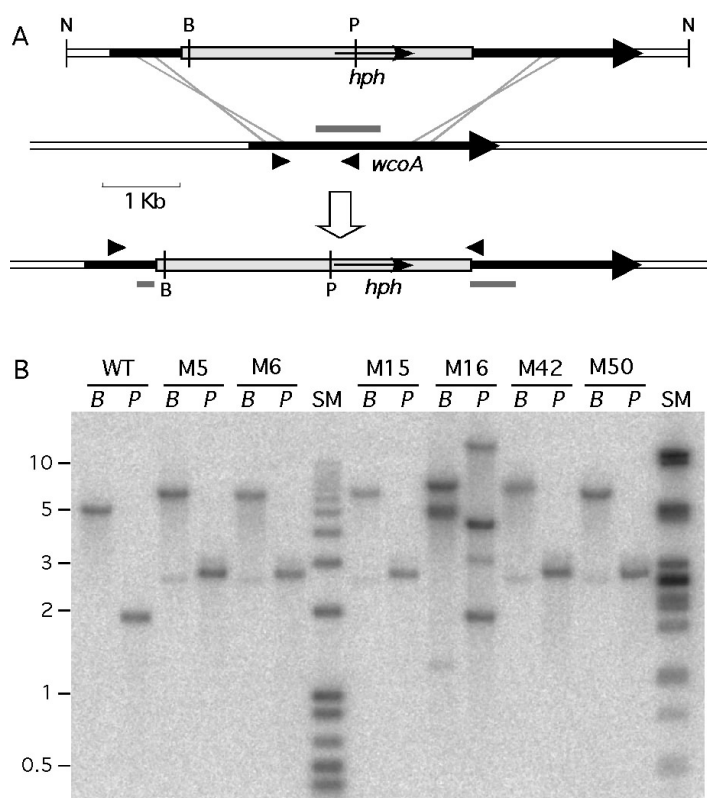


**Fig. C3.4. Generation of *wcoA* disruptant mutants.** (a) Physical map of the *hph* insertion (grey box) in the *wcoA* gene (black thick arrow) in plasmid pAlex7 and expected double recombination events leading to *wcoA* disruption. The grey bar indicates the probe used in the southern blot shown below. N: *NotI* sites used to obtain the linear DNA segment for transformation. Internal *BglII* (B) or *PvuI* (P) sites are indicated. (b) Southern blots of genomic DNA from the wild type (WT) and six selected transformants digested with *BglII* (B) or *PvuI* (P) and hybridized with the *wcoA* probe indicated in the scheme. SM: Size marker (relevant sizes shown on the left in Kb).

### 3.4. Carotenoid biosynthesis in *wcoA* disruptant strains

According to the photoreceptor role tentatively attributed to the WcoA protein, the disruptant mutants are expected to lose the light-induced carotenogenesis. To check this prediction, four of the identified *wcoA* mutants were chosen for detailed carotenoid analyses compared to the wild type grown in the dark or under continuous illumination. The five strains exhibited differences in their external appearance and pigmentation that became more patent with culture aging. Thus, the mutants slowly acquired a purple color, barely present in the wild type. As expected, all the strains lacked the orange pigmentation in the dark, a trait especially visible on young colonies (Fig. C3.5a). Accordingly, the

chemical analyses found only traces of colored carotenoids in their mycelia (less than 5 µg / g dry mass). However, the five strains exhibited an orange pigmentation in the light (Fig. C3.5a), indicating a functional photocarotenogenesis in the *wcoA* disruptants. The presence of carotenoids in light-grown mycelia was confirmed by column chromatography (Fig. C3.5b), TLC (Fig. C3.5c) and HPLC analyses (Fig. C3.5d). The three analytical methods showed a lower proportion of polar carotenoids in the *wcoA* disruptants compared to the control strain, but the four mutants accumulated in the light at least the same amount of carotenoids than the wild type (Fig. C3.4b). We infer from these results that the photoinduction of carotenoid biosynthesis in *F. fujikuroi* does not need a functional WcoA protein.

To confirm that the structural carotenoid genes maintain the regulation by light in the *wcoA* mutants, RT-PCR experiments were done with mycelia from the wild type and two disruptant strains (M5 and M6) grown in the dark and exposed to different light pulses (Fig. C3.6). As already shown (Fig. C3.3a), the low amounts of *carB* mRNA in the dark increased following illumination up to one hour and decreased afterwards, a result that fits previous observations (Prado et al., 2004). The RT-PCR protocol showed a 50-fold increase in the amounts of *carB* mRNA in the wild type one hour after light onset, and a weaker response in the two mutants tested (Fig. C3.6), suggesting a partial role of *wcoA* plays in the light induction of the gene. The gene *carT*, coding for the carotenoid oxygenase responsible for the oxidative break of torulene, the neurosporaxanthin precursor, was also reported to be induced by light (Prado-Cabrero et al., 2007a). Our data showed a more modest light induction of *carT* mRNA compared to *carB* (Fig. C3.6), also found in the *wcoA* disruptants. However, in this case the overall amounts of *carT* mRNA in the mutants were comparable to the ones of the wild type.

The same RNA samples were checked for *wcoA* mRNA levels using primers for a gene segment located upstream of the *hph* insertion site, expected to be expressed in the mutants to produce a truncated WcoA protein. The RT-PCR analyses (Fig. C3.6) confirmed the lack of light regulation of *wcoA* mRNA shown in Fig. C3.3b. Interestingly, the mutants exhibited a 3-fold increase in the amounts of *wcoA* mRNA compared to those of the wild type, a difference that could be explained either by a self-regulation of *wcoA* expression by the WcoA protein, or by differences in mRNA stability of the truncated mRNA produced by the mutants.

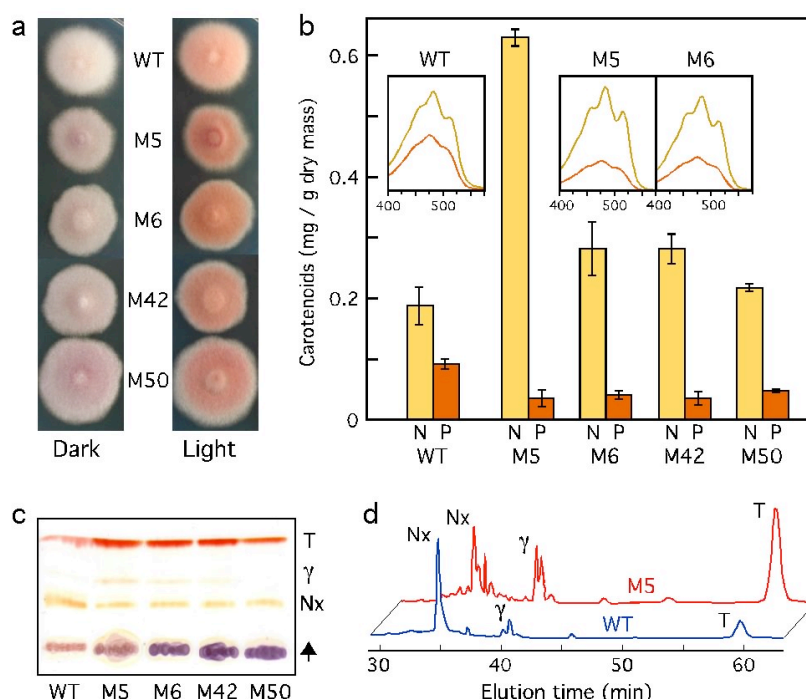


**Fig. C3.5. Production of carotenoids by *wcoA* disruptant mutants.** (a) Colonies of the wild type and four *wcoA* mutants grown four 4 days at 22°C on minimal agar in the dark or under continuous illumination. (b) Concentrations of neutral (N) and polar (P) carotenoids in the mycelia of the wild type and four *wcoA* mutants grown for 7 days at 22°C on minimal agar under continuous illumination. The data show the average and standard deviations from 4 independent determinations. Absorption spectra of representative neutral (yellow line) and polar (orange line) carotenoids fractions are indicated in inner boxes. The numbers below each spectrum indicate wavelength (nm). (c) Thin layer chromatography of crude extracts from the wild type and the four mutants grown for 7 days at 22°C on minimal agar under continuous illumination. The arrow indicates the origin and direction of chromatographic separation. T: torulene; Nx, neurosporaxanthin; γ, γ-carotene. (d) HPLC elution profiles at 473 nm of the carotenoids accumulated by the wild type and the *wcoA* mutant M5 under the same culture conditions. The profiles obtained with the mutants M6, M42 and M50 were similar to the one from M5

### 3.5. Production of other metabolites by the *wcoA* disruptant strains

The purple pigmentation acquired by the aging colonies of the *wcoA* mutants on agar, less apparent or absent in the control strain, suggests alterations in the production of other secondary metabolites. The purple pigment, retained in the origin on the TLC plates because of its high polarity (Fig. C3.5c), was eluted and identified as bikaverin from its typical absorption spectrum in chloroform, with maximal absorbance at 518 nm (Balan et al., 1970). To check the effect of the *wcoA* mutation on secondary metabolism, the wild type and the two selected *wcoA* disruptant strains were grown under appropriate culture conditions for fusarin, bikaverin and gibberellin production. Analysis of fusarin content in surface cultures at 30°C (Barrero et al., 1991) showed the accumulation of high amounts by the wild-type strain used in this work either in the dark or in the light (Fig. C3.7a). The amounts of this metabolite in the two mutants were higher in the dark but negligible in the

light. This result suggests a light-dependent regulatory role of WcoA on fusarin biosynthesis.

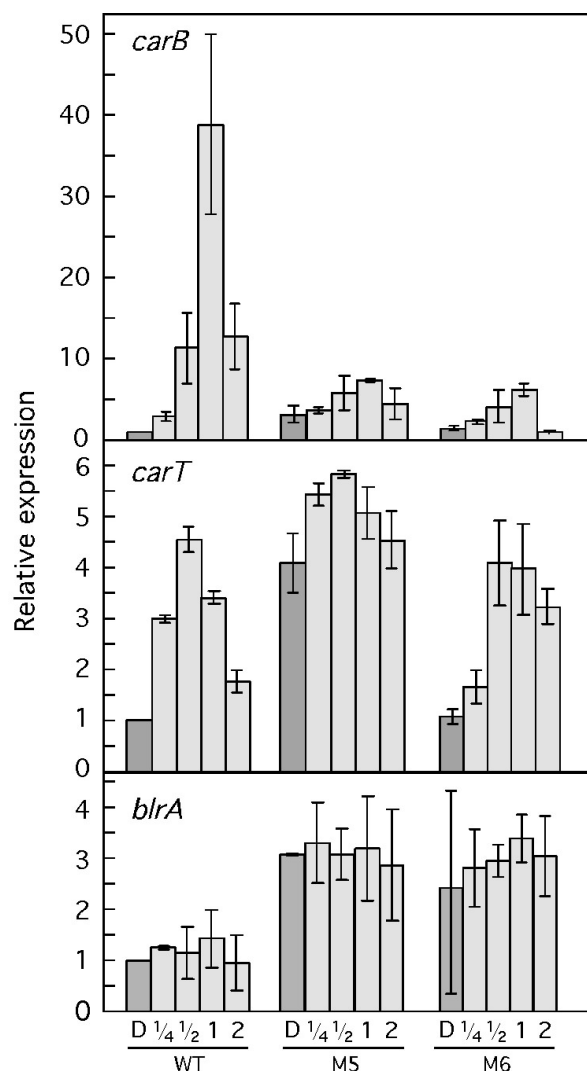


**Fig. C3.6.** Effect of light on the expression of the structural genes of the carotenoid pathway *carB* and *carT*, and of gene *wcoA*, in the wild type and in the *wcoA* disruptant mutants M5 and M6. The data show RT-PCR analyses from RNA samples of the strains grown in the dark and exposed to light for the times indicated (hours). Relative expression was referred to the value of the wild type in the dark. The bars represent the standard deviation for 4 determinations from two independent experiments.

To check the production of gibberellins and bikaverins, shaken cultures were grown under different nitrogen concentrations. Although illumination is less efficient on submerged mycelia, the effect of continuous light was also investigated. In three independent experiments, there were differences in the color of the mutant cultures compared to the one of the wild type, especially in low nitrogen medium (Fig. C3.7b). Under nitrogen starvation, the *wcoA* mutants accumulated less gibberellins (Fig. C3.7c) and more bikaverins (Fig. C3.7d) than the wild type. In agreement with the nitrogen repression of the pathway, only traces of gibberellins were produced by the mutant and control strains in high nitrogen medium.

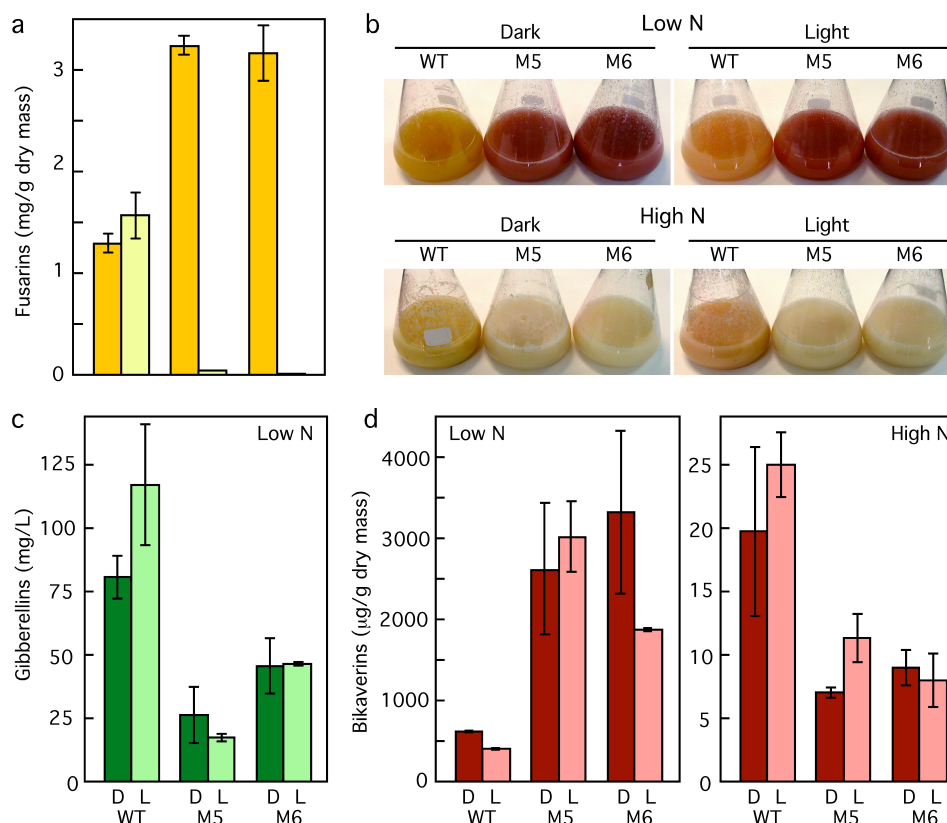


**Fig. C3.7. Secondary metabolite production by the wild type and *wcoA* disruptant mutants.** (a) Concentrations of fusarins in the mycelia of the wild type and the *wcoA* mutants M5 and M6 grown for 7 days at 30°C on minimal agar in the dark (D) or under continuous illumination (L). (b) Representative shake cultures of the same strains grown for 7 days at 30°C in high nitrogen or low nitrogen media in the dark or under continuous illumination. (c) Gibberellic acid concentrations in the filtrates of the shake cultures grown for 7 days at 30°C in low nitrogen medium in the dark (D) or under continuous illumination (L). (d) Bikaverin concentrations in the mycelia of the shake cultures grown for 7 days at 30°C in low or high nitrogen medium in the dark (D) or under continuous illumination (L). The data displayed on (a), (c) and (d) show the average and standard deviations from 4 independent determinations.

As expected from the similar nitrogen regulation of the bikaverin pathway, the wild type produced in high nitrogen medium about 5% of the amounts of bikaverins accumulated in low nitrogen medium. However, in contrast to the result found under nitrogen starvation, the mutants produced less bikaverins under these conditions than the wild type. In both cases (gibberellin and bikaverin production) only minor differences were observed between light and dark cultures, indicating a light-independent effect of the *wcoA* mutation.

### 3.6. Effect of the *wcoA* mutation on conidiation

In contrast to *N. crassa*, light does not significantly affect conidia production in the wild type of *F. fujikuroi* used in this work (Prado et al., 2004). Because of the pleiotropic effect of the *wcoA* mutation, conidia production was investigated in the culture conditions



described in the former sections. Conidiation levels on minimal agar were severely reduced in the mutants compared to the wild type (Fig. C3.8a). The same effect was observed in submerged cultures in high nitrogen medium (Fig. C3.8b). Conidia were more abundant in the low nitrogen cultures, indicating a stimulation of conidiation under nitrogen-starving conditions. In this case, however, higher amounts of conidia were found in the cultures of the mutants (Fig. C3.8b).

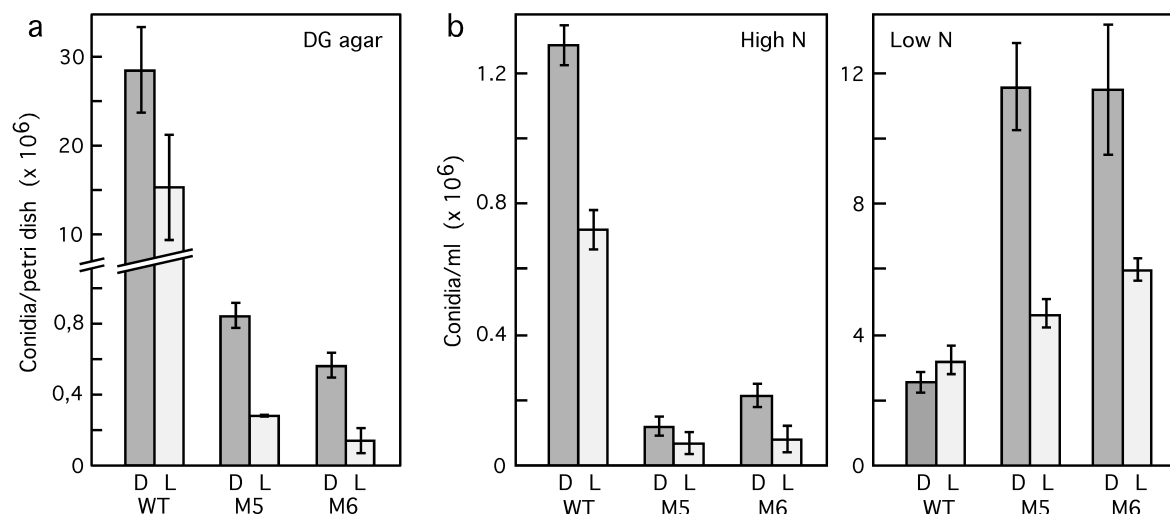


**Fig. C3.8. Production of conidia by the wild type and *wcoA* disruptant mutants.** (a) Conidia produced by the wild type and the *wcoA* mutants M5 and M6 grown for 7 days at 22°C on minimal agar in the dark (D) or under continuous illumination (L). (b) Conidia found in the filtrates of the cultures shown on Fig. C3.7b. The data show the average and standard deviations from 6 independent determinations.

The mycelial surface of the *wcoA* mutants grown on minimal agar was less hydrophobic than the one of the wild type, as shown by their different water-absorbing properties. Flooding of the agar cultures shown on Fig. C3.5a with distilled water during one hour resulted in water embedding of the surface of the *wcoA* mutant colonies, while the wild-type colonies did not absorb water (Fig. C3.S1, supplementary material), an effect that indicates external biochemical differences.

#### 4. Discussion

The proteins of the WC family govern many light-controlled processes in fungi (Corrochano, 2007). White Collar-1 (WC-1) works in *N. crassa* in coordination with a partner protein, WC-2 (Linden and Macino, 2007), forming a functional photosensitive heterodimer in which WC-1 plays the photoreceptor role (He et al., 2002). Similar complexes have been described in ascomycete and basidiomycete species (Casas-Flores et al., 2004; Idnurm and Heitman, 2005), and are probably present also in zygomycetes

(Idnurm et al., 2006; Silva et al., 2006), pointing to the WC complex system as a highly conserved fungal regulatory mechanism.

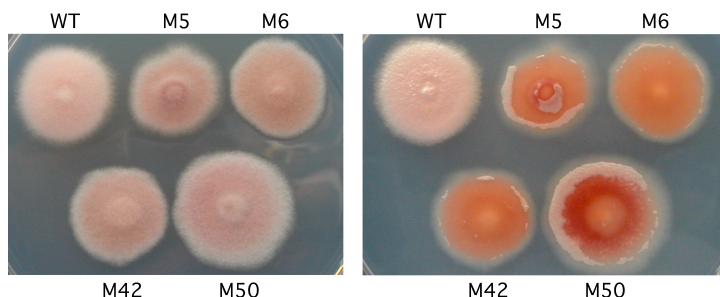


**Fig. C3.S1.** Colonies of the wild type and four *wcoA* mutants grown four 4 days at 22°C on minimal agar under illumination. The picture shows the same colonies before (left) or after gentle addition of 25 ml water and incubation for 1 h (right).

A paradigmatic example of a fungal light-regulated process is the photoinduction of carotenoid biosynthesis (Avalos et al. 1993), a WC-governed response in *N. crassa* (Harding et al. 1981). The carotenoid pathways of *F. fujikuroi* and *N. crassa* are very similar, from the usual early reactions shared by other carotenogenic fungi (Linnemanstöns et al., 2002a) to the highly specific late reactions. Thus, *F. fujikuroi* and *N. crassa* share a unique gene for a carotenoid oxygenase, which catalyzes the rare asymmetric oxidative break needed to produce their apocarotenoid end-product, the acidic neurosporaxanthin (Prado-Cabrero et al., 2007a; Saelices et al., 2007). The pathway is stimulated by light in both fungi (Harding and Turner, 1981; Avalos and Cerdá-Olmedo, 1987), and the structural genes are subject of a similar transcriptional photoinduction (Schmidhauser et al., 1994; Saelices et al., 2007; Prado et al., 2004; Prado-Cabrero et al., 2007a), suggesting the mediation in *F. fujikuroi* of an orthologous WC complex. As observed in other ascomycetes, a single *wc-1*-like gene is found in the available *Fusarium* genomes (*F. graminearum*, *F. verticillioides*, and *F. oxysporum*). We have cloned the *F. fujikuroi* version of this gene, that we called *wcoA*. The predicted WcoA protein is structurally similar to WC-1, with the same PAS and zinc finger domains in equivalent relative positions. This structural pattern is maintained in all the WC-1-like proteins analyzed in ascomycetes and zygomycetes (Fig. C3.1b). Actually, WcoA is more similar to WC-1 than other orthologues because of the presence of poly-glutamine tracts close to the amino end of the protein, absent in the majority of the WC-1 counterparts.

In *N. crassa*, the *wc-1* mRNA levels are strongly induced by light (Ballario et al., 1996), a transient activation mediated by the own Wc-1 gene product, but we found no relevant effect of light on the amounts of *wcoA* mRNA in *F. fujikuroi*. This is not against a photoreceptor role for WcoA. Thus, the products of the genes *cwc-1* from the basidiomycete *C. neoformans* and *madA* from the zygomycete *P. blakesleeanus* mediate light-regulated processes, but their mRNA levels are not induced by light (Idnurm and Heitman, 2005; Idnurm et al., 2006). Only one of the three *wc-1*-like genes of *M.*

*circinelloides*, *mcwc-1a*, is transcriptionally activated by light, but this photoinduction is lost upon mutation of another *wc* gene, *mcwc-1c*, whose mRNA levels are not affected by light (Silva et al., 2006). The *mcwc-1c* orthologue of *P. blakesleeanus*, *wcoA*, is also photoinducible (Idnurm et al., 2006), as are the genes for other WC-1-like proteins, such as *Tbwc-1* from *Tuber borchii* (Ambra et al., 2004).

To confirm the mediation of WcoA on the control by light of *F. fujikuroi* carotenogenesis, we obtained strains carrying a mutated *wcoA* allele. For this purpose, we interrupted the coding sequence with the *E. coli hph* gene surrounded by *A. nidulans* promoter and termination sequences. The insertion was done in a position of the *wcoA* coding region preceding the PAS segments, so that the synthesis of a truncated protein lacking all relevant WC-1 functional domains must be expected. Against our prediction, the mutants conserved the light induction of carotenoid biosynthesis. The WcoA apparently contributes partially to the transcriptional induction of the structural genes of the pathway, as indicated by the lowered light stimulation of the *carB* mRNA levels. However, the *carB* gene was still induced by light and, most importantly, there was no reduction in the amounts of carotenoids synthesized in response to illumination. Therefore, photocarotenogenesis in *F. fujikuroi* relies in a different photoreceptor. Moreover, mutants overproducing carotenoids in the dark are easily isolated in *F. fujikuroi* (Avalos and Cerdá-Olmedo, 1987) but are unknown in *N. crassa*, suggesting deeper regulatory differences between both fungi that remain to be clarified.

The fungal genomes contain genes for other putative photoreceptors, such as phytochromes, cryptochromes and opsins (Herrera-Estrella and Horwitz, 2007; Corrochano, 2007). Phytochromes absorb red light, which does not induce carotenogenesis in *Fusarium* (Schrott et al., 1982). Opsins use as light-absorbing prosthetic group the apocarotenoid retinal, a side-product of the *F. fujikuroi* carotenoid pathway (Prado-Cabrero et al., 2007b). The *carB* mutants are unable to synthesize retinal, but conserve the photoinduction of the pathway (Fernández-Martín et al., 2000). Additionally, a mutant devoid of one of the two opsins of *F. fujikuroi* exhibits a normal carotenoid photoinduction (Prado et al., 2004). These experimental observations leave cryptochromes as likely candidates to mediate light induction of carotenogenesis in *F. fujikuroi*, a hypothesis that awaits experimental demonstration.

The *wcoA* mutants exhibit alterations in their pigmentation under different culture conditions, indicating changes in the production of other secondary metabolites. Thus, their agar cultures in the dark acquire a pale purple color that turns deeper as the colonies become older. Furthermore, a detailed phenotypic analysis of two representative mutants showed alterations in the production of fusarins, bikaverins and gibberellins. In contrast to the wild type, the mutants produced no fusarins under light at 30°C, indicating a light-dependent role of WcoA in the regulation of the biosynthesis of this polyketide.

Additionally, nitrogen-starving cultures of the same mutants produced less gibberellins and more bikaverins than the control strain. This effect of the *wcoA* mutation reminds the one of the *areA* mutation, which also results in reduced gibberellin production (Tudzynski et al., 1999; Mihlan et al., 2003) and enhanced bikaverin production (Linnemanstöns et al., 2002b). The result was similar irrespective of illumination, suggesting a light-independent role of WcoA in the nitrogen regulation of secondary metabolism in *F. fujikuroi*.

The participation of WcoA in the regulation of different pathways of secondary metabolism reminds the role of other global regulators, such as Tor or LaeA. Mutants of the *laeA* gene of *A. nidulans* simultaneously lose the expression of some secondary metabolism gene clusters and derepress others (Bok and Keller, 2004). The LaeA protein was identified as a methyl transferase, suggesting a role in a general cluster silencing mechanism (Bok et al., 2006). The Tor protein, recently found in *F. fujikuroi* (Teichert et al., 2006), is homologous to the yeast proteins Tor1p and Tor2p, targets for the antibiotic rapamycin and involved in coupling nutrient signaling to cell growth control. Rapamycin inhibition shows that the Tor protein plays a role in the nitrogen regulation of gibberellin and bikaverin biosynthesis by *F. fujikuroi*, although this protein is also associated to many other cellular processes (Teichert et al., 2006).

In contrast to the WC-1 like photoreceptors, LaeA or Tor are not DNA binding proteins and they have no relation with light. The regulatory role of WcoA probably involves activation or repression of target genes by direct binding to their promoters, an activity that could be modulated by the interaction with other regulatory proteins or, at least in some cases, by light. The *Fusarium* genomes contain an orthologous gene for *wc-2* (FVEG\_00478.3 in *F. verticillioides*, 50% identity with WC-2), hereafter *wcoB*. The formation of a heterodimeric WC complex in *F. fujikuroi* must be considered a very likely hypothesis. The need of WcoB for appropriate WcoA function awaits for experimental demonstration, starting with the targeted mutagenesis of *wcoB* gene.

The pleiotropic effect of the *wcoA* mutation includes developmental alterations, as shown by the reduction in conidia formation or the lower hydrophobicity of aerial mycelia, the latter probably reflecting changes in the amount of secreted hydrophobins (Kershaw and Talbot, 1998). In fungal species taxonomically close to *F. fujikuroi*, as *T. atroviride* (Casas-Flores et al., 2004) or *N. crassa* (Lauter and Russo, 1991), light induce conidia formation through the action of WC regulatory complexes. In contrast, conidiation is not induced by light in *F. fujikuroi*, at least in the wild type used in this work. Actually, our data rather suggest a negative effect of illumination on the wild type and on the *wcoA* mutants. In contrast, conidiation is strongly influenced by nitrogen availability, as indicated by the higher amounts of conidia found in low nitrogen medium. Similar regulations have been observed in other fungi. Thus, conidiation by *A. nidulans* is stimulated when transferred from complete nutrient conditions to a medium lacking

nitrogen or carbon sources, a regulation controlled through the regulatory gene *blrA* (Skromne et al., 1995). The reduced conidiation resulting from the *wcoA* mutation is not observed under nitrogen starvation, providing further evidence on a role of WcoA in nitrogen regulation and, consequently, in the control of secondary metabolism. Regulatory connections between sporulation and the production of secondary metabolites have been described in other fungi, and thoroughly investigated in *Aspergillus* species (Calvo et al., 2002).

Our results on the *wcoA* mutant phenotype in *F. fujikuroi* provide an outstanding example of light-independent roles for a fungal WC-1-like protein. The functional diversity of these proteins may be higher than expected from the first examples characterized in detail. Thus, the WC-1 proteins from basidiomycetes lack the zinc finger motif, suggesting differences in their regulatory modes of action, involved with light in at least one case investigated (Terashima et al., 2005). WcoA stands out among the proteins described from this family in that the regulation by light seems to play a secondary role in its biological functions.

### **Acknowledgements**

We thank L. Roberto Rodríguez-Ortíz and R. Dueñas for help in RT-PCR analyses, S. Al-Babili for help with HPLC analysis, and L. Perez de Camino for technical assistance. This work was supported by the Spanish Government (Ministerio de Ciencia y Tecnología, projects BIO2003-01548 and BIO2006-01323).

## CAPÍTULO 4

Regulación y mutación dirigida del gen *opsA*, que determina la opsina ortóloga de NOP-1 en *Fusarium fujikuroi*

Regulation and targeted mutation of *opsA*, coding for the NOP-1 opsin orthologue in *Fusarium fujikuroi*

Alejandro F. Estrada and Javier Avalos\*

*Department of Genetics, Faculty of Biology, University of Seville, E-41012 Seville, Spain*



**Abstract**

Opsins are widespread photoreceptor proteins, involved in a diversity of light-driven processes in all major taxa, that use the apocarotenoid retinal as light-absorbing prosthetic group. Proteins from the opsin family are also found in filamentous fungi, but no functions have been attributed to them. The fungus *Fusarium fujikuroi* contains two genes for presumptive retinal-binding opsins, that we call *carO* and *opsA*, and a gene for an opsin-related protein (ORP), called *hspO*. A former report showed that *carO* is linked and coregulated with the enzymatic genes of the carotenoid pathway *carRA*, *carB* and *carX*, but its mutation produced no detectable phenotype. Sequence analyses suggest that OpsA but not CarO is the orthologue of the *Neurospora* opsin NOP1. mRNA levels for the three *Fusarium* opsin genes are induced by heat shock and those for *carO* and *opsA* are induced by light. This photoinduction is lost in mutants of the White collar gene *wcoA*, which contain much higher *carO* and *opsA* mRNA levels than the wild type, indicating a down-regulation of both genes by WcoA. Conversely to *carO*, *opsA* mRNA levels are not enhanced in carotenoid-overproducing mutants. Targeted *opsA* mutants have no discernible external phenotype, but they exhibit a significant decrease in mRNA levels for structural genes of the carotenoid pathway. Similar reductions are produced by mutations in the enzymatic genes *carRA* and *carB*, but not in *carX*, responsible for retinal biosynthesis.

**Keywords:** opsin; retinal; carotenoid; photoinduction; white collar



## 1. Introduction

Opsins are a widespread group of transmembrane photoreactive proteins that use the apocarotenoid retinal as their chromophore (reviewed by Spudich et al., 2000; Spudich, 2006). Knowledge on this chromophore-retinal complex, also known as rhodopsin, started with the identification of bacteriorhodopsin (BR) and halorhodopsin in halophilic archaea, which mediate proton and chloride membrane transport, respectively, using light as the sole energy source (Spudich, 1998). New members of this protein family were later discovered in all major microbial groups, where they play different light-dependent functions (Spudich, 2006). Research on these proteins, called type I rhodopsins, has associated many of them to specific photoreception roles, such as phototaxis in algae (Ridge, 2002), or photoadaptation in eubacteria (Jung et al., 2003). Structurally related to them are animal opsins, also called type 2 rhodopsins, responsible for vision in the retina (Menon et al., 2001). Three dimensional structure, resolved for several opsin proteins, revealed a conserved tertiary organization consisting of seven transmembrane domains (Spudich, 2006; Terakita, 2005). The spatial organization includes an internal pocket with a highly conserved lysine residue, to which retinal is covalently bound.

Putative opsin-encoding genes are also found in fungal genomes (Brown, 2004). Some of them have been subject of detailed investigation. This is the case of *nop-1* from *Neurospora crassa* (Bieszke et al., 1999a), discovered from an EST library, which stood out as the first opsin-like sequence found in a fungus. NOP-1 binds retinal in vitro (Bieszke et al., 1999b) and shows a photochemical reaction cycle (Brown et al., 2001). Targeted mutation of *nop-1* revealed no apparent phenotypic alteration, except a light-dependent change of colony morphology on oligomycin-supplemented medium (Bieszke et al., 1999a). Analyses on *nop-1* mRNA levels indicated a role associated to airborne-induced production of the asexual spores, the conidia, as indicated by its parallel induction with the conidiation specific gene *con-10*, and the lower *nop-1* mRNA amounts in regulatory mutants affected in different stages of conidia development (Bieszke et al., 2007).

Another fungal opsin, OPS from *Leptosphaeria maculans* (Idnurm and Howlett, 2001), differs from NOP-1 and resembles BR in that it exhibits a fast photocycle and an efficient light-driven proton pumping activity (Brown et al., 2001; Waschuk et al., 2005; Furutani et al., 2006). Also, in contrast to *nop-1*, *ops* mRNA levels are not affected by light. Despite their high sequence similarity, the biochemical properties of NOP-1 and OPS suggest different functions, involved in light sensing and proton pumping, respectively. As for other fungal opsins, the biological role for OPS in *L. maculans* has not been elucidated, and the effect of *ops* mutation has not been investigated.

Nop-1 and OPS are just two examples from the diversity of fungal opsin proteins identified in low number in ascomycetes and basidiomycetes species as new fungal proteomes become available (Brown, 2004). In some cases, despite their typical opsin tertiary structure, these proteins lack the conserved retinal-binding lysine present in the seventh transmembrane domain of photoactive opsins, to which retinal is covalently linked. These proteins, called opsin-related proteins or ORPs (Spudich et al., 2000), presumably lack light-dependent functions. To this group belongs a subfamily of heat-shock chaperones (Zhai et al., 2001), represented by HSP30 from *S. cerevisiae* or similar proteins in other fungi, e.g. Cvhsp30/1 and Cvhsp30/2 from *Coriolus versicolor* (Limura and Tatsumi, 2002). Other presumptive opsins contain the conserved lysine residue, but retinal binding or photoreactivity have not been demonstrated; we shall refer here to them as predictable photoactive opsins or PPOs.

The opsin chromophore retinal (C20) is produced through the oxidative cleavage of  $\beta$ carotene (C40), a reaction mediated by enzymes from the carotene oxygenase family (Wyss, 2004). Recently, a retinal-forming oxygenase, encoded by gene *carX*, has been described in *Fusarium fujikuroi* (*Gibberella fujikuroi* mating group C) (Prado-Cabrero et al., 2007a). This fungus stands out for its capacity to produce gibberellins (Tudzynski, 1999; Avalos et al., 2007), growth-promoting plant hormones (MacMillan, 1997) with agricultural applications. Surface cultures of *F. fujikuroi* become orange under light because of the accumulation of an acidic apocarotenoid, neurosporaxanthin, and minor amounts of carotenoid precursors (Avalos and Cerdá-Olmedo, 1987). Neurosporaxanthin biosynthesis is mediated in this fungus by at least three enzymes, encoded by genes *carRA*, *carB* and *carT* (Linnemannstöns et al., 2002; Prado-Cabrero et al., 2007b). CarRA is a bifunctional protein with phytoene synthase and carotene cyclase activities, and CarB is a desaturase, able to introduce up to five conjugated double bonds in the aliphatic carotene chain (Fig. C4.1). The sequential activities of these enzymes produce the monocyclic torulene (C40), which is cleaved by the CarT oxygenase to yield  $\beta$ apo4'carotenal (C35), the aldehyde precursor of neurosporaxanthin (Prado-Cabrero et al., 2007b). The cyclase activity of CarRA also yields the bicyclic  $\beta$ -carotene, substrate of the CarX oxygenase (Prado-Cabrero et al., 2007a).

Biosynthesis of neurosporaxanthin by *F. fujikuroi* is induced by light in wild type strains (Avalos and Cerdá-Olmedo, 1987; Avalos and Schrott, 1990), but high amounts of carotenoids are accumulated in the dark by deregulated mutants (*carS*) (Avalos and Cerdá-Olmedo, 1987; Rodríguez-Ortiz et al., 2009). Carotenoid content correlates with mRNA levels from the enzymatic genes *carRA*, *carB*, and *carT* (Linnemannstöns et al., 2002; Prado-Cabrero et al., 2007b; Prado et al., 2004), as well as with those from *carX*, coding for the retinal forming enzyme (Thewes et al., 2005). Accordingly, these mRNA levels are

low in the dark, increase rapidly upon illumination and decrease afterwards (photoadaptation), while they are high irrespective of light in the *carS* mutants.

Light-induced carotenogenesis has been thoroughly investigated in a *Fusarium* relative, the ascomycete *N. crassa*, in which neurosporaxanthin was firstly described (Aasen and Jensen, 1965). The photoresponse in this fungus is mediated by the White Collar (WC) complex (Talora et al., 1999), formed by the PAS-mediated interaction of the WC-1 and WC-2 proteins (Liu et al., 2003). Activation by light of this heterodimer allows it to bind the promoters of target genes and stimulate their transcription (Liu et al., 2003). Light detection in the WC complex is achieved by WC-1, which absorbs blue light through a FAD molecule (He et al., 2002), bound to a special PAS domain known as LOV from “light, oxygen and voltage” (Cheng et al., 2003). Similar WC proteins are responsible for photocarotenogenesis and other photoresponses in the zygomycetes *Phycomyces blakesleeanus* (Idnurnm et al., 2006) and *Mucor circinelloides* (Silva et al., 2006). Against the findings in *Neurospora* and other fungi, mutation of the only *wc-1* like gene in *F. fujikuroi* did not prevent the stimulation by light of the carotenoid pathway (Estrada and Avalos, 2008), indicating the participation of a different photoreceptor. We recently described in *F. fujikuroi* the gene *carO*, coding for a PPO protein (Prado et al., 2004). This gene is clustered and coregulated with *carRA*, *carB* and *carX*, i.e. the genes needed for retinal formation (Fig. C4.1). The similar light-dependent expression of the four linked genes suggest a functional organization as a regulon for production of photoactive retinal-CarO complex. The gene *carT*, needed for neurosporaxanthin biosynthesis but not for retinal formation, shares a similar regulation but it is not linked to the cluster (Prado-Cabrero et al., 2007b). As found for *nop-1* in *Neurospora*, targeted *carO* mutants lack a discernible phenotype under laboratory conditions (Prado et al., 2004). Genomic analysis of *Fusarium graminearum* (*Gibberella zeae*) revealed three genes for structurally related opsin proteins (Brown, 2004), including the *carO* counterpart and a putative *nop-1* orthologue, that we denominate *opsA*. Similar genes were found in the other *Fusarium* genomes recently available. Here, we report the cloning and characterization of the *opsA* gene from *F. fujikuroi*. To evaluate its biological role in this fungus, we have investigated its regulation and we have analyzed the phenotype of targeted *opsA* mutants. As found for *nop-1*, *opsA* mutations produced no morphological or color alteration either under light or in the dark. However, the *opsA* mutants contained lower mRNA levels for key genes of the carotenoid pathway.

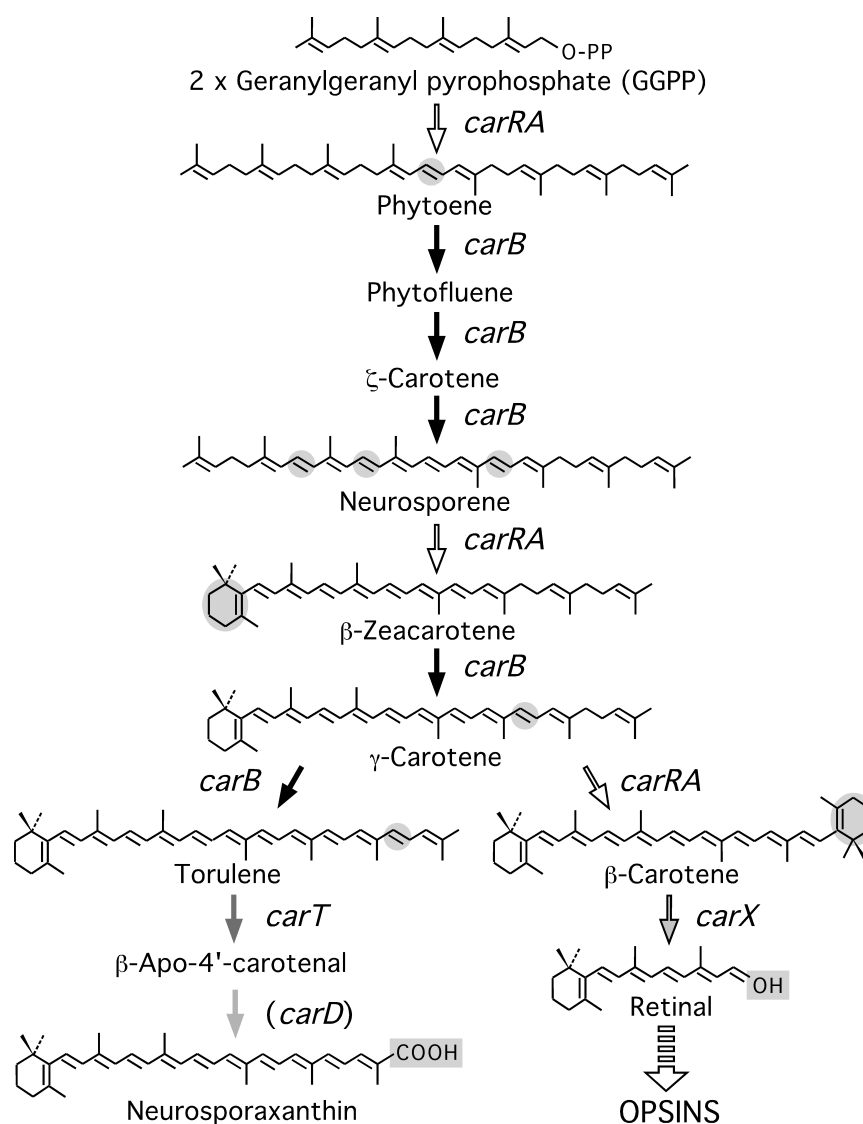


**Fig. C4.1. Biosynthesis of the opsin chromophore retinal from the diterpenoid precursor GGPP and relation with the neurosporaxanthin biosynthetic pathway in *F. fujikuroi*.** The genes responsible for each step are indicated. Identification of the *carD* gene is currently in progress. Chemical modifications on the intermediate products are shaded.

## 2. Results

### 2.1 Proteins from the opsin family in *Fusarium*

Blast searches of genes coding for structurally opsin-like proteins were carried out in *Fusarium* genomes recently available in addition to that of *F. graminearum*, i.e. those of *F. verticillioides* and *F. oxysporum*. The results confirmed the occurrence of three genes coding for proteins from this structural family in the three species. One of them is the *carO* orthologue, already mentioned. The other two genes are called here *opsA* coding for a

PPO, and *hspO*, coding for an ORP. We analyzed the sequences of the proteins encoded by the three genes in the genome of *F. verticillioides*, the closest *F. fujikuroi* relative among these three *Fusarium* species. As expected from their sequence similarities to archaeal opsins, computer-based hydrophobicity prediction of transmembrane tendencies showed a pattern in the three *Fusarium* proteins very similar to that of BR, with the prototypical seven-transmembrane structure (Fig. C4.2a).

Crystal BR structure has been determined at increasing resolution levels and the residues closer to the retinal binding pocket (light gray boxes, Fig. C4.2b) and the ones involved in the proton translocation process (outlined boxes) have been identified (Thewes et al., 2005). The lysine to which retinal is linked through a Schiff base bond (black box, Bayley et al., 1981) and the proton donor to the Schiff base, aspartic acid (dark gray box, Cao et al., 1993), were formerly known. To gain information on their sequence relations, the *F. verticillioides* CarO, OpsA and HspO proteins were aligned with BR from *H. salinarum*, NOP-1 and YRO-2 from *N. crassa*, OPS from *L. maculans* and the heat-shock protein HSP30 from *S. cerevisiae*. Residues corresponding to BR relevant positions at the fungal proteins were represented (Fig. C4.2b). CarO and OpsA from *Fusarium*, and NOP-1 from *Neurospora* contain the highly conserved retinal binding-lysine (black boxes), absent in the other three fungal proteins. However, only CarO and OPS coincide with BR in the presence of the proton donor aspartic acid (dark gray boxes). Glutamic acid, found at the same location in NOP-1 and OpsA, could be inefficient as proton donor, as suggested by the photochemical properties of a targeted *ops* mutant of *L. maculans* (Furutani et al., 2006). The NOP-1 and OPS opsins and the CarO and OpsA PPOs show a higher conservation for the BR residues involved in proton translocation (7, 6 and 8 out of 10, respectively, outlined boxes in Fig. C4.2b) than in YRO-2, HspO and HSP30 (6 to 8 out of 10). A similar conservation was found for the residues that generate the retinal binding pocket, except for those located in transmembrane helix VI. In overall, the conservation was higher for the proteins containing the retinal binding lysine (8 or 9 out of 13) compared to those lacking this critical residue (ORPs). Taken together, these observations suggest light-dependent functions for CarO and OpsA, as already demonstrated for NOP-1, and light-independent functions for HspO and YRO-2.

As formerly described (Brown, 2004), PPO and ORP genes were identified in variable numbers in the different fungi and they were unevenly distributed. E.g., ORPs were not found in *U. maydis* and PPOs were not found in *S. cerevisiae* or in *Aspergillus* species. No PPO or ORP genes were found in the genomes of the zygomycetes *P. blakesleeana*, *M. circinelloides* and *Rhizopus oryzae*. To evaluate the phylogenetic relations between the proteins analyzed in Fig. C4.2b and other fungal and archaeal proteins from the opsin family, a

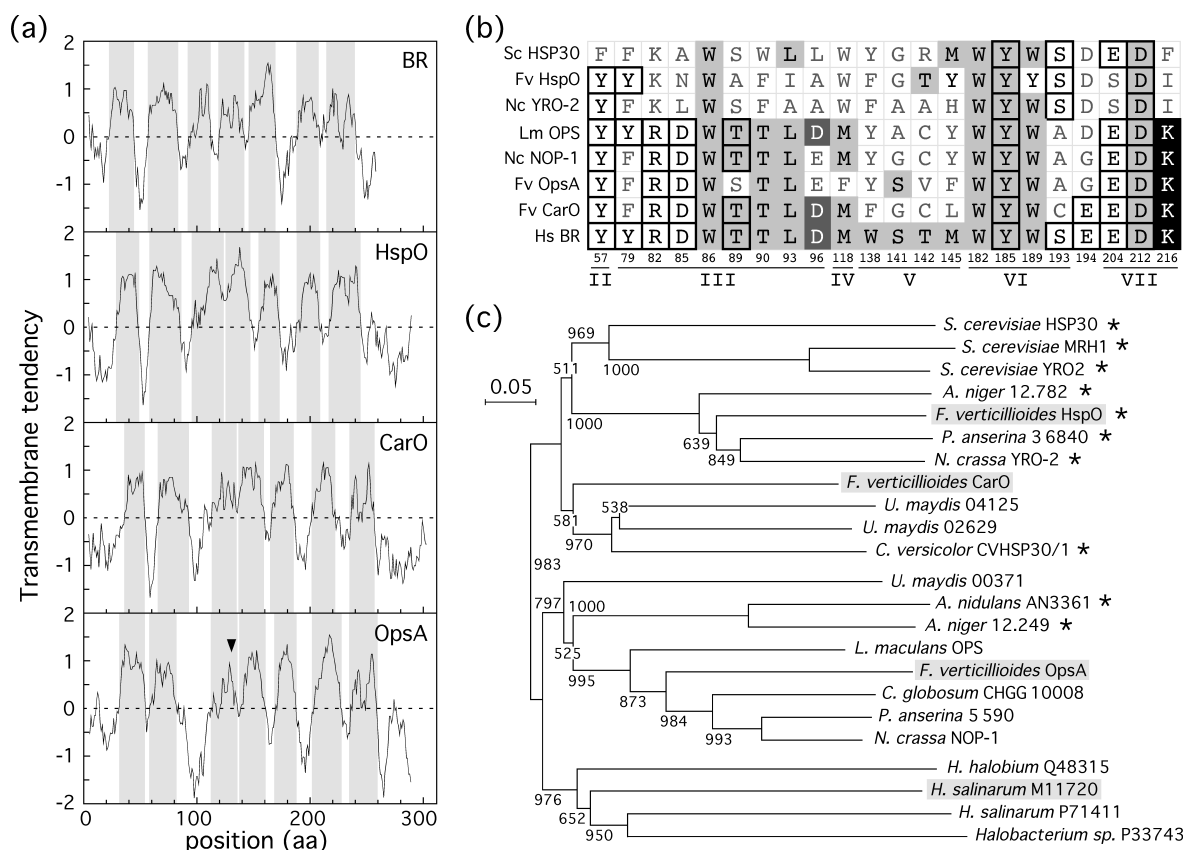


**Fig. C4.2. Analysis of polypeptide sequences of the *Fusarium* CarO, OpsA and HspO proteins.** (a) Transmembrane tendency profiles in comparison with bacteriorhodopsin from *Halobacterium salinarum* (BR, accession No. **M11720**). The arrowhead indicates the insertion point of the *hph* cassette to generate *opsA* mutants (see Fig. C4.5) (b) Conservation of residues involved in retinal photocycle and proton translocation in *H. salinarum* in the same proteins, NOP-1 and YRO-2 from *N. crassa*, OPS from *L. maculans*, and HSP30 from *S. cerevisiae*. Black boxes: Retinal binding lysine through the Schiff base bond link. Dark gray boxes: donor acceptor from the Schiff base (aspartic acid). Outlined boxes: residues participating in the hydrogen-bond network from the retinal Schiff base to the extracellular bacteriorhodopsin. Light gray boxes: residues whose side chains are in the immediate surroundings of the retinal molecule (minimal distance, 3.6 Å from polyene chain or  $\beta$ ionone ring). Numbers below refer to amino acid positions in BR. Lower bars indicate transmembrane helices, from I to VII. (c) Phylogram of representative fungal PPOs and ORPs and archaeal opsins. Numbers in nodes indicate bootstrap values. SPTREMBL accession numbers are indicated for proteins lacking a specific denomination. The asterisk indicates proteins lacking the conserved retinal-binding lysine (ORPs).

phylogram was generated from a Clustal alignment between representative proteins from both taxonomic groups and four representative archaeal opsins. We included in the analysis the formerly described *C. versicolor* ORP, and different proteins found in available annotated fungal genomes: three predicted PPOs from the basidiomycete *U. maydis* (basidiomycete) and one from the ascomycetes *Podospora anserina* and *Chaetomium globosum*, and three ORPs from *S. cerevisiae*, two from *Aspergillus nidulans* and one *Aspergillus niger*. The phylogram revealed different major classes (Fig. C4.2c). Most of the ORPs, including YRO-2 and HspO, were grouped in the phylogram, suggesting the origin from an early common ancestor. Their similarity to HSP30 from *S.*

*cerevisiae* suggests a role as heat shock response chaperones. The conserved lysine has been independently lost in different ancestors, as indicated by the different phylogenetic locations of the ORP from *C. versicolor* and the one from *A. nidulans* and its *A. niger* orthologue.

## 2.2 Gene *opsA* from *F. fujikuroi*

PPOs were distributed in two major groups, one that included OpsA, NOP-1 and OPS, and another one that included CarO and two *U. maydis* ORPs (Fig. C4.2c). This phylogenetic distribution points to OpsA as the NOP-1 orthologue in *Fusarium*. This was corroborated by pairwise sequence comparisons of NOP-1 with the *F. verticillioides* proteins: NOP-1 and OpsA share 155 identical positions (51% of NOP-1), compared to 87 (29%) in the case of NOP-1 and CarO.

To carry out a functional characterization of *opsA*, we cloned by PCR the *F. fujikuroi opsA* gene using appropriate oligonucleotides from the *F. verticillioides* genomic sequence. A 1.8 kb DNA segment, containing the whole 982 bp coding sequence surrounded by 610 and 210 bp of upstream and downstream non-coding DNA, was sequenced from both chains and the final sequence (accession number **FM213121**) was compared to that of the same DNA segment from *F. verticillioides*. As expected, the *F. fujikuroi opsA* gene is highly similar to that from *F. verticillioides*: their respective 982 bp coding sequences contain 95% identities (94,2% if their 54 and 46 bp introns are included), a percentage that drops to 84,9 % in the case of their closer 610 bp promoter segments. The respective OpsA proteins only differ in three of the 294 residues, i.e., 99% identity, a percentage that decreases to 92% when any of these proteins is compared to the orthologous one from *F. graminearum* (FGSG 07554).

## 2.3 Regulation of *Fusarium* opsin-like genes

To gain insights on the putative functions of the *carO*, *opsA* and *hspO* genes, we investigated their mRNA levels under different culture conditions. Their relatedness with the yeast HSP30 protein suggests possible roles in the heat shock response. Moreover, a detectable induction upon heat exposure was already described for *carO* and the closely linked enzymatic gene for the carotenoid pathway, *carB* (Prado et al., 2004; Estrada and Avalos, 2008). We evaluated the effect of heat shock on *hspO* and *opsA* expression in comparison to that of *carO* and *carB*. The mRNA levels of the four genes increased notably after one or two hours incubation at 38°C (Fig. C4.3a), a temperature under which growth of this fungus is drastically impaired.

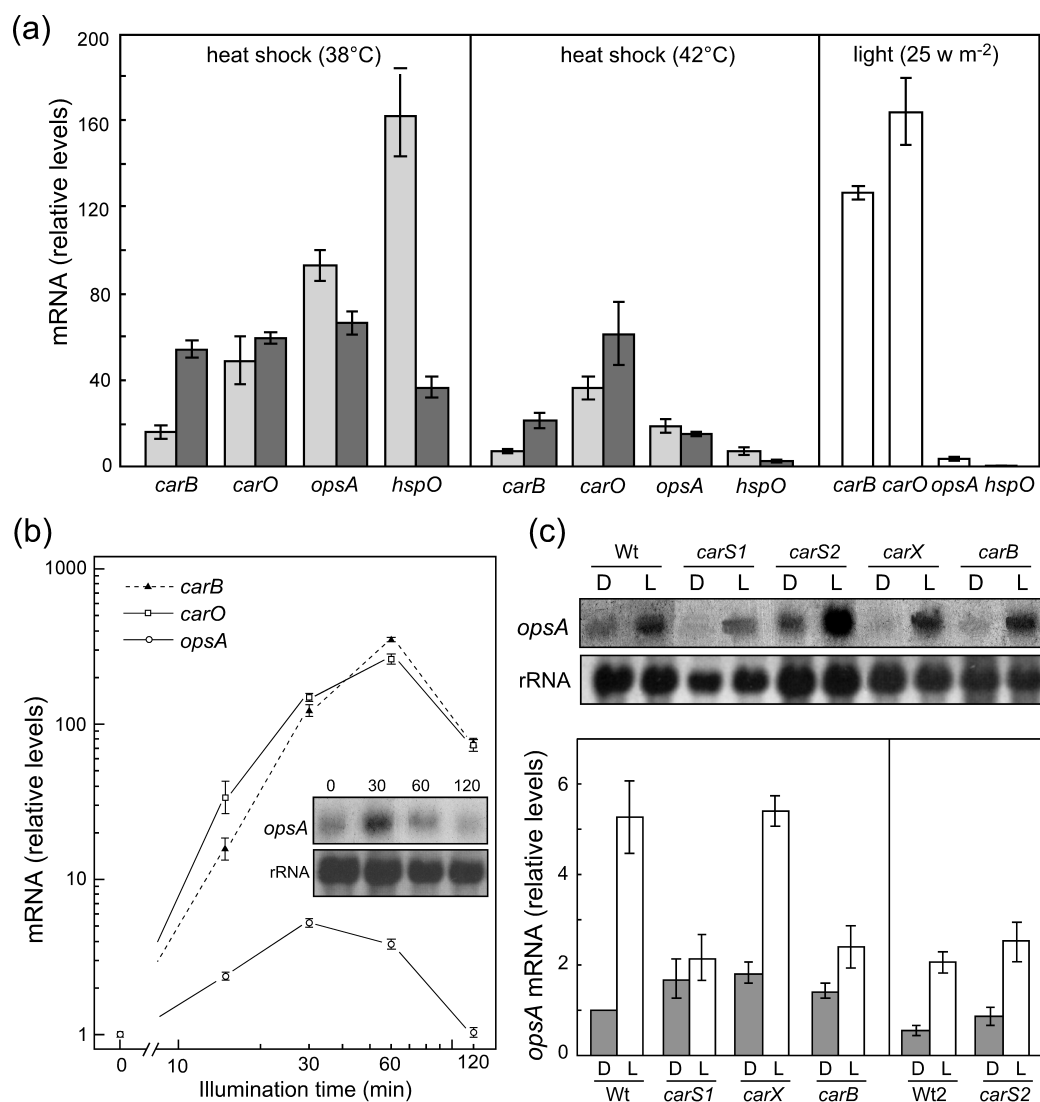


**Fig. C4.3. Effect of heat-shock, light and the genetic background on expression of *F. fujikuroi* genes for opsin-like proteins and gene *carB*.** (a) Real-time RT-PCR analyses of the indicated genes from RNA samples of the wild-type strain grown in the dark and exposed to either 38 or 42°C during 1 h (light gray bars) or 2h (dark gray bars), or to light during 30 min (white bars). Relative mRNA levels are referred to the value for each gene from unexposed mycelia. (b) Real-time RT-PCR analyses of the genes *carB*, *carO* and *opsA* from RNA samples of the wild-type strain grown in the dark and exposed for 15', 30', 1h or 2 h to light. Relative mRNA levels are referred to the values from non-illuminated mycelia. A representative northern blot experiment for *opsA* is shown in the inner box. (c) Northern blot and real-time RT-PCR analyses of the gene *opsA* from RNA samples of the wild-type and mutant strains for the indicated genes grown in the dark (gray bars) or exposed to light during 30 min (white bars). Real-time RT-PCR data represent average and standard deviation for four determinations from two independent experiments.

The highest increase was found for *hspO* after one-hour heat exposure, although the mRNA levels decreased rapidly after two hours. Incubation at 42°C resulted in more modest increases for all genes except *carO*. As already stated, expression of *carO* and *carB* is induced by light (Prado et al., 2004), a regulation shared by other genes of the carotenoid pathway. As expected, 30 min illumination produced a remarkable increase of *carB* and



*carO* mRNA levels. In contrast, only a mild induction was apparent in the case of *opsA* and no effect of light was appreciated for *hspO* (Fig. C4.3a). The modest *hspO* induction could be attributed to the need for longer light exposures than the ones needed for *carO* and *carB*. Extension of the experiment to illumination times ranging from 15 to 120 min confirmed a weaker response for *opsA*, with a maximal induction of 5-6 fold, compared to 300-fold in the case of the *carO* and *carB* genes (Fig. C4.3b). In contrast to these genes, illumination during 60 or 120 min did not affect the *hspO* mRNA levels (data not shown).

Expression of *carO* and other *car* genes is derepressed irrespective of light in *carS* mutants (Prado-Cabrero et al., 2007b; Rodríguez-Ortiz et al., 2009; Prado et al., 2004; Thewes et al., 2005). In contrast to the *car* genes, *carS* mutations did not result in higher levels of *opsA* mRNA either in the dark or after 30 min illumination (Fig. C4.3c), attesting a regulation independent from that of the carotenoid pathway. *opsA* mRNA levels did not suffer major variations in *carB* and *carX* mutants either. These genes are required for the synthesis of carotenes and retinal, respectively, indicating that lack of the presumptive OpsA chromophore has no effect on *opsA* expression.

The mutation of the *white collar* gene *wcoA* affected but did not preclude light induction of the enzymatic genes for the carotenoid pathway *carRA*, *carB* and *carT* (Estrada and Avalos, 2008). We evaluated the effect of the *wcoA* mutation on *carO*, *opsA* and *hspO* mRNA levels either in dark-grown or in illuminated cultures. The results were compared with those obtained with *carX*, and *carB*, the latter as control for former results (Estrada and Avalos, 2008). Lack of functional WcoA had no significant effect on *hspO* mRNA, which remained similar to those of the wild type either in the dark or after one-hour illumination (results not shown). However, the *wcoA* mutation had drastic effects on *carO* and *opsA* expression (Fig. C4.4). mRNA levels for these genes increased in two independent *wcoA* mutants in the dark about 50 fold for *carO* and about 20 fold for *opsA*, pointing to a repressing role for the WcoA protein. Moreover, *carO* and *opsA* mRNA levels kept unaltered following illumination, indicating that photoinduction of these genes is mediated by the WcoA protein. As found before (Estrada and Avalos, 2008), the *wcoA* mutation had quite a different effect on *carB* mRNA: the photoinduction was drastically reduced but it was still apparent in the mutant background. Similar but not identical results were found for gene *carX*. Light induction of *carX* mRNA levels in the wild type was less pronounced than for those of *carB* and *carO*, but it was equally manifest in the *wcoA* mutants. However, *carX* mRNA levels were significantly reduced in the *wcoA* mutants.

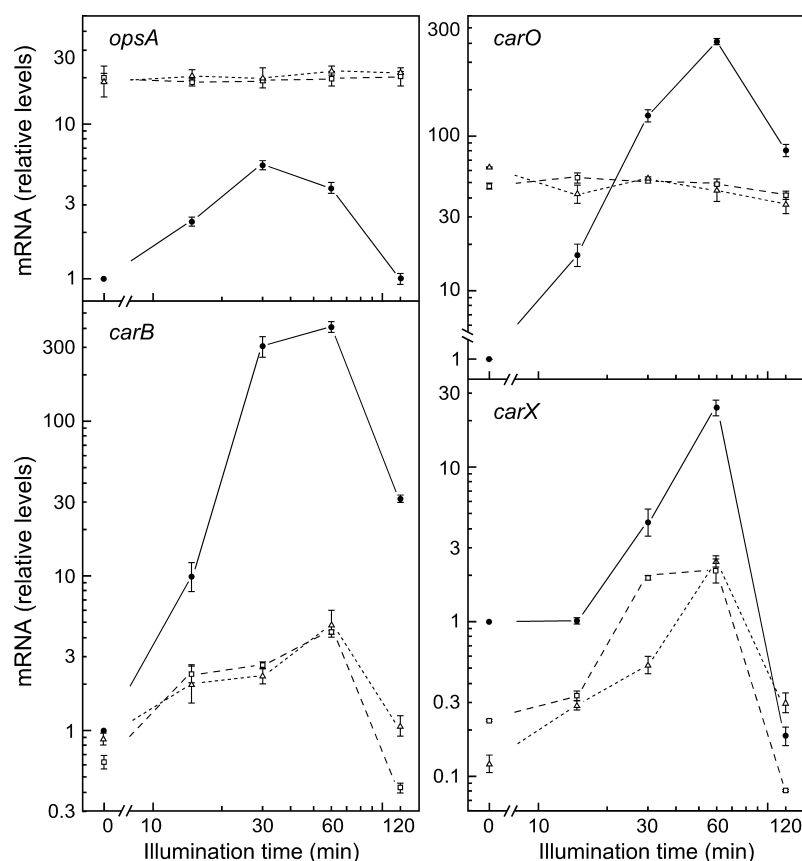


**Fig. C4.4. Effect of WcoA loss on *carO*, *opsA*, *carX* and *carB* expression.** Real-time RT-PCR analyses of mRNA of the gene indicated from RNA samples of the wild-type (continuous lines, closed symbols) and two *wcoA* mutants (*wcoA6*, squares, long dashed lines; and *wcoA7*, triangles, short-dashed lines) grown in the dark or exposed to light during 15 min, 30 min, 1h or 2 h. Relative mRNA levels are referred to the values from non-illuminated wild type mycelia. Data represent average and standard deviation for four determinations from two independent experiments.

### 2.3 Generation and phenotypic characterization of *opsA* mutants

To obtain targeted *opsA* mutants, we incubated wild type protoplasts with a linear fragment of plasmid pALEX10, containing a truncated version of gene *opsA*. This plasmid was designed to obtain the replacement of the wild type *opsA* sequence by the interrupted counterpart by two homologous recombination events (Fig. C4.5a). DNA samples from 36 presumptive transformant colonies, able to grow on hygromycin-supplemented medium, were subjected to a preliminary PCR test with primers surrounding the integration site. The results showed the absence of the wild type amplification product in 31 of the 36 transformants (Fig. C4.5b), suggesting the loss of the functional *opsA* gene by double recombination at the expected target site. Five independent transformants lacking the wild type PCR product were checked by southern blot after digestion of their genomic DNA samples with *SacI* and *Sall*. Three of them, T7, T15 and T25, produced a pattern consistent with the expected single gene replacement (Fig. C4.5c). The other two transformants

exhibited a more complex pattern, indicating further recombination events, and were discarded for further analyses.

The three *opsA* mutants exhibited similar growth and morphology than the wild type, either under normal aeration or under partial anoxia (incubation in sealed Petri dishes) or at different temperatures (16°C, 22°C, 30°C, 34°C and 37°C, data not shown). Also, they did not differ from the wild type in pathogenic capacity in a tomato infection test or in gibberellin production in low nitrogen broth (Fig. C4.S1 supplementary). Mutants of the *Neurospora* orthologue, *nop1*, showed morphological alterations in the light in the presence of oligomycin. As formerly found with *carO* mutants (Prado et al., 2004), the morphology of *opsA* mutant colonies grown on illuminated oligomycin-supplemented medium was comparable to that of the wild type. Regulation of *nop-1* has been associated to conidiation in *Neurospora* (Bieszke et al., 2007). Surface cultures of the *opsA* mutants produced similar amounts of conidia than those of the wild type, irrespective of the presence of oligomycin (Fig. C4.6a). As formerly found (Estrada and Avalos, 2008), the amount of conidia was lower in the light, an effect that was enhanced in the presence of oligomycin. Surface cultures of the three *opsA* mutants exhibited the same pigmentation under light and contained similar amounts of carotenoids (Fig. C4.6b) and carotenoid mixtures (Fig. C4.6c) than those of the wild type. Carotenoid contents in the dark were similarly low in wild type and *opsA* mutants, indicating a fully operative photoinduction of the carotenoid pathway. To confirm this, a RT-PCR experiment was achieved with one of the mutants to test the effect of light on the mRNA levels for a enzymatic gene of the carotenoid pathway. Unexpectedly, the *opsA* mutant investigated exhibited reduced levels of *carB* mRNA either in the dark (ca. 40% of the wild type level) or after illumination (Fig. C4.6d).

#### 2.4 Effect of *opsA* and *car* mutations on the expression of *car* genes

The effect of the *opsA* mutation on *carB* expression prompted a more detailed analysis of the effect of this and other relevant mutations on the mRNA levels of the *car* genes. The reduced light-induction of *carB* mRNA levels observed in an *opsA* mutant was confirmed for the three *opsA* mutants investigated, and was also observed for *carRA* and *carO* (Fig. C4.7). Interestingly, *carB*, *carRA* and *carO* mRNA levels were reduced to similar extents in dark-grown *opsA* mutants compared to those of the wild type, revealing an unaltered photoinduction. Mutation of gene *carX*, responsible for retinal formation, results in enhanced carotenoid production irrespective of illumination (Thewes et al., 2005), an effect accompanied by increased *carRA* and *carB* mRNA levels (Fig. C4.7). Therefore, lack of the retinal-forming enzyme CarX and lack of OpsA had opposite effects on carotenogenesis. To find out if the effect of the *carX* mutation is due to lack of retinal,

we generated targeted *carB* and *carRA* mutants in the same wild type background. Both albino mutants are blocked in different steps of the common branch for neurosporaxanthin and retinal biosynthesis (Fig. C4.1). *carB* mutants accumulated about 70  $\mu\text{g}$  of phytoene per g dry mass under light and only traces in the dark. As in *opsA* mutants, *carRA* and *carB* mRNA levels were reduced in *carRA* or *carB* mutants compared to those of the wild type, suggesting that this effect is produced by lack of functional OpsA protein.

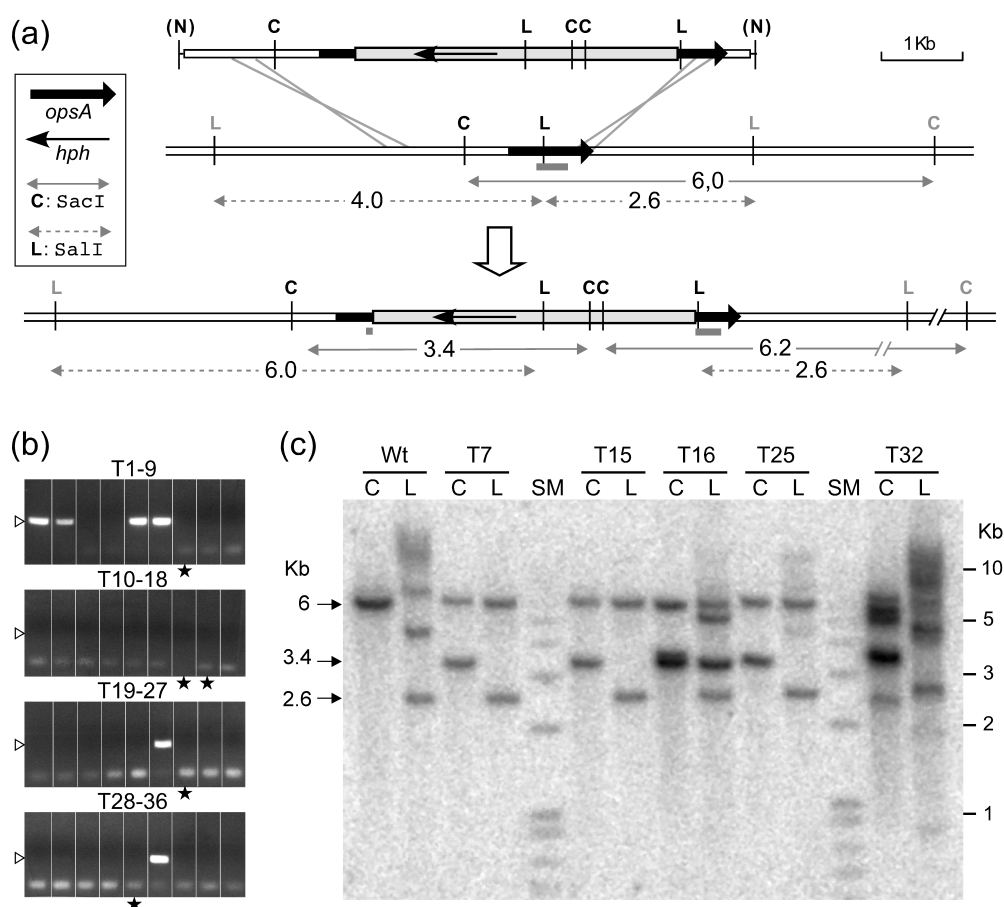


**Fig. C4.5. Generation of targeted *opsA* mutants.** (a) Physical maps of the *hph* cassette (gray box) inserted in the *opsA* gene in plasmid pALEX10 digested with NotI (N) and the *opsA* genomic region in *F. fujikuroi*. The recombination events leading to *opsA* disruption and the resulting physical map in the generated *opsA* mutants are also displayed. The gray bar indicates the probe used in the southern blot shown below. Relevant fragments produced by digestion with SacI (C) or SalI (L) are indicated. Restriction sites in gray were deduced from southern blot analyses. (b) Detection of wild type *opsA* alleles. Electrophoretic profiles of PCR amplification of an internal *opsA* segment that includes the *hph* integration site, amplified by PCR from 37 transformants obtained with pALEX10. The 386 bp amplification product (indicated by an empty arrowhead) indicates the presence of the wild type allele. The stars indicate transformants analyzed in the southern blot displayed on the right. (c) Southern blot of genomic DNA from the wild type (WT) and five transformants digested with SacI (C) or SalI (L) and hybridized with the *opsA* probe indicated above. SM: Size markers (relevant sizes shown on the right in Kb). Sizes of relevant DNA segments produced by enzymatic digestions are indicated on the left.

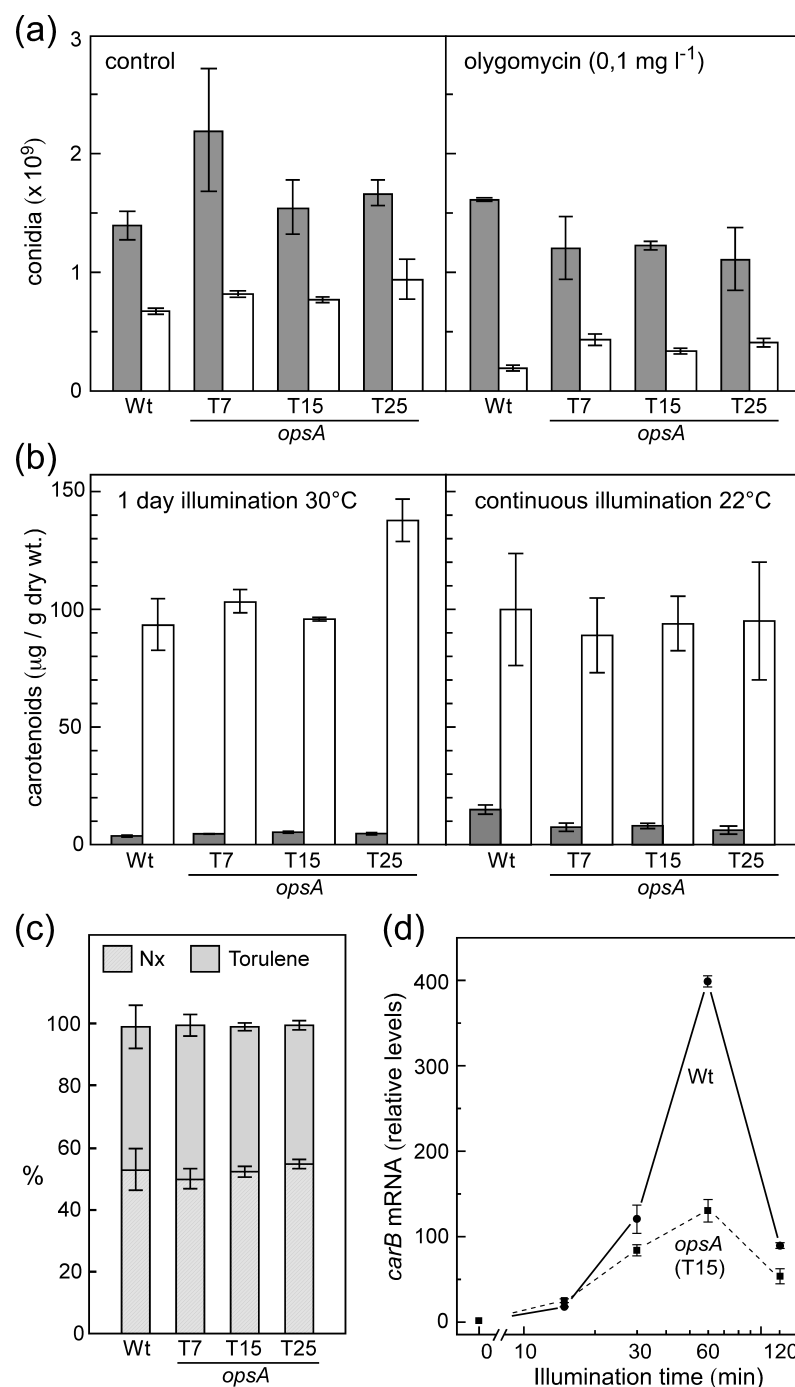


**Fig. C4.6. Effect of *opsA* mutation on carotenogenesis and conidiation.** (a) Conidia produced by the wild type and the *opsA* mutants 7, 15 and 25 grown for 7 days at  $22^\circ\text{C}$  on minimal agar in the dark (grey bars) or under continuous illumination (white bars). (b) Carotenoids in the mycelia of the wild type and the three *opsA* mutants. Left graph: top agar cultures grown for four days at  $30^\circ\text{C}$  in the dark (grey bars) or for three days in the dark and one day under illumination (white bars). Right graph: surface cultures grown for seven days on minimal agar at  $22^\circ\text{C}$  either in the dark (grey bars) or under continuous illumination (white bars). (c) Relative proportions of neurosporaxanthin (NX) and torulene in the carotenoid samples from the top agar cultures shown above (calculated from peak surfaces in the HPLC chromatograms). Proportions of other carotenoids were below 1%. (d) Real-time RT-PCR analyses of *carB* mRNA from RNA samples of the wild-type strain and the *opsA* mutant T15 grown in the dark and exposed for 15 min, 30 min, 1 h or 2 h to light. Relative data are referred to the values from non-illuminated mycelia. All data show average and standard deviation for four determinations from two independent experiments.

As found for *carRA* and *carB*, *carO* mRNA levels were reduced in *opsA* mutants, but in this case the reduction was more severe (Fig. C4.7). A significant *carO* mRNA reduction was also apparent in the *carRA* mutant but, unexpectedly, not in the *carB* one. The derepression produced by the *carX* mutation on *carRA* and *carB* applied also to *CarO* mRNA levels, providing a new example of coordinated regulation of these three *car* genes. This result contrasts with the lack of effect of the *carX* mutation on *opsA* mRNA levels (Fig. C4.3c)

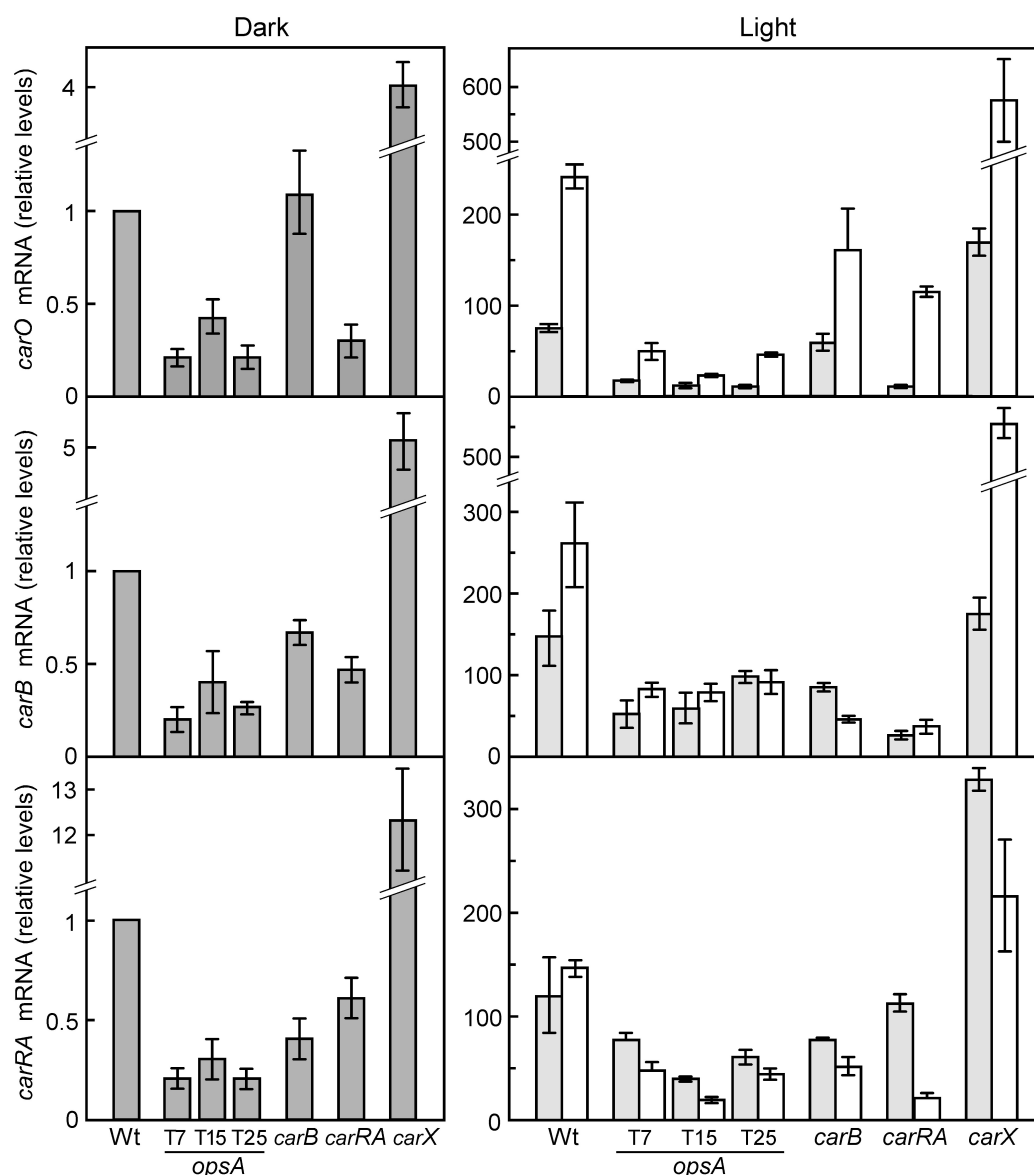


**Fig. C4.7. Effect of mutations at *opsA* and at relevant *car* genes on the expression of the enzymatic genes *carB* and *carRA*.** Real-time RT-PCR analyses of the genes *carB* and *carRA* from RNA samples of the wild-type strain, the *opsA* mutants T7, T15 and T25, and targeted mutants at genes *carRA*, *carB* and *carX* grown in the dark (left graph) or illuminated during 30 min or 1 h (gray and white bars, respectively, on right graph). Data represent average and standard deviations for four determinations from two independent experiments. Relative mRNA levels for each gene are referred to the value from non-illuminated wild type mycelia in each experiment.

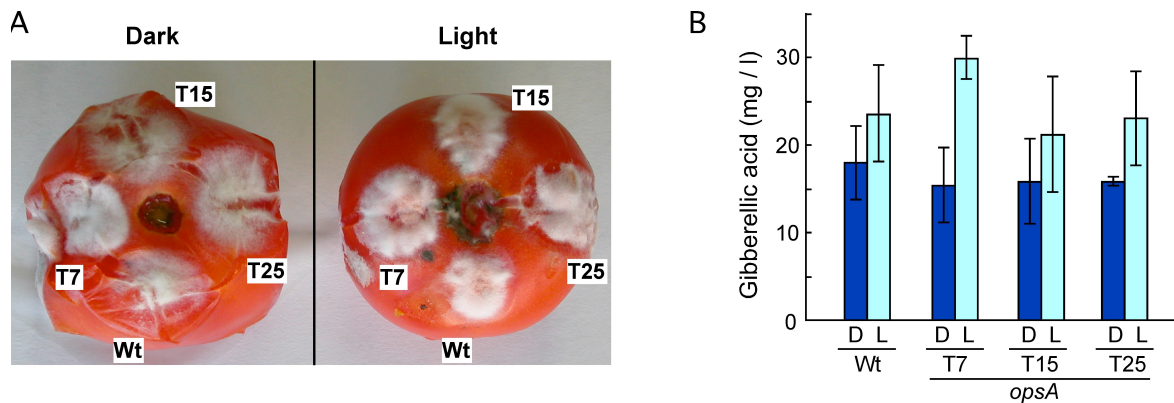


**Fig. C4.S1. a.** Infection test of the wild type (Wt) and three *opsA* mutants (T7, T15 and T25) on tomato fruits.  $5 \cdot 10^6$  conidia of the indicated strains were inoculated on the surface and incubated for 5 days at 30°C in the dark or under 10 W m<sup>2</sup> light. **b.** Gibberellin production by the wild type (Wt) and three *opsA* mutants grown in low nitrogen broth (10% ICI) at 30°C in the dark (D) or under 10 W m<sup>2</sup> white light (L).

### 3. Discussion

Opsins are a well defined group of transmembrane proteins widespread in all major phylogenetic groups. Their functions, initially associated to light-driven ion pumping activities in archaea, have been extended to a diversity of light-related roles in other organisms, with examples in archaea and bacteria as well as in lower and higher eukaryotes (Spudich et al., 2000; Spudich, 2006). So far, however, no specific function has been attributed to any fungal photoactive opsin. Lack of knowledge on the function of fungal opsins also applies to NOP-1, the one that has received more experimental attention. In contrast to *N. crassa* and other ascomycete relatives, the *Fusarium* species contain two genes, *carO* and *opsA*, encoding predictable photoactive opsins. They also contain a ORP gene, *hspO*, encoding a presumptive non-photoactive protein. Sequence comparisons point to OpsA and HspO as orthologous proteins for NOP-1 and YRO-2 from *N. crassa*, respectively, while CarO is unique to *Fusarium*.

The similarity of HspO from *F. fujikuroi* and YRO-2 from *N. crassa* with the stress-induced yeast proteins HSP30 or YRO2 suggests a similar stress-related function. HSP30 and YRO2 are putative chaperones, a family of proteins activated by heat shock or other stressing factors producing protein denaturation (Lindquist, 1992). Heat shock proteins prevent protein aggregation and facilitate protein degradation or refolding. HSP30 or YRO2-like fungal chaperones presumably act on unfolded extracytoplasmic proteins through a proton-flux-activated mechanism, a process functionally analogous to ATP-driven protein folding by cytoplasmic chaperones (Zhai et al., 2001). This is supported by the predictions in YRO2 of a proton conducting pathway, based on structure modeling techniques (Zhai et al., 2001). Proton transfer could induce conformational changes in YRO2 able to promote substrate protein unfolding. Similar mechanisms could also apply

to HspO in *F. fujikuroi* and YRO-2 in *N. crassa*. The heat-shock activation of genes *carO* and *opsA* and the presence of conserved proton transfer residues in the presumptive encoded proteins could also be explained by stress alleviating functions, in this case using light as driving force. Light is associated with stress signals in other organisms, as indicated by the light-triggered ten-fold increase of the mRNA levels for the heat-shock Hsp100-like gene *hspA* in *P. blakesleeanus* (Rodríguez-Romero and Corrochano, 2004). Photoinduction of this gene is mediated by regulatory gene products required for other photoresponses in this fungus, such as the WC1-like proteins MADA and its likely WC-2 partner, MADB (Rodríguez-Romero and Corrochano, 2006).

In contraposition to *hspO*, *opsA* mRNA levels are affected by light. Photoactivation of this gene is less prominent than the one exhibited by *carO* or by other *car* genes, but this difference may be partially attributed to higher *opsA* mRNA levels in the dark compared to *carO* rather than to lower *opsA* mRNA levels after illumination. In support to this, *opsA* mRNA is easily detected in northern blots on RNA samples from dark-grown mycelia (Fig. C4.3b and c) while *carO* mRNA is hardly detectable (Prado et al., 2004), and CT values in RT-PCR reactions were lower for *opsA* than for *carO* in the same total RNA samples. As an additional difference with *carO* regulation, *opsA* mRNA levels are not derepressed in carotenoid overproducing mutants, a phenotype tentatively explained by the loss of a key repressor of the carotenoid pathway. The low amounts of *carO* mRNA in the dark could be explained by efficient down-regulation of this gene by a putative CarS repressor, a regulatory mechanism that would not operate on *opsA*.

Induction of *opsA* and *carO* by light requires an active WcoA protein. In the case of *carO*, this is an unexpected result because of its coregulation with the enzymatic genes for the carotenoid pathway. In contrast to other fungi, this *Fusarium* WC-1-like protein is only partially involved in light activation of *carB*, *carRA* and *carT* (Estrada and Avalos, 2008), a result corroborated at the level of carotenoid production in a equivalent mutant of *F. oxysporum* (Ruiz-Roldán et al., 2008). Our results show that, as WC-1 in *N. crassa*, WcoA is a fully active photoreceptor in *F. fujikuroi*. This seems to be also the case for the WcoA counterpart in *F. oxysporum*, whose mutants lacking this protein have lost the photoinduced accumulation of mRNA for the photolyase gene *phr1* (Ruiz-Roldán et al., 2008). Additionally, this *Fusarium* WC-1-like protein has light-independent roles, as indicated by the effects in the dark on the regulation of secondary metabolism in *F. fujikuroi* (Estrada and Avalos, 2008), or its need for the expression of a hydrophobin gene in *F. oxysporum* (Ruiz-Roldán et al., 2008). Our results show a novel repressing effect for a WC-1 protein associated to the regulation of PPO genes in *F. fujikuroi*: *opsA* and *carO* mRNA levels increase 20- and 40-fold in *wcoA* mutants in a light-independent manner. This could be an indirect effect of the *wcoA* mutation, e.g., WcoA could activate a *opsA*/*carO* repressor. As a simpler hypothesis, WcoA could bind the *opsA* and *carO* promoters in



the dark to block its transcription, and its DNA binding activity could be reduced in light-activated WcoA. Future experiments with *in vitro* purified WcoA will be achieved to throw light on the repressing/activating functions of this versatile protein. Interestingly, a similar repressing effect was found for *nop-1* mRNA in *Neurospora* in a *wc-2* mutant but not in its *wc-1* counterpart (Bieszke et al., 2007). The role of the *F. fujikuroi* WC-2 orthologue in the regulation of *carO*, *opsA* and enzymatic *car* genes awaits to be investigated.

As found for the *carO* mutation (Prado et al., 2004), loss of a functional *opsA* gene produced no apparent phenotype, including unaltered morphology, pigmentation, conidiation, gibberellin production, pathogenic capacity or ability to grow at different non-optimal conditions. Unexpectedly, the *opsA* mutants contained lower mRNA levels for enzymatic genes of the carotenoid pathway, although they conserved their photoinduction. This effect is opposite to that produced by the *carX* mutation (Thewes et al., 2005), confirmed with more accurate mRNA analyses in this work (Fig. C4.7). The effect of the *carX* mutation was accompanied by an increased accumulation of carotenoids. However, the *opsA* mutants produced similar amounts of carotenoids than the parental strain, either in the dark or under light. A similar phenotype was exhibited by the *carB* mutant, which accumulated similar amounts of phytoene than those of colored carotenoids in the parental strain, despite it contained lower *carRA* mRNA levels. Furthermore, the reduced *carB* photoinduction in *wcoA* mutants (Estrada and Avalos, 2008, Fig. C4.4) was not accompanied by a concomitant reduction in their carotenoid content (Estrada and Avalos, 2008). Post-transcriptional effects, e.g., more efficient mRNA translation or enhanced enzymatic activity, could compensate the lower mRNA levels in the *wcoA*, *carB* and *opsA* mutants. An example of such effect is evident in the *carB* mutants of *P. blakesleeana*: they accumulate up to 20 fold more phytoene than  $\beta$ -carotene in the wild type, but their *carRA* and *carB* mRNA levels remain practically unchanged (Almeida and Cerdá-Olmedo, 2008). The similar reductions of *carB* and *carRA* mRNA levels, extended also to *carO* mRNA, found in *carRA*, *carB* and *opsA* null mutants may be attributed the lack of functional OpsA protein, which depends on the CarRA and CarB enzymes for production of retinal precursors (Fig. C4.1). Therefore, the opposite effect of the *carX* mutation must be attributed to loss of the CarX enzyme and not to lack of its enzymatic product, retinal. CarX is also active on other intermediates of the pathway, as  $\gamma$ -carotene or torulene, to produce acycloretnal and 3,4-didehydro-acycloretnal, respectively, in addition to retinal (Prado-Cabrero et al., 2007a). The regulatory effect of the *carX* mutation could be explained by a repressing role of any of these compounds.

The abilities of NOP-1 to bind retinal and to suffer a photocycle (Bieszke et al 1999a, Brown et al., 2001) suggest similar characteristics for OpsA. Photoreactivity was also experimentally demonstrated for OPS from *L. maculans* (Waschuk et al., 2005). As found for BR from *H. salinarum*, the OPS protein exhibited a fast photocycle, which

contrasts with the slow photocycle found for NOP-1 (Brown et al., 2001; Furutani et al., 2006). This disparity, which suggests a different biological role for NOP-1, was attributed to the presence of glutamic acid instead of the aspartic acid acting as proton donor in the BR protein (D96, labeled by dark gray boxes in Fig. C4.2B; Furutani et al., 2006; Fan et al., 2007). Interestingly, OpsA contains glutamic acid at this position while CarO contains aspartic acid. As proposed for OPS, the high conservation of residues involved in proton transfer in CarO led to suggest a similar light-driven ion transport function for this protein in *F. fujikuroi* (Prado et al., 2004). Pairwise protein comparisons reveal a higher similarity of OPS to NOP-1 from *N. crassa* and OpsA from *F. fujikuroi* (52% and 44% identical positions in the OPS protein, respectively) than to CarO (31%), but the presence of critical residues suggests a fast OPS-like photocycle for CarO and a slow NOP-1-like photocycle for OpsA. It must be noted, however, that the association between Glu/Asp and slow/fast photocycle is not solidly established. Bacterial proteorhodopsin uses glutamic acid as proton donor (Dioumaev et al., 2002), but carries out a highly efficient proton pumping photocycle (Rupenyan et al., 2008). Furthermore, the slow photocycle attributed to Nop-1 derives from its behavior under in vitro experimental conditions (Bieszke et al., 1999b), which significantly differ from those in its real in vivo environment. Thus, the available information does not totally discard light-driven ion pumping functions for NOP-1 or OpsA.

The similarity between NOP-1 and OpsA suggest analogous functions and we could expect similar effects for their respective mutations. In an indirect manner, this was really the case: none of these mutations produced any apparent phenotypic change under laboratory conditions. However, the only visible effect found in the null *nop-1* strain, a light-dependent morphological alteration in the presence of oligomycin (Bieszke et al., 1999a), was not visible in our *F. fujikuroi opsA* mutants. Recent data in *Neurospora* point to a connection between NOP-1 and conidiation (Bieszke et al., 2007), but the role that this protein could play in this process remains unsolved. Both fungi differ in the control of conidiation, induced by light in *Neurospora* but not in *F. fujikuroi* (Estrada and Avalos, 2008; and this work). Furthermore, the *opsA* mutants produced similar amounts of conidia than the wild type, suggesting that this gene is not involved in conidiation in *F. fujikuroi*. As found for the orthologous WC-1 and WcoA proteins, NOP-1 and OpsA could have evolved to fit different biological demands in these related fungi.

## 4. Material and methods

### 4.1 Strains and culture conditions

Unless otherwise stated, the wild type strain of *Fusarium fujikuroi* (*Gibberella fujikuroi* mating population C; O'Donnell et al., 1998) used in this work was FKMC1995 (Leslie, 1991; Kansas State University Collection, Manhattan, KS, USA), abbreviated Wt. In some cases, the wild type strain IMI58289 (Commonwealth Mycological Institute, London, England), abbreviated Wt2, was also used. SF134 and SG22 are neurosporaxanthin-overproducing strains obtained from FKMC1995 and IMI58289, respectively, by exposure to N-methyl-N'-nitro-N-nitrosoguanidine (Avalos et al., 1985). The *carX* mutant T.2.1, obtained from IMI58289, was described before (Thewes et., 2005).

For sporulation analyses,  $10^6$  conidia were spread on plates of DG minimal medium (Avalos et al., 1985) with 3 g l<sup>-1</sup> asparagine instead of NaNO<sub>3</sub> as the nitrogen source (DGasn) and grown for 7 days in the dark or under 25 W m<sup>2</sup> of white light. When required, the medium was supplemented with 100 mg l<sup>-1</sup> oligomycin (Sigma) or with 100 mg l<sup>-1</sup> hygromycin (Roche). For DNA isolation the strains were grown in 250 ml Erlenmayer flasks with 50 ml DGasn broth for 2 days in an orbital shaker and separated from the medium by filtration through Whatman paper. For gene expression analyses, the strains were grown in 15 cm Petri dishes with 80 ml of DGasn broth inoculated with  $10^6$  spores. The Petri dishes were incubated for three days in the dark and the mycelia were recovered under safe red light. When indicated, the Petri dishes were illuminated under 25 W m<sup>2</sup> before mycelia collection. The same protocol was used for carotenoid analyses, except that 8,5 cm agar cultures were used instead of submerged cultures, the conidia were inoculated in 2 ml top agar (8 g l<sup>-1</sup> of agar in water), and incubation under light lasted 24 h. As an alternative approach, the strains were grown as surface colonies for seven days on DGasn at 22°C either in the dark or under 10 W m<sup>2</sup>. In the case of heat shock, the Petri dishes were incubated at 38°C or 42°C for one or two hours before mycelia collection. For gibberellin biosynthesis, the strains were grown in low nitrogen broth as described (Estrada and Avalos, 2008). Unless otherwise stated, incubations were carried out at 30°C.

### 4.2 Cloning and sequencing of *opsA*

The complete *opsA* gene sequence was obtained in three steps. (a) An internal *opsA* segment was obtained by PCR using the degenerate oligonucleotides 5'-TTYGTYGC-YATGACYGTYGT-3' and 5'-CCARAARCCRATRACRGCYTT-3', deduced from the amino acid sequences FVAMTVV and KAVIGFW from the *F. graminearum* FGSG\_07554 annotated protein. DNA sequence analysis confirmed that the cloned segment was genuine.

(b) DNA segments surrounding *opsA* were cloned by PCR using forward and reverse primers from the available internal gene segment and predictably conserved external sequences. An upstream DNA segment was cloned using the *opsA* reverse primer 5'-GAGGGATCACCACAAGCATG-3', and the degenerate primer 5'-TTCCAYTCRTCTT-NCCYTC-3', designed from a conserved domain of the upstream annotated gene FGSG\_07553. A downstream DNA segment was cloned using the *opsA* forward primer 5'-GTTGAAGTACGATGTCTGGC-3', and the degenerate primer 5'-GGYTTYATYC-ARGCNTGGAA-3', designed from a conserved domain of the downstream annotated gene FGSG\_07555. (c) Both surrounding DNA segments were sequenced from their ends and used to choose the primer sets 5'-GCCATTGCTTGTGACGTCTG-3' / 5'-GTTTGGTAGTGAGTCGGTTC-3', 5'-GTTCATCCTTACCCGTGGTG-3' / 5'-CAACAAGATAGACGAGCCAG-3', and 5'-ATCGCTCGCCTCTTTGGCTC-3' / 5'-TCGTATTTCGTGTCCCATCAC-3'. The resulting PCR products, three overlapping DNA segments covering the entire gene, were sequenced to obtain the complete *opsA* sequence from FKMC1995 DNA. To enhance amplification fidelity, the PCR reactions were performed with the Triplmaster PCR system (Eppendorf AG, Hamburg, Germany). The sequences from each segment were determined for both DNA strands from at least two independent PCR products using an ABI Prism® 3100 Genetic Analyzer (Applied Biosystems, Foster City, CA. USA).

#### 4.3 *Fusarium* transformation

For protoplast formation,  $5 \cdot 10^8$  conidia were incubated in 100 ml YPED-2G (20 g l<sup>-1</sup> glucose, 10 g l<sup>-1</sup> peptone and 3 g l<sup>-1</sup> yeast extract) at 28°C for 7 h, checking under microscope development of germination tubes. Germinated conidia were filtered through Whatman paper previously soaked in NaCl 0,7 M, transferred with a sterile spatula to an empty Petri dish, mixed with 15 ml of enzymatic solution, and transferred to a 100 ml Erlenmayer flask to be incubated in an orbital shaker for 45 min, 40 r.p.m. (protoplasts formation monitored under microscope every 15 min). The enzymatic solution contained 2 g Lysing enzymes of *Trichoderma harzianum*, 5 g Driselase basidiomycetes sp, and 10 mg Chitinase from *Streptomyces grisea* (the three chemicals from Sigma) dissolved in 200 ml NaCl 0.7 M. The newly formed protoplasts were passed through two borosilicat filters (first one, porosity 0.40 mm Ø, second one, porosity 1, Robu Glasfilter-geräte, GMBH) previously soaked in NaCl 0.7 M. 50 ml of the filtered protoplast suspension were collected in a Falcon tube and centrifuged at room temperature for 10 min, 1,500 r.p.m. (1240 g). The pellet was resuspended in 50 ml NaCl 0.7 M, centrifuged as described above, resuspended in 50 ml STC buffer (1.2 M sorbitol, 10 mM Tris-HCl pH 8, 50 mM CaCl<sub>2</sub>), centrifuged again and finally resuspended in 200 ul STC buffer. Protoplasts

concentration was calculated in an haemocytometer and diluted to a final concentration of  $3 \cdot 10^8$  protoplasts  $\text{ml}^{-1}$ . The protoplast suspension was used immediately for transformation following the protocol by Proctor et al., 1997.

#### 4.4 Generation of *opsA*, *carB* and *carRA* mutants

The *opsA* gene was obtained by PCR from FKMC1995 genomic DNA with primers 5'-GGCCTGGCTGGTCAGTTGAG-3' and 5'-TCGTATTCGTGTCCCATCAC-3'. The resulting 3.4 kb DNA product, which includes 2.1 and 0.3 kb of upstream and downstream untranslated sequences, respectively, was cloned into the pGem®-T vector (Promega, Mannheim, Germany), to yield plasmid pALEX8A. The hygromycin resistance cassette (gene *hph* and regulatory sequences), obtained from plasmid pHJA2 (Fernández-Martín et al., 2000) with primers 5'-CTTGCATGGGCCCAAAGCTATTG-3' and 5'-GAATGTGGGCCCTGTAGGCTTG-3', was introduced into pALEX8A at the *ApaI* restriction site of the *opsA* gene, 392 nucleotides downstream from the ATG start codon, giving plasmid pALEX10. FKMC1995 protoplasts were transformed with plasmid pALEX10 linearized with *NotI*. For preliminary detection of *opsA* truncation, DNA samples from isolated transformants were checked for amplification with two primers surrounding the integration site (5'-GAGGGATCACCACAAGCATG-3' and 5'-CAACAAGATAGACGAGCCAG-3').

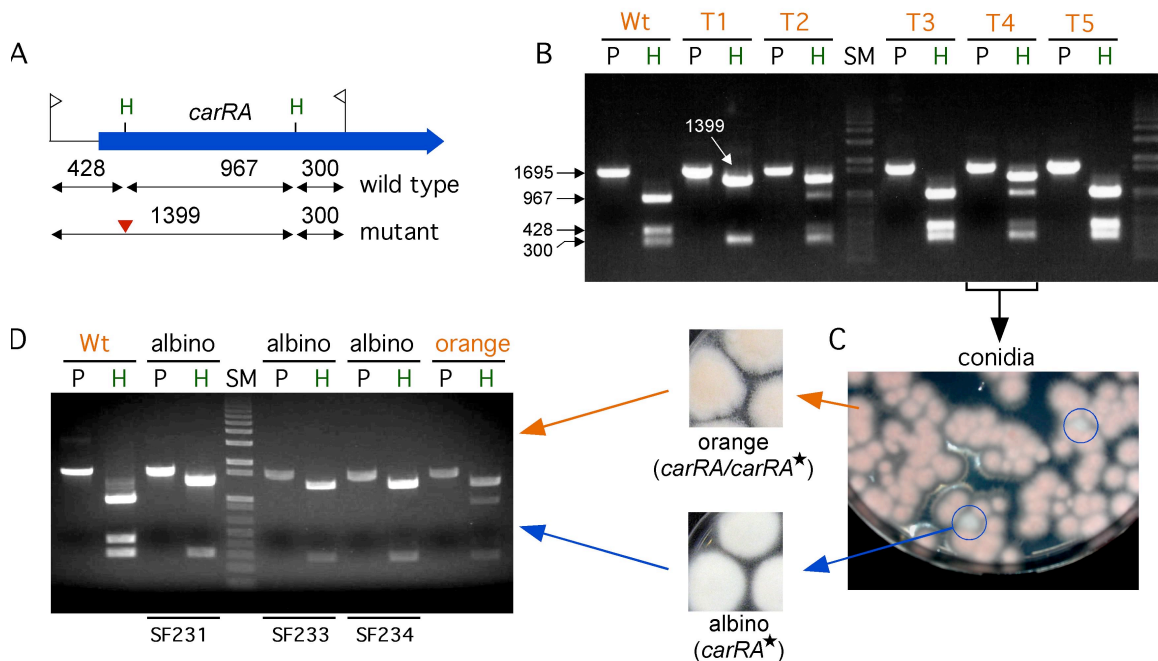
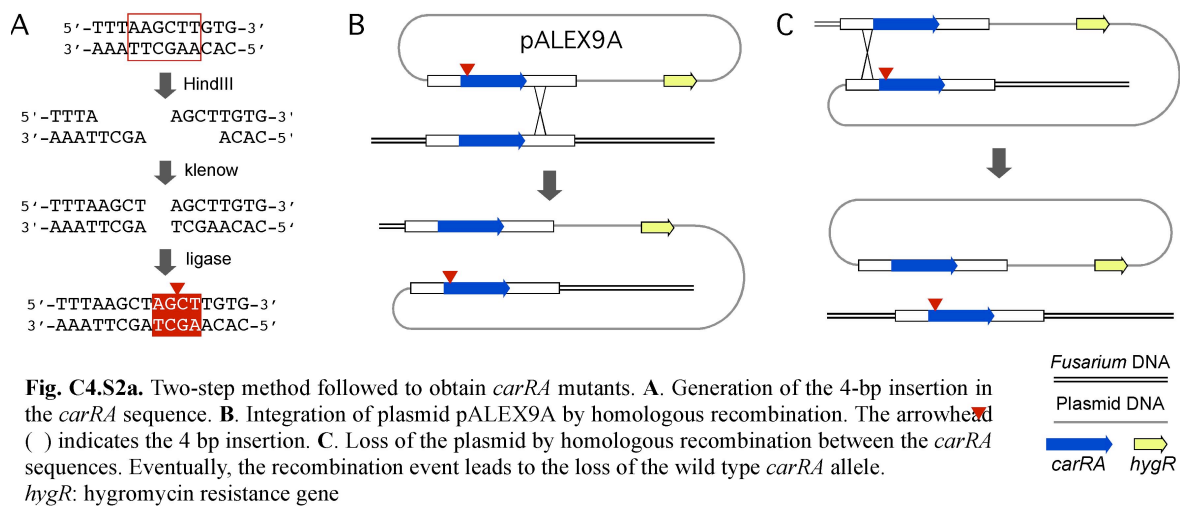
Targeted *carRA* mutants were obtained from FKMC1995 using a two-step allelic replacement method (Fig. C4.S2a, adapted from Fernández-Martín et al., 2000). In detail, the *carRA* gene was obtained by PCR from FKMC1995 genomic DNA with primers 5'-CGCTCAGAACGACACCGTTTG-3' and 5'-GCCGGTAAGATATCTGTGAC-3', resulting in a 4.47 kb DNA product with 0.97 kb and 1.55 kb of upstream and downstream *carRA* sequences, respectively. This PCR product was cloned into pGem®-T, removed by digestion with *NotI*, and subcloned into the *NotI* site at the polylinker sequence of plasmid pHJA2 to produce plasmid pALEX9. This plasmid, which contains a hygromycin resistance cassette, was partially digested with *HindIII*, endfilled with klenow and self-ligated to generate an AGCT insertion 153 nucleotides downstream from the ATG start codon (Fig. C4.S2a), yielding plasmid pALEX9A. FKMC1995 protoplasts were transformed with plasmid pALEX9A previously linearized with *ApaI*, leading to the isolation of 14 hygromycin-resistant transformants. Two of them were albino, indicating the occurrence of gene conversion by homologous recombination (Fernández-Martín et al., 2000). Five of the transformants, including one of the albino strains, were analyzed by PCR to check the presence of the wild type and mutant *carRA* alleles. For this purpose, a 2.4 kb *carRA* gene segment was obtained from each strain by PCR with primers 5'-GCCGGTAA-GATATCTGTGAC-3' and 5'-TTGTTCAATGCAGACCATGC-3' and

digested with HindIII (Fig. C4.S2a). Conidia obtained from one of the transformants containing both *carRA* alleles were plated on non-selecting media and incubated under light to check the generation of spontaneous albino mutants, which are expected to have lost the wild type *carRA* allele by a single recombination event (Fig. C4.S2b). Genomic DNA was extracted from five albino strains and one orange strain and used to confirm the absence of the wild type *carRA* alleles. All the albino strains tested contained only the mutated *carRA* allele (Fig. C4.S2b). One of them, called SF233, was used in this work as null *carRA* mutant.

Targeted *carB* mutants were obtained from FKMC1995 as described by Fernández-Martín et al., 2000.

#### 4.5 Molecular techniques

RNA samples were isolated using Trizol (Invitrogen, USA) following manufacturer instructions. DNA for Southern blot analyses were obtained with the GenElute Plant Genomic DNA Miniprep Kit (Sigma). DNA samples for PCR analyses were obtained from 0.2 g of mycelial fragment following the method described by Hoffman and Winston, 1987. Southern and northern blot hybridizations were performed as described (Sambrook and Russell, 2001). In both cases, nylon membranes were probed with an internal 386 bp segment from the *opsA* gene obtained by PCR with primers 5'-GAGGGATCACC-ACAAGCATG-3' and 5'-CAACAAGATAGACGAGCCAG-3'. Real time PCR (RT-PCR) expression analyses were performed using total RNA samples as template. The reactions, carried out in 25 µl volumes with an ABI 7500 (Applied biosystems), consisted of a 30 min retrotranscription step at 48°C, 10 min at 95°C and 40 cycles of 95°C denaturation for 15 s and 60°C polymerization for 1 min. Dissociation curves were achieved afterwards. Genes and primer sets for the RT-PCR reactions, chosen with the software Primer Express™ v2.0.0 (Applied Biosystems) were *carB* (5'-TCGGTGTCGAGTACCGTCTCT-3' and 5'-TGCCTTGCCGGTTGCTT-3'), *carRA* (5'-CAGAAGCTGTTCCCGAAGACA-3' and 5'-TGCGATGCCCATTTCTTGA-3'), *carO* (5'-TGGGCAACGCAGTGACAT-3' and 5'-TGCGCAGACAGCCCAGTA-3'), *opsA* (5'-GTGTTGATGGTGCGCATACC-3' and 5'-ACCCGCGAGGACAAAGATC-3'), *hspO* (5'-TTCCCACGCAGCGTAACC-3' and 5'-CCCAGTTGATGTACTTGGCAAA-3'), and *carX* (5'-GCCGCCCATGAGGATACA-3' and 5'-TCAGCTTCAACACCGTCGAA-3'). Optimized RTPCR conditions were described before (38).  $\beta$ -tubulin gene from *F. fujikuroi* (5'-CCGGTGCTGGAAA-CAACTG-3' and 5'-CGAGGACCTGGTCGACAAGT-3') was used as control for constitutive expression.



Relative gene expression was calculated with the  $2^{\Delta\Delta CT}$  method with the Sequence Detection Software v1.2.2 (Applied Biosystems). Each RTPCR analysis was performed four times (duplicated samples from two independent experiments) and standard deviations calculated to ensure statistical accuracy. Primers (HPLC grade) were synthesized by StabVida (Oeiras, Portugal).

#### 4.6 Analytical methods, conidia production and pathogenicity assay

Carotenoid extractions were performed from lyophilized mycelial samples as described by Youssar and Avalos (2007) except that the extractions were done breaking the dry mycelial samples in a Fastprep®-24 device (MP biomedical, Irvine, CA, USA). Total carotenoid samples were determined by optical absorbance in hexane in a Beckman DU® 640 spectrophotometer. For low carotenoid amounts, the samples were concentrated and measured in a 100 µl 8 mm high micro cell. HPLC analyses were done with a Hewlett Packard 1100 series system (Waldbronn, Germany), equipped with a photodiode array detector and a C30-reversed phase column (Waters, hypersil ODS). The separations were performed using MeOH/tert-butylmethylether, 500:500, v/v (solvent A) and MeOH/tertbutylmethylether/water, 600:120:120, v/v/v (solvent B). The column was developed at a flow rate of 1 ml min<sup>-1</sup> with a linear gradient from 100% solvent B to 57% solvent A 43% solvent B within 25 min, followed by a linear gradient to 100% solvent A with a flow rate of 1.5 ml within 7 min. The flow was then increased to 2 ml min<sup>-1</sup> of 100% solvent A maintaining these conditions for 32 min. Gibberellins (gibberellic acid) was quantified with the same HPLC equipment as described (Barendse et al., 1980).

Conidia production on agar cultures was quantified following by Prado et al., 2004. Pathogenicity assays were done on fresh tomato fruits by inoculation of 5 x 10<sup>5</sup> conidia as described by Di Pietro et al., 2001, followed by five days incubation at 30°C either in the dark or under light (10 W m<sup>-2</sup>).

#### 4.7 Sequence analyses

Blast analyses were done through the NCBI server ([www.ncbi.nlm.nih.gov/blast/](http://www.ncbi.nlm.nih.gov/blast/)). BlastP was carried out against the non-redundant Swissprot database. Alignments and bootstrapped NJ trees were achieved with the ClustalX 1.83 program (Thompson et al., 1997). Positions with gaps were excluded in the analysis. DNA sequences were obtained through the server [www.broad.mit.edu/annotation/fungi/](http://www.broad.mit.edu/annotation/fungi/) of the Broad Institute (Cambridge, MA. USA). Transmembrane tendencies of PPO and ORP sequences were calculated through the Expasy server (<http://us.expasy.org/tools/protscale.html>) following Zhao and London (Zhao and London, 2006).

#### Acknowledgments

This work was supported by the Spanish Government (Ministerio de Ciencia y Tecnología, projects BIO2003-01548 and BIO2006-01323) and the Andalusian Government (project P07-CVI-02813).





## CAPÍTULO 5

### **Biosíntesis de $\beta$ -caroteno y retinal en *Ustilago maydis***

### **$\beta$ -carotene and retinal biosynthesis in *Ustilago maydis***

Alejandro F. Estrada<sup>1</sup>, Thomas Brefort<sup>2</sup>, Carina Mengel<sup>2</sup>, Violeta Díaz-Sánchez<sup>1</sup>, Adrian Alder<sup>3</sup>, Salim Al-Babili<sup>3</sup> and Javier Avalos<sup>1\*</sup>

<sup>1</sup>Departamento de Genética, Facultad de Biología, Universidad de Sevilla, E41080 Sevilla, Spain

<sup>2</sup>Department of Organismic Interactions. Max Planck Institute for terrestrial Microbiology. D-35043 Marburg, Germany

<sup>3</sup>Faculty of Biology, Albert-Ludwigs University of Freiburg, D-79104 Freiburg, Germany.



## Abstract

The basidiomycete *Ustilago maydis*, the causative agent of corn smut disease, has emerged as a model organism for dimorphism and fungal phytopathogenicity. Availability of an annotated genome sequence and amenability to genetic manipulation make this fungus an ideal system to investigate other biological processes. We show that *U. maydis* accumulates  $\beta$ -carotene and that its genome encodes key conserved enzymes for the synthesis of this pigment. The amounts of  $\beta$ -carotene depended on culture pH and aeration and was not affected by light or oxidative stress. Moreover, we identified an *U. maydis* gene, *cco1*, which codes for a potential  $\beta$ -carotene dioxygenase. Heterologous overexpression and in vitro analyses of Cco1 demonstrated that it catalyzes the oxidative cleavage of  $\beta$ -carotene to yield two molecules of the apocarotenoid retinal. This enzymatic activity was confirmed in vivo by the analyses of  $\beta$ -carotene and retinal contents of *U. maydis cco1* deletion and over-expression strains. The *U. maydis* genome also encodes three potential opsins, a family of photoactive proteins that use retinal as chromophore. Two opsin genes showed different light-regulated expression patterns, suggesting specialized roles in photobiology, but no mRNA was detected for the third opsin gene in the same experiments. Deletion of the *cco1* gene, which should abolish function of all the retinal-dependent opsins, did not affect growth, morphology or pathogenicity, indicating that retinal and opsin proteins play no relevant role in *U. maydis* under the tested conditions.

**Keywords:** carotenogenesis, light regulation, opsins, carotene dioxygenase, apocarotenoids

## 1. Introduction

Carotenoids are terpenoid pigments widely spread in nature, where they are synthesized by photosynthetic species and many non-photosynthetic microorganisms, such as heterotrophic bacteria and fungi (Britton et al., 1998; Sandmann and Misawa 2002). In plants and algae they are essential accessory pigments of the photosynthetic machinery (Telfer 2005). Carotenoids are responsible for the bright colors of many fruits and flowers as well as of some animals. Well known examples are the pink color of flamingos or salmons, due to the accumulation of astaxanthin. Animals are unable to synthesize carotenoids, but depend on their dietary acquisition as vitamins to generate such crucial compounds as retinal, the central light-absorbing pigment in vision, or retinoic acid, a critical morphogen in vertebrate development (Blomhoff and Blomhoff 2006). In addition, carotenoids serve as antioxidants and have commercial applications in cosmetics and food industry, where algae and fungi are employed as biotechnological carotenoid producers (Avalos and Cerdá-Olmedo 2004; Del Campo et al., 2007).

Chemically, the carotenoids are fat-soluble compounds which contain a long aliphatic polyene chain, usually composed of eight isoprene units. Their synthesis is initiated by the condensation of two geranylgeranyl pyrophosphate units to generate the colorless carotenoid precursor phytoene (Fig. C5.1). Hundreds of different carotenoids have been found in nature, but only a few are widely distributed. One of them is  $\beta$ -carotene, which is synthesized from phytoene by the oxidative introduction of four conjugated double bonds and two  $\beta$  rings. Some carotenoids are subject to additional oxidative modifications to yield xanthophylls.

The genes and enzymes involved in carotenoid biosynthesis have been described in different species, including several fungi, i. e. the ascomycetes *Neurospora crassa* and *Fusarium fujikuroi*, the zygomycetes *Phycomyces blakesleeanus*, *Mucor circinelloides*, and *Blakeslea trispora*, and the basidiomycete *Xanthophyllomyces dendrorhous* (formerly *Phaffia rhodozyma*) (reviewed by Avalos and Cerdá-Olmedo 2004). In contrast to photosynthetic species, fungal phytoene synthase and cyclase activities reside on a single bifunctional polypeptide encoded by a highly conserved gene, i. e. *carRA* in *P. blakesleeanus*, *B. trispora* and *F. fujikuroi*, *carRP* in *M. circinelloides*, *al-2* in *N. crassa*, and *crtYB* in *X. dendrorhous*. The desaturation step from the phytoene precursor to lycopene is catalysed by conserved phytoene desaturases, encoded by the *carB* gene in most of the mentioned fungi except *N. crassa* (*al-1*) and *X. dendrorhous* (*crtI*). The sequential action of these enzymes drives  $\beta$ -carotene biosynthesis in the mentioned zygomycete species, but additional enzymes catalyse further oxidation steps in other fungi to yield different carotenoid derivatives. The carotenoid pathways in *F. fujikuroi* and *N. crassa* involve a fifth desaturation step instead of the second cyclization and two additional oxidative reactions yielding neurosporaxanthin, a carboxylic apocarotenoid (Prado-

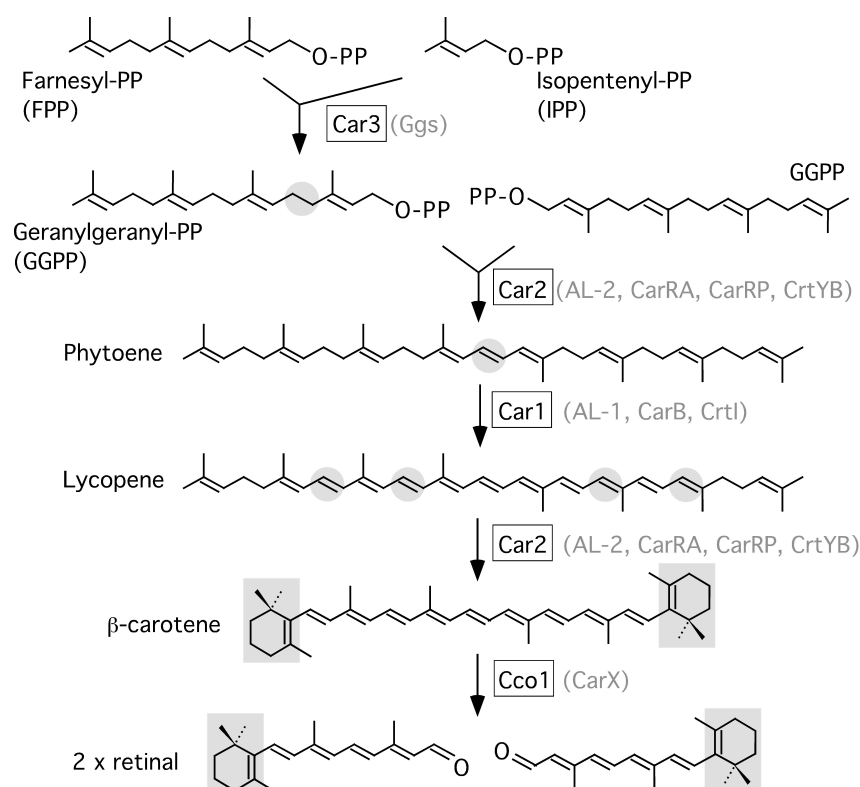


**Fig. C5.1. Biosynthetic pathway for  $\beta$ -carotene and retinal.** Putative gene products responsible for each enzymatic reaction in *U. maydis* are boxed. Orthologous proteins for each reaction in representative fungi are indicated in parentheses. Chemical changes from precursor molecules are highlighted as shaded areas. Attribution of the Cco1 gene product to  $\beta$ -carotene cleavage derives from results of this work.

Cabrero et al., 2007a; Saelices et al., 2007; Estrada et al., 2008).

In *X. dendrorhous*, the main pathway leads to the formation of astaxanthin through the introduction of keto and hydroxy groups in the  $\beta$  rings of  $\beta$ -carotene to produce astaxanthin (Alvarez et al., 2006; Ojima et al., 2006; Visser et al., 2003).

These carotenoids may be subject to oxidative cleavage by a class of dioxygenases, which generate two molecules of respective apocarotenoids from one carotenoid precursor, e. g. two molecules of retinal from one of  $\beta$ -carotene (Wyss 2004). Retinal serves as the chromophore of opsins, a widespread group of transmembrane photoreactive proteins (Sharma et al., 2006; Spudich 2006). Best known members of this protein family are the bacterial bacteriorhodopsins and halorhodopsins, which act as light-driven proton and chloride pumps, respectively (Spudich, 1998). Opsins are found in all major taxonomic groups, where they mediate different photoreceptor functions (Sharma et al., 2006), such as phototaxis in algae (Ridge 2002) or vision in animals (Menon et al., 2001). Putative opsin-encoding genes are also found in fungal genomes (Brown 2004). Many of them are potentially photoactive, as indicated by the presence of a highly conserved lysine residue

for covalent binding of the retinal chromophore. A thoroughly investigated example is *nop-1* from *N. crassa* (Bieszke et al., 1999a), whose ability to bind retinal and to undergo a photochemical reaction cycle have been demonstrated (Bieszke et al., 1999b; Brown et al., 2001).

Carotenoids are not essential for fungi, as deduced from viability upon mutational or chemical block of the pathway in different species, e. g. in *F. fujikuroi* (Avalos and Cerdá-Olmedo 1986, 1987) and in *P. blakesleeanus* (Cerdá-Olmedo 1987). However, carotenoids provide protection against oxidative stress (Edge et al., 1997). Consistently, hydrogen peroxide treatment results in enhanced production of astahaxanthin in *X. dendrorhous* (Liu and Wu 2006) and of neurosporaxanthin in *N. crassa* (Iigusa et al., 2005). Furthermore, carotenoid biosynthesis is stimulated by light in different fungi (Avalos et al., 1993), a regulation that has been attributed to the protective properties of carotenoids in *Neurospora* (Yoshida and Hasunuma 2004; Iigusa et al., 2005). Additionally, carotenoid biosynthesis provides a source for several compounds with distinct features and activities. In zygomycetes,  $\beta$ -carotene is used for the synthesis of the sexual hormones, the trisporic acids (Burmester et al., 2007). The first fungal gene for a retinal-forming dioxygenase, CarX, has recently been described in *F. fujikuroi* (Prado-Cabrero et al., 2007b), demonstrating that carotenoids also serve as retinal precursors in fungi. In *F. fujikuroi* the *carX* gene is part of a coregulated gene cluster together with the  $\beta$ -carotene biosynthesis genes, *carRA* and *carB*, and that for one of the two potentially photoactive opsins of this fungus, *carO* (Prado et al., 2004; Thewes et al., 2005; Prado-Cabrero et al., 2007b).

Genome databases for an increasing number of fungi have become available in the recent years, allowing the identification of carotenoid genes in model fungi in which this biosynthetic pathway has not received attention. A relevant example is the biotrophic basidiomycete *Ustilago maydis*, the causative agent of corn smut disease (Kahmann et al. 2000). Signaling pathways involved in different developmental stages in *U. maydis* life cycle have been subject to detailed analyses (Feldbrügge et al., 2004, Nadal et al., 2008, Klosterman et al., 2007, Garcia-Pedrajas et al., 2008), establishing this basidiomycete as a leading model in the research of the molecular mechanisms involved in dimorphism (Sánchez-Martínez and Pérez-Martín 2001), mating (Bakkeren et al., 2008) and other basic biological processes (Steinberg and Pérez-Martín 2008). Furthermore, the identification of secreted effectors for pathogenic development made *U. maydis* a valuable model system to unravel the molecular mechanisms of fungal biotrophy (Kämper et al., 2006).

*U. maydis* produces different secondary metabolites, such as ferrichrome or ustilagic acid, that contribute to its survival in natural habitats (Bölker et al., 2008). Carotenoid biosynthesis has not received attention in this fungus, probably because lack of a patent pigmentation. However, carotenoids were formerly found in *Ustilago violacea*, the causing agent of anther smut in *Silene alba*. Strains from this species show different colors, ranging

from pink to yellow, and accumulate different mixtures of phytoene-derived carotenoids in the pathway from phytoene to  $\beta$ -carotene (Fig. C5.1) (Will et al., 1994). We have found in the *U. maydis* genome sequence orthologous genes for fungal  $\beta$ -carotene biosynthesis enzymes, and for a CarX-like retinal forming enzyme. Moreover, the genome includes three genes for putative photoactive opsins (Brown 2004), indicating the need for retinal and, therefore, for an active carotenoid pathway. In this study, we show that *U. maydis* accumulates moderate amounts of  $\beta$ -carotene and present the functional characterization of the *U. maydis carX* ortholog, named *cco1*. We demonstrate by genetic and biochemical approaches that Cco1 acts as an enzyme that cleaves/oxidizes  $\beta$ -carotene to retinal. Consistently, targeted deletion of *cco1* in *U. maydis* resulted in higher  $\beta$ -carotene accumulation, but no other evident phenotype. This indicates that retinal and the potential photoactive opsins play no relevant biological role in *U. maydis* under the tested conditions.

## 2. Results

### 2.1 *U. maydis* accumulates $\beta$ -carotene as the sole carotenoid

Pellets from submerged cultures of *U. maydis* grown at pH 7 exhibit a yellow color, indicating the accumulation of carotenoids. To confirm the occurrence of these pigments and to determine their biochemical pattern, lipophilic extracts were analyzed by HPLC. As shown in Fig. C5.2, the HPLC chromatogram revealed the accumulation of  $\beta$ -carotene, identified by its UV-Vis spectrum and elution time, which were identical to those of an authentic standard. The HPLC analyses did not show any detectable amounts of  $\beta$ -carotene precursors or other carotenoids. Similar results were obtained from cells grown on Petri dishes at neutral pH.

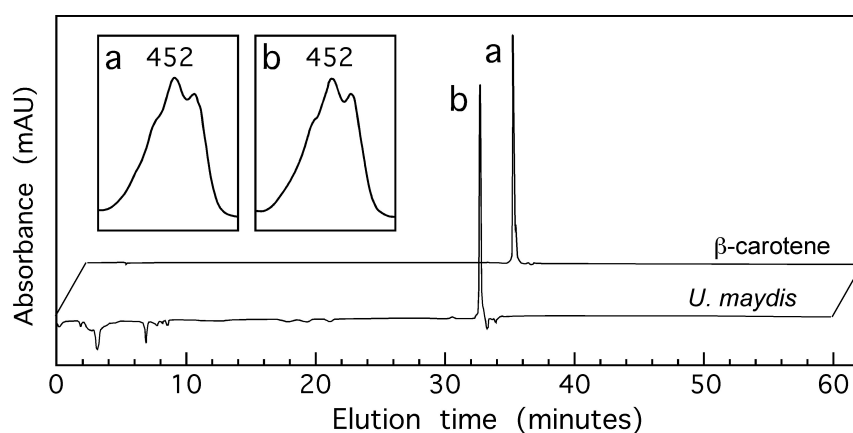


**Fig. C5.2. Carotene biosynthesis by wild-type *U. maydis*.** HPLC analyses of  $\beta$ -carotene standard, purified from wild type *P. blakes-leeanus*, and the carotenes accumulated by a 6 day-old culture grown at pH 7. UV-visible light absorption spectra of the major peaks are displayed in the inner boxes.



## 2.2 *U. maydis* $\beta$ -carotene content is reduced by low pH value and not affected by light or $H_2O_2$

Light is known to induce carotenoid biosynthesis in several fungal species (Avalos et al., 1993). Lowering the pH value of the culture medium may also affect the pigment content, since it causes global changes in *U. maydis* morphology and physiology (Martínez-Espinoza et al., 2004). To investigate the impact of these factors, cultures were grown on agar either in the dark or under continuous illumination at pH 7 or 3 for twelve days, and the  $\beta$ -carotene contents were determined at different time points. As shown in Fig. C5.3A, the amount of  $\beta$ -carotene increased about three-fold between the second and twelfth day of incubation under continuous illumination at neutral pH. Similar  $\beta$ -carotene contents were observed in the dark, excluding light regulation of the pathway under the conditions used. The growth under acidic conditions (pH 3) led to striking morphological changes and a paler pigmentation. In contrast to the typical yeast-like appearance at pH 7, the cells exhibited pseudohyphal growth, which was accompanied by a general reduction of  $\beta$ -carotene contents, irrespective of culture age or illumination. Similarly, young cultures (12 and 24 h-old) grown in liquid minimal medium at pH 7 contained about 30  $\mu\text{g g}^{-1}$  dry wt, while only about 15  $\mu\text{g g}^{-1}$  dry wt were accumulated upon cultivation at pH 3. Incubations for longer times in liquid cultures at both pH values led to lower carotene amounts than those of surface cultures. This effect could be attributed to low aeration, since long-term incubations of smaller culture volumes in larger flasks resulted in enhanced carotene accumulation (Fig. C5.3B). The positive impact of higher aeration conditions may be the result of an induction by oxidative stress. Thus, carotene biosynthesis is moderately induced in *X. dendrorhous* grown in media supplemented with 10 mM  $H_2O_2$  (Liu and Wu 2006). To check its impact on carotene content in *U. maydis*, cells were cultivated in the presence of different  $H_2O_2$  concentrations. Total inhibition of the growth was observed at 3 mM, whilst a  $H_2O_2$  concentration of 1mM was tolerated. However, the application of  $H_2O_2$  at this concentration did not lead to significant changes in the  $\beta$ -carotene content, as shown by the carotene analyses of cultures treated for four days at the two pH values investigated (Fig. C5.3B).

## 2.3 $\beta$ -carotene biosynthesis genes occur in *U. maydis*

The synthesis of  $\beta$ -carotene by *U. maydis* implies the occurrence of corresponding structural genes, likely to be similar to those of formerly investigated carotenogenic fungi. Blast searches against fungal GGPP synthases, phytoene synthase/carotene cyclases and phytoene desaturases revealed three clear orthologs in the *U. maydis* genome, UM04459,

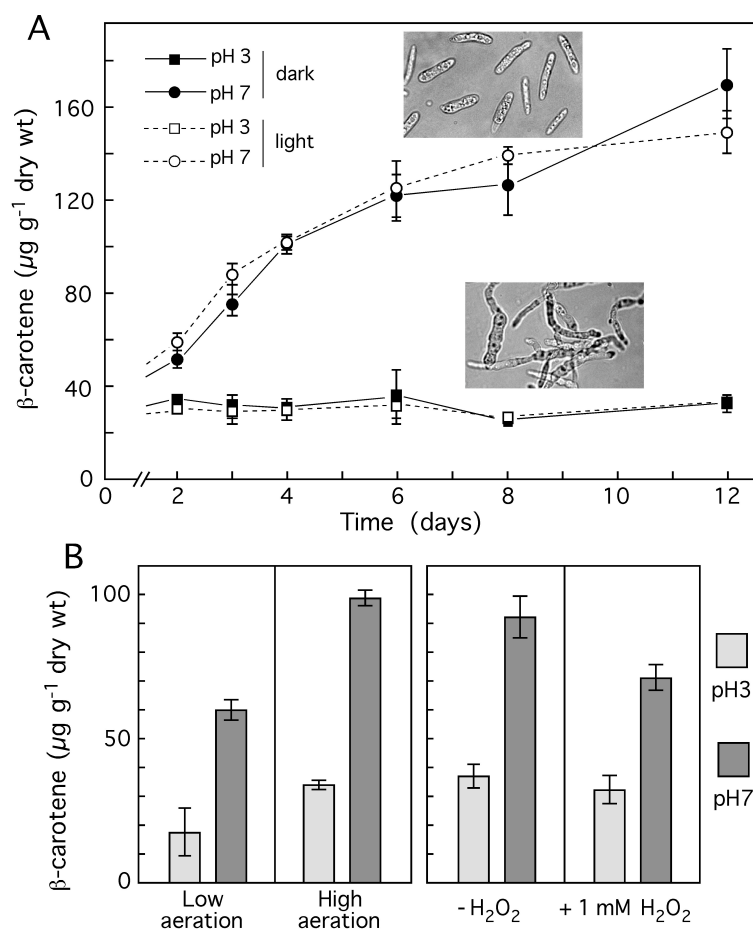


**Fig. C5.3. Effect of culture conditions on  $\beta$ -carotene biosynthesis by wild-type *U. maydis*.** A. Time-course of carotene accumulation of agar cultures at pH 3 and pH 7 in the dark or under continuous illumination ( $10 \text{ W m}^{-2}$ ). Inner microscope pictures show cell morphology at the pHs investigated. B. Effect of aeration (6 days growth; high aeration: 10 ml in 500 ml Erlenmeyer flasks; low aeration: 50 ml in 250 ml Erlenmeyer flasks) and oxidative stress (4 days growth in 1 mM  $\text{H}_2\text{O}_2$ ) on carotene production by wild type cells grown as submerged cultures in minimal medium.

UM06287 and UM04210, respectively. The three *U. maydis* genes were named *car1*, *car2* and *car3*, following the *al-1*, *al-2* and *al-3* *N. crassa* terminology (Fig. C5.1).

Clustal alignments of the predicted Car1, Car2 and Car3 proteins showed different degrees of homology to their orthologs from three different fungal classes (Fig. C5.4). GGPP synthases from ascomycetes, zygomycetes and basidiomycetes showed considerable structural divergence, but the six proteins included in the analysis contained highly conserved internal domains.

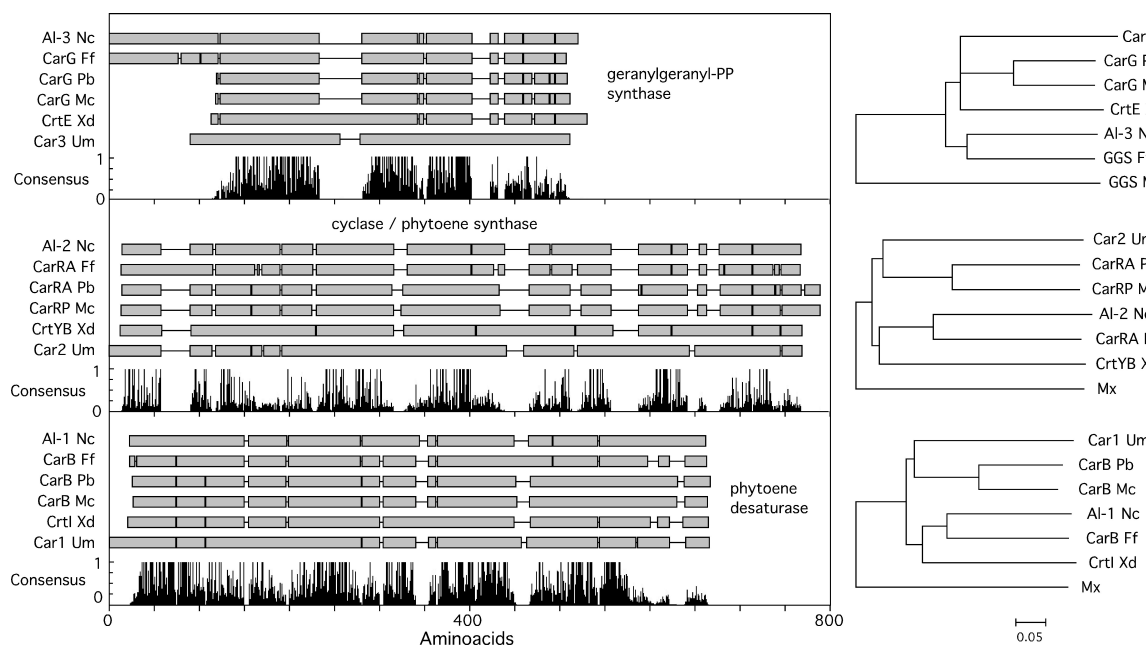


**Fig. C5.4. Sequence analysis of the *U. maydis* predicted proteins Car3 (UM04459), Car2 (UM06287) and Car1 (UM04210).** A. Simplified representation of the Clustal comparison between the three Car proteins and their respective counterparts in five representative fungi. Geranylgeranyl PP synthases: AL-3 from *N. crassa* (accession number P24322), CarG from *F. fujikuroi* (X96943), *P. blakesleeanus* (33722) and *M. circinelloides* (CAB89115), and CrtE from *X. dendrorhous* (AAY33921). Cyclases / phytoene synthases: AL-2 from *N. crassa* (L27652), CarRA from *F. fujikuroi* (AJ426417) and *P. blakesleeanus* (CAB93661), CarRP from *M. circinelloides* (AJ250827), and CrtYB from *X. dendrorhous* (AAO47570). Phytoene desaturases: AL-1 from *N. crassa* (P21334), CarB from *F. fujikuroi* (AJ426418), *P. blakesleeanus* (P54982), and *M. circinelloides* (CAB40843) and CrtI from *X. dendrorhous* (CAA75240). Breaks between the boxes represent gaps introduced by the Clustal program to facilitate alignment. Lower diagrams plot the presence of consensus aminoacids. B. Phylograms of the proteins displayed on the left graph. Orthologous proteins from *Myxococcus xanthus* (Geranylgeranyl PP synthase, CAA79955; phytoene synthase, CAA79957; phytoene dehydrogenase, M94727) were used as outgroups.

The structures of these enzymes were very similar in each taxonomic group, except those from *U. maydis* and *X. dendrorhous*, which differed markedly. At amino acid level, the ascomycete and zygomycete GGPP synthases were highly related to each other (about 50% of identical positions), with the exception of N-terminal extensions only found in the ascomycete enzymes. The phytoene synthases/carotene cyclases and phytoene desaturases from the six species showed higher overall structural similarity than GGPP synthases (Fig. C5.4). However, the carotene cyclase/phytoene synthases, especially those from *X. dendrorhous* and *U. maydis*, exhibited lower sequence conservation. Taken together, sequence comparisons strongly indicate the occurrence of the complete set of genes required for  $\beta$ -carotene biosynthesis in *U. maydis*. Moreover, phylogenetic analyses of the deduced amino acid sequences show that the *U. maydis* enzymes are more related to their zygomycetes than to their *X. dendrorhous* or ascomycetes counterparts (Fig. C5.4).

## 2.4 The *U. maydis* enzyme Cco1 catalyzes retinal synthesis in vitro

The *U. maydis* genome encodes three putative photoactive opsins (Brown 2004) that imply the ability to synthesize the chromophore, retinal. In the ascomycete *F. fujikuroi*, retinal is synthesized via symmetrical cleavage of  $\beta$ -carotene, which is catalyzed by the carotenoid cleavage oxygenases CarX (Prado-Cabrero et al., 2007b). To identify an ortholog, blast analyses of the *U. maydis* proteome were performed, revealing the putative carotenoid oxygenase, UM00965, termed here as carotene cleaving oxygenase 1 (Cco1). Comparison of Cco1 with CarX or with the human retinal-forming enzyme  $\beta$ -carotene oxygenase I (BCMO 1; accession no. Q9HAY6) showed significant overall conservation (Fig. C5.5). The two fungal proteins are larger (696 aa for CarX and 787 aa for UM00965 against 547 aa for BCMO1) and are, as expected, more similar to each other (310 identical positions) than to BCMO1, sharing 92 and 97 identical amino acids with CarX and Cco1, respectively. To confirm the Cco1 activity as a retinal-forming,  $\beta$ -carotene-cleaving enzyme, the corresponding cDNA was cloned by RT-PCR. Cco1 was then expressed in *E. coli* cells as a GST-fusion, purified using glutathione-sepharose and released by the protease factor Xa (Fig. C5.6). *In vitro*-incubation with  $\beta$ -carotene resulted in the formation of a product, which exhibited an UV/Vis spectrum and a chromatographic behavior identical to those of retinal standard. The nature of the product was further confirmed by LC-MS analysis (data not shown).

## 2.5 *U. maydis* $\beta$ -carotene content is determined by Cco1

To investigate the function of Cco1 in *U. maydis*, we generated solopathogenic SG200 strains deleted for the *cco1* gene (hereafter  $\Delta cco1$ ) or expressing an additional ectopic copy of the gene under the control of the constitutive *o2tef* promoter (hereafter *cco1*<sup>con</sup>) (Spellig et al., 1996). Haploid SG200 strains can infect maize plants without the requirement for mating and cell fusion.

To analyze transcriptional regulation of *cco1* and confirm *cco1* overexpression in *cco1*<sup>con</sup> strains we performed quantitative real time PCR analyses. *cco1* mRNA levels were similar at pH 3 and pH 7 when prepared from cells incubated in the dark. However, a three fold induction in *cco1* expression was detected upon illumination at acidic pH, while at neutral pH hardly any light induction could be observed (Fig. C5.7A).

```

Cco1      MVKGSSNRQRHSASLQGLPSSQHCAPVISIPSPPPPAEDHAYPPS
Cco1      SFTIPLSKDEELAEAGPSRPGSSAISRRPVLSRRRTSKKEYVHPY
CarX      MKFLQQNSFTQTSMSP--HEDVS--PAIR-----HPY
BCMO1     MDI

Cco1      LSGNFAPVTTECPLTDCLFEGTIPEEFAGSQYVRNGGNPLANSER
CarX      LTGNFAPIHKTNNLTPTCTYSGCIPPELTGGQYVRNGGNPVSHQDL
BCMO1     IFG--RRNRQQLPEPVRAKVTGKIPAWLQG-TLLRNGPG-MHTVGE

Cco1      DRDAHWFADAGMLAGVLFRRTP-KGTIQPCFLNRFILTDLLSTP
CarX      GKDAHWFADGMLSGVAFRKASIDGKTIPEFVNQYILTDLYLSRK
BCMO1     SRYNHWFDGLALLHSFTIRDG-----EVYYSKYLRSDTYNTNI

Cco1      EHSR-LPYVPSIATLVNPHTSVFWLLCEIIRTFVLAMLTWLPGLG
CarX      TTSIASPIMPSITTLVNPLSTMFQIMFATFRITFLVILSNLP---
BCMO1     EANRIVSEFGTMAYPDECKNIFSKAFSYLSHTIPDFT-----

Cco1      LGGNQKLKRISVANTSVFWDHGKAMAGCESGPPMRIMLPGLTAG
CarX      -GSQQAIKRISVANTAVLYHDGRALATCESGPPMRIQLPSLDTVG
BCMO1     -----DNCLINIMKCGEDFYATSETNYIRKINPQTLLETLE

Cco1      WYTGEEDKEKETCDKNSGNSLTSSSSKGGGGPPIVSMLEFRTTA
CarX      WFDGVEAEAGE-----PEISQAGSDDSPFGG-SGIFSMKEWTTG
BCMO1     KVDYRKYVAVN-----LATSHPHYDEAGN-----VLNMG

Cco1      HPKIDPRTOELLLYHMCFEPPYLRLSVIPASQSKKTDLPAAKTI
CarX      HPKVDPTVTEMLLYHNTFMPPYVHCSVLPKSNEK-----APGHRLL
BCMO1     TSIVEKGKTKYVIFKIP-----ATVPEGKQKQKSPWKHTEVF

Cco1      KGKAVRGLKQPKMMHDFGATATQTVIIDVPLSLDMMNLVRG----
CarX      VNQPVLGVSARMHDFGASRSHITIMDLPLSLDPLNTMKG----
BCMO1     CSIPSRSLLSFSYYHSFGVTENYVIFLEQPFRLDILKMATAYIRR

Cco1      ---KPIHLYDPSQPTRFGILPRYEPERVRWYSAEACCIYHTANS
CarX      ---KEVVADPTKPSRFGVFPRLPSSVRWFHTAP-CCIFHTANT
BCMO1     MSWASCLAFHREKTYIHIIDQRTQRPVQTKFYTDAMVVFHVNNA

Cco1      WDDDGKFDASHEHATRSAIRGVNMLGCRLNSATLVYSAGNLLPPS
CarX      WDSQ-----SSEGELSVNLLACRMTSSTLVYTAGNIRPPV
BCMO1     YEED-----GCIVFDVIAYEDNSLYQLFYLANLNQDF

Cco1      -----HVLPPNCP-----
CarX      RSRCTQARVWSDEREETACRYKEAPALESPGESTGLADYFPITAE
BCMO1     K-----

Cco1      ----EKCOLYYWRFDLHAETNTISHEFALSDIPFEFPTINEDYS
CarX      SDDYDQCRLYYYEFDLAMESRNHVKSQWALSAIPFEFPSVRPDRE
BCMO1     ----ENSRLTSVPTLRRFAVPLHVDKNAEVTNLIKVASTTATAL

Cco1      MQQACYVYGTSMRDGTFDAGLGKAAKIDALVKLDAQALIRKGKAM
CarX      MQEARYIYGCTSTSTSCFGVALGRADKVDLLVKMDAKTLIQRGKKM
BCMO1     KEEDGQVY---CQPEFLYEGLELPRVNYAHNGKQYRYVFATGVQW

Cco1      WSQGRLLKAGDSVDTRTVEEVLTQORDGSASPEDPIKIFEMPRGWY
CarX      NATS---ITGCVDRRSVCEILQEQRK-----DDPIYIFRLPPNHY
BCMO1     SPIP---TKI IKYDILT KSSLKWR-----DDCW

Cco1      AQETTFVPRRSSTNETSQEDDGWLVCYVFDEATGLHPSTGEVLP
CarX      AQEPRFVPACST---EEDDGYLIFYVFDESQ-LLPS-GDCPPS
BCMO1     PAEPLFVPAPGAK---DEDDGVILSAIVSTDP-----Q

Cco1      ASSELWIIDAKLMSRVVCRIKLPQRPVYGLHGTFTTEEQTASQKP
CarX      ATSELWILDAKNMRDVVAKVRLPQRPVYGLHGTWFSSQDIESQRS
BCMO1     KLPFLLILDAKSFT-ELARASVDVDMHMDLHGLFITDMDWDTKKQ

Cco1      IDPSQVRSWALSINLADPFSSSALGSTVYSAGKAATSKFKNREE
CarX      VES--LRSLEVVRKKEEWVNSGG-----
BCMO1     AASEEQDRASDCHGAPLT

Cco1      TYAAFIKDPTRIGAWVVKRNIELLIA
CarX      -----QIRKSWMLREKLEKAVG

```

**Fig. C5.5.** CLUSTAL alignment of the predicted Cco1 protein with  $\beta$ -carotene dioxygenases CarX (AJ854252, *F. fujikuroi*) and BCMO1 (Q9HAY6, *H. sapiens*). Residues present at the same position in at least two proteins are shaded.

Expression of *cco1* under control of the *o2tef* promoter resulted in a seven fold increase in its mRNA levels and this was further increased by light irrespective of the culture pH, clearly demonstrating that the ectopic *cco1*<sup>con</sup> allele results in overexpression of the gene. Interestingly, *cco1* mRNA levels in the *cco1*<sup>con</sup> strain were further induced by light (Fig. C5.7A). At pH 3 this can at least in part be attributed to the light induced expression of the

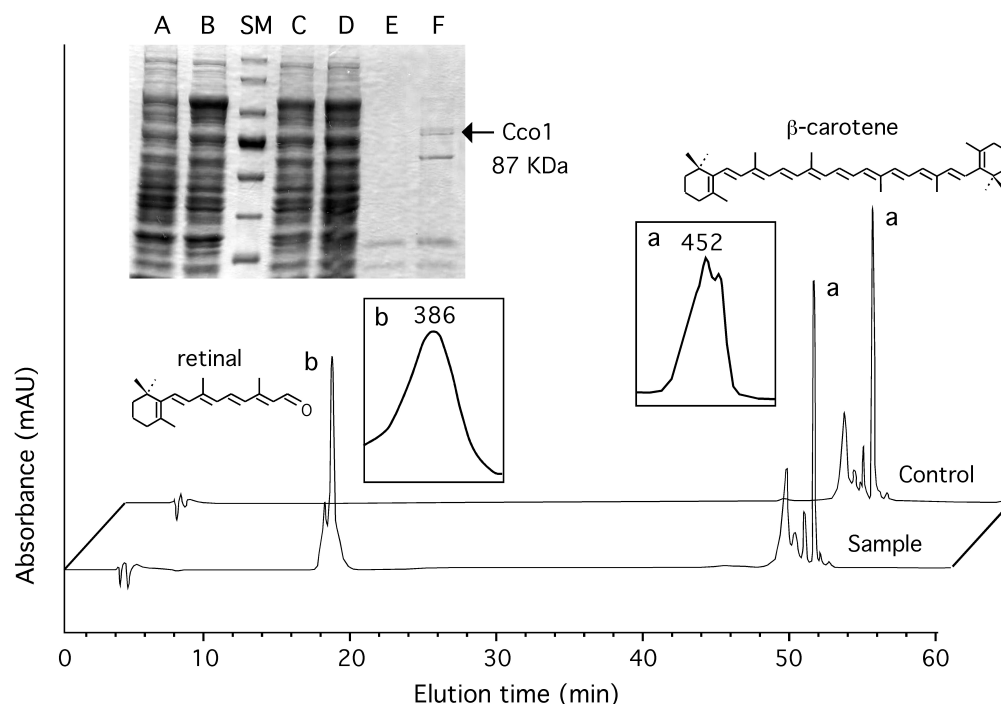


**Fig. C5.6. In vitro Cco1 activity on  $\beta$ -carotene.** HPLC analysis of the in vitro assay products obtained after incubation of purified Cco1 protein with  $\beta$ -carotene. Inner boxes show UV-visible light spectra of peaks a and b. The picture shows a coomassie-stained SDS gel showing GST-Cco1 purification. Lanes: A, total lysate of cells expressing GST (control); B, total lysate of cells expressing GST-Cco1; C, sample B after removal of inclusion bodies; D, non binding supernatant of sample C; E, elution fraction of the control; F, protein sample of eluted GST-Cco1.

native *cco1* gene, which is present in addition to the ectopic *cco1*<sup>con</sup> allele in this strain.

We determined the effects of the *cco1* deletion and overexpression on cellular  $\beta$ -carotene content. Cell pellets from cultures of  $\Delta cco1$  strains exhibited a deeper yellow pigmentation than those of the SG200 wild type (Fig. C5.7B), and contained more  $\beta$ -carotene irrespective of illumination (Fig. C5.7C). In contrast to the wild type, which produced about two-fold less  $\beta$ -carotene at pH 3 than at pH 7 ( $\sim 15$ - $20 \mu\text{g/g}$  and  $\sim 35 \mu\text{g/g}$  dry weight, respectively; Fig. C5.7C), the amount of  $\beta$ -carotene accumulated by the  $\Delta cco1$  strains was similarly high at both pH conditions ( $\sim 50 \mu\text{g/g}$ ; Fig. C5.7C). Consequently, the difference to the wild type was higher at pH 3 than at pH 7. Consistently, analyses of the *cco1*<sup>con</sup> strains revealed a much paler pigmentation of the cell pellets than the control strain (Fig. C5.7B) and accordingly, showed drastically reduced  $\beta$ -carotene contents, irrespective of light and culture pH (Fig. C5.7C). These *in vivo* findings are in perfect agreement with the demonstrated *in vitro* function of the heterologously expressed Cco1 enzyme as a  $\beta$ -carotene cleaving dioxygenase. The higher  $\beta$ -carotene accumulation in the  $\Delta cco1$  mutants can be explained by the lack of  $\beta$ -carotene conversion in the absence of *cco1*. Likewise the strongly reduced  $\beta$ -carotene content in *cco1*<sup>con</sup> strains can be explained by the almost

complete conversion of the  $\beta$ -carotene precursor to retinal by action of the overexpressed Cco1 dioxygenase.

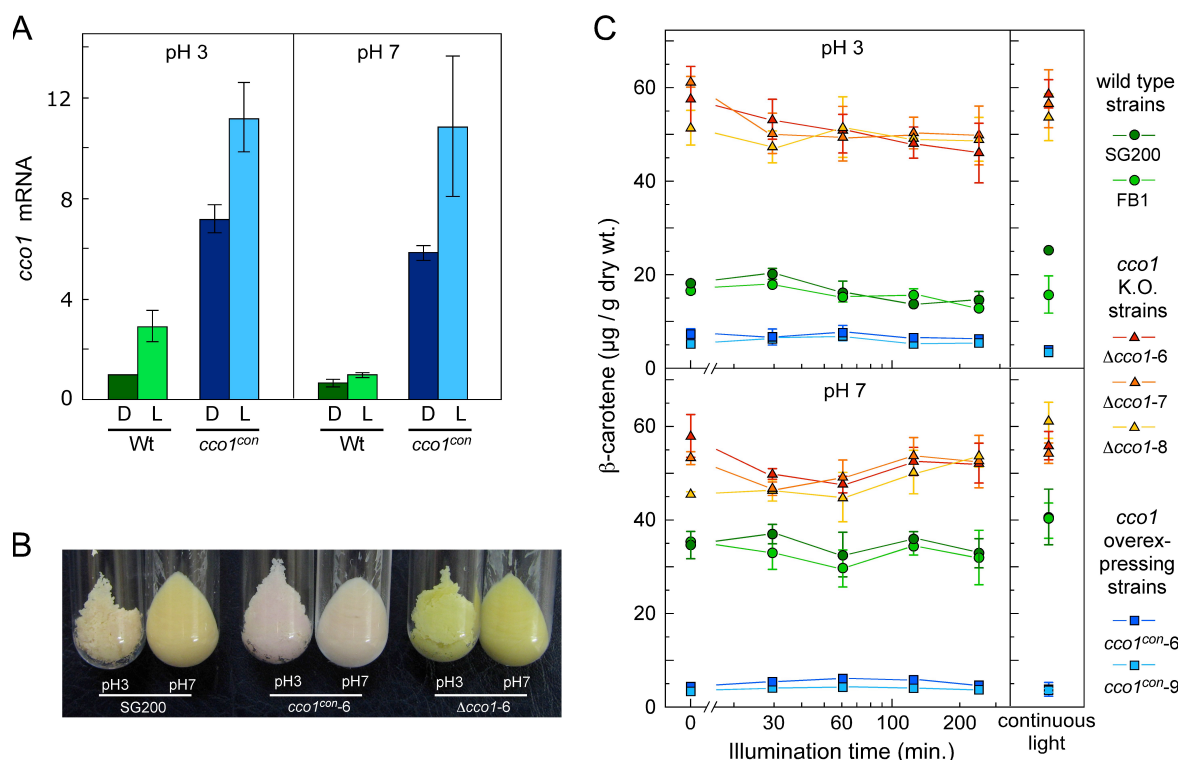


**Fig. C5.7. Effect of alteration of gene *cco1* on  $\beta$ -carotene production.** A. Real-time RT-PCR analyses of *cco1* mRNA in the wild type and *cco1<sup>con</sup>* strain from cells grown in the dark or following 30 min illumination. B. Pellets from cultures of  $\Delta cco1$  and *cco1<sup>con</sup>* strains grown in the dark at the indicated pH. C. Carotene accumulation by the same strains in the dark, following illumination for the indicated times or under continuous light.

## 2.6 Retinal is not found in *U. maydis* $\Delta cco1$ mutants

To confirm the function of Cco1 in *U. maydis*, retinal contents of wild type and mutant cells were determined. For this purpose, a formaldehyde-based extraction protocol was developed, which allowed the isolation of free and protein-bound retinal. HPLC analyses of wild type cell extracts grown at pH 7 indicated the occurrence of retinal, as suggested by its UV-Vis spectrum and elution time (Fig. C5.8). Slight variations in maximal absorption values suggest the occurrence of a *cis*-retinal isomer, distinct from commercial all-trans retinal used as a control. As expected, retinal was also found in the samples from *cco1<sup>con</sup>* strains. However, the amounts were similar to those determined in the wild type. The total amount estimated in both strains,  $\sim 6 \mu\text{g g}^{-1}$  dry wt, was much lower than that of  $\beta$ -carotene under the same culture conditions,  $\sim 120 \mu\text{g g}^{-1}$  dry wt. This result suggests that the content of this compound is not only determined by the Cco1 cleaving activity, but also by retinal degradation or metabolization, which could specially

affect to excess free retinal. Noticeably, retinal was not detected in the  $\Delta cco1$  strain, supporting the biological role of Cco1 as the retinal-forming enzyme in *U. maydis*.

### 2.7 *car* and *ops* genes are differentially regulated

Analyses of the Cco1 transcript levels revealed an induction upon illumination at pH3. To check the possible correlation between the transcript levels of Cco1 and  $\beta$ -carotene synthesis genes, real-time RT-PCR analyses of the phytoene desaturase gene *car1* were performed, using mRNA isolated from wild type and Cco1 mutants grown under different conditions.

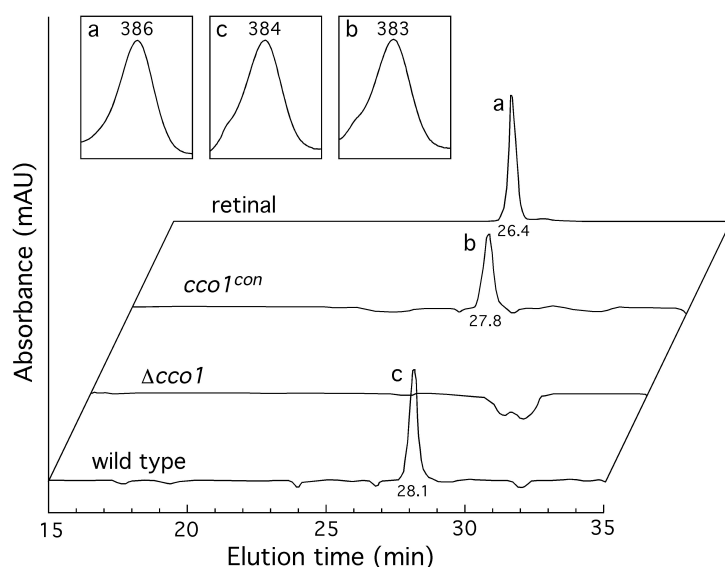


**Fig. C5.8. Detection of retinal-like compounds in *U. maydis*.** HPLC analysis of a all-*trans* retinal standard and cell extracts from wild type,  $\Delta cco1$  and *cco1*<sup>con</sup> strains. Only the relevant segment of the HPLC profile is shown. Inner boxes show UV-visible light spectra and maximal absorption wavelengths of labeled peaks.

As shown in Fig. C5.9, *car1* mRNA exhibited a three-fold increase after 30 min illumination of cells grown at pH 3, while such effect was not manifest at pH 7. Analyses of the *cco1*<sup>con</sup> strain grown at pH 3 revealed a slight induction of *car1* mRNA upon illumination. In contrast, the three  $\Delta cco1$  mutants did not show significant changes under the same conditions. The lack of induction in the  $\Delta cco1$  strains may be rather explained by their increased *car1* mRNA levels in the dark. The deregulation of *car1* in the  $\Delta cco1$  strains may be a result of the absence of retinal, suggesting an end-product feed-back inhibition of the carotenoid pathway. The availability of the chromophore, retinal, may affect the expression of the three opsin genes found in the *U. maydis* genome (Brown 2004), named here as *ops1* (UM02629), *ops2* (UM00371) and *ops3* (UM04125). To check this hypothesis, real time RT-PCR analyses of the opsin genes were performed. The transcript levels of *ops1* and *ops2* were sufficiently abundant, allowing reliable detection.



In contrast, no *ops3* mRNA levels could be detected in the same mRNA samples, albeit the usage of two different primer sets. Therefore, we concluded that *ops3* is not expressed under the standard culture conditions used in this work. The amounts of *ops1* and *ops2* mRNA were not significantly affected, neither by the pH nor by deletion or overexpression of *cco1* in the corresponding mutants. However, the *ops1* and *ops2* transcript levels

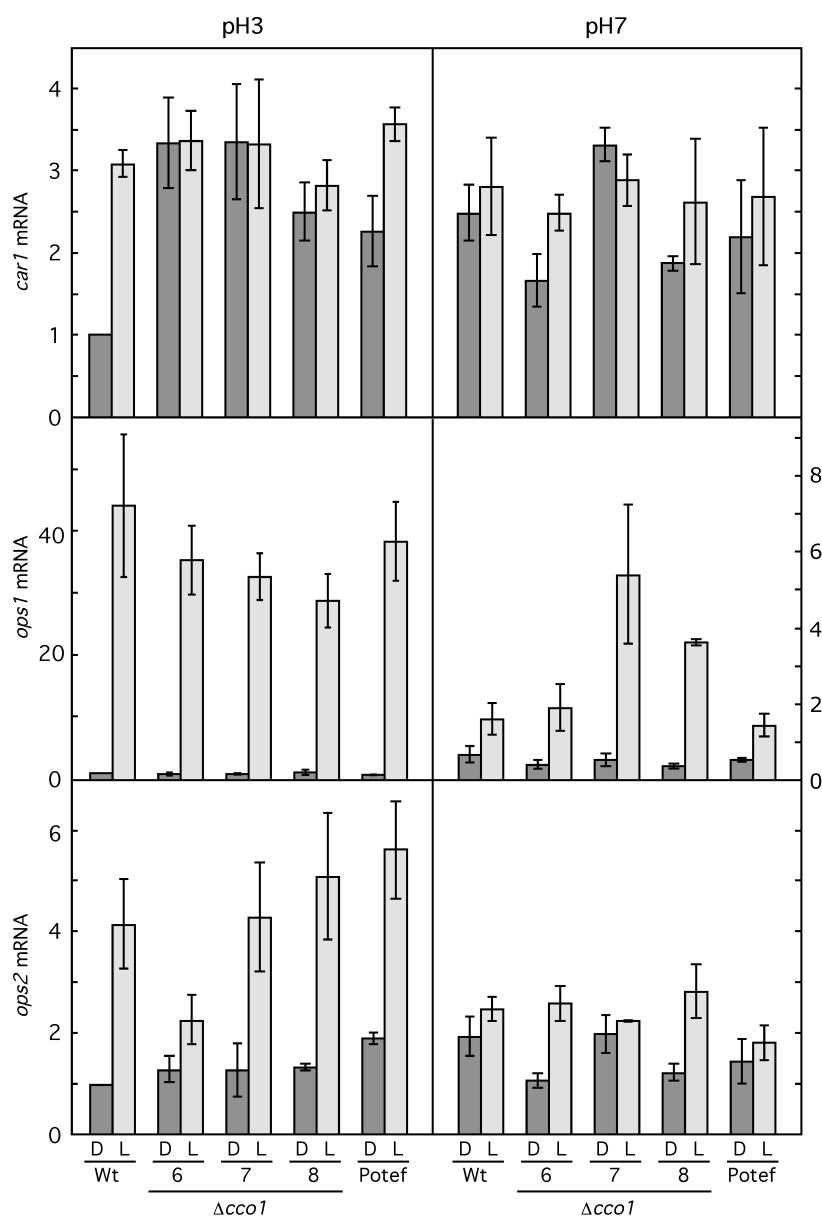


**Fig. C5.9. Effect of *cco1* deletion and overexpression on *car2*, *ops1* and *ops2* gene expression.** Real-time RT-PCR analyses from RNA samples of the wild-type strain, three  $\Delta cco1$  mutants and the *cco1*<sup>con-6</sup> strain displayed in Fig. C5.7. The cells were grown in the dark (D) or illuminated during 30 min before RNA extraction (L). Data represent average and standard deviations for four determinations from two independent experiments. To improve visualization, scale was enlarged for *ops1* mRNA samples at pH 7. Relative mRNA levels for each gene are referred to the value from non-illuminated wild type mycelia in each experiment.

increased about 40- and 4-fold, respectively, upon illumination at pH 3. The induction of both genes by light was severely reduced at pH 7, although it was still apparent in the case of *ops1*. The regulatory effect of light on *ops1* and *ops2* mRNA levels was not significantly affected by disruption of *cco1*, although a higher light induction of *ops1* was apparent at pH 7 in two of the  $\Delta cco1$  mutants. Taken together, the real time RT-PCR analyses of *ops1* and *ops2* indicate that the expression of these genes is not significantly affected by retinal availability.

### 3. Discussion

Accumulation of carotenoids is common in different taxa, including fungi (Avalos and Cerdá-Olmedo 2004; Sandmann and Misawa, 2002) that represent preferred sources for the biotechnological production of these compounds. Here we report that the biotrophic plant pathogen *U. maydis* accumulates moderate amounts of  $\beta$ -carotene, which is responsible for the pale yellow pigmentation exhibited by their cell pellets. The finding of  $\beta$ -carotene in *U. maydis* is not surprising, since different strains of another *Ustilago* species, *U. violacea*, were shown to accumulate carotenoids (Will et al., 1984). The synthesis of  $\beta$ -carotene implies the occurrence of the corresponding genes. Indeed, the *U. maydis* genome encodes orthologs of fungal carotene biosynthesis enzymes. The presumptive phytoene desaturase, lycopene cyclase /phytoene synthase and geranylgeranyl pyrophosphate synthase, encoded by the *U. maydis* genes *car1*, *car2* and *car3*, show unequivocal sequence and structural similarities to formerly investigated fungal enzymes.

Our phylogenetic analyses place the *U. maydis* enzymes closer to the orthologs from zygomycetes than to those from ascomycetes or even to those from the basidiomycete *X. dendrorhous*. The zygomycete species considered, *P. blakesleeanus*, *M. circinelloides* and *B. trispora*, coincide with *U. maydis* in accumulating  $\beta$ -carotene as the major carotenoid, produced from phytoene via four desaturation and two cyclization reactions. In contrast, the ascomycetes *F. fujikuroi* and *N. crassa* accumulate the acidic apocarotenoid neurosporaxanthin, produced from phytoene via five desaturation reactions, a single cyclization step and an asymmetrical cleavage reaction, achieved by a carotene oxygenase (Prado-Cabrero et al., 2007a; Saelices et al., 2007). To our knowledge, *Ustilago* is the only basidiomycete described so far accumulating  $\beta$ -carotene as the sole carotene. The other investigated *Ustilago* species, *U. violacea*, contains a carotene mixture, consisting of  $\beta$ -carotene and variable precursor amounts, depending on the strain investigated (Will et al., 1984). The second basidiomycete included in our analysis, *X. dendrorhous*, accumulates astaxanthin (Johnson 2003), a xanthophyll produced from  $\beta$ -carotene through hydroxylation and ketolation reactions. Both enzymatic activities have been attributed to a single enzyme from the cytochrome P450 monooxygenase family (Alvarez et al., 2006;

Ojima et al., 2006). The *U. maydis* genome contains several genes from this protein family and an eventual enzymatic activity introducing similar  $\beta$ -carotene modifications under different growth conditions can not be discarded. Other basidiomycete yeasts, i.e. *Rhodotorula minuta* (Buzzini et al., 2007), synthesize torularhodin, a carboxylic carotenoid produced from torulene (Frengova and Beshkova 2008), implying the ability of its phytoene desaturase to carry out five desaturation steps. This trait is also exhibited by the CrtI enzyme from *X. dendrorhous*, in which the carotenoid pathway includes a side branch leading to torulene production (Visser et al., 2003). Nonetheless, appropriate mutations allow the predominant accumulation of  $\beta$ -carotene in naturally xanthophyll-producing yeasts, as shown in *X. dendrorhous* (Johnson 2003) and *R. minuta* (Bhosale and Gadre 2001).

Photoinduction of carotenoid biosynthesis is a widespread trait in carotenogenic fungi (Avalos et al., 1993).  $\beta$ -carotene accumulation in *U. maydis* was not induced by light at either of the two pHs investigated. However, a moderate photoinduction was exhibited at pH 3 by *car1* mRNA, used here as control for a structural gene of the *U. maydis*  $\beta$ -carotene pathway. A similar result was obtained in *B. trispora*: mRNA levels for the structural genes of its  $\beta$ -carotene pathway are transiently induced by a short light pulse, but the total carotene content is lowered under permanent illumination (Quiles-Rosillo et al., 2005). In the basidiomycetes group, *U. maydis* resembles *X. dendrorhous* in the lack of photoinduction of astaxanthin biosynthesis (An and Johnson 1990), but contrasts with *Rhodotorula glutinis*, whose  $\beta$ -carotene and torularhodin contents increase under illumination (Sakaki et al., 2001).

The *U. maydis* genome contains three genes for presumptive photoactive opsins, whose function relies on light absorption by a retinal chromophore (Spudich 2006). We identified a gene in *U. maydis*, *cco1*, encoding a presumptive enzyme for retinal biosynthesis. Moreover, we demonstrated that Cco1 is a carotene oxygenase that catalyzes the symmetrical cleavage of  $\beta$ -carotene to produce retinal. This conclusion was drawn from the *in vitro* activity of purified enzyme and from the correlation between Cco1 availability and  $\beta$ -carotene level *in vivo*. Furthermore, we could identify retinal in *cco-1* expressing strains but not in  $\Delta cco1$  mutants. Taken together, our data suggest retinal biosynthesis as the specific biological function for this protein, the second one described in fungi with this enzymatic activity (Prado-Cabrero et al., 2007b) and the first one in basidiomycetes. Furthermore, they suggest that the major function of  $\beta$ -carotene in *U. maydis* is the supply of retinal.

Carotenoids protect against reactive oxygen species and, accordingly, oxidative stress induces carotenoid biosynthesis in different fungi, among them *X. dendrorhous* (Schroeder and Johnson 1995; Liu and Wu 2006) and *R. minuta* (Sakaki et al., 2002). However, incubation of *U. maydis* in the presence of the highly reactive  $H_2O_2$  did not lead to changes

in carotene accumulation. In fact, *U. maydis* was more sensitive than other fungi to this oxidative agent: it did not grow at 3 mM H<sub>2</sub>O<sub>2</sub> while *X. dendrorhous* tolerates much higher concentrations (Liu and Wu 2006). H<sub>2</sub>O<sub>2</sub> sensitivity was not affected by *cco1* deletion or overexpression (results not shown), suggesting that carotene content in this fungus does not significantly contribute to reactive oxygen detoxification or tolerance. *U. maydis* possess specific H<sub>2</sub>O<sub>2</sub> detoxification enzymes, unveiled by the high H<sub>2</sub>O<sub>2</sub> sensitivity exhibited by mutants lacking the presumptive redox regulatory protein Yap1 (Molina and Kahmann, 2007). Interestingly, the *yap1* mutants exhibit a reduced virulence, indicating that oxidative stress plays a role in the plant defense mechanisms.

$\beta$ -carotene accumulation in *U. maydis* was affected by external pH, a relevant environmental signal for this fungus. Carotene accumulation was reduced under acidic conditions, which induce a developmental shift from yeast-like budding to hyphal growth (Martínez-Espinoza et al., 2004; Ruiz-Herrera et al., 1995). This reduction was probably due to different  $\beta$ -carotene degradation activities of Cco1, as indicated by the similar  $\beta$ -carotene levels in the  $\Delta cco1$  mutants at either of the two pHs investigated. Supportingly, *cco1* mRNA levels were higher at pH 3 than at pH 7. The influence of pH on  $\beta$ -carotene or retinal biosynthetic activities could be a direct regulatory effect or it could be integrated via the conserved cAMP- or MAPK pathways involved in controlling the pH-induced morphological transition (Martínez-Espinoza et al., 2004). To address this, the  $\beta$ -carotene contents in *U. maydis* strains bearing a genetically activated or disrupted cAMP- or MAPK pathway could be analysed. Furthermore, the  $\beta$ -carotene production could be monitored during biotrophic growth of the fungus *in planta*. However, this would be a technically challenging task.

Our expression analyses showed a moderate induction of *cco1* mRNA levels by light at pH 3, comparable to that showed by the gene *car1* under the same culture conditions. The modest mRNA increase, just a three-fold, contradicts the huge photoresponse showed by the mRNA of *carX*, the *cco1* counterpart in *F. fujikuroi* (Thewes et al., 2005), or by mRNAs for structural genes of the carotene pathway in other fungi (see e.g. Prado et al., 2004; Saelices et al., 2007). Cco1 induction by light at pH 3 is biologically meaningful: the needs for retinal are predictably higher because of the strong photoactivation of *ops1* mRNA under these conditions. The parallel *cco1* and *car1* photoactivation provide an explanation to the lack of effect of light on carotene content: the expected increase of  $\beta$ -carotene biosynthesis is probably compensated by an enhanced degradation to produce retinal. In support to this interpretation, the difference in  $\beta$ -carotene content between the wild type and  $\Delta cco1$  mutants was more pronounced at pH 3 than at pH 7.

The function of fungal opsins remains an unsolved problem. Targeted mutants of opsin genes did not show phenotypic alterations in *N. crassa* (Bieszke et al., 1999a) and *F. fujikuroi* (Prado et al., 2004; Estrada and Avalos 2009). Likewise, setting aside the

increased  $\beta$ -carotene content, lack of phenotypic alterations in the  $\Delta cc1$  mutants, including virulence on maize (results not shown), indicate that none of the three *U. maydis* opsins play a relevant photoactive role under laboratory conditions or during pathogenic development in the host plant. Expression experiments showed diverse regulatory patterns for the three *ops* genes in this fungus, suggesting different biological functions. Under our culture conditions, *ops1* was strongly induced after 30 min illumination, a regulation that reminds that of *carO* in *F. fujikuroi* (Prado et al., 2004; Estrada and Avalos 2009). In this case, the same regulatory pattern was exhibited by the structural genes of the carotenoid pathway, linked to *carO* in a coregulated cluster. In contrast, *ops2* exhibited only a mild photoinduction under the same conditions, reminding the regulation of *opsA* (Estrada and Avalos 2009), the second opsin gene from *F. fujikuroi*. Contrary to *ops1* and *ops2*, no *ops3* mRNA could be detected in the same RNA samples. No doubt, *U. maydis* is a promising tool in the unraveling of the biological functions of fungal opsins. Its complex life cycle, with switches from heterotrophy to biotrophy and from budding to filamentous growth, offers different biological scenarios in which light might be a key environmental signal, and where opsins might play relevant biological roles, which await to be elucidated.

## Material and methods

### 4.1 Strains and Growth conditions

*U. maydis* strains used in this study are listed in Table 1. The *Escherichia coli* K-12 derivatives DH5 $\alpha$  (Bethesda Research Laboratories) and Top10 (Invitrogen) were used for cloning purposes, and *E. coli* Rosetta (DE3) (pLysS) (Novagen) was used for protein expression.

Hygromycin B, nourseothricin (ClonNAT) and carboxin were obtained from Roche (Pensberg, Germany), the Hans-Knöll-Institute (Jena, Germany), and Riedel de Haen (Seelze, Germany), respectively. All other chemicals were of analytical grade and were obtained from Sigma or Merck.

For genetic manipulations, *U. maydis* strains were grown at 28°C in liquid CM (Holliday 1974), YEPSL (0.4% yeast extract, 0.4% peptone, 2% sucrose), or solid potato dextrose (PD) agar (2.4% PD broth, Difco). For carotenoid analyses they were grown in minimal medium (Holliday 1974), liquid or solidified with agar, either at pH7 or adjusted to pH3, or in YPD (Sherman et al., 1986). Each Petri dish was spread with 10<sup>8</sup> fresh-grown cells and incubated in the dark or under 10 W m<sup>-2</sup> of white light at 30°C. When indicated, H<sub>2</sub>O<sub>2</sub> was added after sterilization to reach a final concentration of 1 mM. For incubations in liquid medium, 10<sup>8</sup> cells were grown in a 250 ml Erlenmeyer with 50 ml of minimal medium. For improved aeration, 10 ml samples were incubated in 500 ml Erlenmeyer

flasks.

**Table I.** *U. maydis* strains used in this work.

Strain	Reference transformed	Plasmid locus	Integration strain	Progenitor
FB1 ( <i>a1 b1</i> )	Banuett and Herskowitz, 1989			
FB2 ( <i>a2 b2</i> )	Banuett and Herskowitz, 1989			
SG200 ( <i>a1:mfa2 bE1bW2</i> )	Kämper et al., 2006			
SG200Δ <i>cco1</i> #6; #7; #8	This study	pCRII-Δ <i>cco1</i> -hyg	<i>cco1</i>	SG200
SG200 <i>cco1</i> <sup>con</sup> #6; #9	This study	p123- <i>cco1</i>	<i>ip</i>	SG200

#### 4.2 Plasmid and strain constructions

Plasmid pCRII-TOPO (Invitrogen) was used for cloning and sequencing of fragments generated by PCR. Sequence analyses were performed with an automated sequencer (ABI 377) and standard informatic tools. pMF1h contains a hygromycin resistance cassette as an *SfiI* fragment (Brachmann et al., 2004). p123 is a pSP72 (Promega) derivative which contains the carboxin resistance cassette for integration into the genomic *ip*-locus of *U. maydis* and carries the *egfp* gene (Clontech) under control of the constitutive *o2tef* promoter and the *nos* terminator (Wedlich-Söldner et al., 2000).

Deletion constructs were generated according to Kämper (2004). For pCRII-Δ*cco1*-hyg, a 1.0 kb fragment comprising the 5'-flank and a 1.0 kb fragment comprising the 3'-flank of the *cco1* ORF were generated by PCR on *U. maydis* SG200 DNA with primer combinations 965-L-uni (5'-GAACGTGATTGCACAGGAAACCG-3') / 965-L-Sfi-rev (5'-GTGGGCCATCTAGGCCTATCGAGGATGTTGATGGAAGC-3') and 965-R-Sfi-uni (5'-CACGGCCTGAGTGGCCAGCTCACTTTTGTGAGGTTAGG-3') / 965-R-rev (5'-CTGTCGGTACTTCTACCGTTCAGG-3'), respectively. These fragments were then digested with *SfiI* and ligated to the 2.7 kb *SfiI* hygromycin resistance cassette from pMF1h (Brachmann et al., 2004). The resulting ligation products were cloned into pCRII-TOPO (Invitrogen). Plasmid pCRII-Δ*cco1*-hyg was subsequently used as a template to amplify the *cco1* deletion construct with primers 965-L-uni and 965-R-rev.

Plasmid p123-umc4 was constructed by replacing the 0.7 kb *NcoI*-*NotI* *egfp* ORF fragment of p123 with a 2.4 kb *NcoI*-*NotI* fragment obtained by PCR on *U. maydis* SG200 DNA using the primer set 965-NcoI-uni (5'-GCCCATGGTGAAAGGCTCGAG-TAACCG-3') / 965-NotI-rev (5'-TAGCGGCCGCTGATGGCTTAAGCAATCA-

GCAGC-3'), comprising the *cco1* ORF. The resulting plasmid p123-cco1 for integration into the genomic *ip*-locus of *U. maydis* carries the *cco1* ORF under control of the constitutive *o2tef* promoter (Wedlich-Söldner et al., 2000).

For transformation of *U. maydis*, the linear deletion construct was generated from the respective deletion plasmid pCRII-Δ*cco1*-hyg by PCR as described above. Plasmid p123-cco1 was linearized with *SspI* prior to transformation. In all cases, homologous integration events into the respective loci were verified by Southern blot analysis.

For heterologous overexpression in *E. coli*, the *cco1* gene was amplified by PCR with the primer set 5'-ATGGTGAAAGGCTCGAGTAAC-3' / 5'-GATTGCTTAAGCCA-TCAGCTC-3') and cloned into pGemT-easy (Promega) to get pGem-cco1. The gene was removed from pGem-cco1 by *EcoRI* digestion and subcloned into *EcoRI*-treated pGEX-5X-1 (Amersham Biosciences, NJ, USA) to give plasmid pGex-cco1.

#### 4.3 DNA and RNA procedures

DNA and RNA manipulations were done following standard protocols (Sambrook et al., 2001). *U. maydis* transformation and DNA isolation were performed as previously published (Hoffman and Winston 1987, Schulz et al., 1990, respectively). For Southern blot analyses the *cco1* deletion construct or a 0.7 kb *cbx* fragment were labeled with the PCR DIG-labeling Mix according to manufacturer's instructions (Roche, Mannheim). Hybridization and detection by alkaline phosphatase-coupled anti-DIG-antibodies using CDP-Star as chemiluminescence substrate were carried out according to manufacturer's instructions (Roche, Mannheim).

#### 4.4 Expression analyses

RNA samples were isolated using Trizol (Invitrogen, USA) following manufacturer recommendations. The samples were treated with DNAase to avoid DNA contamination. RT-PCR expression analyses were performed using total RNA samples as template. The reactions, carried out in 25 µl volumes with an ABI 7500 (Applied biosystems), consisted of a 30 min retrotranscription step at 48°C, 10 min at 95°C and 40 cycles of 95°C denaturation for 15 s and 60°C polymerization for 1 min. Dissociation curves were achieved afterwards. Genes and primer sets for the RT-PCR reactions, chosen with the software Primer Express™ v2.0.0 (Applied Biosystems) were *car1*, (5'-GGCCATGGTC-GGTGTCATG-3' / 5'-CAAGCCTAGCAAGATGAATG-3'), *ops1* (5'-GTCGTATCCGAGCTGCTGAAG-3' / 5'-GTAATGTCGATGTCAGCGAC-3'), *ops2* (5'-GGCTTCTCGCTGCTCTTCTTC-3' / 5'-GGTGTGCATGAGGCGGTAAC-3'), *ops3* (two primer sets: 5'-TCGGAAGAAGACAGCGATGTAC-3' / 5'-CCAATGCGCTCG-

TGATCCTTC-3' and 5'-CCTGCCCAGAAAGAGGAGAA-3' / 5'-CGAGATGGTGGA-GATTGCAA-3'), and *cco1* (5'-CCACCCGCTTCGGAATTT-3' / 5'-TCCGCGCTTTCGTACCAA-3'). Optimized RTPCR conditions were described before (Estrada and Avalos., 2008). The actin gene UM06217 (5'-GAGCGAGGCTACCC-CTTCA-3' / 5'-GAGCTTCTCCTTGATGTCACGAA-3') was used as control for constitutive expression. Relative gene expression was calculated with the  $2^{\Delta\Delta CT}$  method with the Sequence Detection Software v1.2.2 (Applied Biosystems). Each RTPCR analysis was performed four times (duplicated samples from two independent experiments) and standard deviations calculated to ensure statistical accuracy. Primers (HPLC grade) were synthesized by StabVida (Oeiras, Portugal).

#### 4.5 Carotenoid analyses

Cell samples were frozen, lyophilized and weighed prior analysis. Carotenoid extractions were performed as described by Saelices et al. (2007).  $\beta$ -carotene concentrations were calculated from absorption spectra in hexane (Davies 1976).

For retinal analysis, lyophilized cell samples were homogenized with 425-600  $\mu$ m glass beads (Sigma) in 20% formaldehyde (15 cycles of 1 min vigorous vortexing and 30 s in ice). Then one volume of methanol was added and the mixtures were incubated under shaking for 20 minutes. The retinal containing fraction was recovered by partition with light petroleum.

HPLC separations were performed in a Waters system (Eschborn, Germany) equipped with a photodiode array detector (model 996) and a C30-reversed phase column (YMC Europe, Schermbeck, Germany) or in a Hewlett Packard 1100 series system (Waldbronn, Germany) equipped with a photodiode array detector and a C30 column (ProntoSIL, 250 x 4.6 mm i.d., 5  $\mu$ m), using the solvent systems A (MeOH/ tert-butylmethylether, 1:1, v/v), and B (MeOH/ tertbutylmethylether/ water, 30:1:10, v/v/v). Either of both columns were developed at a flow rate of 1 ml min<sup>-1</sup> with a linear gradient from 100% B to 57% A 43% B within 30 min, followed by a linear gradient to 100% A with the same flow rate within 10 min. The flow was then increased to 2 ml min<sup>-1</sup> of 100% A maintaining these conditions for 10 min. All trans retinal standard was obtained from Sigma.  $\beta$ -carotene was extracted from mycelia of wild type *P. blakesleeanus* NRRL1555 and purified by TLC (DC-Plate F<sub>254</sub> in light petroleum: diethyl ether: acetone [40:10:7; v/v/v]).

#### 4.6 Enzymatic assays

BL21 *E. coli* cells were transformed with pGex-cco1. The transformed cells were



grown, induced with 0.1 mM IPTG, and the protein was purified as described by Ruch et al. (2005). To produce micelles, about 50 mM of the substrates were mixed with 50  $\mu$ l of 4% (v/v) octyl- $\beta$ -glucoside in ethanol and dried in a vacuum centrifuge or in an ethanolic detergent mixture consisting of 0.7% (vol/vol) Triton X-100 and 1.6% (vol/vol) Triton X-405. The resulting gel was carefully resuspended in 100  $\mu$ l of an incubation buffer consisting of 200 mM HEPES-NaOH, pH 8.0, 2 mM TCEP (Tris 2-carboxy-ethylphosphine hydrochloride) obtained from Sigma-Aldrich (Deisenhofen, Germany), 0.4 mM FeSO<sub>4</sub> and 2 mg ml<sup>-1</sup> catalase (Sigma-Aldrich, Deisenhofen, Germany). The assays were performed as described by Prado-Cabrero et al. (2007b). Protein concentration was determined using the BioRad protein assay kit (BioRad, Hercules, CA). Incubations were done at 28°C for 2 h, stopped by addition of 1 volume acetone, extracted with light petroleum/diethylether (1:4, v/v) and subjected to HPLC analyses.  $\beta$ -carotene was quantified spectrophotometrically at their individual  $\lambda_{\text{max}}$  using extinction coefficients as given by Barua and Olson (2000) or Davies (1976). The products obtained from the assay were run directly in the HPLC as described above.

#### *4.7 Pathogenicity assay*

Plant infections of the corn variety Early Golden Bantam (Olds Seeds, Madison, Wisconsin) were performed as described by Müller et al., (1999).

#### *4.8 Sequence analyses*

Blast analyses were done through the NCBI server ([www.ncbi.nlm.nih.gov/blast/](http://www.ncbi.nlm.nih.gov/blast/)). BlastP was carried out against the non-redundant Swissprot database. Alignments were achieved with the ClustalX 1.83 program (Thompson et al., 1997).

### **Acknowledgments**

This work was supported by the Governments from Spain (Ministerio de Ciencia y Tecnología, projects BIO2003-01548 and BIO2006-01323), Andalusia (project P07-CVI-02813) and Germany (German Science Foundation, DFG, Collaborative Research Center 593 and Grant AL 892/1-3). *P. blakesleeanus* mycelium was kindly provided by L. Pérez de Camino.

## **Discusión general**



## Discusión general

Los hongos filamentosos han sido excelentes modelos para el estudio de las enzimas responsables de la biosíntesis de carotenoides y su regulación (Sandmann y Misawa, 2002). Son buenos ejemplos los avances alcanzados en zigomicetos como *P. blakesleeanus*, *M. circinelloides* y *B. trispora*, que acumulan mayoritariamente  $\beta$ -caroteno, y el basidiomiceto *X. dendrorhous* y los ascomicetos *N. crassa* y *F. fujikuroi*, que producen xantofilas (Avalos y Cerda-Olmedo, 2004). El interés aplicado de los carotenoides da especial relevancia a las investigaciones sobre sus rutas biosintéticas y los mecanismos que las controlan, y en algunos hongos ha llevado a su explotación biotecnológica. Son ejemplo de ello *B. trispora* y *X. dendrorhous* (anteriormente *Phaffia rhodozyma*), empleados para la síntesis a nivel industrial de  $\beta$ -caroteno y astaxantina, respectivamente (Feofilova, 2006; Frengova et al., 2008).

La carotenogénesis ha sido estudiada en especial detalle en dos de los hongos utilizados en esta Tesis, *N. crassa* y *F. fujikuroi*. Ambas especies acumulan neurosporaxantina, una xantofila con un grupo carboxilo, infrecuente en los carotenoides. La mayoría de los genes responsables de su síntesis se conocen tanto en una especie (Schmidhauser et al., 1990; Sandmann et al., 1993; Schmidhauser et al., 1994; Saelices et al., 2007) como en la otra (Prado-Cabrero et al. 2007a; Prado-Cabrero et al. 2007b; Thewes et al., 2005; Prado et al., 2004; Linnemannstöns et al., 2002; Fernandez-Martin et al., 2000). Por el contrario, no había sido objeto de atención la síntesis de carotenoides en el tercer hongo estudiado en esta Tesis, *U. maydis*. Existía sin embargo el precedente de la acumulación de diferentes mezclas de carotenos en la especie *Ustilago violacea*, aunque no se llegó a abordar el estudio de los genes y enzimas responsables. El interés por *U. maydis* proviene de las facilidades que ofrece su manipulación molecular en el laboratorio y la disponibilidad de la secuencia de su genoma, siendo un modelo biológico de creciente importancia dentro de los hongos. Los resultados obtenidos sobre el metabolismo de los carotenoides con este organismo han iniciado una línea de investigación prometedora tanto en sus aspectos básicos como en su posible potencial aplicado.

Esta Tesis ha profundizado en el conocimiento de las rutas biosintéticas de hongos, completando la información de un modelo clásico, *N. crassa*, y abordando un modelo nuevo, *U. maydis*. Por otro lado, ha abordado el análisis funcional de dos fotorreceptores del hongo *F. fujikuroi*, la proteína ortóloga a Wc-1 y una opsina, y ha iniciado el estudio de las opsinas de *U. maydis*.

### D.1 Rutas biosintéticas de carotenoides en *Neurospora*

En los últimos años, *N. crassa* se ha convertido en un organismo de referencia en diversas áreas de investigación básica, en especial en el campo de la fotobiología y sus

conexiones con el ritmo circadiano (Dunlap et al., 2007). A causa posiblemente de las dificultades técnicas del análisis de las mezclas complejas de carotenoides acumuladas por este hongo, los estudios sobre su ruta biosintética han sido muy limitados. De esta forma, son numerosas las publicaciones en *N. crassa* en las que se hace referencia a la síntesis de carotenoides de forma global, realizando estimas de sus contenidos totales a partir del espectro de absorción de muestras crudas (ver, por ejemplo, Harding et al., 1969; Goldie y Subden, 1973a; Mitzka-Schnabel y Rau, 1980; Harding y Turner, 1981; Youssar et al., 2005).

El estudio de la síntesis de carotenoides en *N. crassa* tiene su origen en la fácil identificación de mutantes albinos, conocidos desde hace más de 60 años (Hungate, 1945), y utilizados como marcadores fácilmente rastreables. Los análisis bioquímicos de estas estirpes mostraron la ausencia de carotenoides en los mutantes *al-2* y *al-3* y la acumulación de fitoeno por los mutantes *al-1*. En combinación con datos bioquímicos obtenidos en otros organismos, los análisis de estos mutantes condujeron a la identificación de los primeros enzimas de la ruta, la sintetasa de pirofosfato de geraniogeraniol (AL-3, Nelson et al., 1989), la sintasa de fitoeno (AL-2, Schmidhauser et al., 1994) y la desaturasa (AL-1, Schmidhauser et al., 1990). A diferencia de otros grupos taxonómicos, como bacterias y organismos fotosintéticos, la actividad ciclasa se encuentra en la misma proteína AL-2, a la postre un polipéptido bifuncional. El descubrimiento de la bifuncionalidad de esta proteína (Arrach et al., 2002) tiene su origen en la demostración bioquímica de ambas actividades en la enzima ortóloga del basidiomiceto *X. dendrorhous* (Verdoes et al., 1999a).

Los pasos siguientes a las desaturaciones, que usan como primer sustrato el fitoeno, fueron durante muchos años una incógnita debido a la ausencia de mutantes que acumulen intermediarios de pasos más avanzados de la ruta. La dificultad de identificar tales mutantes fue superada mediante el empleo de técnicas adecuadas de búsqueda, en particular la iluminación a baja temperatura. En las condiciones de cultivo normalmente empleadas en el laboratorio, este hongo acumula una mezcla rica en carotenoides intermediarios, pero si se ilumina a temperaturas inferiores a 16 °C, aumenta tanto la cantidad de carotenoides acumulados (Harding, 1974) como la proporción de neurosporaxantina. Es decir, por causas aún no esclarecidas, las enzimas de la ruta funcionan más eficazmente a baja temperatura. Como consecuencia de la alta proporción del producto final al iluminar en frío, si se produce un bloqueo de la ruta se acumula el carotenoide inmediatamente anterior, es decir, el sustrato de la enzima afectada. El empleo de esta forma de cultivo permitió la identificación de dos tipos de mutantes de tonalidad rojiza, afectados en un caso en la actividad ciclasa de AL-2 (Arrach et al., 2002) y en el otro en la enzima que produce el corte oxidativo necesario para la síntesis de neurosporaxantina, que se denominó CAO-2 (Saelices et al., 2007). El carotenoide acumulado por el mutante *cao-2* fue identificado como toruleno, conocido anteriormente

por su presencia mayoritaria en un mutante equivalente en *F. fujikuroi*, aislado hace más de 20 años (Avalos y Cerdá-Olmedo, 1987) y cuyo gen fue identificado recientemente (*carT*, Prado-Cabrero et al., 2007). Sin embargo, no existía precedente que permitiera identificar el carotenoide acumulado por el mutante de la actividad ciclasa de AL-2, aunque por su comportamiento cromatográfico y su espectro de absorción se especuló con la posibilidad de que fuera la versión acíclica de la neurosporaxantina (Arrach et al., 2002).

El esclarecimiento definitivo de la ruta carotenogénica de *N. crassa* ha sido posible gracias al análisis del mutante *ylo-1* llevado a cabo en esta Tesis. Este mutante, conocido desde hace más de 35 años (Goldie y Subden, 1973), debe su nombre a la pigmentación amarilla de sus micelios y conidios. Sus primeros análisis bioquímicos mostraron la ausencia de neurosporaxantina (Goldie y Subden, 1973), y la acumulación de una mezcla de intermediarios entre los que se encontraban en mayor proporción el  $\gamma$ -caroteno y el  $\zeta$ -caroteno (Sandmann, 1993). Este patrón de carotenoides no es fácilmente atribuible a ningún bloqueo enzimático concreto de la ruta, por lo que estos primeros trabajos no proporcionaron una explicación satisfactoria. Como posibles explicaciones, se propuso un bloqueo en el corte oxidativo del toruleno o en la desaturación del licopeno, pero la ausencia de toruleno o 3,4-didehidrolicopeno en el mutante no encajaba con estas propuestas. La identificación del gen *cao-2* como responsable del corte del toruleno (Saelices et al., 2007) descartó la primera hipótesis, y el mapeo genético de la mutación *ylo-1* (Wan et al., 1997) descartó las mutaciones en el gen de la desaturasa, *al-1*, o en cualquiera de los otros genes *al*.

Las oxigenasas de carotenoides generan extremos aldehído en los extremos de sus productos apocarotenoides (Giuliano et al., 2003; Wyss, 2004; Kloer y Schulz, 2006). No sorprendió, por tanto, que el análisis de la actividad bioquímica de la oxigenasa CAO-2 no mostrara la síntesis de neurosporaxantina, sino de su versión aldehído, el  $\beta$ -apo-4'-carotenal, carotenoide no identificado previamente en *N. crassa* o en cualquier otro organismo. La conversión de este aldehído en neurosporaxantina, es decir, ácido  $\beta$ -apo-4'-carotenoico, requiere la deshidrogenación del grupo aldehído para generar el grupo ácido, reacción para la que supuestamente hace falta una nueva enzima. La posibilidad de que YLO-1 fuese responsable de esta reacción enzimática surgió como una hipótesis plausible, más aún si se tiene en cuenta que datos no publicados del T. J. Schmidhauser indicaron que el locus *ylo-1* determina una enzima de la familia de las deshidrogenasas de aldehído (Perkins et al., 2001). Esta Tesis ha sacado provecho de las distintas informaciones disponibles, (a) la secuencia del genoma, (b) el mapeo genético del gen y (c) la naturaleza química de la enzima YLO-1, para identificar un gen candidato. La confirmación de que dicho gen era realmente el genuino *ylo-1* la proporcionó el hallazgo de mutaciones en dos mutantes *ylo-1* independientes y su capacidad para complementar uno de los dos mutantes.

Las deshidrogenasas de aldehído (ALDHs) constituyen una vasta y heterogénea familia de proteínas que llevan a cabo una actividad enzimática similar sobre una gran diversidad de compuestos químicos. En todos los casos, la reacción enzimática consiste en la oxidación de un grupo aldehído (R-CHO) a un grupo carboxilo (R-COOH). Cuatro de cada cinco de las ALDHs conocidas están formadas por un único dominio funcional denominado Aldeh. El resto, entre las que se incluye YLO-1, poseen una mayor complejidad estructural, ya que combinan el dominio Aldeh con otros dominios funcionales. En el caso de YLO-1, su extremo carboxilo presenta un dominio de anclaje a membrana (dominio transmembrana o TM), una característica no carente de lógica, ya que los carotenos son moléculas hidrófobas presuntamente ubicadas en membranas, como lo están también las enzimas de la carotenogénesis investigadas (Mitzka-Schnabel y Rau, 1980). El dominio TM es muy infrecuente en las enzimas de la familia ALDH, pero no es exclusivo de YLO-1. Lo posee también un tipo de ALDH que oxida aldehídos de cadenas alifáticas para convertirlos en ácidos grasos. YLO-1 puede compartir con estas enzimas un modo de acción similar; ambas estarían ancladas en la membrana plasmática y actuarían sobre compuestos hidrofóbicos embebidos en la membrana. Entre el dominio Aldeh y el dominio TM poseen una región desestructurada que facilitaría movilidad sobre la superficie de la membrana para poder localizar y actuar sobre su sustrato.

Desde otro punto de vista, YLO-1 destaca también dentro de la familia de las ALDHs por ser una de las pocas enzimas que reconoce un carotenoide como sustrato. Se une así a las ALDHs que convierten el 9-*cis*- o el todo-*trans* retinal en ácido retinoico. La actividad enzimática de estas ALDHs es muy similar, ya que sus sustratos solo difieren en la longitud de la cadena alifática (35 carbonos del  $\beta$ -apo-4'-carotenal frente a 20 en el caso del 9-*cis*- o el todo-*trans* retinal). Sin embargo, los ensayos *in vitro* con proteína YLO-1 obtenida tras expresión en *E. coli* no mostraron actividad enzimática sobre todo-*trans* retinal. No se puede descartar que YLO-1 posea un origen evolutivo distinto, ya que la similitud de sus dominios Aldeh no es excesivamente alto (22%) y las deshidrogenasas de retinal carecen de dominio TM.

La proteína YLO-1 reconoce  $\beta$ -apo-4'-carotenal *in vitro* y lo convierte en neurosporaxantina. Cabe esperar por tanto que esta sea su actividad enzimática *in vivo*, y que los mutantes nulos del gen acumulen  $\beta$ -apo-4'-carotenal. El espectro de absorción de este compuesto en éter de petróleo, con un máximo a 485 nm, permite anticipar una pigmentación más rojiza que el típico color anaranjado producido por la neurosporaxantina (472 nm). Además, debido a que es la última enzima de la ruta, el efecto de la mutación debería ser escaso en condiciones de cultivo en las que la mayoría de los carotenoides acumulados por el hongo son intermediarios anteriores al  $\beta$ -apo-4'-carotenal. Cualquiera de estos argumentos es suficiente para no esperar que la mutación *ylo-1* produzca un cambio significativo en la pigmentación, y menos aún que este cambio se produzca hacia el color

amarillo, es decir, hacia una longitud de onda más corta. El fenotipo amarillo del mutante *ylo-1* parece indicar que la pérdida de la enzima YLO-1 interfiere en la actividad de otras enzimas de la ruta. No se puede descartar que YLO-1 posea otra función, por ejemplo, como ALDH de ácidos grasos. En apoyo a una actividad enzimática poco específica, YLO-1 es capaz de metabolizar *in vitro* otros sustratos independientemente de la longitud de la cadena alifática, como el  $\beta$ -apo-10'-carotenal (27 átomos de carbono) o incluso algún apocarotenoide que no posee un anillo en su extremo, como el apo-8'-licopenal (30 átomos de carbono). En congruencia con una segunda función, al contrario que otros genes para enzimas de la carotenogénesis, los niveles de ARNm del gen *ylo-1* apenas son influidos por la luz.

Sin embargo, las consideraciones anteriores no son suficientes para entender la base molecular del patrón de carotenoides acumulado por el mutante *ylo-1*, responsable en definitiva de su pigmentación amarilla. El fenotipo amarillo persiste cuando el mutante se incuba a baja temperatura (iluminación a 8°C de un cultivo sumergido), condiciones bajo las cuales más del 95% de los carotenoides acumulados por la estirpe silvestre es neurosporaxantina. La identificación química de los carotenoides presentes en el micelio del mutante *ylo-1* iluminado en frío, llevada a cabo tanto por HPLC como por LC-MS y usando como referencias apocarotenoides producidos por estirpes de *E. coli* adecuadamente modificadas, muestran la acumulación de apo-4'-licopenal, versión no ciclada del  $\beta$ -apo-4'-carotenal, y cantidades menores de licopeno y apo-4'-licopenol. Parece por tanto que el mutante *ylo-1* tiene mermada su actividad ciclasa, lo que puede explicar la ausencia de  $\beta$ -apo-4'-carotenal. También cabe pensar en una menor capacidad de llevar a cabo la quinta desaturación, como parece indicar la presencia de licopeno y la ausencia de su derivado pentadesaturado, el 3,4 didehidrolicopeno. Estos datos confirman que la ausencia de YLO-1 tiene consecuencias sobre otras actividades de la ruta, quizás asociadas a otra función biológica de la enzima. El desconocimiento de la base molecular de dicha interferencia, unida a los diferentes patrones de carotenoides de la estirpe silvestre en función de las condiciones de cultivo e iluminación, complican enormemente la interpretación de su fenotipo.

Una consecuencia interesante de los experimentos realizados iluminando *N. crassa* a baja temperatura es la identificación de un orden alternativo en la ejecución de las reacciones enzimáticas. En esta Tesis hemos demostrado que CAO-2 es capaz de reconocer 3,4-didehidrolicopeno como sustrato para producir apo-4'-licopenal, y que este puede ser metabolizado por YLO-1 para convertirlo en ácido apo-4'-licopenoico. Hemos confirmado además que este último compuesto es acumulado por los mutantes *al-2* carentes de actividad ciclasa, tal como se propuso originalmente (Arrach et al., 2002), lo que demuestra que los pasos enzimáticos mencionados tienen lugar *in vivo*. Si a esto se une que los mutantes YLO-1 no acumulan compuestos ciclados, llegamos a la conclusión de



que el sustrato natural de la ciclasa AL-2 es un apocarotenoide, el ácido apo-4'-licopenoico. La capacidad de AL-2 de ciclar este apocarotenoide ácido para producir neurosporaxantina es una deducción de los resultados citados, pero no ha sido aún demostrada *in vitro*. Eso no quiere decir que la enzima no sea capaz de ciclar con baja eficiencia otros sustratos, como ocurre con el 3,4-didehidrolicopeno, presuntamente ciclado para dar toruleno en los mutantes *cao-2*.

La iluminación de *N. crassa* a 30°C en las condiciones empleadas en esta Tesis (cultivos sumergidos de 200 ml en matraces de 500 ml) da lugar a la acumulación de una mezcla de intermediarios, entre los que podemos encontrar fitoeno, fitoflueno, neurosporeno,  $\beta$ -zeacaroteno,  $\gamma$ -caroteno y  $\beta$ -caroteno, y cantidades relativamente bajas de neurosporaxantina. Este patrón puede ser explicado por una termosensibilidad de la desaturasa AL-1, de tal forma que se acumulan intermediarios que pueden ser reconocidos con baja eficiencia por la actividad ciclasa. En apoyo de esta interpretación, la actividad desaturasa obtenida por expresión de *al-1* en *E. coli* es baja a 24°C pero mejora si la temperatura de incubación se baja a 18°C (resultados no mostrados). Por tanto, la baja proporción de neurosporaxantina puede tener su causa en la escasa cantidad de 3,4-didehidrolicopeno producido en estas condiciones. Interesantemente, la iluminación del mutante *ylo-1* a 30°C da lugar a una mezcla de carotenoides intermediarios similar a la observada en la estirpe silvestre pero carente de neurosporaxantina. Sin embargo, las cantidades de carotenoides producidas en estas condiciones son muy inferiores a las producidas a baja temperatura, de hecho apenas suficientes para pigmentar el micelio. Los cultivos sumergidos difieren considerablemente de los tubos de agar inclinado, en los que una gran parte de la biomasa está formada por cadenas de conidios y el grado de aireación es máximo. Por la intensidad de su pigmentación, los cultivos aéreos acumulan cantidades particularmente elevadas de carotenoides, condiciones en las que destaca especialmente la pigmentación amarilla de los mutantes *ylo-1*. Por la mayor dificultad metodológica de su manipulación, los carotenoides acumulados en micelio aéreo no han sido aún objeto de investigación.

En conclusión, el análisis de los mutantes y los estudios enzimáticos nos llevan a proponer modificaciones en la ruta biosintética en *N. crassa*. El orden de las reacciones vendrían determinadas por la eficiencia de la desaturasa, dependiente de la temperatura y de la disponibilidad de sustratos, ya que CAO-2 e YLO-1 son activas tanto sobre sustratos cíclicos como acíclicos. Debido a la baja eficacia de AL-1 a alta temperatura, es importante tener en cuenta que esta ruta rige solo a baja temperatura (igual o inferior a 16 °C), y que la ruta observada a la temperatura habitual de cultivo de *N. crassa* en el laboratorio es resultado del funcionamiento anómalo de dicha enzima. Es posible que el efecto de la temperatura tenga un significado biológico, permitiendo al hongo responder con eficacia a los primeros rayos del sol en las temperaturas frescas del amanecer.

Al contrario que en *N. crassa*, la ruta biosintética de carotenoides funciona eficazmente a alta temperatura en *F. fujikuroi*, acumulando una alta proporción de neurosporaxantina. Por los carotenoides acumulados, especialmente la presencia de  $\beta$ -zeacaroteno, se deduce además que la ruta sigue un orden diferente, usando como intermediarios posteriores el  $\gamma$ -caroteno, el toruleno y el  $\beta$ -apo-4'-carotenal. El último gen de la ruta, ortólogo a *ylo-1*, está siendo actualmente investigado (Violeta Díaz, Tesis doctoral en ejecución). En esta Tesis hemos dedicado la atención a los mecanismos de regulación por la luz en este hongo, en particular a las proteínas fotorreceptoras.

## D.2 La proteína WcoA de *Fusarium*

Como ya se indicó en la introducción, el primer sistema fotorreceptor identificado en hongos fue el complejo White Collar de *N. crassa*, heterodímero formado por las proteínas WC-1 y WC-2 (Linden et al., 1997a) en el que WC-1 actúa como fotorreceptor de luz azul (He et al., 2002). Este complejo es responsable de todas las fotorrespuestas conocidas en este hongo, incluyendo la fotoinducción de la carotenogénesis. El complejo White Collar (WC) ha sido descrito en otros hongos ascomicetos, así como en basidiomicetos y zigomicetos (Casas-Flores et al., 2004; Idnurm and Heitman, 2005; Idnurm et al., 2006; Silva et al., 2006), y su presencia reiterada en los genomas fúngicos apunta a un mecanismo regulador altamente conservado.

La síntesis de carotenoides es inducida por la luz también en *Fusarium*, donde se utilizó la especie *F. aquaeductuum* como modelo para llevar a cabo un estudio muy detallado de este fenómeno (ver por ej. Schrott et al., 1982). Una de las contribuciones más relevantes en este hongo fue el esclarecimiento del espectro de acción, que indica que es mediado por un fotorreceptor de luz azul (Rau et al., 1967). Posteriormente se demostró la fotoinducción de la carotenogénesis en *F. fujikuroi* y en otros dos grupos de cruzamiento del complejo *Gibberella fujikuroi* (Avalos y Cerdá-Olmedo, 1987) y se esclareció la cinética de la respuesta en esta especie (Avalos y Schrott, 1990). Teniendo en cuenta la relativa proximidad filogenética entre *F. fujikuroi* y *N. crassa*, la similitud entre sus rutas biosintéticas de carotenoides, y la conservación de los sistemas WC en hongos, se consideró altamente probable que la fotoinducción de la carotenogénesis en *F. fujikuroi* dependiera de su versión ortóloga de este complejo proteico. Como apoyo adicional a esta hipótesis, los niveles de ARNm de sus genes *car* aumentan al iluminarse el micelio (Prado et al., 2004; Thewes et al. 2005; Prado-Cabrero et al., 2007a), de forma similar a como lo hacen los genes de la carotenogénesis de *N. crassa* (Schmidhauser et al., 1990; Baima et al., 1992; Schmidhauser et al., 1994; Saelices et al., 2007). Con esta base, se decidió abordar el estudio de la función de la proteína WcoA (ortóloga de WC-1) en *F. fujikuroi*.

El análisis de los genomas disponibles de *Fusarium* (*F. graminearum*, *F. verticillioides*, y *F. oxysporum*) muestra un único gen candidato a *wc-1*. La proteína

codificada posee una estructura muy similar a la de WC-1, con los dominios PAS y el dedo de zinc en las mismas posiciones. De hecho WcoA es más similar a WC-1 que otras proteínas ortólogas de otros hongos. Por ejemplo, WcoA coincide con WC-1 en la presencia de un dominio poliglutamina en su extremo amino, ausente en otras versiones ortólogas. Sin embargo, a partir de ahí solo hemos encontrado diferencias. La primera alude a la propia regulación de *wcoA*. En *N. crassa* los niveles de ARNm de *wc-1* se inducen por la luz, aunque la inducción es transitoria (Ballario et al., 1996). Sin embargo, en *F. fujikuroi* los niveles de ARNm de *wcoA* no se ven afectados por la luz. Este hecho no es novedoso, pues ya se observó con otros genes de tipo *wc-1* en otros hongos, como *C. neoformans* y *P. blakesleanus* (Idnurm y Heitman, 2005; Idnurm et al., 2006).

Un experimento obligado a la hora de estudiar la función de un gen es el análisis fenotípico de su mutación. En contra de nuestras predicciones, la mutación dirigida del gen *wcoA* no alteró la fotoinducción de la síntesis de carotenoides en *F. fujikuroi*, resultado corroborado en un experimento similar en *F. oxysporum* (Ruiz-Roldán et al., 2008). A pesar de ello, la mutación *wcoA* dio lugar a alteraciones en el patrón de inducción por la luz de los genes de la carotenogénesis, especialmente en el caso del gen *carB*. Sin embargo, la mutación no tuvo consecuencias a nivel de acumulación de carotenoides. La conclusión inevitable es que WcoA no es el fotorreceptor principal de la carotenogénesis, lo que obliga a pensar en fotorreceptores alternativos. Está en marcha el análisis del único gen para criptocromo encontrado en el genoma de *Fusarium*, excluyendo el gen de la fotoliasa (Alejandre-Durán et al., 2003), como único gen candidato a mediar una respuesta a luz azul acorde con el espectro de acción publicado (Rau, 1967).

Estos resultados ponen en evidencia diferencias significativas en la regulación de la carotenogénesis por la luz entre *N. crassa* y *F. fujikuroi*. Las diferencias regulatorias entre ambos hongos son resaltadas por la existencia en *F. fujikuroi* de al menos un gen represor cuyos mutantes poseen altas concentraciones de carotenoides tanto en luz como en oscuridad (Avalos y Cerdá-Olmedo, 1987). Tales mutantes, denominados genéricamente *carS*, se obtienen con facilidad en este hongo, pero no se han descrito en *N. crassa*, a pesar de haberse realizado una exhaustiva búsqueda con este único objetivo (J. Avalos, comunicación personal). Los mutantes *carS* están afectados en la producción de otros metabolitos, como las giberelinas y las bikaverinas, lo que implica conexiones regulatorias entre la síntesis de carotenoides y la de estos compuestos (Rodríguez-Ortiz et al. 2009). La producción de estos metabolitos en *F. fujikuroi* se induce en condiciones de hambre de nitrógeno, un mecanismo de regulación que se extiende también a la síntesis de carotenoides (Rodríguez-Ortiz et al. 2009).

La falta de efecto de la mutación *wcoA* sobre la fotocarotenogénesis no significa que la proteína WcoA no sea un fotorreceptor funcional. La caída en la fotoinducción del gen *carB* en los mutantes *wcoA* (Fig. C3.6) demuestra que WcoA participa al menos

parcialmente en esta respuesta. Es más, la fotoinducción del gen *carO* es totalmente dependiente de este fotorreceptor, como lo es también la fotoinducción más leve del gen *opsA* (Fig. C4.6), discutido en la siguiente sección. Estos resultados demuestran que, como WC-1, WcoA es un fotorreceptor activo en *F. fujikuroi*. Sin embargo, llama la atención que los genes *car* analizados tengan diferentes dependencias regulatorias de WcoA, aún mostrando un patrón similar de inducción de sus niveles de ARNm por la luz (Prado et al., 2004; Thewes et al., 2005).

La información disponible sugiere que un segundo fotorreceptor ha irrumpido recientemente en la línea evolutiva de *Fusarium*, suplantando parcialmente algunas de las funciones asumidas por WC-1 en *N. crassa*, y por proteínas ortólogas en otros hongos. Más aún, es posible que la participación de este segundo fotorreceptor haya relajado la presión evolutiva sobre WcoA y haya facilitado que esta proteína haya asumido nuevas funciones. Es especialmente llamativo a este respecto la desrepresión de los niveles de ARNm de los genes *carO* y *opsA* en la oscuridad en los mutantes *wcoA*, mientras que los genes *carRA* o *carB* apenas se ven afectados (Figura C4.4). La proteína Wc-1 de *N. crassa* es un activador transcripcional, y solo se ha descrito un efecto represor sobre un gen, *cut-1*, siendo probablemente un efecto indirecto (Youssar y Avalos, 2006). Queda por ver también el papel que puede jugar la proteína ortóloga a Wc-2, que llamamos WcoB, para el cual existe en los genomas de *Fusarium* un gen candidato obvio cuyo estudio se emprenderá en breve. Dada las peculiaridades observadas para WcoA, su posible interacción con WcoB pasa a ser un objetivo experimental relevante, como lo es también la eventual existencia de un mecanismo de regulación por fosforilación, como el observado para el complejo WC en *N. crassa* (He et al., 2006).

La adquisición de otras funciones por WcoA es puesta de manifiesto por el fenotipo complejo causado por la mutación del gen sobre el metabolismo secundario o la conidiación, procesos generalmente asociados en este hongo a la disponibilidad de nitrógeno. Los mutantes *wcoA* muestran alteraciones de distinto signo en la producción de conidios, giberelinas, bicaverinas y fusarinas, indicando que en algunos casos la proteína WcoA silvestre ejerce una influencia positiva y en otros casos negativa. Además, los mutantes se vuelven más hidrófilos, indicando cambios en la regulación de la síntesis de hidrofobinas. Las alteraciones observadas son diversas y generalmente no drásticas, lo que indica que los procesos afectados no son mediados en exclusiva por WcoA, sino que esta proteína reguladora es una pieza de un rompecabezas más complejo, asociado a la regulación por nitrógeno, en el que pueden participar otras proteínas reguladoras, como AreA (Tudzynski et al., 1999) o Tor (Teichert et al., 2006). La importancia de la regulación por nitrógeno en este hongo, y sus numerosas conexiones metabólicas, es resaltada también por el efecto represor de este nutriente sobre la carotenogénesis, en el que posiblemente la propia proteína WcoA juegue un papel, aún por investigar.

La regulación de la conidiación en *F. fujikuroi* diferencia también a esta especie de *N. crassa* o de otros ascomicetos. La conidiación es inducida por la luz en *N. crassa* (Lauter y Russo, 1991), *A. nidulans* (Mooney y Yager, 1990) o *Trichoderma viridae* (Casas-Flores et al., 2004). Sin embargo, los micelios de *F. fujikuroi*, tanto aéreos como sumergidos, producen cantidades similares o incluso menores de conidios en la luz que en la oscuridad. En contraste con la falta de influencia de la luz, la disponibilidad de nitrógeno influye drásticamente sobre la cantidad de conidios producidos. La mutación *wcoA* altera significativamente el patrón de conidiación y, más interesante aún, la consecuencia de la mutación es diferente en función de la presencia de nitrógeno en el medio, resaltando aún más la conexión regulatoria entre WcoA y los mecanismos de control asociados al hambre de nitrógeno en este hongo. Los mutantes *wcoA* muestran una reducción de la cantidad de conidios en exceso de nitrógeno, pero el fenotipo contrario en hambre de nitrógeno. Este resultado destaca de nuevo la versatilidad funcional de esta proteína, capaz de ejercer un papel activador o represor en función del proceso estudiado o de las condiciones de cultivo.

El número de proteínas investigadas de la familia WC en hongos no es muy elevado, y cabe esperar que WcoA no sea el único ejemplo de proteína de esta familia con funciones no asociadas a la luz. En los genomas de basidiomicetos se han encontrado proteínas similares a WC-1 pero carentes de dedo de zinc, lo que ya de por sí implica una forma de acción diferente a la representada por WC-1 (Terashima et al., 2005). El análisis funcional de WcoA proporciona un ejemplo sobre como las comparaciones de secuencias no siempre permiten anticipar las funciones de las proteínas, por muy conservadas que estas parezcan estar. El ejemplo de WcoA ha abierto nuevas perspectivas sobre el papel de estas proteínas en los hongos, y nos llama la atención a la capacidad de los seres vivos para adaptar proteínas preexistentes a nuevas funciones.

Esta Tesis ha dedicado atención también a la síntesis de carotenoides en el hongo *U. maydis* y a su eventual regulación por la luz. Aunque el resultado fue que la luz no ejerce ningún efecto aparente sobre este proceso biosintético, el genoma de este hongo posee genes ortólogos para proteínas WC-1 y WC-2. La función de este sistema regulador será objeto de atención en el laboratorio del Dr. Thomas Brefort, en colaboración con quien se han hecho algunos de los experimentos descritos en esta Tesis.

Las proteínas de tipo WC no son más que uno de los diferentes tipos de fotorreceptores de que disponen los hongos (Corrochano, 2007). En la interfase entre síntesis de carotenoides y detección de la luz se encuentran las opsinas, una familia de fotorreceptores que utiliza como grupo prostético para la absorción de luz un apocarotenoide, el retinal (Bayley et al., 1981). A la función de este tipo de proteínas en hongos ha dedicado especial atención también esta Tesis.

### D.3 Las opsinas de *Fusarium* y *Ustilago*

Las opsinas son un grupo de proteínas transmembrana presentes en diferentes grupos taxonómicos, desde arqueas y bacterias hasta animales. La proteína mejor conocida, y origen de su descubrimiento, es la bacteriorrodopsina de arqueas, una bomba de protones que usa la luz como fuente de energía (Cao et al., 1993) a través del uso del gradiente de protones para la generación de ATP. La investigación de esta proteína se ha extendido al descubrimiento de una extensa familia de fotorreceptores, que se han diversificado en la evolución para cumplir diferentes funciones asociadas a la detección de luz (Spudich et al., 2000; Spudich, 2006).

Las opsinas se descubrieron tardíamente en hongos. Su presencia en este grupo taxonómico no fue anticipada y el estudio de la primera de ellas, NOP-1 en *N. crassa*, tuvo su origen en su descubrimiento casual en el análisis de secuencias de ADN complementario (Bieszke et al. 1999a). Las opsinas fotoactivas son proteínas de estructura bien definida, formada por siete hélices TM, una de las cuales contiene un residuo de lisina altamente conservado de anclaje del retinal. La presencia de esta lisina permite distinguir las opsinas teóricamente fotoactivas de una subclase de proteínas de esta familia, supuestamente no fotoactivas por carecer de este aminoácido crítico, y que han recibido el nombre genérico de ORPs (de “opsin related proteins”). De los hongos investigados en esta Tesis, dos poseen un gen para una ORP, YRO-2 en *N. crassa* y HspO en *F. fujikuroi*, y *U. maydis* no posee ninguno. Algunos genes de esta familia habían sido ya identificados por su inducción por choque térmico (familia HSP30). Aunque la falta de relación de estas proteínas con la luz no ha sido demostrada, se atribuye a estas proteínas funciones de chaperonas (Lindquist, 1992).

No todos los hongos poseen genes para opsinas presumiblemente fotoactivas (PPOs o “predictable photoactive opsins”), lo que indica que no juegan ningún papel esencial en este grupo taxonómico. De hecho, no se han encontrado aún en zigomicetos, y no se encuentran en todos los ascomicetos. Especialmente llamativa es la ausencia no solo de opsinas, sino de otros tipos de fotorreceptores, en la levadura *S. cerevisiae*, un microorganismo presumiblemente ciego. *Fusarium* destaca entre los ascomicetos estudiados por la presencia de dos PPOs, CarO y OpsA, mientras que *N. crassa* posee solo una, NOP-1. Por el contrario, *U. maydis*, un organismo al que no se le conoce aún ninguna función regulada por la luz, posee tres PPOs, que hemos denominado Ops1, Ops2 y Ops3.

Una de las dos opsinas de *F. fujikuroi*, CarO, fue descubierta por su ligamiento a los genes estructurales *carRA*, *carB* y *carO*, con los que forma un cluster corregulado o regulón (Prado et al., 2004; Thewes et al., 2005). Los cuatro genes dependen de la luz para su expresión. A causa de su baja expresión en la oscuridad, el efecto inductor de la luz es especialmente llamativo (más de 100 veces de incremento de los niveles de ARNm) y transitorio (los niveles alcanzan su máximo a los 30-60 min y decaen en la hora siguiente).

Es de resaltar que los cuatro genes son necesarios y suficientes para la síntesis de opsina CarO funcional, por lo cual su coregulación tiene una lógica evidente. La ausencia de fenotipo de la mutación *carO* hace que desconozcamos la función de esta opsina en *F. fujikuroi*, aunque nos permite concluir que no juega ningún papel relevante en las condiciones de cultivo del laboratorio. Los mutantes *carS* muestran una desrepresión en luz y en oscuridad del regulón completo, por lo que son *de facto* estirpes superproductoras de opsina CarO. Además de la superproducción de carotenoides, estas estirpes muestran alteraciones en el metabolismo secundario (Rodríguez-Ortiz et al. 2009), pero este fenotipo debe atribuirse a efectos pleiotrópicos de la mutación *carS* y no a la superproducción de la opsina, ya que los mutantes *carO* no parecen estar afectados en estos procesos (Prado et al. 2004). Datos no publicados permiten sospechar una relación de CarO con la regulación del ciclo sexual, inducido por la luz en este hongo (Leslie y Summerell, 2006). Desgraciadamente, *F. fujikuroi* destaca dentro de las especies del complejo *Gibberella fujikuroi* por su baja fertilidad, lo que dificulta su uso para fines de cruzamiento. El estudio del papel de CarO en la fertilidad de *Fusarium* será abordado en el futuro en especies más proclives a producir peritecios, como *F. verticillioides* o *F. proliferatum*.

En esta Tesis se ha prestado especial atención a la función de la opsina OpsA en *F. fujikuroi*. La similitud de su secuencia identifica a OpsA como ortólogo de Nop-1 de *N. crassa*, por lo que el gen *carO* carece de ortólogo en este hongo. Tanto OpsA como NOP-1 poseen los residuos conservados característicos de las bombas de protones, por lo que cabe suponer que esa es la función que cumplen en los respectivos hongos. Sin embargo, de forma análoga a lo observado con la mutación *nop-1* en *N. crassa* (Bieszke et al. 1999a), la mutación del gen *opsA* no dio lugar a ninguna alteración fenotípica externa en las condiciones de cultivo en el laboratorio.

Una consecuencia particularmente inesperada de la mutación *opsA* es la disminución de los niveles de ARNm de los genes enzimáticos de la carotenogénesis (Fig. C4.7). Este efecto contrasta con el efecto contrario producido por la mutación en el gen *carX*, que determina la enzima que produce el propio cromóforo de la opsina (Thewes et al., 2005). La observación de una reducción similar en los niveles de ARNm de *carB*, *carRA* y *carO* en los mutantes nulos *carRA* y *carB* puede atribuirse a la falta de proteína OpsA funcional, ya que las actividades enzimáticas CarRA y CarB son necesarias para la síntesis de retinal. De ser cierta esta hipótesis, la proteína OpsA unida a su cromóforo estimularía por algún mecanismo desconocido la transcripción de los ARNm de los genes *car* o su estabilidad. Sin embargo, se observa el efecto contrario en el caso de que el gen mutado sea *carX*, igualmente incapaz de producir retinal. El aumento de la carotenogénesis observado en este caso puede ser un efecto de la ausencia de la propia enzima, y no de su producto. CarX no solo es activo sobre el  $\beta$ -caroteno, sino que también es capaz de metabolizar  $\gamma$ -caroteno y toruleno para producir respectivamente acicloretilal y 3,4-didehidro-

acicloretinal (Prado-Cabrero et al., 2007b). Es posible que alguno de estos compuestos sea utilizado por la célula como señal represora de la carotenogénesis.

Una explicación alternativa al efecto de la mutación del gen *opsA* es que la versión carente de retinal de esta opsina ejerza un efecto estimulador de la expresión de los genes *car* en un intento de aumentar la cantidad de cromóforo. Este hecho explicaría el efecto contrario de la mutación *carX*, que daría lugar a la acumulación de opsina sin retinal. Sin embargo, esta hipótesis no explicaría la disminución observada de los niveles de ARNm en los propios mutantes de los genes *carRA* y *carB*, bloqueados en pasos anteriores en la ruta biosintética del retinal. Cualquiera que sea la explicación, llama la atención que la disminución en los niveles de ARNm de los genes *car* en los mutantes *opsA* no se traduzca en una menor cantidad de caroteno, lo que indica la existencia de otros mecanismos de regulación postrascriptcional, por ej. a nivel de traducción o de actividad enzimática. Este resultado concuerda con la falta de efecto de la mutación *wcoA* sobre la acumulación de carotenoides en la luz, a pesar de la significativa reducción en los niveles de ARNm del gen *carB* (Fig. C3.6).

La regulación del gen *opsA* es independiente del regulón de los genes *car*. Aunque sus niveles de ARNm son inducidos por la luz, se detectan también en la oscuridad y la fotoactivación es mucho menos prominente. Además, muy significativamente, las mutaciones *carS* no le afectan. Sin embargo, comparte con *carO* la mediación de WcoA en su regulación por la luz y la represión de los niveles de ARNm en oscuridad. La necesidad de proteína WcoA funcional es también patente para la fotoinducción del gen *phr1* de la fotoliasa en *F. oxysporum*, pero en este caso la mutación del gen ortólogo de *wcoA* en esta especie no da lugar a una desrepresión en la oscuridad de sus niveles de ARNm (Ruiz-Róldan et al., 2008). La regulación por *wcoA* de los genes de ambas opsinas sugiere una conexión de estas fotoproteínas con otras señales ambientales, como puede ser la disponibilidad de nitrógeno, aún por investigar.

Un organismo de especial interés para el estudio funcional de las opsinas fúngicas es la levadura *U. maydis*. Como ya se ha indicado, su genoma contiene tres genes para presumibles opsinas fotoactivas, que hemos denominado *ops1*, *ops2* y *ops3*, lo que indica la existencia de una ruta de síntesis de retinal. Los resultados descritos en esta Tesis indican que *U. maydis* acumula cantidades moderadas de  $\beta$ -caroteno en estado prácticamente puro, y que la síntesis no se ve influida por la luz o el estrés oxidativo. Sin embargo, los niveles de  $\beta$ -caroteno son diferentes en función del pH del medio, una señal ambiental que ejerce notable influencia en la morfología de sus células. La eficiencia de su ruta biosintética, en la que no se ha podido detectar cantidad alguna de carotenos intermediarios predecesores del  $\beta$ -caroteno, y sus peculiaridades regulatorias, unido a las facilidades que ofrece su manipulación genética, hacen de *U. maydis* un modelo particularmente atractivo dentro de los hongos para estudios de carotenogénesis.



La función del  $\beta$ -caroteno en esta levadura es puesta en evidencia por los resultados de la mutación y sobreexpresión del gen *cco1*, ortólogo al gen *carX* y presunto responsable de la síntesis de retinal en este organismo. La función de este gen han quedado sólidamente demostrados por una combinación de enfoques experimentales, que abarcan desde el efecto de la mutación *in vivo* a la actividad de la enzima Cco1 *in vitro*. El análisis de los niveles de ARNm del gen *cco1* mostró una leve fotoinducción a pH 3, comparable al de uno de los genes enzimáticos de la carotenogénesis en las mismas condiciones. El aumento, apenas tres veces, está muy lejos de la fuerte inducción mostrada en experimentos de northern por su ortólogo *carX* en *F. fujikuroi* (Thewes et al., 2005). La fotoinducción, sin embargo, no se detectó a pH 7, condiciones bajo las cuales se prevé una menor cantidad de opsinas, a juzgar por los niveles de ARNm de los genes *ops1* y *ops2*.

Los resultados obtenidos con estirpes alteradas en el gen *cco1* muestran una relación inversa entre su expresión y los niveles de  $\beta$ -caroteno en *U. maydis*, indicando que una de las finalidades más relevantes de la síntesis de este caroteno por este hongo, si no la más importante, es la de proporcionar un *pool* de sustrato para la producción de retinal. De ser así, su carotenogénesis debe estar sujeta a algún tipo de regulación que asegure la existencia de un nivel suficientes de  $\beta$ -caroteno disponible para la enzima Cco1. Es también evidente que los niveles de retinal los determina en primera instancia la actividad Cco1, y que las tres opsinas dependen de esta enzima para la disponibilidad de su cromóforo. Sin embargo, los similares niveles de retinal observados en la estirpe silvestre y en un mutante desregulado para Cco1 sugieren la existencia de mecanismos de eliminación del retinal sobrante, lo que hace más improbable un posible papel de la actividad Cco1 como factor limitante para la funcionalidad de las opsinas. Este papel reside probablemente en la propia regulación de los genes de las opsinas, cuyos diferentes patrones de regulación sugieren funciones muy dispares.

El análisis comparativo de las tres opsinas de *U. maydis* con las PPOs de *F. fujikuroi* y *N. crassa* indica que Ops2 es el probable ortólogo de OpsA y NOP-1, mientras que Ops1 y Ops3 muestran una mayor similitud con CarO. Estas correlaciones son particularmente reveladoras, ya que la regulación del gen *ops1* es muy similar a la del gen *carO*, con una fuerte inducción por la luz de sus niveles de ARNm, mientras que la fotoinducción más modesta observada para el gen *ops2* recuerda a la manifestada por el gen *opsA*. Estas coincidencias regulatorias sugieren equivalencias funcionales para las correspondientes opsinas en *U. maydis* y *F. fujikuroi*. Sin embargo, el gen de la tercera opsina, *ops3*, no se expresa en las condiciones experimentales empleadas. Es probable que la función de esta tercera opsina esté asociada a un proceso específico de *U. maydis*, como es la patogénesis del maíz. Una hipótesis tentadora es su activación en fases tardías del proceso de patogénesis, en el que el hongo aflora al exterior de la mazorca infectada para la liberación de las teliosporas. El elevado parecido entre Ops3 y Ops1 sugiere una duplicación reciente

en la línea evolutiva de *Ustilago* y una especialización funcional posterior de uno de los dos genes duplicados.

La dependencia de las tres opsinas de *U. maydis* de una única enzima proporcionadora de su cromóforo convierte al mutante *cco1* en un triple mutante de opsinas funcionales. La viabilidad de la mutación *cco1* y la ausencia de alteraciones fenotípicas detectables, con la salvedad de los cambios en el contenido de  $\beta$ -caroteno, proporciona un nuevo ejemplo de ausencia de un papel biológico relevante de las opsinas fúngicas.



## **Conclusiones**



## Conclusiones

1. El gen *ylo-1* de *Neurospora crassa* determina una deshidrogenasa de aldehído con un dominio transmembrana inusual en las enzimas de esta familia. *In vitro*, la enzima YLO-1 convierte  $\beta$ -apo-4'-carotenal en ácido  $\beta$ -apo-4'-carotenoico o neurosporaxantina, el producto final de la ruta carotenogénica en este hongo. Además realiza la misma reacción sobre apo-4'-licopenal, la versión no ciclada de este sustrato, para convertirlo en ácido apo-4'-licopenoico.
2. El análisis químico de los carotenoides acumulados por el mutante *ylo-1* y los mutantes *al-2* carentes de actividad ciclasa en condiciones óptimas para la síntesis de neurosporaxantina ha permitido identificar tres nuevos apocarotenoides: apo-4'-licopenal, apo-4'-licopenol, y ácido apo-4'-licopenoico. Es la primera vez que estos compuestos se encuentran en la naturaleza.
3. La presencia de estos apocarotenoides indica un nuevo orden de las reacciones finales en la carotenogénesis de *N. crassa*. De acuerdo con este orden, la oxigenasa CAO-2 introduce un corte oxidativo en el precursor pentasaturado 3,4-didehidrolicopeno para producir apo-4'-licopenal, el cual es oxidado por la deshidrogenasa de aldehído YLO-1 para generar ácido apo-4'-licopenoico, el cual es ciclado finalmente por AL-2 para producir neurosporaxantina.
4. La proteína WcoA de *Fusarium fujikuroi*, ortóloga de WC-1 de *Neurospora crassa*, no es el fotorreceptor principal de la carotenogénesis en este hongo. Sin embargo, es el fotorreceptor responsable de la fotoinducción de los niveles de ARNm de los genes de las opsinas CarO y OpsA. Además, WcoA reprime la expresión de dichos genes en la oscuridad.
5. Los mutantes *wcoA* muestran alteraciones de distinto signo en la síntesis de giberelinas, bicaverinas y fusarinas, así como en la producción de conidios o en la hidrofobicidad del micelio. Por tanto, la proteína WcoA juega un papel en los mecanismos que controlan el metabolismo secundario de *Fusarium fujikuroi* y otros procesos celulares, en especial aquellos asociados a la regulación por disponibilidad de nitrógeno.
6. La pérdida de la opsina OpsA no produce cambios fenotípicos externos detectables en *Fusarium fujikuroi* en condiciones de laboratorio. Los niveles de ARNm de los genes *car* disminuyen en los mutantes *opsA*, pero el contenido de caroteno total no se ve alterado.

7. El gen *opsA* muestra un patrón de regulación diferente que el gen *carO*, que determina otra opsina anteriormente investigada en el mismo hongo. A diferencia de *carO*, los niveles de ARNm de *opsA* son detectables en la oscuridad, muestran una inducción mucho más débil en respuesta a la luz y no cambian significativamente en los mutantes superproductores de carotenoides.

8. La levadura *Ustilago maydis* sintetiza cantidades moderadas de  $\beta$ -caroteno y su genoma contiene genes ortólogos a los ya descritos para su síntesis en otros hongos. La síntesis de  $\beta$ -caroteno no es afectada por la luz o el estrés oxidativo, pero sí por el pH, un factor ambiental determinante en su desarrollo.

9. El gen *ccoI* de *Ustilago maydis* determina una oxigenasa de carotenoides ortóloga del gen *carX* de *Fusarium fujikuroi*. La proteína Cco1 produce *in vitro* retinal a partir de  $\beta$ -caroteno, la expresión de su gen correlaciona inversamente con la concentración de  $\beta$ -caroteno *in vivo* y los mutantes *ccoI* carecen de retinal. Por tanto, la función de la enzima Cco1 en esta levadura es sintetizar retinal.

10. Los tres genes para opsinas del genoma de *Ustilago maydis* muestran patrones diferentes de regulación, y dos de ellos son inducidos por la luz. Los mutantes *ccoI*, presumiblemente carentes de opsinas fotoactivas, no muestran alteraciones fenotípicas detectables excepto un aumento en la acumulación de  $\beta$ -caroteno.

## **Bibliografía**





## Bibliografía

- Aasen, A.J., and Jensen, S.L. (1965) Fungal carotenoids II. The structure of the carotenoid acid neurosporaxanthin. *Acta Chem. Scand.* **19**: 1843-1853.
- Accoceberry, I., and Noel, T. (2006) Antifungals cellular targets and mechanisms of resistance. *Therapie* **61**: 195-199.
- Adams, G., Johnson, N., Leslie, J.F., and Hart, L.P. (1987) Heterokaryons of *Gibberella zeae* formed following hyphal anastomosis or protoplast fusion. *Exp. Mycol.* **11**: 339-353.
- Addicott, F.T. (1983) *Abscisic Acid*. New York: Praeger Publishers.
- Agrios, G.N. (2005) *Plant Pathology*. New York: Academic Press.
- Akiyama, K. (2007) Chemical identification and functional analysis of apocarotenoids involved in the development of arbuscular mycorrhizal symbiosis. *Biosci Biotechnol Biochem* **71**: 1405-1414.
- Alder, A., Holdermann, I., Beyer, P., and Al-Babili, S. (2008) Carotenoid oxygenases involved in plant branching catalyse a highly specific conserved apocarotenoid cleavage reaction. *Biochem J* **416**: 289-296.
- Alejandre-Duran, E., Roldan-Arjona, T., Ariza, R.R., and Ruiz-Rubio, M. (2003) The photolyase gene from the plant pathogen *Fusarium oxysporum f. sp. lycopersici* is induced by visible light and alpha-tomatine from tomato plant. *Fungal Genet Biol* **40**: 159-165.
- Almeida, E.R., and Cerda-Olmedo, E. (2008) Gene expression in the regulation of carotene biosynthesis in *Phycomyces*. *Curr. Genet.* **53**: 129-137.
- Alvarez, V., Rodriguez-Saiz, M., de la Fuente, J.L., Gudina, E.J., Godio, R.P., Martin, J.F., and Barredo, J.L. (2006) The *crtS* gene of *Xanthophyllomyces dendrorhous* encodes a novel cytochrome-P450 hydroxylase involved in the conversion of beta-carotene into astaxanthin and other xanthophylls. *Fungal Genet. Biol.* **43**: 261-272.
- Ambra, R., Grimaldi, B., Zamboni, S., Filetici, P., Macino, G., and Ballario, P. (2004) Photomorphogenesis in the hypogeous fungus *Tuber borchii*: isolation and characterization of Tbwc-1, the homologue of the blue-light photoreceptor of *Neurospora crassa*. *Fungal Genet. Biol.* **41**: 688-697.
- An, G.H., and Johnson, E.A. (1990) Influence of light on growth and pigmentation of the yeast *Phaffia rhodozyma*. *Antonie Van Leeuwenhoek* **57**: 191-203.
- Andrewes, A.G., Borch, G., and Liaaen-Jensen, S. (1976) Bacterial carotenoids. XLVIII. C50-Carotenoids. 16. Synthesis and chiroptical properties of the model compounds (2R, 6R, 2'R,6'R)-2,2'-dimethyl-epsilon,epsilon-carotene and (2R, 6S, 2'R, 6'S)-2,2'-dimethyl-epsilon,epsilon-carotene. *Acta Chem Scand B* **30**: 214-218.
- Andrianopoulos, A., Kourambas, S., Sharp, J.A., Davis, M.A., and Hynes, M.J. (1998) Characterization of the *Aspergillus nidulans nmrA* gene involved in nitrogen metabolite repression. *J Bacteriol* **180**: 1973-1977.
- Armaleo, D., Ye, G.N., Klein, T.M., Shark, K.B., Sanford, J.C., and Johnston, S.A. (1990) Biolistic nuclear transformation of *Saccharomyces cerevisiae* and other fungi. *Curr Genet* **17**: 97-103.

- Armstrong, G.A. (1997) Genetics of eubacterial carotenoid biosynthesis: a colorful tale. *Annu Rev Microbiol* **51**: 629-659.
- Arpaia, G., Loros, J.J., Dunlap, J.C., Morelli, G., and Macino, G. (1993) The interplay of light and the circadian clock. Independent dual regulation of clock-controlled gene *cgc-2(eas)*. *Plant Physiol* **102**: 1299-1305.
- Arpaia, G., Carattoli, A., and Macino, G. (1995a) Light and development regulate the expression of the *albino-3* gene in *Neurospora crassa*. *Dev Biol* **170**: 626-635.
- Arpaia, G., Loros, J.J., Dunlap, J.C., Morelli, G., and Macino, G. (1995b) Light induction of the clock-controlled gene *cgc-1* is not transduced through the circadian clock in *Neurospora crassa*. *Mol Gen Genet* **247**: 157-163.
- Arpaia, G., Cerri, F., Baima, S., and Macino, G. (1999) Involvement of protein kinase C in the response of *Neurospora crassa* to blue light. *Mol Gen Genet* **262**: 314-322.
- Arrach, N., Fernandez-Martin, R., Cerda-Olmedo, E., and Avalos, J. (2001) A single gene for lycopene cyclase, phytoene synthase, and regulation of carotene biosynthesis in *Phycomyces*. *Proc Natl Acad Sci U S A* **98**: 1687-1692.
- Arrach, N., Schmidhauser, T.J., and Avalos, J. (2002) Mutants of the carotene cyclase domain of *al-2* from *Neurospora crassa*. *Mol Genet Genomics* **266**: 914-921.
- Auldridge, M.E., McCarty, D.R., and Klee, H.J. (2006) Plant carotenoid cleavage oxygenases and their apocarotenoid products. *Curr Opin Plant Biol* **9**: 315-321.
- Austwick, P.K.C. (1984) *Fusarium* infections in man and animals. In *The applied Mycology of Fusarium*. Cambridge University press (M.O. Moss and J.E. Smith). London, pp. 129-140.
- Avalos, J., Casadesus, J., and Cerda-Olmedo, E. (1985) *Gibberella fujikuroi* mutants obtained with UV radiation and N-methyl-N'-nitro-N-nitrosoguanidine. *Appl. Environ. Microbiol.* **49**: 187-191.
- Avalos, J., and Cerdá-Olmedo, E. (1986) Chemical modification of carotenogenesis in *Gibberella fujikuroi*. *Phytochemistry* **25**: 1837-1841.
- Avalos, J., and Cerda-Olmedo, E. (1987) Carotenoid mutants of *Gibberella fujikuroi*. *Curr. Genet.* **25**: 1837-1841.
- Avalos, J., and Cerdá-Olmedo, E. (1987) Carotenoid mutants of *Gibberella fujikuroi*. *Curr. Genet.* **11**: 505-511.
- Avalos, J., and Schrott, E.L. (1990) Photoinduction of carotenoid biosynthesis in *Gibberella fujikuroi*. *FEMS Microbiol. lett.* **66**: 295-298.
- Avalos, J., Bejarano, E.R., and Cerdá-Olmedo, E. (1993) Photoinduction of carotenoid biosynthesis. *Methods Enzymol.* **214**: 283-294.
- Avalos, J., Fernandez-Martin, R., Prado, M.M., and Cerda-Olmedo, E. (1999) Gibberellin biosynthesis in *Gibberella*. *J. Bot. Gall.* **146**: 55-65.
- Avalos, J., and Cerdá-Olmedo, E. (2004) Fungal carotenoid production. In *Handbook of Fungal Biotechnology*. Arora, D.K. (ed). New York: Marcel Dekker, Inc., pp. 367-378.
- Avalos, J., Cerda-Olmedo, E., Reyes, F., and Barrero, A.F. (2007) Gibberellins and other metabolites of *Fusarium fujikuroi* and related fungi. *Curr. Org. Chem.* **11**: 721-737.
- Bacon, C.W., Porter, J.K., Norred, W.P., and Leslie, J.F. (1996) Production of fusaric acid by *Fusarium* species. *Appl Environ Microbiol* **62**: 4039-4043.

- 
- Baima, S., Macino, G., and Morelli, G. (1991) Photoregulation of the *albino-3* gene in *Neurospora crassa*. *J Photochem Photobiol B* **11**: 107-115.
  - Baima, S., Carattoli, A., Macino, G., and Morelli, G. (1992) Photoinduction of *albino-3* gene expression in *Neurospora crassa* conidia. *J Photochem Photobiol B* **15**: 233-238.
  - Bakkeren, G., Kamper, J., and Schirawski, J. (2008) Sex in smut fungi: Structure, function and evolution of mating-type complexes. *Fungal Genet Biol* **45 Suppl 1**: S15-21.
  - Balan, J., Fuska, J., Kuhr, I., and Kuhrova, V. (1970) Bikaverin, an antibiotic from *Gibberella fujikuroi*, effective against *Leishmania brasiliensis*. *Folia Microbiol. (Praha)* **15**: 479-484.
  - Ballario, P., Vittorioso, P., Magrelli, A., Talora, C., Cabibbo, A., and Macino, G. (1996) White collar-1, a central regulator of blue light responses in *Neurospora*, is a zinc finger protein. *Embo J.* **15**: 1650-1657.
  - Ballario, P., Talora, C., Galli, D., Linden, H., and Macino, G. (1998) Roles in dimerization and blue light photoresponse of the PAS and LOV domains of *Neurospora crassa* white collar proteins. *Mol Microbiol* **29**: 719-729.
  - Banno, S., Ochiai, N., Noguchi, R., Kimura, M., Yamaguchi, I., Kanzaki, S., Murayama, T., and Fujimura, M. (2005) A catalytic subunit of cyclic AMP-dependent protein kinase, PKAC-1, regulates asexual differentiation in *Neurospora crassa*. *Genes Genet Syst* **80**: 25-34.
  - Banuett, F., and Herskowitz, I. (1989) Different alleles of *Ustilago maydis* are necessary for maintenance of filamentous growth but not for meiosis. *Proc. Natl. Acad. Sci. USA* **86**: 5878-5882.
  - Banuett, F. (1992) *Ustilago maydis*, the delightful blight. *Trends Genet* **8**: 174-180.
  - Banuett, F. (1995) Genetics of *Ustilago maydis*, a fungal pathogen that induces tumors in maize. *Annu Rev Genet* **29**: 179-208.
  - Banuett, F., and Herskowitz, I. (1996) Discrete developmental stages during teliospore formation in the corn smut fungus, *Ustilago maydis*. *Development* **122**: 2965-2976.
  - Barendse, G.W.M., van de Werken, P.H., and Takahashi, N. (1980) High performance liquid chromatography of gibberellins. *J. Chromatogr.* **198**: 449-455.
  - Barrero, A.F., Sánchez, J.F., Oltra, J.E., Tamayo, N., Cerdá-Olmedo, E., Candau, R., and Avalos, J. (1991) Fusarin C and 8Z-Fusarin C from *Gibberella fujikuroi*. *Phytochemistry* **30**: 2259-2263.
  - Barua, A.B., and Olson, J.A. (2000) Beta-carotene is converted primarily to retinoids in rats *in vivo*. *J. Nutr.* **130**: 1996-2001.
  - Basse, C.W., and Steinberg, G. (2004) *Ustilago maydis*, model system for analysis of the molecular basis of fungal pathogenicity. *Mol. Plant Pathol.* **5**: 83-92.
  - Bayley, H., Huang, K.S., Radhakrishnan, R., Ross, A.H., Takagaki, Y., and Khorana, H.G. (1981) Site of attachment of retinal in bacteriorhodopsin. *Proc. Natl. Acad. Sci. USA* **78**: 2225-2229.
  - Beadle, G.W., and Tatum, E.L. (1941) Genetic Control of Biochemical Reactions in *Neurospora*. *Proc Natl Acad Sci U S A* **27**: 499-506.
  - Bell, A.A., Wheeler, M.H., Liu, J., Stipanovic, R.D., Puckhaber, L.S., and Orta, H. (2003) United States Department of Agriculture-Agricultural Research Service

- studies on polyketide toxins of *Fusarium oxysporum f sp vasinfectum*: potential targets for disease control. *Pest Manag Sci* **59**: 736-747.
- Belozerskaia, T.A., Burikhanov Sh, S., Kritskii, M.S., L'Vov N, P., and Chernysheva, E.K. (1982) Photoinduction of carotenoid synthesis by *Neurospora crassa* on different structural and functional states of nitrate reductase. *Prikl Biokhim Mikrobiol* **18**: 231-236.
  - Bhosale, P.B., and Gadre, R.V. (2001) Production of  $\beta$ -carotene by a mutant of *Rhodotorula glutinis*. *Appl. Microbiol. Biotechnol.* **55**: 423-427.
  - Bieszke, J.A., Braun, E.L., Bean, L.E., Kang, S., Natvig, D.O., and Borkovich, K.A. (1999a) The *nop-1* gene of *Neurospora crassa* encodes a seven transmembrane helix retinal-binding protein homologous to archaeal rhodopsins. *Proc. Natl. Acad. Sci. USA* **96**: 8034-8039.
  - Bieszke, J.A., Spudich, E.N., Scott, K.L., Borkovich, K.A., and Spudich, J.L. (1999b) A eukaryotic protein, NOP-1, binds retinal to form an archaeal rhodopsin-like photochemically reactive pigment. *Biochemistry* **38**: 14138-14145.
  - Bieszke, J.A., Li, L., and Borkovich, K.A. (2007) The fungal opsin gene *nop-1* is negatively-regulated by a component of the blue light sensing pathway and influences conidiation-specific gene expression in *Neurospora crassa*. *Curr. Genet.* **52**: 149-157.
  - Bindl, E., Lang, W., and Rau, W. (1970) Untersuchungen über die lichtabhängige Carotinoidsynthese. VI. Zeitlicher Verlauf der Synthese der einzelnen Carotinoide bei *Fusarium aquaeductuum* unter verschiedenen Induktionsbedingungen. *Planta* **94**: 156-174.
  - Bistis, G.N. (1996) Trichogynes and Fertilization in Uni- and Bimating Type Colonies of *Neurospora tetrasperma*. *Fungal Genet Biol* **20**: 93-98.
  - Blomhoff, R., and Blomhoff, H.K. (2006) Overview of retinoid metabolism and function. *J. Neurobiol.* **66**: 606-630.
  - Bogomolni, R.A., and Spudich, J.L. (1982) Identification of a third rhodopsin-like pigment in phototactic *Halobacterium halobium*. *Proc Natl Acad Sci U S A* **79**: 6250-6254.
  - Bok, J.W., and Keller, N.P. (2004) LaeA, a regulator of secondary metabolism in *Aspergillus spp.* *Eukaryot. Cell* **3**: 527-535.
  - Bok, J.W., Noordermeer, D., Kale, S.P., and Keller, N.P. (2006) Secondary metabolic gene cluster silencing in *Aspergillus nidulans*. *Mol. Microbiol.* **61**: 1636-1645.
  - Bolker, M., Basse, C.W., and Schirawski, J. (2008) *Ustilago maydis* secondary metabolism-from genomics to biochemistry. *Fungal Genet Biol* **45 Suppl 1**: S88-93.
  - Booth, C. (1971) *The genus Fusarium*. Kew: Commonwealth Mycological Institute.
  - Borkovich, K.A., Alex, L.A., Yarden, O., Freitag, M., Turner, G.E., Read, N.D., Seiler, S., Bell-Pedersen, D., Paietta, J., Plesofsky, N., Plamann, M., Goodrich-Tanrikulu, M., Schulte, U., Mannhaupt, G., Nargang, F.E., Radford, A., Selitrennikoff, C., Galagan, J.E., Dunlap, J.C., Loros, J.J., Catcheside, D., Inoue, H., Aramayo, R., Polymenis, M., Selker, E.U., Sachs, M.S., Marzluf, G.A., Paulsen, I., Davis, R., Ebbole, D.J., Zelter, A., Kalkman, E.R., O'Rourke, R., Bowring, F., Yeadon, J., Ishii, C., Suzuki, K., Sakai, W., and Pratt, R. (2004) Lessons from the genome

- sequence of *Neurospora crassa*: tracing the path from genomic blueprint to multicellular organism. *Microbiol Mol Biol Rev* **68**: 1-108.
- Bouvier, F., Isner, J.C., Dogbo, O., and Camara, B. (2005) Oxidative tailoring of carotenoids: a prospect towards novel functions in plants. *Trends Plant Sci* **10**: 187-194.
  - Bouwmeester, H.J., Roux, C., Lopez-Raez, J.A., and Becard, G. (2007) Rhizosphere communication of plants, parasitic plants and AM fungi. *Trends Plant Sci* **12**: 224-230.
  - Brachmann, A., König, J., Julius, C., and Feldbrügge, M. (2004) A reverse genetic approach for generating gene replacement mutants in *Ustilago maydis*. *Mol. Genet. Genomics* **272**: 216-226.
  - Briggs, W.R. (2007) The LOV domain: a chromophore module servicing multiple photoreceptors. *J Biomed Sci* **14**: 499-504.
  - Britton, G., Liaaen-Jensen, S., and Pfander, H. (1998) *Carotenoids*. Basel: Birkhäuser Verlag.
  - Britton, G., Liaaen-Jensen, S., and Pfander, H. (2004) *Carotenoids: Handbook*. Boston: Birkhauser.
  - Brown, L.S., Dioumaev, A.K., Lanyi, J.K., Spudich, E.N., and Spudich, J.L. (2001) Photochemical reaction cycle and proton transfers in *Neurospora* rhodopsin. *J. Biol. Chem.* **276**: 32495-32505.
  - Brown, L.S. (2004) Fungal rhodopsins and opsin-related proteins: eukaryotic homologues of bacteriorhodopsin with unknown functions. *Photochem. Photobiol. Sci.* **3**: 555-565.
  - Bubrick, P. (1991) Production of astaxanthin from *Haematococcus*. *Biores. Tech.* **38**: 237-239.
  - Burmester, A., Richter, M., Schultze, K., Voelz, K., Schachtschabel, D., Boland, W., Wostemeyer, J., and Schimek, C. (2007) Cleavage of beta-carotene as the first step in sexual hormone synthesis in zygomycetes is mediated by a trisporic acid regulated beta-carotene oxygenase. *Fungal Genet. Biol.* **44**: 1096-1108.
  - Buzzini, P., Innocenti, M., Turchetti, B., Libkind, D., van Broock, M., and Mulinacci, N. (2007) Carotenoid profiles of yeasts belonging to the genera *Rhodotorula*, *Rhodospiridium*, *Sporobolomyces*, and *Sporidiobolus*. *Can. J. Microbiol.* **53**: 1024-1031.
  - Caddick, M.X., Arst, H.N., Jr., Taylor, L.H., Johnson, R.I., and Brownlee, A.G. (1986) Cloning of the regulatory gene *areA* mediating nitrogen metabolite repression in *Aspergillus nidulans*. *Embo J.* **5**: 1087-1090.
  - Calvo, A.M., Wilson, R.A., Bok, J.W., and Keller, N.P. (2002) Relationship between secondary metabolism and fungal development. *Microbiol. Mol. Biol. Rev.* **66**: 447-459.
  - Cambareri, E.B., Singer, M.J., and Selker, E.U. (1991) Recurrence of repeat-induced point mutation (RIP) in *Neurospora crassa*. *Genetics* **127**: 699-710.
  - Candau, R., Avalos, J., and Cerda-Olmedo, E. (1991) Gibberellins and Carotenoids in the Wild Type and Mutants of *Gibberella fujikuroi*. *Appl Environ Microbiol* **57**: 3378-3382.

- Candau, R., Avalos, J., and Cerda-Olmedo, E. (1992) Regulation of Gibberellin Biosynthesis in *Gibberella fujikuroi*. *Plant Physiol* **100**: 1184-1188.
- Cano-Dominguez, N., Alvarez-Delfin, K., Hansberg, W., and Aguirre, J. (2008) NADPH oxidases NOX-1 and NOX-2 require the regulatory subunit NOR-1 to control cell differentiation and growth in *Neurospora crassa*. *Eukaryot Cell* **7**: 1352-1361.
- Cao, Y., Váró, G., Klinger, A.L., Czajkowsky, D.M., Braiman, M.S., Needleman, R., and Lanyi, J.K. (1993) Proton transfer from Asp-96 to the bacteriorhodopsin Schiff base is caused by decrease of the pK<sub>a</sub> of Asp-96 which follows a protein backbone conformation change. *Biochemistry* **32**: 1981-1990.
- Casas-Flores, S., Rios-Momberg, M., Bibbins, M., Ponce-Noyola, P., and Herrera-Estrella, A. (2004) BLR-1 and BLR-2, key regulatory elements of photoconidiation and mycelial growth in *Trichoderma atroviride*. *Microbiology* **150**: 3561-3569.
- Case, M.E., Schweizer, M., Kushner, S.R., and Giles, N.H. (1979) Efficient transformation of *Neurospora crassa* by utilizing hybrid plasmid DNA. *Proc Natl Acad Sci U S A* **76**: 5259-5263.
- Catalanotto, C., Pallotta, M., ReFalo, P., Sachs, M.S., Vayssie, L., Macino, G., and Cogoni, C. (2004) Redundancy of the two dicer genes in transgene-induced posttranscriptional gene silencing in *Neurospora crassa*. *Mol Cell Biol* **24**: 2536-2545.
- Cerda-Olmedo, E. (1985) Carotene Mutants of *Phycomyces*. *Methods in Enzymology* **110**: 220-243.
- Cerda-Olmedo, E., Fernandez-Martin, R., and Avalos, J. (1994) Genetics and gibberellin production in *Gibberella fujikuroi*. *Antonie Van Leeuwenhoek* **65**: 217-225.
- Cerda-Olmedo, E. (2001) *Phycomyces* and the biology of light and color. *FEMS Microbiol. Rev.* **25**: 503-512.
- Cerdá-Olmedo, E. (1987) Carotene. In *Phycomyces*. Cerdá-Olmedo, E. and Lipson, E.D. (eds). Cold Spring Harbor: Cold Spring Harbor Laboratory Press, pp. 199-222.
- Cha, J., Chang, S.S., Huang, G., Cheng, P., and Liu, Y. (2008) Control of WHITE COLLAR localization by phosphorylation is a critical step in the circadian negative feedback process. *Embo J* **27**: 3246-3255.
- Chakraborty, B.N., Patterson, N.A., and Kapoor, M. (1991) An electroporation-based system for high-efficiency transformation of germinated conidia of filamentous fungi. *Can J Microbiol* **37**: 858-863.
- Chang, C., and Yoshida, A. (1997) Human fatty aldehyde dehydrogenase gene (ALDH10): organization and tissue-dependent expression. *Genomics* **40**: 80-85.
- Cheng, P., Yang, Y., and Liu, Y. (2001) Interlocked feedback loops contribute to the robustness of the *Neurospora* circadian clock. *Proc Natl Acad Sci U S A* **98**: 7408-7413.
- Cheng, P., He, Q., Yang, Y., Wang, L., and Liu, Y. (2003) Functional conservation of light, oxygen, or voltage domains in light sensing. *Proc. Natl. Acad. Sci. U S A* **100**: 5938-5943.
- Christie, J.M., Corchnoy, S.B., Swartz, T.E., Hokenson, M., Han, I.S., Briggs, W.R., and Bogomolni, R.A. (2007) Steric interactions stabilize the signaling state of the LOV2 domain of phototropin 1. *Biochemistry* **46**: 9310-9319.

- 
- Cogoni, C., and Macino, G. (1999a) Posttranscriptional gene silencing in *Neurospora* by a RecQ DNA helicase. *Science* **286**: 2342-2344.
  - Cogoni, C., and Macino, G. (1999b) Homology-dependent gene silencing in plants and fungi: a number of variations on the same theme. *Curr Opin Microbiol* **2**: 657-662.
  - Conlon, H., Zadra, I., Haas, H., Arst, H.N., Jr., Jones, M.G., and Caddick, M.X. (2001) The *Aspergillus nidulans* GATA transcription factor gene *areB* encodes at least three proteins and features three classes of mutation. *Mol Microbiol* **40**: 361-375.
  - Correll, J.D., Klittich, C.J.R., and Leslie, J.F. (1987) Nitrate nonutilizing mutants of *Fusarium oxysporum* and their use in vegetative compatibility tests. *Phytopathology* **77**: 1640-1646.
  - Corrochano, L.M., and Cerda-Olmedo, E. (1992) Sex, light and carotenes: the development of *Phycomyces*. *Trends Genet.* **8**: 268-274.
  - Corrochano, L.M. (2007) Fungal photoreceptors: sensory molecules for fungal development and behaviour. *Photochem. Photobiol. Sci.* **6**: 725-736.
  - Cunningham, F.X., and Gantt, E. (1998) Genes and Enzymes of Carotenoid Biosynthesis in Plants. *Annu Rev Plant Physiol Plant Mol Biol* **49**: 557-583.
  - Davies, B.H. (1976) Carotenoids. Goodwin, T.W. (ed). London: Academic Press, pp. 38-165.
  - Davis, R.H., and de Serres, F.J. (1970) Genetic and microbiological research techniques for *Neurospora crassa*. *Methods Enzymol.* **71A**: 79-143.
  - Davis, R.H. (2000) *Neurospora. Contributions of a model organism*. New York: Oxford University Press.
  - Davis, R.H., and Perkins, D.D. (2002) Timeline: *Neurospora*: a model of model microbes. *Nat Rev Genet* **3**: 397-403.
  - De Fabo, E.C., Harding, R.W., and Shropshire, W. (1976) Action Spectrum between 260 and 800 Nanometers for the Photoinduction of Carotenoid Biosynthesis in *Neurospora crassa*. *Plant Physiol* **57**: 440-445.
  - de Groot, M.J., Bundock, P., Hooykaas, P.J., and Beijersbergen, A.G. (1998) *Agrobacterium tumefaciens*-mediated transformation of filamentous fungi. *Nat Biotechnol* **16**: 839-842.
  - Degli-Innocenti, F., Chambers, J.A., and Russo, V.E. (1984) Conidia induce the formation of protoperithecia in *Neurospora crassa*: further characterization of white collar mutants. *J Bacteriol* **159**: 808-810.
  - Degli-Innocenti, F., and Russo, V.E. (1984) Isolation of new white collar mutants of *Neurospora crassa* and studies on their behavior in the blue light-induced formation of protoperithecia. *J Bacteriol* **159**: 757-761.
  - Deising, H.B., Werner, S., and Wernitz, M. (2000) The role of fungal appressoria in plant infection. *Microbes Infect* **2**: 1631-1641.
  - Del Campo, J.A., Garcia-Gonzalez, M., and Guerrero, M.G. (2007) Outdoor cultivation of microalgae for carotenoid production: current state and perspectives. *Appl. Microbiol. Biotechnol.* **74**: 1163-1174.
  - DellaPenna, D., and Pogson, B.J. (2006) Vitamin synthesis in plants: tocopherols and carotenoids. *Annu Rev Plant Biol* **57**: 711-738.
  - Demmig-Adams, B., and Adams, W.W., 3rd (2002) Antioxidants in photosynthesis and human nutrition. *Science* **298**: 2149-2153.



- Denault, D.L., Loros, J.J., and Dunlap, J.C. (2001) WC-2 mediates WC-1-FRQ interaction within the PAS protein-linked circadian feedback loop of *Neurospora*. *Embo J* **20**: 109-117.
- Desjardins, A.E., Manandhar, H.K., Plattner, R.D., Manandhar, G.G., Poling, S.M., and Maragos, C.M. (2000) *Fusarium* species from nepalese rice and production of mycotoxins and gibberellic acid by selected species. *Appl Environ Microbiol* **66**: 1020-1025.
- Desjardins, A.E. (2006) *Fusarium mycotoxins. Chemistry, Genetics and Biology*. St. Paul: APS Press.
- Desjardins, A.E., and Proctor, R.H. (2007) Molecular biology of *Fusarium* mycotoxins. *Int J Food Microbiol* **119**: 47-50.
- Di Pietro, A., Garcia-MacEira, F.I., Meglecz, E., and Roncero, M.I. (2001) A MAP kinase of the vascular wilt fungus *Fusarium oxysporum* is essential for root penetration and pathogenesis. *Mol Microbiol* **39**: 1140-1152.
- Dodge, B.O., Singleton, J.R., and Rolnick, A. (1948) Studies relative to a temporary revision of *Neurospora tetrasperma* to an 8-spored type. *Science* **108**: 680.
- Domenech, C.E., Giordano, W., Avalos, J., and Cerda-Olmedo, E. (1996.) Separate compartments for the production of sterols, carotenoids and gibberellins in *Gibberella fujikuroi*. *Eur J Biochem* **239**: 720-725.
- Duester, G. (2000) Families of retinoid dehydrogenases regulating vitamin A function. Production of visual pigment and retinoic acid. *Eur J Biochem*. **267**: 4315-4324.
- Dunlap, J.C., and Loros, J.J. (2005) Analysis of circadian rhythms in *neurospora*: overview of assays and genetic and molecular biological manipulation. *Methods Enzymol* **393**: 3-22.
- Dunlap, J.C. (2006) Physiology. Running a clock requires quality time together. *Science* **311**: 184-186.
- Dunlap, J.C., Borkovich, K.A., Henn, M.R., Turner, G.E., Sachs, M.S., Glass, N.L., McCluskey, K., Plamann, M., Galagan, J.E., Birren, B.W., Weiss, R.L., Townsend, J.P., Loros, J.J., Nelson, M.A., Lambregts, R., Colot, H.V., Park, G., Collopy, P., Ringelberg, C., Crew, C., Litvinkova, L., DeCaprio, D., Hood, H.M., Curilla, S., Shi, M., Crawford, M., Koerhsen, M., Montgomery, P., Larson, L., Pearson, M., Kasuga, T., Tian, C., Basturkmen, M., Altamirano, L., and Xu, J. (2007a) Enabling a community to dissect an organism: overview of the *Neurospora* functional genomics project. *Adv Genet* **57**: 49-96.
- Dunlap, J.C., Loros, J.J., Colot, H.V., Mehra, A., Belden, W.J., Shi, M., Hong, C.I., Larrondo, L.F., Baker, C.L., Chen, C.H., Schwerdtfeger, C., Collopy, P.D., Gamsby, J.J., and Lambregts, R. (2007b) A circadian clock in *Neurospora*: how genes and proteins cooperate to produce a sustained, entrainable, and compensated biological oscillator with a period of about a day. *Cold Spring Harb Symp Quant Biol* **72**: 57-68.
- Dutta, S.K. (1976) DNA homologies among heterothallic species of *Neurospora*. *Mycologia* **68**: 388-401.
- Dutta, S.K., Sheikh, I., Choppala, J., Aulakh, G.S., and Nelson, W.H. (1976) DNA homologies among homothallic, pseudo-homothallic and heterothallic species of *Neurospora*. *Mol Gen Genet* **147**: 325-330.

- Edge, R., McGarvey, D.J., and Truscott, T.G. (1997) The carotenoids as anti-oxidants, a review. *J Photochem Photobiol B* **41**: 189-200.
- Eisenreich, W., Menhard, B., Hylands, P.J., Zenk, M.H., and Bacher, A. (1996) Studies on the biosynthesis of taxol: the taxane carbon skeleton is not of mevalonoid origin. *Proc Natl Acad Sci U S A* **93**: 6431-6436.
- Elvin, M., Loros, J.J., Dunlap, J.C., and Heintzen, C. (2005) The PAS/LOV protein VIVID supports a rapidly dampened daytime oscillator that facilitates entrainment of the *Neurospora* circadian clock. *Genes Dev* **19**: 2593-2605.
- Estrada, A.F., and Avalos, J. (2008) The White Collar protein WcoA of *Fusarium fujikuroi* is not essential for photocarotenogenesis, but is involved in the regulation of secondary metabolism and conidiation. *Fung. Genet. Biol.* **45**: 45: 705-718.
- Estrada, A.F., Youssar, L., Scherzinger, D., Al-Babili, S., and Avalos, J. (2008) The *ylo-1* gene encodes an aldehyde dehydrogenase responsible for the last reaction in the *Neurospora* carotenoid pathway. *Mol. Microbiol.* **69**: 1207-1220.
- Estrada, A.F., and Avalos, J. (2009) Regulation and targeted mutation of *opsA*, coding for the NOP-1 opsin orthologue in *Fusarium fujikuroi*. *J. Mol. Biol.* *In press*
- Fan, Y., Shi, L., and Brown, L.S. (2007) Structural basis of diversification of fungal retinal proteins probed by site-directed mutagenesis of *Leptosphaeria* rhodopsin. *FEBS Lett.* **581**: 2557-2561.
- Feldbrugge, M., Kamper, J., Steinberg, G., and Kahmann, R. (2004) Regulation of mating and pathogenic development in *Ustilago maydis*. *Curr Opin Microbiol* **7**: 666-672.
- Feofilova, E.P. (2006) Heterothallism of mucoraceous molds: a review of biological implications and uses in biotechnology. *Prikl Biokhim Mikrobiol* **42**: 501-519.
- Fernandez-Martin, R., Reyes, F., Domenech, C.E., Cabrera, E., Bramley, P.M., Barrero, A.F., Avalos, J., and Cerda-Olmedo, E. (1995) Gibberellin biosynthesis in mutants of *Gibberella fujikuroi*. *J Biol Chem* **270**: 14970-14974.
- Fernandez-Martin, R., Cerda-Olmedo, E., and Avalos, J. (2000) Homologous recombination and allele replacement in transformants of *Fusarium fujikuroi*. *Mol. Gen. Genet.* **263**: 838-845.
- Fischer, G.W., and Holton, C.S. (1957) *Biology and Control of the Smut Fungi*. New York.: Ronald Press Company.
- Flor-Parra, I., Vranes, M., Kamper, J., and Perez-Martin, J. (2006) Biz1, a zinc finger protein required for plant invasion by *Ustilago maydis*, regulates the levels of a mitotic cyclin. *Plant Cell* **18**: 2369-2387.
- Flor-Parra, I., Castillo-Lluva, S., and Perez-Martin, J. (2007) Polar growth in the infectious hyphae of the phytopathogen *Ustilago maydis* depends on a virulence-specific cyclin. *Plant Cell* **19**: 3280-3296.
- Franklin, K.A., Allen, T., and Whitelam, G.C. (2007) Phytochrome A is an irradiance-dependent red light sensor. *Plant J* **50**: 108-117.
- Fraser, P.D., and Bramley, P.M. (2004) The biosynthesis and nutritional uses of carotenoids. *Prog Lipid Res* **43**: 228-265.
- Frengova, G.I., and Beshkova, D.M. (2008) Carotenoids from *Rhodotorula* and *Phaffia*: yeasts of biotechnological importance. *J. Ind. Microbiol. Biotechnol.*: On line preprint.

- Froehlich, A.C., Liu, Y., Loros, J.J., and Dunlap, J.C. (2002) White Collar-1, a circadian blue light photoreceptor, binding to the frequency promoter. *Science* **297**: 815-819.
- Furutani, Y., Sumii, M., Fan, Y., Shi, L., Waschuk, S.A., Brown, L.S., and Kandori, H. (2006) Conformational coupling between the cytoplasmic carboxylic acid and the retinal in a fungal light-driven proton pump. *Biochemistry* **45**: 15349-15358.
- Gaffoor, I., Brown, D.W., Plattner, R., Proctor, R.H., Qi, W., and Trail, F. (2005) Functional analysis of the polyketide synthase genes in the filamentous fungus *Gibberella zeae* (anamorph *Fusarium graminearum*). *Eukaryot Cell* **4**: 1926-1933.
- Galagan, J.E., Calvo, S.E., Borkovich, K.A., Selker, E.U., Read, N.D., Jaffe, D., FitzHugh, W., Ma, L.J., Smirnov, S., Purcell, S., Rehman, B., Elkins, T., Engels, R., Wang, S., Nielsen, C.B., Butler, J., Endrizzi, M., Qui, D., Ianakiev, P., Bell-Pedersen, D., Nelson, M.A., Werner-Washburne, M., Selitrennikoff, C.P., Kinsey, J.A., Braun, E.L., Zelter, A., Schulte, U., Kothe, G.O., Jedd, G., Mewes, W., Staben, C., Marcotte, E., Greenberg, D., Roy, A., Foley, K., Naylor, J., Stange-Thomann, N., Barrett, R., Gnerre, S., Kamal, M., Kamvysselis, M., Mauceli, E., Bielke, C., Rudd, S., Frishman, D., Krystofova, S., Rasmussen, C., Metzenberg, R.L., Perkins, D.D., Kroken, S., Cogoni, C., Macino, G., Catcheside, D., Li, W., Pratt, R.J., Osmani, S.A., DeSouza, C.P., Glass, L., Orbach, M.J., Berglund, J.A., Voelker, R., Yarden, O., Plamann, M., Seiler, S., Dunlap, J., Radford, A., Aramayo, R., Natvig, D.O., Alex, L.A., Mannhaupt, G., Ebbole, D.J., Freitag, M., Paulsen, I., Sachs, M.S., Lander, E.S., Nusbaum, C., and Birren, B. (2003) The genome sequence of the filamentous fungus *Neurospora crassa*. *Nature* **422**: 859-868.
- Galagan, J.E., and Selker, E.U. (2004) RIP: the evolutionary cost of genome defense. *Trends Genet* **20**: 417-423.
- Garcia-Muse, T., Steinberg, G., and Perez-Martin, J. (2004) Characterization of B-type cyclins in the smut fungus *Ustilago maydis*: roles in morphogenesis and pathogenicity. *J Cell Sci* **117**: 487-506.
- Garcia-Pedrajas, M.D., Nadal, M., Bolker, M., Gold, S.E., and Perlin, M.H. (2008) Sending mixed signals: redundancy vs. uniqueness of signaling components in the plant pathogen, *Ustilago maydis*. *Fungal Genet Biol* **45 Suppl 1**: S22-30.
- Geissman, T.A., Verbiscar, A.J., Phinney, B.O., and Cragg, G. (1966) Studies on the biosynthesis of gibberellins from (-)-kaurenoic acid in cultures of *Gibberella fujikuroi*. *Phytochemistry* **5**: 933-947.
- Gelderblom, W.C., Jaskiewicz, K., Marasas, W.F., Thiel, P.G., Horak, R.M., Vleggaar, R., and Kriek, N.P. (1988) Fumonisin, novel mycotoxins with cancer-promoting activity produced by *Fusarium moniliforme*. *Appl Environ Microbiol* **54**: 1806-1811.
- Gilmartin, P.M., Sarokin, L., Memelink, J., and Chua, N.H. (1990) Molecular light switches for plant genes. *Plant Cell* **2**: 369-378.
- Giordano, W., Avalos, J., Cerdá-Olmedo, E., and Domenech, C.E. (1999a) Nitrogen availability and production of bikaverin and gibberellins in *Gibberella fujikuroi*. *FEMS lett.* **173**: 389-393.
- Giordano, W., Avalos, J., Fernandez-Martin, R., Cerdá-Olmedo, E., and Domenech, C.E. (1999b) Lovastatin inhibits the production of gibberellins but not sterol or

- carotenoid biosynthesis in *Gibberella fujikuroi*. *Microbiology* **145** ( Pt 10): 2997-3002.
- Giordano, W., and Domenech, C.E. (1999) Aeration affects acetate destination in *Gibberella fujikuroi*. *FEMS Microbiol Lett* **180**: 111-116.
  - Giovannucci, E., Rimm, E.B., Liu, Y., Stampfer, M.J., and Willett, W.C. (2002) A prospective study of tomato products, lycopene, and prostate cancer risk. *J Natl Cancer Inst* **94**: 391-398.
  - Giuliano, G., Al-Babili, S., and von Lintig, J. (2003) Carotenoid oxygenases: cleave it or leave it. *Trends Plant Sci* **8**: 145-149.
  - Glass, N.L., Vollmer, S.J., Staben, C., Grotelueschen, J., Metzenberg, R.L., and Yanofsky, C. (1988) DNAs of the two mating-type alleles of *Neurospora crassa* are highly dissimilar. *Science* **241**: 570-573.
  - Gold, S.E., Garcia-Pedrajas, M.D., and Martinez-Espinoza, A.D. (2001) New (and used) approaches to the study of fungal pathogenicity. *Annu Rev Phytopathol* **39**: 337-365.
  - Goldie, A.H., and Subden, R.E. (1973a) The neutral carotenoids of wild-type and mutant strains of *Neurospora crassa*. *Biochem Genet* **10**: 275-284.
  - Goldie, A.H., and Subden, R.E. (1973b) Separation of the neutral carotenoids of *Neurospora crassa* using concave gradient elution chromatography. *J Chromatogr* **84**: 192-194.
  - Golubev, W.I. (1995) Perfect state of *Rhodymyces dendrorhous* (*Phaffia rhodozyma*). *Yeast* **11**: 101-110.
  - Gomez-Roldan, V., Feras, S., Brewer, P.B., Puech-Pages, V., Dun, E.A., Pillot, J.P., Letisse, F., Matusova, R., Danoun, S., Portais, J.C., Bouwmeester, H., Becard, G., Beveridge, C.A., Rameau, C., and Rochange, S.F. (2008) Strigolactone inhibition of shoot branching. *Nature* **455**: 189-194.
  - Goodwin, T.W., and Lijinsky, W. (1951) Studies in carotenogenesis. II. Carotene production by *Phycomyces blakesleeana*; the effect of different amino-acids when used in media containing low concentrations of glucose. *Biochem J* **50**: 268-273.
  - Goodwin, T.W., and Srisukh, S. (1949) Some observations on astaxanthin distribution in marine crustacea. *Biochem J* **45**: 268-270.
  - Govind, N.S., and Cerdá-Olmedo, E. (1986) Sexual activation of carotenogenesis in *Phycomyces blakesleeana*. *J. Gen. Microbiol.* **132**: 2775-2780.
  - Grimaldi, B., Coiro, P., Filetici, P., Berge, E., Dobosy, J.R., Freitag, M., Selker, E.U., and Ballario, P. (2006) The *Neurospora crassa* White Collar-1 dependent blue light response requires acetylation of histone H3 lysine 14 by NGF-1. *Mol Biol Cell* **17**: 4576-4583.
  - Hadley, C.W., Miller, E.C., Schwartz, S.J., and Clinton, S.K. (2002) Tomatoes, lycopene, and prostate cancer: progress and promise. *Exp Biol Med (Maywood)* **227**: 869-880.
  - Handelsman, J. (2004) Metagenomics: application of genomics to uncultured microorganisms. *Microbiol Mol Biol Rev* **68**: 669-685.
  - Hanson, J.R., and Fraga, B.M. (2008) Fugenal, a diterpenoid saga of neighbouring group participation. *Phytochemistry* **69**: 2104-2109.

- Harding, R.W., Huang, P.C., and Mitchell, H.K. (1969) Photochemical studies of the carotenoid biosynthetic pathway in *Neurospora crassa*. *Arch. Biochem. Biophys.* **129**: 696-707.
- Harding, R.W. (1974) The effect of temperature on photo-induced carotenoid biosynthesis in *Neurospora crassa*. *Plant Physiol* **54**: 142-147.
- Harding, R.W., and Turner, R.V. (1981) Photoregulation of the carotenoid biosynthetic pathway in albino and *white collar* mutants of *Neurospora crassa*. *Plant Physiol.* **68**: 745-749.
- Harding, R.W., and Melles, S. (1983) Genetic Analysis of Phototropism of *Neurospora crassa* Perithecial Beaks Using White Collar and Albino Mutants. *Plant Physiol* **72**: 996-1000.
- Harding, R.W., Philip, D.Q., Drozdowicz, B.Z., and Williams, N.O. (1984) A *Neurospora crassa* mutant whit overaccumulates carotenoids pigments. *Neurospora newsletter* **31**: 23-25.
- Haug, S., and Braun-Falco, M. (2006) Restoration of fatty aldehyde dehydrogenase deficiency in Sjögren-Larsson syndrome. *Gene Ther.* **13**: 1021-1026.
- Hausmann, A., and Sandmann, G. (2000) A single five-step desaturase is involved in the carotenoid biosynthesis pathway to beta-carotene and torulene in *Neurospora crassa*. *Fungal Genet Biol* **30**: 147-153.
- He, Q., Cha, J., He, Q., Lee, H.C., Yang, Y., and Liu, Y. (2006) CKI and CKII mediate the FREQUENCY-dependent phosphorylation of the WHITE COLLAR complex to close the *Neurospora* circadian negative feedback loop. *Genes Dev* **20**: 2552-2565.
- He, Q., Cheng, P., Yang, Y., Wang, L., Gardner, K.H., and Liu, Y. (2002) White collar-1, a DNA binding transcription factor and a light sensor. *Science* **297**: 840-843.
- He, Q., and Liu, Y. (2005) Molecular mechanism of light responses in *Neurospora*: from light-induced transcription to photoadaptation. *Genes Dev* **19**: 2888-2899.
- Heintzen, C., Loros, J.J., and Dunlap, J.C. (2001) The PAS protein VIVID defines a clock-associated feedback loop that represses light input, modulates gating, and regulates clock resetting. *Cell* **104**: 453-464.
- Herrera-Estrella, A., and Horwitz, B.A. (2007) Looking through the eyes of fungi: molecular genetics of photoreception. *Mol. Microbiol.* **64**: 5-15.
- Hirschberg, J. (2001) Carotenoid biosynthesis in flowering plants. *Curr Opin Plant Biol* **4**: 210-218.
- Hoffman, C.S., and Winston, F. (1987) A ten-minute DNA preparation from yeast efficiently releases autonomous plasmids for transformation of *Escherichia coli*. *Gene* **57**: 267-272.
- Holliday, R. (1974a) *Ustilago maydis*. In *Handbook. of genetics*. Vol. I. King, R.C. (ed). New York: Plenum Press, pp. 575-595.
- Holliday, R. (1974b) Molecular aspects of genetic exchange and gene conversion. *Genetics* **78**: 273-287.
- Horbach, S., Sahm, H., and Welle, R. (1993) Isoprenoid biosynthesis in bacteria: two different pathways? *FEMS Microbiol Lett* **111**: 135-140.
- Hori, S. (1898) Some observations on 'bakanae' disease of the rice plant. *Mem. Agric. Res. Sta. (Tokyo)* **12**: 110-119.

- 
- Hundle, B., Alberti, M., Nievelstein, V., Beyer, P., Kleinig, H., Armstrong, G.A., Burke, D.H., and Hearst, J.E. (1994) Functional assignment of *Erwinia herbicola* Eho10 carotenoid genes expressed in *Escherichia coli*. *Mol Gen Genet* **245**: 406-416.
  - Hungate, M.V.G. (1945) *Genetic study of albino mutants of Neurospora crassa*. Stanford, California: Stanford University.
  - Hynes, M.J. (2003) The *Neurospora crassa* genome opens up the world of filamentous fungi. *Genome Biol* **4**: 217.
  - Idnurm, A., and Howlett, B.J. (2001) Characterization of an opsin gene from the ascomycete *Leptosphaeria maculans*. *Genome* **44**: 167-171.
  - Idnurm, A., and Heitman, J. (2005) Light controls growth and development via a conserved pathway in the fungal kingdom. *PLoS Biol.* **3**: e95.
  - Idnurm, A., Rodriguez-Romero, J., Corrochano, L.M., Sanz, C., Iturriaga, E.A., Eslava, A.P., and Heitman, J. (2006) The *Phycomyces mada* gene encodes a blue-light photoreceptor for phototropism and other light responses. *Proc. Natl. Acad. Sci. U S A* **103**: 4546-4551.
  - Iigusa, H., Yoshida, Y., and Hasunuma, K. (2005) Oxygen and hydrogen peroxide enhance light-induced carotenoid synthesis in *Neurospora crassa*. *FEBS Lett.* **579**: 4012-4016.
  - Iimura, Y., and Tatsumi, K. (2002) Structure of genes for Hsp30 from the white-rot fungus *Coriolus versicolor* and the increase of their expression by heat shock and exposure to a hazardous chemical. *Biosci. Biotechnol. Biochem.* **66**: 1567-1570.
  - Innocenti, F.D., Pohl, U., and Russo, V.E. (1983) Photoinduction of protoperithecia in *Neurospora crassa* by blue light. *Photochem Photobiol* **37**: 49-51.
  - Ishibashi, K., Suzuki, K., Ando, Y., Takakura, C., and Inoue, H. (2006) Nonhomologous chromosomal integration of foreign DNA is completely dependent on MUS-53 (human Lig4 homolog) in *Neurospora*. *Proc Natl Acad Sci U S A* **103**: 14871-14876.
  - Jacobson, D.J., Dettman, J.R., Adams, R.I., Boesl, C., Sultana, S., Roenneberg, T., Merrow, M., Duarte, M., Marques, I., Ushakova, A., Carneiro, P., Videira, A., Navarro-Sampedro, L., Olmedo, M., Corrochano, L.M., and Taylor, J.W. (2006) New findings of *Neurospora* in Europe and comparisons of diversity in temperate climates on continental scales. *Mycologia* **98**: 550-559.
  - Johnson, E.A., and Lewis, M.J. (1979) "Astaxanthin Formation by the Yeast *Phaffia rhodozyma*". *Gen. Microbiol.* **115**: 173-183.
  - Johnson, E.A., and Schroeder, W.A. (1996) Microbial carotenoids. *Adv. Biochem. Eng. Biotechnol.* **53**: 119-178.
  - Johnson, E.A. (2003) *Phaffia rhodozyma*: colorful odyssey. *Int. Microbiol.* **6**: 169-174.
  - Jung, K.H., Trivedi, V.D., and Spudich, J.L. (2003a) Demonstration of a sensory rhodopsin in eubacteria. *Mol Microbiol* **47**: 1513-1522.
  - Juttner, F. (1984) Dynamics of the Volatile Organic Substances Associated with Cyanobacteria and Algae in a Eutrophic Shallow Lake. *Appl Environ Microbiol* **47**: 814-820.
  - Jyonouchi, H., Zhang, L., and Tomita, Y. (1993) Studies of immunomodulating actions of carotenoids. II. Astaxanthin enhances in vitro antibody production to T-dependent antigens without facilitating polyclonal B-cell activation. *Nutr Cancer* **19**: 269-280.

- Kahmann, R., Basse, C., and Feldbrugge, M. (1999) Fungal-plant signalling in the *Ustilago maydis*-maize pathosystem. *Curr Opin Microbiol* **2**: 647-650.
- Kahmann, R., Steinberg, G., Basse, C., Feldbrügge, M., and Kämper, J. (2000) *Ustilago maydis*, the causative agent of corn smut disease. Dordrecht, The Netherlands: Kluwer.
- Kaldi, K., Gonzalez, B.H., and Brunner, M. (2006) Transcriptional regulation of the *Neurospora* circadian clock gene *wc-1* affects the phase of circadian output. *EMBO Rep* **7**: 199-204.
- Kämper, J. (2004) A PCR-based system for highly efficient generation of gene replacement mutants in *Ustilago maydis*. *Mol. Genet. Genomics* **271**: 103-110.
- Kämper, J., Kahmann, R., Bolker, M., Ma, L.J., Brefort, T., Saville, B.J., Banuett, F., Kronstad, J.W., Gold, S.E., Muller, O., Perlin, M.H., Wosten, H.A., de Vries, R., Ruiz-Herrera, J., Reynaga-Pena, C.G., Snetselaar, K., McCann, M., Perez-Martin, J., Feldbrugge, M., Basse, C.W., Steinberg, G., Ibeas, J.I., Holloman, W., Guzman, P., Farman, M., Stajich, J.E., Sentandreu, R., Gonzalez-Prieto, J.M., Kennell, J.C., Molina, L., Schirawski, J., Mendoza-Mendoza, A., Greilinger, D., Munch, K., Rossel, N., Scherer, M., Vranes, M., Ladendorf, O., Vincon, V., Fuchs, U., Sandrock, B., Meng, S., Ho, E.C., Cahill, M.J., Boyce, K.J., Klose, J., Klosterman, S.J., Deelstra, H.J., Ortiz-Castellanos, L., Li, W., Sanchez-Alonso, P., Schreier, P.H., Hauser-Hahn, I., Vaupel, M., Koopmann, E., Friedrich, G., Voss, H., Schluter, T., Margolis, J., Platt, D., Swimmer, C., Gnirke, A., Chen, F., Vysotskaia, V., Mannhaupt, G., Guldener, U., Munsterkotter, M., Haase, D., Oesterheld, M., Mewes, H.W., Mauceli, E.W., DeCaprio, D., Wade, C.M., Butler, J., Young, S., Jaffe, D.B., Calvo, S., Nusbaum, C., Galagan, J., and Birren, B.W. (2006) Insights from the genome of the biotrophic fungal plant pathogen *Ustilago maydis*. *Nature* **444**: 97-101.
- Kerenyi, Z., Moretti, A., Waalwijk, C., Olah, B., and Hornok, L. (2004) Mating type sequences in asexually reproducing *Fusarium* species. *Appl Environ Microbiol* **70**: 4419-4423.
- Kershaw, M.J., and Talbot, N.J. (1998) Hydrophobins and Repellents: Proteins with fundamental roles in fungal morphogenesis. *Fungal Genet. Biol.* **23**: 18-33.
- Klein, R.M. (1992) Effects of green light on biological systems. *Biol Rev Camb Philos Soc* **67**: 199-284.
- Klittich, C., and Leslie, J.F. (1988) Nitrate Reduction Mutants of *Fusarium moniliforme* (*Gibberella Fujikuroi*). *Genetics* **118**: 417-423.
- Kloer, D.P., Ruch, S., Al-Babili, S., Beyer, P., and Schulz, G.E. (2005) The structure of a retinal-forming carotenoid oxygenase. *Science* **308**: 267-269.
- Kloer, D.P., and Schulz, G.E. (2006) Structural and biological aspects of carotenoid cleavage. *Cell Mol Life Sci* **63**: 2291-2303.
- Klosterman, S.J., Perlin, M.H., Garcia-Pedrajas, M., Covert, S.F., and Gold, S.E. (2007) Genetics of morphogenesis and pathogenic development of *Ustilago maydis*. *Adv Genet* **57**: 1-47.
- Krinsky, N.I., Landrum, J.T., and Bone, R.A. (2003) Biologic mechanisms of the protective role of lutein and zeaxanthin in the eye. *Annu Rev Nutr* **23**: 171-201.

- Krubasik, P., and Sandmann, G. (2000) Molecular evolution of lycopene cyclases involved in the formation of carotenoids with ionone end groups. *Biochem Soc Trans* **28**: 806-810.
- Kuhlman, E.G. (1983) Varieties of *Gibberella fujikuroi* with anamorphs in *Fusarium* section *Liseola*. *Mycologia* **74**: 759-768.
- Kumagai, T., Yoshioka, N., and Oda, Y. (1976) Further studies on the blue and near ultraviolet reversible photoreaction with an intracellular particulate fraction of the fungus, *Alternaria tomato*. *Biochim Biophys Acta* **421**: 133-140.
- Lauter, F.R., and Russo, V.E. (1991) Blue light induction of conidiation-specific genes in *Neurospora crassa*. *Nucleic Acids Res.* **19**: 6883-6886.
- Lauter, F.R., Russo, V.E., and Yanofsky, C. (1992) Developmental and light regulation of *ea*s, the structural gene for the rodlet protein of *Neurospora*. *Genes Dev* **6**: 2373-2381.
- Lauter, F.R., Yamashiro, C.T., and Yanofsky, C. (1997) Light stimulation of conidiation in *Neurospora crassa*: studies with the wild-type strain and mutants *wc-1*, *wc-2* and *acon-2*. *J Photochem Photobiol B: Biology* **37**: 203-211.
- Lee, B., Yoshida, Y., and Hasunuma, K. (2006) Photomorphogenetic characteristics are severely affected in nucleoside diphosphate kinase-1 (*ndk-1*)-disrupted mutants in *Neurospora crassa*. *Mol Genet Genomics* **275**: 9-17.
- Leslie, J. (1991) Mating populations in *Gibberella fujikuroi* (*Fusarium* section *Liseola*). *Phytopathology* **81**: 1058-1060.
- Leslie, J.F., and Klein, K.K. (1996) Female fertility and mating type effects on effective population size and evolution in filamentous fungi. *Genetics* **144**: 557-567.
- Leslie, J.F., and Summerell, B.A. (2006) *The Fusarium laboratory manual*: Blackwell Publishing.
- Lew, R.R. (2005) Mass flow and pressure-driven hyphal extension in *Neurospora crassa*. *Microbiology* **151**: 2685-2692.
- Lewis, Z.A., Correa, A., Schwerdtfeger, C., Link, K.L., Xie, X., Gomer, R.H., Thomas, T., Ebbole, D.J., and Bell-Pedersen, D. (2002) Overexpression of White Collar-1 (WC-1) activates circadian clock-associated genes, but is not sufficient to induce most light-regulated gene expression in *Neurospora crassa*. *Mol Microbiol* **45**: 917-931.
- Li, C., and Schmidhauser, T.J. (1995) Developmental and photoregulation of *al-1* and *al-2*, structural genes for two enzymes essential for carotenoid biosynthesis in *Neurospora*. *Dev Biol* **169**: 90-95.
- Li, Q.H., and Yang, H.Q. (2007) Cryptochrome signaling in plants. *Photochem Photobiol* **83**: 94-101.
- Lichtenthaler, H.K., Schwender, J., Disch, A., and Rohmer, M. (1997) Biosynthesis of isoprenoids in higher plant chloroplasts proceeds via a mevalonate-independent pathway. *FEBS Lett* **400**: 271-274.
- Limura, Y., and Tatsumi, K. (2002) Structure of genes for Hsp30 from the white-rot fungus *Coriolus versicolor* and the increase of their expression by heat shock and exposure to a hazardous chemical. *Biosci Biotechnol Biochem* **66**: 1567-1570.
- Linden, H., Ballario, P., and Macino, G. (1997a) Blue light regulation in *Neurospora crassa*. *Fungal Genet. Biol.* **22**: 141-150.



- Linden, H., and Macino, G. (1997) White collar 2, a partner in blue-light signal transduction, controlling expression of light-regulated genes in *Neurospora crassa*. *Embo J.* **16**: 98-109.
- Linden, H., Rodriguez-Franco, M., and Macino, G. (1997b) Mutants of *Neurospora crassa* defective in regulation of blue light perception. *Mol Gen Genet* **254**: 111-118.
- Linden, H., Ballario, P., Arpaia, G., and Macino, G. (1999) Seeing the light: news in *Neurospora* blue light signal transduction. *Adv Genet* **41**: 35-54.
- Linden, H. (2002) Blue light perception and signal transduction in *Neurospora crassa*. In *Molecular Biology of Fungal Development*. Osiewacz, H.D. (ed). New York: Marcel Dekker, pp. 165–185.
- Lindquist, S. (1992) Heat-shock proteins and stress tolerance in microorganisms. *Curr Opin. Genet. Dev.* **2**: 748-755.
- Linnemannstons, P., Prado, M.M., Fernandez-Martin, R., Tudzynski, B., and Avalos, J. (2002a) A carotenoid biosynthesis gene cluster in *Fusarium fujikuroi*: the genes *carB* and *carRA*. *Mol. Genet. Genomics* **267**: 593-602.
- Linnemannstons, P., Schulte, J., del Mar Prado, M., Proctor, R.H., Avalos, J., and Tudzynski, B. (2002b) The polyketide synthase gene *pk4* from *Gibberella fujikuroi* encodes a key enzyme in the biosynthesis of the red pigment bikaverin. *Fungal Genet. Biol.* **37**: 134-148.
- Liu, Y., He, Q., and Cheng, P. (2003) Photoreception in *Neurospora*: a tale of two White Collar proteins. *Cell. Mol. Life Sci.* **60**: 2131-2138.
- Liu, Y.S., and Wu, J.Y. (2006) Hydrogen peroxide-induced astaxanthin biosynthesis and catalase activity in *Xanthophyllomyces dendrorhous*. *Appl. Microbiol. Biotechnol.* **73**: 663-668.
- Lowry, R.J., Durkee, T.L., and Sussman, A.S. (1967) Ultrastructural studies of microconidium formation in *Neurospora crassa*. *J Bacteriol* **94**: 1757-1763.
- Lu, S., and Li, L. (2008) Carotenoid metabolism: biosynthesis, regulation, and beyond. *J Integr Plant Biol* **50**: 778-785.
- Lu, Y.K., Sun, K.H., and Shen, W.C. (2005) Blue light negatively regulates the sexual filamentation via the Cwc1 and Cwc2 proteins in *Cryptococcus neoformans*. *Mol. Microbiol.* **56**: 480-491.
- Luecke, H., Schobert, B., Richter, H.T., Cartailier, J.P., and Lanyi, J.K. (1999) Structure of bacteriorhodopsin at 1.55 Å resolution. *J. Mol. Biol.* **291**: 899-911.
- Luecke, H., Schobert, B., Stagno, J., Imasheva, E.S., Wang, J.M., Balashov, S.P., and Lanyi, J.K. (2008) Crystallographic structure of xanthorhodopsin, the light-driven proton pump with a dual chromophore. *Proc Natl Acad Sci U S A* **105**: 16561-16565.
- MacMillan, J. (1997) Biosynthesis of the gibberellin plant hormones. *Nat. Prod. Rep.* **14**: 221–244.
- MacMillan, J. (2001) Occurrence of Gibberellins in Vascular Plants, Fungi, and Bacteria. *J. Plant Growth Regul.* **20**: 387-442.
- Maiani, G., Periago Caston, M.J., Catasta, G., Toti, E., Cambrodon, I.G., Bysted, A., Granado-Lorencio, F., Olmedilla-Alonso, B., Knuthsen, P., Valoti, M., Bohm, V., Mayer-Miebach, E., Behnlian, D., and Schlemmer, U. (2008) Carotenoids: Actual

- knowledge on food sources, intakes, stability and bioavailability and their protective role in humans. *Mol Nutr Food Res*.
- Malonek, S., Bomke, C., Bornberg-Bauer, E., Rojas, M.C., Hedden, P., Hopkins, P., and Tudzynski, B. (2005) Distribution of gibberellin biosynthetic genes and gibberellin production in the *Gibberella fujikuroi* species complex. *Phytochemistry* **66**: 1296-1311.
  - Marasas, W.F., and Van Rensburg, S.J. (1986) Mycotoxicological investigations on maize and groundnuts from the endemic area of Mseleni joint disease in Kwazulu. *S Afr Med J* **69**: 369-374.
  - Marasas, W.F., Jaskiewicz, K., Venter, F.S., and Van Schalkwyk, D.J. (1988) *Fusarium moniliforme* contamination of maize in oesophageal cancer areas in Transkei. *S Afr Med J* **74**: 110-114.
  - Mares-Perlman, J.A., Millen, A.E., Ficek, T.L., and Hankinson, S.E. (2002) The body of evidence to support a protective role for lutein and zeaxanthin in delaying chronic disease. Overview. *J Nutr* **132**: 518S-524S.
  - Martinez-Espinoza, A.D., Garcia-Pedrajas, M.D., and Gold, S.E. (2002) The Ustilaginales as plant pests and model systems. *Fungal Genet Biol* **35**: 1-20.
  - Martinez-Espinoza, A.D., Ruiz-Herrera, J., Leon-Ramirez, C.G., and Gold, S.E. (2004) MAP kinase and cAMP signaling pathways modulate the pH-induced yeast-to-mycelium dimorphic transition in the corn smut fungus *Ustilago maydis*. *Curr Microbiol* **49**: 274-281.
  - Marzluf, G.A. (1997) Genetic regulation of nitrogen metabolism in the fungi. *Microbiol Mol Biol Rev* **61**: 17-32.
  - McCluskey, K. (2003) The Fungal Genetics Stock Center: from molds to molecules. *Adv. Appl. Microbiol.* **52**: 245-262.
  - Medentsev, A.G., and Akimenko, V.K. (1998) Naphthoquinone metabolites of the fungi. *Phytochemistry* **47**: 935-959.
  - Mehta, B., and Cerdá-Olmedo, E. (1995) Mutants of Carotene Production in *Blakeslea trispora*. *Applied Microbiology and Biotechnology* **42**: 836-838.
  - Mehta, B.J., Salgado, L.M., Bejarano, E.R., and Cerda-Olmedo, E. (1997) New Mutants of *Phycomyces blakesleeanus* for (beta)-Carotene Production. *Appl Environ Microbiol* **63**: 3657-3661.
  - Mehta, B.J., Obratsova, I.N., and Cerda-Olmedo, E. (2003) Mutants and intersexual heterokaryons of *Blakeslea trispora* for production of beta-carotene and lycopene. *Appl. Environ. Microbiol.* **69**: 4043-4048.
  - Mein, J.R., Lian, F., and Wang, X.D. (2008) Biological activity of lycopene metabolites: implications for cancer prevention. *Nutr Rev* **66**: 667-683.
  - Mende, K., Homann, V., and Tudzynski, B. (1997) The geranylgeranyl diphosphate synthase gene of *Gibberella fujikuroi*: isolation and expression. *Mol Gen Genet* **255**: 96-105.
  - Mendgen, K., Hahn, M., and Deising, H. (1996) Morphogenesis and mechanisms of penetration by plant pathogenic fungi. *Annu Rev Phytopathol* **34**: 367-386.
  - Menon, S., T., Han, M., and Sakmar, T.P. (2001) Rhodopsin: structural basis of molecular physiology. *Physiol. Rev.* **81**: 1659-1688.

- Menzella, H.G., Reid, R., Carney, J.R., Chandran, S.S., Reisinger, S.J., Patel, K.G., Hopwood, D.A., and Santi, D.V. (2005) Combinatorial polyketide biosynthesis by de novo design and rearrangement of modular polyketide synthase genes. *Nat Biotechnol* **23**: 1171-1176.
- Michan, S., Lledias, F., and Hansberg, W. (2003) Asexual development is increased in *Neurospora crassa* cat-3-null mutant strains. *Eukaryot Cell* **2**: 798-808.
- Mihlan, M., Homann, V., Liu, T.W., and Tudzynski, B. (2003) AREA directly mediates nitrogen regulation of gibberellin biosynthesis in *Gibberella fujikuroi*, but its activity is not affected by NMR. *Mol. Microbiol.* **47**: 975-991.
- Ming, Y.N., Lin, P.C., and Yu, T.F. (1966) Heterokaryosis in *Fusarium fujikuroi* (Saw.) Wr. *Sci Sin* **15**: 371-378.
- Misawa, N., Satomi, Y., Kondo, K., Yokoyama, A., Kajiwarra, S., Saito, T., Ohtani, T., and Miki, W. (1995) Structure and functional analysis of a marine bacterial carotenoid biosynthesis gene cluster and astaxanthin biosynthetic pathway proposed at the gene level. *J Bacteriol* **177**: 6575-6584.
- Mishra, N.C., and Tatum, E.L. (1973) Non-Mendelian inheritance of DNA-induced inositol independence in *Neurospora*. *Proc Natl Acad Sci U S A* **70**: 3875-3879.
- Mitzka-Schnabel, U., and Rau, W. (1980) The subcellular distribution of carotenoids in *Neurospora crassa*. *Phytochemistry* **19**: 1409-1413.
- Mitzka-Schnabel, U. (1985) Carotenogenic enzymes from *Neurospora*. *Pure & Appl. Chem.* **57**: 667-669.
- Moise, A.R., von Lintig, J., and Palczewski, K. (2005) Related enzymes solve evolutionarily recurrent problems in the metabolism of carotenoids. *Trends Plant Sci* **10**: 178-186.
- Molina, L., and Kahmann, R. (2007) An *Ustilago maydis* gene involved in H<sub>2</sub>O<sub>2</sub> detoxification is required for virulence. *Plant Cell* **19**: 2293-2309.
- Mooney, J.L., and Yager, L.N. (1990) Light is required for conidiation in *Aspergillus nidulans*. *Genes Dev* **4**: 1473-1482.
- Moretti, A., Mule, G., Ritieni, A., and Logrieco, A. (2007) Further data on the production of beauvericin, enniatins and fusaproliferin and toxicity to *Artemia salina* by *Fusarium* species of *Gibberella fujikuroi* species complex. *Int J Food Microbiol* **118**: 158-163.
- Müller, P., Aichinger, C., Feldbrügge, M., and Kahmann, R. (1999) The MAP kinase kpp2 regulates mating and pathogenic development in *Ustilago maydis*. *Mol. Microbiol.* **34**: 1007-1017.
- Murillo, F.J., and Cerda-Olmedo, E. (1976) Regulation of carotene synthesis in *Phycomyces*. *Mol Gen Genet* **148**: 19-24.
- Nadal, M., Garcia-Pedrajas, M.D., and Gold, S.E. (2008) Dimorphism in fungal plant pathogens. *FEMS Microbiol Lett* **284**: 127-134.
- Nambara, E., and Marion-Poll, A. (2005) Absciscic acid biosynthesis and catabolism. *Annu Rev Plant Biol* **56**: 165-185.
- Napoli, J.L. (1996) Biochemical pathways of retinoid transport, metabolism, and signal transduction. *Clin. Immunol. Immunopathol.* **80**: S52-S62.

- Navarro, E., Ruiz-Perez, V.L., and Torres-Martinez, S. (2000) Overexpression of the *crgA* gene abolishes light requirement for carotenoid biosynthesis in *Mucor circinelloides*. *Eur J Biochem* **267**: 800-807.
- Navarro, E., Lorca-Pascual, J.M., Quiles-Rosillo, M.D., Nicolas, F.E., Garre, V., Torres-Martinez, S., and Ruiz-Vazquez, R.M. (2001) A negative regulator of light-inducible carotenogenesis in *Mucor circinelloides*. *Mol Genet Genomics* **266**: 463-470.
- Navarro-Sampedro, L., Yanofsky, C., and Corrochano, L.M. (2008) A genetic selection for *Neurospora crassa* mutants altered in their light regulation of transcription. *Genetics* **178**: 171-183.
- Nelson, M.A., Morelli, G., Carattoli, A., Romano, N., and Macino, G. (1989) Molecular cloning of a *Neurospora crassa* carotenoid biosynthetic gene (*albino-3*) regulated by blue light and the products of the white collar genes. *Mol Cell Biol* **9**: 1271-1276.
- Nelson, P.E., Dignani, M.C., and Anaissie, E.J. (1994) Taxonomy, biology, and clinical aspects of *Fusarium* species. *Clin Microbiol Rev* **7**: 479-504.
- Neutze, R., Pebay-Peyroula, E., Edman, K., Royant, A., Navarro, J., and Landau, E.M. (2002) Bacteriorhodopsin: a high-resolution structural view of vectorial proton transport. *Biochim Biophys Acta* **1565**: 144-167.
- Ninnemann, H. (1991) Photostimulation of conidiation in mutants of *Neurospora crassa*. *J Photochem Photobiol B* **9**: 189-199.
- Ninomiya, Y., Suzuki, K., Ishii, C., and Inoue, H. (2004) Highly efficient gene replacements in *Neurospora* strains deficient for nonhomologous end-joining. *Proc Natl Acad Sci U S A* **101**: 12248-12253.
- Nirenberg, H., and O'Donnell, K. (1998) New *Fusarium* species and combinations within the *Gibberella fujikuroi* species complex. *Mycologia* **90**: 434-458.
- O'Donnell, K., Cigelnik, E., and Nirenberg, H.I. (1998) Molecular systematics and phylogeography of the *Gibberella fujikuroi* species complex. *Mycologia* **90**: 465-493.
- O'Hagan, D. (1993) Biosynthesis of fatty acid and polyketide metabolites. *Nat Prod Rep* **10**: 593-624.
- Ojima, K., Breitenbach, J., Visser, H., Setoguchi, Y., Tabata, K., Hoshino, T., van den Berg, J., and Sandmann, G. (2006) Cloning of the astaxanthin synthase gene from *Xanthophyllomyces dendrorhous* (*Phaffia rhodozyma*) and its assignment as a beta-carotene 3-hydroxylase/4-ketolase. *Mol. Genet. Genomics* **275**: 148-158.
- Ortoneda, M., Guarro, J., Madrid, M.P., Caracuel, Z., Roncero, M.I., Mayayo, E., and Di Pietro, A. (2004) *Fusarium oxysporum* as a multihost model for the genetic dissection of fungal virulence in plants and mammals. *Infect Immun* **72**: 1760-1766.
- Pan, J.J., Baumgarten, A.M., and May, G. (2008) Effects of host plant environment and *Ustilago maydis* infection on the fungal endophyte community of maize (*Zea mays*). *New Phytol* **178**: 147-156.
- Pappa, A., Estey, T., Manzer, R., Brown, D., and Vasiliou, V. (2003) Human aldehyde dehydrogenase 3A1 (ALDH3A1): biochemical characterization and immunohistochemical localization in the cornea. *Biochem J* **376**: 615-623.

- Perkins, D.D. (1949) Biochemical mutants in the smut fungus *Ustilago maydis*. *Genetics* **34**: 607-626.
- Perkins, D.D., and Davis, R.H. (2000a) Evidence for safety of *Neurospora* species for academic and commercial uses. *Appl Environ Microbiol* **66**: 5107-5109.
- Perkins, D.D., and Davis, R.H. (2000b) *Neurospora* at the millennium. *Fungal Genet Biol* **31**: 153-167.
- Perkins, D.D., Radford, A., and Sachs, M.S. (2001) *The Neurospora compendium. Chromosomal loci*. San Diego, Calif.: Academic Press, Inc.
- Posch, K.C., Burns, R.D., and Napoli, J.L. (1992) Biosynthesis of all trans-retinoic acid from retinal: recognition of retinal bound to cellular retinol binding protein (type I) as substrate by a purified cytosolic dehydrogenase. *J. Biol. Chem.* **267**: 19676-19682.
- Prado, M.M., Prado-Cabrero, A., Fernandez-Martin, R., and Avalos, J. (2004) A gene of the opsin family in the carotenoid gene cluster of *Fusarium fujikuroi*. *Curr. Genet.* **46**: 47-58.
- Prado-Cabrero, A., Estrada, A.F., Al-Babili, S., and Avalos, J. (2007a) Identification and biochemical characterization of a novel carotenoid oxygenase: elucidation of the cleavage step in the *Fusarium* carotenoid pathway. *Mol. Microbiol.* **64**: 448-460.
- Prado-Cabrero, A., Scherzinger, D., Avalos, J., and Al-Babili, S. (2007b) Retinal biosynthesis in fungi: Characterization of the carotenoid oxygenase CarX from *Fusarium fujikuroi*. *Eukaryot. Cell* **6**: 650-657.
- Proctor, R.H., Hohn, T.M., and McCormick, S.P. (1997) Restoration of wild-type virulence to Tri5 disruption mutants of *Gibberella zeae* via gene reversion and mutant complementation. *Microbiology-Uk* **143**: 2583-2591.
- Puhalla, J.E., and Spieth, P.T. (1983) Heterokaryosis in *Fusarium moniliforme*. *Exp Mycol* **7**: 328-335.
- Puhalla, J.E., and Spieth, P.T. (1985) A comparison of heterokaryosis and vegetative incompatibility among varieties of *Gibberella fujikuroi* (*Fusarium moniliforme*). *Exp Mycol* **9**: 39-47.
- Quiles-Rosillo, M.D., Ruiz-Vázquez, R.M., Torres-Martínez, S., and Garre, V. (2005) Light induction of the carotenoid biosynthesis pathway in *Blakeslea trispora*. *Fungal Genet. Biol.* **42**: 141-153.
- Raju, N.B. (1980) Meiosis and ascospore genesis in *Neurospora*. *Eur J Cell Biol* **23**: 208-223.
- Raju, N.B., and Leslie, J.F. (1992) Cytology of recessive sexual-phase mutants from wild strains of *Neurospora crassa*. *Genome* **35**: 815-826.
- Rau, W., Feuser, B., and Rau-Hund, A. (1967) Substitution of p-chloro- or p-hydroxymercuribenzoate for light in carotenoid synthesis by *Fusarium aquaeductum*. *Biochim Biophys Acta* **136**: 589-590.
- Reyes-Martinez, M.A., and Zavaleta, A. (2005) Bacteriorhodopsina: una molécula peculiar. *Ciencia e investigación*. VIII (1): 48-57
- Ridge, K. (2002) Algal rhodopsins: phototaxis receptors found at last. *Curr. Biol.* **12**: R588-R590.

- 
- Rodriguez-Bustamante, E., and Sanchez, S. (2007) Microbial production of C13-norisoprenoids and other aroma compounds via carotenoid cleavage. *Crit Rev Microbiol* **33**: 211-230.
  - Rodriguez-Ortiz, R., Limon, M.C., and Avalos, J. (2008) Nitrogen regulation of carotenogenesis and secondary metabolism in wild type and carotenoid overproducing mutants of *Fusarium fujikuroi*. *Appl Environ Microbiol*.
  - Rodriguez-Romero, J., and Corrochano, L.M. (2004) The gene for the heat-shock protein HSP100 is induced by blue light and heat-shock in the fungus *Phycomyces blakesleeanus*. *Curr Genet* **46**: 295-303.
  - Rodriguez-Romero, J., and Corrochano, L.M. (2006) Regulation by blue light and heat shock of gene transcription in the fungus *Phycomyces*: proteins required for photoinduction and mechanism for adaptation to light. *Mol. Microbiol.* **61**: 1049-1059.
  - Rohmer, M., Knani, M., Simonin, P., Sutter, B., and Sahm, H. (1993) Isoprenoid biosynthesis in bacteria: a novel pathway for the early steps leading to isopentenyl diphosphate. *Biochem J* **295** ( Pt 2): 517-524.
  - Rojas, M.C., Urrutia, O., Cruz, C., Gaskin, P., Tudzynski, B., and Hedden, P. (2004) Kaurenolides and fujenoic acids are side products of the gibberellin P450-1 monooxygenase in *Gibberella fujikuroi*. *Phytochemistry* **65**: 821-830.
  - Romano, N., and Macino, G. (1992) Quelling: transient inactivation of gene expression in *Neurospora crassa* by transformation with homologous sequences. *Mol Microbiol* **6**: 3343-3353.
  - Romer, S., and Fraser, P.D. (2005) Recent advances in carotenoid biosynthesis, regulation and manipulation. *Planta* **221**: 305-308.
  - Royer, J.C., and Yamashiro, C.T. (1992) Generation of transformable spheroplasts from mycelia, macroconidia, microconidia and germinating ascospores of *Neurospora crassa*. *Fungal Genet. Newslett.* **39**: 76-79.
  - Ruch, S., Beyer, P., Ernst, H., and Al-Babili, S. (2005) Retinal biosynthesis in Eubacteria: in vitro characterization of a novel carotenoid oxygenase from *Synechocystis sp.* PCC 6803. *Mol. Microbiol.* **55**: 1015-1024.
  - Ruiz-Herrera, J., León, G.C., Guevara, L.O., and Cáramez, A.T. (1995 ) Yeast-mycelial dimorphism of haploid and diploid strains of *Ustilago maydis*. *Microbiology* **141**: 695-703.
  - Ruiz-Herrera, J., and Martinez-Espinoza, A.D. (1998) The fungus *Ustilago maydis*, from the aztec cuisine to the research laboratory. *Int Microbiol* **1**: 149-158.
  - Ruiz-Hidalgo, M.J., Benito, E.P., Sandmann, G., and Eslava, A.P. (1997) The phytoene dehydrogenase gene of *Phycomyces*: regulation of its expression by blue light and vitamin A. *Mol Gen Genet* **253**: 734-744.
  - Ruiz-Roldan, M.C., Garre, V., Guarro, J., Marine, M., and Roncero, M.I. (2008) Role of the *white collar 1* photoreceptor in carotenogenesis, UV resistance, hydrophobicity, and virulence of *Fusarium oxysporum*. *Eukaryot Cell* **7**: 1227-1230.
  - Russo, V.E. (1988) Blue light induces circadian rhythms in the *bd* mutant of *Neurospora*: double mutants *bd,wc-1* and *bd,wc-2* are blind. *J Photochem Photobiol B* **2**: 59-65.

- Saelices, L., Youssar, L., Holdermann, I., Al-Babili, S., and Avalos, J. (2007) Identification of the gene responsible for torulene cleavage in the *Neurospora* carotenoid pathway. *Mol. Genet. Genomics*.
- Sakaki, H., Nakanishi, T., Tada, A., Miki, W., and Komemushi, S. (2001) Activation of torularhodin production by *Rhodotorula glutinis* using weak white light irradiation. *J. Biosci. Bioeng.* **92**: 294-297.
- Sakaki, H., Kaneno, H., Sumiya, Y., Tsushima, M., Miki, W., Kishimoto, N., Fujita, T., Matsumoto, S., Komemushi, S., and Sawabe, A. (2002) A new carotenoid glycosyl ester isolated from a marine microorganism, *Fusarium* strain T-1. *J. Nat. Prod.* **65**: 1683-1684.
- Salgado, L.M., and Cerdá Olmedo, E. (1992) Genetic Interactions in the Regulation of Carotenogenesis in *Phycomyces*. *Current Genetics* **21**: 67-71.
- Salomon, M., Christie, J.M., Knieb, E., Lempert, U., and Briggs, W.R. (2000) Photochemical and mutational analysis of the FMN-binding domains of the plant blue light receptor, phototropin. *Biochemistry* **39**: 9401-9410.
- Sambrook, J., and Russell, D.W. (2001) *Molecular cloning: a laboratory manual*. New York: Cold Spring Harbor Laboratory Press.
- Sanchez-Fernandez, R., Avalos, J., and Cerda-Olmedo, E. (1997) Inhibition of gibberellin biosynthesis by nitrate in *Gibberella fujikuroi*. *FEBS Lett* **413**: 35-39.
- Sánchez-Martínez, C., and Pérez-Martín, J. (2001) Dimorphism in fungal pathogens: *Candida albicans* and *Ustilago maydis* - similar inputs, different outputs. *Curr. Opin. Microbiol.* **4**: 214-221.
- Sandmann, G. (1993a) Photoregulation of carotenoid biosynthesis in mutants of *Neurospora crassa*: Activities of enzymes involved in the synthesis and conversion of phytoene. *Z. Naturforsch.* **48c**: 570-574.
- Sandmann, G. (1993b) Carotenoid analysis in mutants from *Escherichia coli* transformed with carotenogenic gene cluster and *Scenedesmus obliquus* mutant C-6D. *Methods Enzymol* **214**: 341-347.
- Sandmann, G., Misawa, N., Wiedemann, M., Vittorioso, P., Carattoli, A., Morelli, G., and Macino, G. (1993) Functional identification of *al-3* from *Neurospora crassa* as the gene for geranylgeranyl pyrophosphate synthase by complementation with crt genes, *in vitro* characterization of the gene product and mutant analysis. *J Photochem Photobiol B* **18**: 245-251.
- Sandmann, G., and Misawa, N. (2002) Fungal carotenoids. In *The Mycota X. Industrial applications*. Osiewacz, H.D. (ed). Berlin Heidelberg: Springer Verlag, pp. 247-262.
- Sato, M., Niki, T., Tokou, T., Suzuki, K., Fujimura, M., and Ichiishi, A. (2008) Genetic analysis of the *Neurospora crassa* RAD14 homolog *mus-43* and the RAD10 homolog *mus-44* reveals that they belong to the *mus-38* pathway of two nucleotide excision repair systems. *Genes Genet Syst* **83**: 1-11.
- Schafmeier, T., Kaldi, K., Diernfellner, A., Mohr, C., and Brunner, M. (2006) Phosphorylation-dependent maturation of *Neurospora* circadian clock protein from a nuclear repressor toward a cytoplasmic activator. *Genes Dev* **20**: 297-306.

- Scherzinger, D., Ruch, S., Kloer, D.P., Wilde, A., and Al-Babili, S. (2006) Retinal is formed from apo-carotenoids in *Nostoc sp.* PCC7120: In vitro characterization of an apo-carotenoid oxygenase. *Biochem. J.* **398**: 361-369.
- Scherzinger, D., and Al-Babili, S. (2008) In vitro characterization of a carotenoid cleavage dioxygenase from *Nostoc sp.* PCC 7120 reveals a novel cleavage pattern, cytosolic localization and induction by highlight. *Mol Microbiol* **69**: 231-244.
- Schlicht, M., Samajova, O., Schachtschabel, D., Mancuso, S., Menzel, D., Boland, W., and Baluska, F. (2008) D'orenone blocks polarized tip growth of root hairs by interfering with the PIN2-mediated auxin transport network in the root apex. *Plant J* **55**: 709-717.
- Schliemann, W., Ammer, C., and Strack, D. (2008) Metabolite profiling of mycorrhizal roots of *Medicago truncatula*. *Phytochemistry* **69**: 112-146.
- Schmidhauser, T.J., Lauter, F.R., Russo, V.E., and Yanofsky, C. (1990) Cloning, sequence, and photoregulation of al-1, a carotenoid biosynthetic gene of *Neurospora crassa*. *Mol Cell Biol* **10**: 5064-5070.
- Schmidhauser, T.J., Lauter, F.R., Schumacher, M., Zhou, W., Russo, V.E., and Yanofsky, C. (1994) Characterization of al-2, the phytoene synthase gene of *Neurospora crassa*. Cloning, sequence analysis, and photoregulation. *J. Biol. Chem.* **269**: 12060-12066.
- Schroeder, W.A., and Johnson, E.A. (1995) Singlet oxygen and peroxy radicals regulate carotenoid biosynthesis in *Phaffia rhodozyma*. *J. Biol. Chem.* **270**: 18374-18379.
- Schrott, E.L., Huber-Willer, A., and Rau, W. (1982) Is phytochrome involved in the light-mediated carotenogenesis in *Fusarium aquaeductuum* and *Neurospora crassa*? *Photochem. Photobiol.* **35**: 213-216.
- Schulz, B., Banuett, F., Dahl, M., Schlesinger, R., Schäfer, W., Martin, T., Herskowitz, I., and Kahmann, R. (1990) The b alleles of *U. maydis*, whose combinations program pathogenic development, code for polypeptides containing a homeodomain-related motif. *Cell* **60**: 295-306.
- Schwartz, S.H., Qin, X., and Zeevaart, J.A. (2003) Elucidation of the indirect pathway of abscisic acid biosynthesis by mutants, genes, and enzymes. *Plant Physiol* **131**: 1591-1601.
- Schwender, J., Seemann, M., Lichtenthaler, H.K., and Rohmer, M. (1996) Biosynthesis of isoprenoids (carotenoids, sterols, prenyl side-chains of chlorophylls and plastoquinone) via a novel pyruvate/glyceraldehyde 3-phosphate non-mevalonate pathway in the green alga *Scenedesmus obliquus*. *Biochem J* **316** ( Pt 1): 73-80.
- Schwerdtfeger, C., and Linden, H. (2001) Blue light adaptation and desensitization of light signal transduction in *Neurospora crassa*. *Mol Microbiol* **39**: 1080-1087.
- Schwerdtfeger, C., and Linden, H. (2003) VIVID is a flavoprotein and serves as a fungal blue light photoreceptor for photoadaptation. *Embo J* **22**: 4846-4855.
- Selker, E.U. (1990) Premeiotic instability of repeated sequences in *Neurospora crassa*. *Annu Rev Genet* **24**: 579-613.
- Sharma, A.K., Spudich, J.L., and Doolittle, W.F. (2006) Microbial rhodopsins: functional versatility and genetic mobility. *Trends Microbiol.* **14**: 463-469.
- Shear, C.L., and Dodge, B.O. (1927) Life histories and heterothallism of the red bread-mold fungi of the *Monilia sitophila* group. *J. Agric. Res.* **34**: 1019-1042.



- Sherman, F., Fink, G.R., and Hicks, J.B. (1986) *Methods in Yeast Genetics*. Cold Spring Harbor, NY: Cold Spring Harbor Laboratory.
- Shiu, P.K., Raju, N.B., Zickler, D., and Metzenberg, R.L. (2001) Meiotic silencing by unpaired DNA. *Cell* **107**: 905-916.
- Shrode, L.B., Lewis, Z.A., White, L.D., Bell-Pedersen, D., and Ebbole, D.J. (2001) vvd is required for light adaptation of conidiation-specific genes of *Neurospora crassa*, but not circadian conidiation. *Fungal Genet Biol* **32**: 169-181.
- Sidhu, G.S. (1983a) Genetics of *Gibberella fujikuroi*. II. Natural occurrence and significance of heterokaryosis in sorghum isolates. *Can J Bot* **61**: 3314-3319.
- Sidhu, G.S. (1983b) Genetics of *Gibberella fujikuroi*. III. Significance of heterokaryosis in natural occurring corn isolates. *Can J Bot* **61**: 3320-3325.
- Sieiro, C., Poza, M., de Miguel, T., and Villa, T.G. (2003) Genetic basis of microbial carotenogenesis. *Int. Microbiol.* **6**: 11-16.
- Silva, F., Torres-Martinez, S., and Garre, V. (2006) Distinct *white collar-1* genes control specific light responses in *Mucor circinelloides*. *Mol. Microbiol.* **61**: 1023-1037.
- Skromne, I., Sanchez, O., and Aguirre, J. (1995) Starvation stress modulates the expression of the *Aspergillus nidulans brlA* regulatory gene. *Microbiology* **141**: 21-28.
- Small, A.J., Hynes, M.J., and Davis, M.A. (1999) The TamA protein fused to a DNA-binding domain can recruit AreA, the major nitrogen regulatory protein, to activate gene expression in *Aspergillus nidulans*. *Genetics* **153**: 95-105.
- Snetselaar, K.M., and Mims, C.W. (1992) Sporidial fusion and infection of maize seedlings by the smut fungus *Ustilago maydis*. *Mycologia* **84**: 193-203.
- Snetselaar, K.M., and Mims, C.W. (1993) Infection of maize stigmas by *Ustilago maydis*: light and electron microscopy. *Phytopathology* **83**: 843-850.
- Snetselaar, K.M., Bolker, M., and Kahmann, R. (1996) *Ustilago maydis* Mating Hyphae Orient Their Growth toward Pheromone Sources. *Fungal Genet Biol* **20**: 299-312.
- Sommer, T., Chambers, J.A., Eberle, J., Lauter, F.R., and Russo, V.E. (1989) Fast light-regulated genes of *Neurospora crassa*. *Nucleic Acids Res* **17**: 5713-5723.
- Song, Z.S., Cox, R.J., Lazarus, C.M., and Simpson, T.J. (2004) Fusarin C biosynthesis in *Fusarium moniliforme* and *Fusarium venenatum*. *Chembiochem.* **5**: 1196-1203.
- Spellig, T., Bottin, A., and Kahmann, R. (1996) Green fluorescent protein (GFP) as a new vital marker in the phytopathogenic fungus *Ustilago maydis*. *Mol. Gen. Genet.* **252**: 503-509.
- Springer, M.L. (1993) Genetic control of fungal differentiation: the three sporulation pathways of *Neurospora crassa*. *Bioessays* **15**: 365-374.
- Spudich, J.L. (1998) Variations on a molecular switch: transport and sensory signalling by archaeal rhodopsins. *Mol Microbiol* **28**: 1051-1058.
- Spudich, J.L., Yang, C.S., Jung, K.H., and Spudich, E.N. (2000) Retinylidene proteins: structures and functions from archaea to humans. *Annu Rev Cell Dev Biol* **16**: 365-392.
- Spudich, J.L. (2006) The multitasking microbial sensory rhodopsins. *Trends Microbiol.* **14**: 480-487.
- Steenkamp, E.T., Wingfield, B.D., Coutinho, T.A., Zeller, K.A., Wingfield, M.J., Marasas, W.F., and Leslie, J.F. (2000) PCR-based identification of MAT-1 and

- MAT-2 in the *Gibberella fujikuroi* species complex. *Appl Environ Microbiol* **66**: 4378-4382.
- Steinberg, G., and Perez-Martin, J. (2008) *Ustilago maydis*, a new fungal model system for cell biology. *Trends Cell Biol* **18**: 61-67.
  - Sweigard, J.A., and Ebbole, D.J. (2001) Functional analysis of pathogenicity genes in a genomics world. *Curr Opin Microbiol* **4**: 387-392.
  - Talbot, N.J. (2003) On the trail of a cereal killer: Exploring the biology of *Magnaporthe grisea*. *Annu Rev Microbiol* **57**: 177-202.
  - Talora, C., Franchi, L., Linden, H., Ballario, P., and Macino, G. (1999) Role of a *white collar-1-white collar-2* complex in blue-light signal transduction. *Embo J.* **18**: 4961-4968.
  - Teichert, S., Wottawa, M., Schonig, B., and Tudzynski, B. (2006) Role of the *Fusarium fujikuroi* TOR kinase in nitrogen regulation and secondary metabolism. *Eukaryot. Cell* **5**: 1807-1819.
  - Telfer, A. (2005) Too much light? How beta-carotene protects the photosystem II reaction centre. *Photochem Photobiol Sci* **4**: 950-956.
  - Terakita, A. (2005) The opsins. *Genome Biol.* **6**: 213.211-213.219.
  - Terashima, K., Yuki, K., Muraguchi, H., Akiyama, M., and Kamada, T. (2005) The *dst1* gene involved in mushroom photomorphogenesis of *Coprinus cinereus* encodes a putative photoreceptor for blue light. *Genetics* **171**: 101-108.
  - Thewes, S., Prado-Cabrero, A., Prado, M.M., Tudzynski, B., and Avalos, J. (2005) Characterization of a gene in the *car* cluster of *Fusarium fujikuroi* that codes for a protein of the carotenoid oxygenase family. *Mol. Genet. Genomics* **274**: 217-228.
  - Thompson, J.D., Gibson, T.J., Plewniak, F., Jeanmougin, F., and Higgins, D.G. (1997) The ClustalX windows interface: flexible strategies for multiple sequence alignment aided by quality analysis tools. *Nucleic Acids Res.* **24**: 4876-4882.
  - Tudzynski, B. (1999) Biosynthesis of gibberellins in *Gibberella fujikuroi*: biomolecular aspects. *Appl. Microbiol. Biotechnol.* **52**: 298-310.
  - Tudzynski, B., and Holter, K. (1998) Gibberellin biosynthetic pathway in *Gibberella fujikuroi*: evidence for a gene cluster. *Fungal Genet Biol* **25**: 157-170.
  - Tudzynski, B., Homann, V., Feng, B., and Marzluf, G.A. (1999) Isolation, characterization and disruption of the *areA* nitrogen regulatory gene of *Gibberella fujikuroi*. *Mol. Gen. Genet.* **261**: 106-114.
  - Tudzynski, B. (2005) Gibberellin biosynthesis in fungi: genes, enzymes, evolution, and impact on biotechnology. *Appl. Microbiol. Biotechnol.* **66**: 597-611.
  - Turner, B.C. (2001) Geographic distribution of *Neurospora* spore killer strains and strains resistant to killing. *Fungal Genet Biol* **32**: 93-104.
  - Uhlinger, C. (1997) Leukoencephalomalacia. *Vet Clin North Am Equine Pract* **13**: 13-20.
  - Umehara, M., Hanada, A., Yoshida, S., Akiyama, K., Arite, T., Takeda-Kamiya, N., Magome, H., Kamiya, Y., Shirasu, K., Yoneyama, K., Kyoizuka, J., and Yamaguchi, S. (2008) Inhibition of shoot branching by new terpenoid plant hormones. *Nature* **455**: 195-200.
  - Vasiliou, V., Bairoch, A., Tipton, K., and Nebert, D. (1999) Eukaryotic aldehyde dehydrogenase (ALDH) genes: human polymorphisms, and recommended

- nomenclature based on divergent evolution and chromosomal mapping. *Pharmacogenetics* **9**: 421-434.
- Velayos, A., Blasco, J.L., Alvarez, M.I., Iturriaga, E.A., and Eslava, A.P. (2000a) Blue-light regulation of phytoene dehydrogenase (*carB*) gene expression in *Mucor circinelloides*. *Planta* **210**: 938-946.
  - Velayos, A., Eslava, A.P., and Iturriaga, E.A. (2000b) A bifunctional enzyme with lycopene cyclase and phytoene synthase activities is encoded by the *carRP* gene of *Mucor circinelloides*. *Eur J Biochem* **267**: 5509-5519.
  - Verdoes, J.C., Krubasik, K.P., Sandmann, G., and van Ooyen, A.J. (1999a) Isolation and functional characterisation of a novel type of carotenoid biosynthetic gene from *Xanthophyllomyces dendrorhous*. *Mol Gen Genet* **262**: 453-461.
  - Verdoes, J.C., Misawa, N., and van Ooyen, A.J. (1999b) Cloning and characterization of the astaxanthin biosynthetic gene encoding phytoene desaturase of *Xanthophyllomyces dendrorhous*. *Biotechnol Bioeng* **63**: 750-755.
  - Visser, H., van Ooyen, A.J., and Verdoes, J.C. (2003) Metabolic engineering of the astaxanthin-biosynthetic pathway of *Xanthophyllomyces dendrorhous*. *FEMS Yeast Res.* **4**: 221-231.
  - Vitalini, M.W., de Paula, R.M., Park, W.D., and Bell-Pedersen, D. (2006) The rhythms of life: circadian output pathways in *Neurospora*. *J Biol Rhythms* **21**: 432-444.
  - Voigt, K., Schleier, S., and Bruckner, B. (1995) Genetic variability in *Gibberella fujikuroi* and some related species of the genus *Fusarium* based on random amplification of polymorphic DNA (RAPD). *Curr Genet* **27**: 528-535.
  - Vollmer, S.J., and Yanofsky, C. (1986) Efficient cloning of genes of *Neurospora crassa*. *Proc Natl Acad Sci U S A* **83**: 4869-4873.
  - Walter, M.H., Fester, T., and Strack, D. (2000) Arbuscular mycorrhizal fungi induce the non-mevalonate methylerythritol phosphate pathway of isoprenoid biosynthesis correlated with accumulation of the 'yellow pigment' and other apocarotenoids. *Plant J* **21**: 571-578.
  - Wan, Y., Liu, H., Li, C., and Schmidhauser, T.J. (1997) Genome analysis on linkage group VI of *Neurospora crassa*. *Fungal Genet. Biol.* **21**: 329-336.
  - Waschuk, S.A., Bezerra, A.G., Jr., Shi, L., and Brown, L.S. (2005) *Leptosphaeria* rhodopsin: bacteriorhodopsin-like proton pump from a eukaryote. *Proc. Natl. Acad. Sci. USA* **102**: 6879-6883.
  - Watanabe, K., Sakuraba, Y., and Inoue, H. (1997) Genetic and molecular characterization of *Neurospora crassa* *mus-23*: a gene involved in recombinational repair. *Mol Gen Genet* **256**: 436-445.
  - Watters, M.K., Randall, T.A., Margolin, B.S., Selker, E.U., and Stadler, D.R. (1999) Action of repeat-induced point mutation on both strands of a duplex and on tandem duplications of various sizes in *Neurospora*. *Genetics* **153**: 705-714.
  - Wedlich-Söldner, R., Bölker, M., Kahmann, R., and Steinberg, G. (2000) A putative endosomal t-SNARE links exo- and endocytosis in the phytopathogenic fungus *Ustilago maydis*. *Embo J.* **19**: 1974-1986.
  - Weete, J.D., and Gandhi, S.R. (1997) Sterols of the phylum zygomycota: phylogenetic implications. *Lipids* **32**: 1309-1316.

- 
- Westergaard, M., and Hirsch, H.M. (1954) Environmental and genetic control of differentiation in *Neurospora*. . *Proc Symp Colson Res Soc* **7**: 171-183.
  - Will, O.H., Newl, N.A., and Reppe, C.R. (1984) The photosensitivity of pigmented and non-pigmented strains of *Ustilago violacea*. *Curr Microbiol* **10**: 295-302
  - Wisniewska, A., Widomska, J., and Subczynski, W.K. (2006) Carotenoid-membrane interactions in liposomes: effect of dipolar, monopolar, and nonpolar carotenoids. *Acta Biochim. Pol.* **53**: 475-484.
  - Wyss, A. (2004) Carotene oxygenases: a new family of double bond cleavage enzymes. *J Nutr* **134**: 246S-250S.
  - Yoshida, Y., and Hasunuma, K. (2004) Reactive oxygen species affect photomorphogenesis in *Neurospora crassa*. *J. Biol. Chem.* **279**: 6986-6993.
  - Youssar, L., and Avalos, J. (2006) Light-dependent regulation of the gene *cut-1* of *Neurospora*, involved in the osmotic stress response. *Fungal Genet Biol* **43**: 752-763.
  - Youssar, L., and Avalos, J. (2007) Genetic basis of the *ovc* phenotype of *Neurospora*: identification and analysis of a 77 kb deletion. *Curr Genet* **51**: 19-30.
  - Zalokar, M. (1954) Studies on biosynthesis of carotenoids in *Neurospora crassa*. *Arch Biochem Biophys* **50**: 71-80.
  - Zhai, Y., Heijne, W.H., Smith, D.W., and Saier, M.H., Jr. (2001) Homologues of archaeal rhodopsins in plants, animals and fungi: structural and functional predications for a putative fungal chaperone protein. *Biochim. Biophys. Acta.* **1511**: 206-223.
  - Zhao, G., and London, E. (2006) An amino acid "transmembrane tendency" scale that approaches the theoretical limit to accuracy for prediction of transmembrane helices: relationship to biological hydrophobicity. *Protein Sci.* **15**: 1987-2001.
  - Zoltowski, B.D., Schwerdtfeger, C., Widom, J., Loros, J.J., Bilwes, A.M., Dunlap, J.C., and Crane, B.R. (2007) Conformational switching in the fungal light sensor Vivid. *Science* **316**: 1054-1057.